JOURNAL OF THE NATIONAL CANCER INSTITUTE

National Institutes of Health • Public Health Service

Volume 27 • Number 4

October 1961

Observations on the Surface Cells of the Mouse Omentum as Studied With the Phase-Contrast and Electron Microscopes [1]

MARIE D. FELIX,[2] *Division of Pathology, Sloan-Kettering Institute for Cancer Research, Sloan-Kettering Division of Cornell University Medical College, New York, New York*

SUMMARY

The conformation and fine structure of the cells covering the surface of the normal, or control, omentum are described. Some of the observations are of particular interest in the light of past controversies concerning the apposition and potentialities of mesothelial cells. Both macrophages and mesothelial cells compose the surface layer of the milky spots. The mesothelial cells, which are contracted, are in the majority, macrophages being interspersed among them. Openings occur between the cells on the milky spots thus exposing the underlying cells or collagen fibers to the surface. No basement membrane appears beneath any of the cells covering the omentum. The surface cells of the netlike areas of the omentum are flattened, tenuous mesothelial cells that appose each other by adjoining or overlapping. The possible significance of the milky spots and their surface modification in relation to the reticuloendothelial system is discussed. Whether the surface macrophages function as sessile phagocytes or migrate in response to stimulation must be determined by experimental studies. Macrophages and mesothelial cells being close neighbors on the omental surface makes this an advantageous region for comparing their reaction to various stimuli.—J. Nat. Cancer Inst. 27: 713-745, 1961.

IN THE 1870's, when achievement of the techniques of staining and embedding enabled advances in light microscopy comparable to those of the 1950's in electron microscopy, the normal omentum of several species of mammals was the subject of studies by Ranvier (*1*, *2*). He described the collagenous fabric of the tissue, the flat surface cells on both sides of the netlike areas, and the relations of the surface cells with each other and with the meshes of the net. He gave one of the first descriptions of the cellular areas of the omentum, calling them "*taches laiteuses*," or "milky spots," a name which has endured. Ranvier's observations were made on spreads of the omentum that had been treated with silver nitrate to outline the surface cells and then stained with picrocarmine. He observed a thickening and irregularity of the mesothelial cells over the milky spots and a widening of the dark lines at the

[1] Received for publication November 22, 1960; revised July 26, 1961.

[2] Public Health Research Fellow of the National Cancer Institute.

603724—61——2

edges of the cells, all of which he interpreted as indicating an interrupted surface. He described macrophages, which he called "motile lymphatic cells," as being not only free in the peritoneal fluid and within the cellular areas but also on the surface among mesothelial cells. He speculated that those on the surface had been caught in passing back and forth between tissue and fluid. Later Buxton and Torrey (*3*) and Maximow (*4*) also observed macrophages among the mesothelial cells covering the milky spots.

Two questions regarding the surface cells of the peritoneal cavity became controversial in the latter part of the 19th century and have continued so to this day. First, what role does the configuration of mesothelial cells play in the passage of fluids, particles, and cells from the cavity? Second, are mesothelial cells capable of being transformed into macrophages?

The idea of stomata or preformed openings between mesothelial cells as a mechanism of passage from the peritoneal cavity was first broached by von Recklinghausen (*5*) and seemingly proved by the use of silver nitrate. Dark lines marking the cell boundaries were seen to be interrupted in places by small, dark, elliptical areas. These areas were thought to be stomata in which a precipitate of albuminate of silver had been caught. In 1870 von Recklinghausen himself (*6*) expressed some doubt of the preformed openings, and in 1901 Hertzler (*7*) pointed to several probable sources of artifact in the making of preparations. There followed a period of conflicting concepts involving theories of passage of fluids and particles through temporary openings between the cells or directly through the cytoplasm. Cunningham (*8*) reviewed the question up to 1926. Since 1926, evidence has been presented again for stomata (*9*), for passage between cell membranes (*10*) and, with the electron microscope, for the passage of very small particles through the cytoplasm (*11*).

The diaphragm appears to be the major site of exit from the peritoneal cavity for experimentally administered fluids and particles. These traverse the lining cells and the subadjacent endothelium of lymphatic lacunae, entering the diaphragmatic lymph plexus within minutes. Thence they travel to the anterior mediastinal lymph nodes and enter the blood stream by way of the right lymph duct (*12*). The omentum had been known to segregate particulate material (*13*, *14*) and to be capable, to some degree, of absorption of fluids (*13*, *15*). In 1930, Higgins and Bain (*16*) isolated part of the omentum of cats into a subcutaneous pocket on the ventral abdominal wall and injected graphite into the pocket. They demonstrated the appearance of graphite particles in the same lymphatics of the diaphragm and the anterior mediastinal lymph nodes within 48 hours. The graphite appeared as free particles and as particles within free macrophages. At no time did they find graphite free in the peritoneal cavity, but they were able to trace its intratissue migration to the diaphragm. Thus it has been demonstrated that a majority of experimentally administered particles leaves the peritoneal cavity by way of a well-defined lymphatic pathway. They can enter this course either

directly via the diaphragm or less directly through the omentum. Their means of traversing the intervening cells is still undecided.

The question as to whether mesothelial cells become transformed into phagocytic cells arose mainly as a result of studies on the free cells present in the peritoneal fluid. A change takes place in the components and proportions of the normal cell population after the introduction of irritating substances into the peritoneal cavity. After an initial influx of neutrophilic granulocytes there is a rise in the number of large macrophages (*14*). Some investigators, observing changes and sometimes desquamation of the lining cells under these conditions, concluded that mesothelial cells were the source of the free phagocytic cells (*17–19*). Other investigators were of the opinion that the free macrophages had migrated from the milky spots of the omentum, with probable additions from the subperitoneal tissue in general and in the form of monocytes, from the blood stream (*20*, *21*). When vital dyes were introduced, extensive studies were made on the lineage of blood and connective-tissues cells. The evidence gained from this technique was against a relationship between macrophages and mesothelial cells (*22–24*).

The electron microscope, in conjunction with the phase-contrast microscope, has proved a valuable tool for the reinvestigation of the questions reviewed. The results of this study confirm the early morphological observations of Ranvier (*2*), Buxton and Torrey (*3*), and Maximow (*4*) that both mesothelial cells and macrophages compose the surface covering the milky spots of the omentum and that discontinuities exist between these cells. Mesothelial cells covering the surfaces of the ovary (*25*), diaphragm or mesentery (*11*), small intestine (*26*, *27*), and liver and spleen (*27*) have already been examined with the electron microscope. Differences between these and the cells covering the omentum will be discussed.

MATERIAL AND METHODS

Omenta were obtained from three different strains of adult mice, 3 C3H/An females, 2 C3H/An males, 2 Swiss males, and 2 DBA/2 females. The mice were raised and fed according to the usual laboratory procedures.

The gross structure of the fixed omenta of all the mice was observed with a dissecting microscope at magnifications ranging from 9× to 45×. Omental spreads from 7 of the mice were examined with the phase-contrast microscope at 200 to 950×.

All except the omentum from 1 Swiss male mouse were embedded in plastic. Cross sections from the omenta of 2 C3H/An females, 1 C3H/An male, and 1 Swiss male were studied with the phase-contrast microscope. Similar areas from a male and a female C3H/An mouse, a Swiss male mouse, and a DBA/2 female mouse were studied with the electron microscope. The material used for the illustrations in this paper came from a C3H/An male and a Swiss male mouse. Unless otherwise stated, the

description of the gross and cellular morphology in the results is generally applicable to all the omenta observed.

The mice were killed by decapitation or neck dislocation. Immediately 3½ ml of chrome-osmium fluid, *p*H 7.2 (*28*), was injected into the peritoneal cavity. The abdomen was gently kneaded for a short time prior to opening to insure complete distribution of the fixative. The omentum was then removed and placed in the fixative for 50 minutes. After washing in several changes of saline or tap water, it was placed in 10 percent neutral formalin for a minimum of one-half hour. Beyond this, the period in neutral formalin was not critical and was allowed to vary, depending upon the time necessary for cutting up the material. Rectangles of about ½ × 3 mm were cut under a dissecting microscope and placed in flat dishes containing warm (47–49° C) liquid 2 percent agar. Pieces of this size were small enough to lie comparatively flat. The agar containing the pieces of omentum was kept warm and fluid for 10 to 15 minutes, then allowed to cool and harden. Primary embedding in agar was advantageous with this tissue, not only as a protection but also as a means of making orientation easier. While in 70 percent alcohol, the agar was cut into small cubes, each containing a piece of omentum, after which dehydration was completed in graded alcohols. The alcohol was then replaced with methacrylate monomer without catalyst and allowed to stand overnight at 4° C. The monomer used for the C3H mice was 1 part methyl to 8 parts *n*-butyl, while that for the Swiss mouse was 1 part methyl to 3 parts *n*-butyl methacrylate.

The agar-embedded tissue from the C3H/An and DBA/2 mice was placed in plastic containing 1 percent benzoyl peroxide as catalyst which had been prepolymerized to a heavy, syrupy consistency. Polymerization was completed at 65° C. That from the Swiss mouse was placed in monomer containing 1.5 percent azodi-iso-butyronitrile (ADIB) (*29*) as catalyst. It was then placed in capsules with a lightly prepolymerized plastic containing 1.5 percent ADIB and 0.07 percent uranyl nitrate (*30*). Polymerization was completed at 47° C. The use of ADIB and uranyl nitrate greatly improved the preservation of the omental tissue as can be observed in the illustrations.

All sections were cut on a Porter-Blum microtome, with a diamond knife. Those used for phase-contrast microscopy were cut at an approximate thickness of 1 μ, mounted in glycerin on a glass slide, and sealed under a coverslip. The electron microscopes used were RCA models EMU 2B and EMU 2C. Electron micrographs were taken at a magnification of 5000 to 6000 and optically magnified to the final enlargement.

To make wholemounts for phase-contrast microscopy, pieces of the fixed omenta were spread on glass slides, glycerin was used as a mounting medium, and the preparations were sealed under coverslips. The phase-contrast microscope was a Zeiss Winkel Standard GFL model equipped with achromatic dark phase-contrast optics.

RESULTS

The greater omentum is formed by an invagination of the dorsal mesogastrium during the early development of the embryo. After the rotation of the stomach it continues to grow downward and becomes a thin-walled, flattened sac, which is dependent from the greater curvature of the stomach and overlies the intestines ventrally. In the mature human the layers of the sac become largely fused below the stomach. In the mature mouse less fusion seems to have occurred so that most of the bursa is patent. Thus, under the dissecting microscope, the greater omentum of the mouse appears as a thin, transparent, saclike structure. Its fat deposits are mainly peripheral, and large areas appear to be avascular. Scattered throughout the transparent tissue are discrete opaque spots. These are the milky spots of Ranvier (*2*); they are composed of mobilized macrophages, lymphocytes, occasional plasma cells, eosinophils, and mast cells, as well as fibroblasts. The number of milky spots varies to some extent from mouse to mouse.

Phase-Contrast Microscopy

Spreads made from fixed omenta were examined under the phase-contrast microscope with a high, dry objective. The main texture of the tissue was composed of bundles of collagen fibers and an occasional elastic fiber (fig. 1). The fibers of the fabric and the cells on the surface are so arranged that numerous openings or meshes are formed having diameters which generally range from less than 1 to 20 μ. Occasionally a mesh is as large as 50 or 60 μ. In some places only a narrow isthmus separates the meshes; in other places an expanse lies between them. A few scattered nuclei can be discerned on the surface of the netlike areas and an occasional cell within the tissue. Occasionally foreign material is segregated in the cellular regions. No meshes are apparent within the milky spots, which are composed of massed cells lying within the tissue. The milky spots measure from less than 100 micra to half a millimeter or more. Meshes occurring at the edges of the milky spots often have cells extending into their openings (fig. 4).

One-micron thick cross sections of methacrylate-embedded tissue from the network of the omentum appear as an aligned series of thin segments (figs. 1*a* and 1*b*). The tissue from the C3H/An mouse (fig. 1*a*) is thinner than that from the Swiss mouse (fig. 1*b*). Mesothelial cells of both tissues are platelike and thin. Their nuclei, though flat, cause a local thickening which, in the case of the C3H/An mouse, tends to project into the tissue (fig. 1*a*). The cytoplasm of the mesothelial cells of the Swiss mouse is not as thin as that of the C3H/An, and the nuclei often project outward (fig. 1*b*). Cross sections through the milky spots assume an appearance different from that of cross sections through the network (figs. 2 and 3). The surface cells are contracted and rounded up, the tissue is thicker, and cells lie among the fibers. The manner of rounding up of the surface cells is distinctive in the 2 mice used for illustration, although the essential

character and relationships are similar. In the C3H/An mouse the longest diameter tends to parallel the tissue, which gives the surface an undulated appearance (fig. 2). In the Swiss mouse the longest diameter of the surface cells tends to extend outward toward the peritoneal cavity (fig. 3). This not only gives a jagged appearance to the surface, but, depending on where the section passes in relation to the cells, it also gives an impression that other cells not a part of the tissue are adherent to or caught against the omentum. A study of serial cross sections shows that this is probably not the situation. Many of the cells on the surface of the cellular areas of the Swiss mouse are anchored to the tissue by a relatively narrow process as shown in figures 4, 4*a*, 4*b*, and 4*c*. Electron micrographs of cross sections often show the process to be wrapped around a bundle of collagen fibers. At the resolution of the phase-contrast microscope, vacuoles can be seen in some surface cells from the C3H/An mouse (*arrow*, fig. 2). For reasons to be presented later, such cells, as well as cells found on the surface of the milky spots of the Swiss mouse, have been tentatively identified as macrophages. That there are discontinuities between the cells is strongly suggested in both figure 2 and figure 3.

Electron Microscopy

The electron micrographs of the omenta are of cross sections. Since the omental bursa was patent in the material from the mice used in this study, one surface was facing the peritoneal cavity and the other the bursa. Nothing has been observed which would indicate any difference in the two surfaces. Therefore no distinction will be made, and in describing the electron micrographs, the peritoneal cavity will be indicated as lying on both sides of the tissue.

Netlike areas.—The fabric of the network of the omentum is covered on both sides by thin, flattened mesothelial cells. The tissue varies in thickness due to the presence of a cell lying within the tissue or to the presence of a mesothelial-cell nucleus. It may be as thin as 1 μ (fig. 6) or as thick as 5 or 6 μ (figs. 14 and 15), the average thickness being about 2 or 3 μ for the C3H/An omentum and 3 or 4 μ for the Swiss omentum. The cytoplasm of the mesothelial cell may become very tenuous, sometimes having a depth of only 20 to 40 mμ (figs. 6 and 7). At the edges of the meshes the surface cells of one side of the net make junctions with the cells covering the other side, as indicated by the arrows in figures 7, 8, and 13. Sometimes part of a cell extends all the way around the fibers at the edge of an opening and continues for a considerable distance on the other side of the net before a juncture is made (fig. 8). In some places the main body of a single cell constitutes the entire breadth of the tissue forming the surface on both sides (fig. 12).

The mesothelial cells that pave the network appose each other by adjoining or overlapping. Junctions of two adjacent cells appear in figures 5 and 8. Figure 5 shows two cells bordering on each other and figure 8 two cells overlapping each other. Figure 9 is an enlargement of a junction which in this case happens to be between two parts of the same cell. A

section which passes through a region where several cells come together may show them overlapping each other as in figure 5 or overlapping and adjoining as in figure 10.

There is no evidence of a basement membrane between the covering cells and the underlying fibers. Occasionally a small amount of material is condensed against the proximal membrane but it is never extensive (fig. 6). On the free surface of the mesothelial cells a variable number of microvilli are found. In normal C3H/An mice they are scanty, although in other mice of this strain which had undergone prolonged peritoneal irritation microvilli were prominent. In the Swiss mouse microvilli are numerous enough to appear in most of the thin sections.

The existence of a single central flagellum on mesothelial cells has been described by Maximow (*31*) and attributed by him to a connection with the centrioles. In two thin sections of mesothelial cells from the omenta of C3H/An mice a flagellum was observed situated above a depression near the center of the nucleus. The one in figure 11 is an approximate longitudinal cut near the center of the flagellum. In general its structure conforms to the description of cilia on the epithelium of the oviduct of the mouse by Fawcett and Porter (*32*) and to those described on β-cells from the islets of the mouse pancreas by Munger (*33*). It is difficult to determine whether the oval body at its base is a centriole as Munger found or a part of the basal corpuscle that appears to be partially separate because of the angle of the structure and the plane of the section. No flagella have been noted in thin sections from the Swiss mouse omentum.

The nuclei of mesothelial cells covering the network show a tendency to extend partly into the tissue. They appear as elongated, flattened ovals whose surfaces have undulant areas as well as an occasional sharp indentation. A typical nuclear membrane surrounds them (figs. 6, 8, and 15). The electron-dense material in the nuclei from C3H/An omenta embedded with benzoyl peroxide as catalyst appears clumped (figs. 6 and 8), while that in the nuclei of the Swiss omentum embedded with ADIB as catalyst and with added uranyl nitrate shows an even, though loose, distribution (fig. 15). The mesothelial-cell nucleus usually contains but one nucleolus, and none appears in these illustrations. In the nuclei in figures 6 and 15 there are several small, dense regions surrounded by less dense halos.

The tiny invaginations at the plasma membrane and the small, usually oval, vesicles within the cytoplasm, which seem to be related to them, are a prominent feature of the omental mesothelial cells even in the more tenuous regions. Readily seen in the sections of the Swiss mouse processed with ADIB and uranyl nitrate, they appear in general to be more numerous beneath the plasma membrane on the peritoneal side of the cell and to have a tendency to be oriented with their longest diameter normal to that of the membrane. Their shortest diameter ranges from 20 to about 70 mμ (figs. 12, 14, and 15).

Small vacuoles are common in the cytoplasm of mesothelial cells from the omenta of both mice (figs. 6, 12, and 15). In the C3H/An mouse they

do not appear membrane-bounded and their contents are either electron-lucent (fig. 6) or of moderate electron density. Vacuoles contained in the cytoplasm of macrophages from the same material are usually bounded by membranes. In the omentum of the Swiss mouse, which shows less polymerization damage, there again appear small vacuoles (figs. 12 and 15). These are membrane-bounded, their interior is electron-lucent, and many are partially or almost completely filled with a particulate material.

Mitochondria are moderate in number and are very dense. The method of fixation made the cristae difficult to see because of the density of the material preserved between them. The Golgi zones are located either beside or above the nucleus, and are composed of double membranes and vesicles (fig. 15). A moderate amount of ergastoplasm is present, occurring in the thin parts of the cytoplasm as short, scattered profiles of double membranes with attached granules (figs. 5 and 14). In the thicker areas near the nuclei, groups of more extensive profiles tend to lie parallel to each other (fig. 15). Occasional lipide droplets are found in mesothelial cells from the Swiss mouse. They are either round or crescent-shaped. Those which are crescent-shaped are related to an electron-lucent space which might be an artifact (fig. 15). Lipide droplets are found only rarely in the other mice.

Milky spots.—In the section on phase-contrast microscopy the general characteristics of the surface cells covering the milky spots of the omentum were described (figs. 2 and 3). Electron microscopy confirms the presence of discontinuities between the cells and shows that macrophages constitute part of the surface layer.

Discontinuities on the surface of the milky spots occur between the thicker parts of the cells as well as between thin cell processes (figs. 16 and 17). It has been deduced from the study of both phase-contrast and electron micrographs that when mesothelial cells become contracted and thickened over the milky spots their edges are usually thinner than the nuclear region and possess a number of processes. These may lie beside adjacent cells or beside the processes of adjacent cells thus forming openings which vary from about 50 mμ to 1 μ or more in width. The processes adjoin or overlap each other as well (fig. 16). At the places where openings occur collagen fibers or underlying cells are exposed to the surface. While the possibility of artifact causing the discontinuities has not been ruled out, it seems that if this were artifactitious it would have been observed frequently on the network where the thin cell edges are merely touching or overlapping and where, at the resolution employed for this study, there is no evidence of a mechanism of intercellular binding. Milky spots can appear and disappear as a result of conditions in the peritoneal cavity (*4*, *34*). It would be reasonable to suppose, therefore, that the flattened mesothelial cells covering the net have the ability to contract and assume the appearance described for those covering the cellular areas. As on the net, there is no evidence of a basement membrane.

The macrophages sharing the surface of the milky spots lie directly on the fibers of the underlying tissue or on thin processes of adjacent cells, as do the mesothelial cells (fig. 16). They may abut directly upon a neighboring mesothelial cell and may overlie cells within the tissue (fig. 18). Mesothelial cells are in the majority, with macrophages interspersed among them. In the Swiss mouse both macrophages and mesothelial cells tend to be anchored to the fabric with a relatively narrow process and to extend outward toward the peritoneal cavity (figs. 4*a*, 4*b*, and 4*c*). Openings may occur between a macrophage and a mesothelial cell as well as between mesothelial cells.

Macrophages differ from mesothelial cells in several characteristic ways (figs. 16, 17, and 18). The free surface of the macrophage lacks the microvilli of more or less uniform dimensions which are present on the free surface of the mesothelial cell. The mesothelial surface gives an impression of smoothness compared to that of the macrophage, which is undulant and exhibits a varying number of blunt processes and small cytoplasmic extensions of diverse form and size. That the character of the surface of the macrophage in fixed material is the result of its surface activity can be seen when living macrophages in the peritoneal fluid of mice are observed with the phase-contrast microscope (*14*). A surface appearance similar to that of the cells in figures 18, 19, and 22 occurs when free macrophages are fixed and sectioned for electron microscopy [(*27*), figs. 20 and 21]. The processes, which are cross sections of thin sheets or folds, often close upon themselves, thus engulfing particles or droplets of the surrounding medium (figs. 18 and 20). The small vacuoles being formed at or occurring near the surface of the macrophage are oval, round, or irregular in shape and variable in size. The small vesicles of the mesothelial cell, which have dimensions of a less marked variation, do not appear to involve the outstretching of processes from the surface but rather a pulling inward of the surface. The two phenomena, while perhaps comparable, seem to show a different morphological involvement of the surface.

Vacuoles ranging from about 40 mμ to as much as 2 μ in diameter appear within the cytoplasm of macrophages on the omental surface. They are particularly striking in macrophages from the C3H/An mouse (fig. 16). Many of the vacuoles in macrophages from the Swiss mouse contain particles and are reminiscent of those in free macrophages that are actively ingesting experimentally inoculated material (figs. 21 and 22). Small vacuoles containing particulate material also occur in the cytoplasm of mesothelial cells from the Swiss mouse (fig. 15).

Membrane-bounded inclusions with a dense matrix typical of those noted in macrophages from other locations (*27*, *35*) are present in the cytoplasm of macrophages from the surface of the milky spots of the mice studied. In the macrophage from a Swiss mouse in figure 18 they appear to contain a relatively homogeneous material of medium electron density. They are comparable to those in the cytoplasm of the free macrophage from the peritoneal fluid of a normal DBA/2 mouse in figure 20. In

another macrophage from the Swiss mouse (fig. 22) the inclusions are difficult to distinguish, being of a density similar to the general cytoplasm. Here they are less homogeneous and seem to have randomly placed membranes among their contents. In a portion of a macrophage from the omental surface of a C3H/An mouse (fig. 19), the two inclusions (IB) exhibit a stippling of tiny, dense 55 to 60 A particles in their matrices. Such particles are often found in the cytoplasm of macrophages both on and within the omentum of this mouse. They are either scattered diffusely through the cytoplasm, adherent to the membranes of vacuoles, or aggregated in dense bodies. Similar particles have been identified as ferritin in macrophages from lung alveoli (*36*), from interstitial-testicular tissue (*37*), and in macrophages from the spleen (*35*). Ferritin-like particles are rarely observed in the macrophages of the omentum of the Swiss mouse. These particles have never been seen in mesothelial cells.

When a macrophage is sectioned through the nuclear region, the nucleocytoplasmic ratio is smaller than that of the contracted mesothelial cell (fig. 18). The nucleus contains material of medium electron density and of even and compact distribution. A nucleolus is rarely seen. The ground cytoplasm is less compact than the cytoplasm of mesothelial cells (fig. 18), a fact which is evident in the cells from the C3H/An mice where greater clumping occurred during polymerization (fig. 16). Scattered through the cytoplasm of macrophages are tiny vesicles with a dense matrix reminiscent in size and character of those which are an element of the Golgi complex. Mitochondria are scattered and tend to show more detail of the cristae than those in the mesothelial cells, with the fixation used for this study. Profiles of ergastoplasmic sacs are usually randomly distributed and the Golgi complex is composed of two elements, stacks of parallel double membranes, and small vesicles, as in the mesothelial cells. Lipide droplets are not often seen. The cellular detail of the contracted mesothelial cells from the surface of the milky spots is similar to that given in the description of those from the net.

DISCUSSION

This study has ascertained the presence of macrophages on the surface above the omental milky spots of normal mice, which thus confirms the early light microscopic observation of Ranvier (*2*) and the later ones of Buxton and Torrey (*3*) and Maximow (*4*). In the section on Results a comparison was made between the characteristics of macrophages on the surface (figs. 18, 19, and 22) and those free in the peritoneal fluid (figs. 20 and 21). A number of electron micrographic studies have illustrated macrophages from widely separated locations in laboratory mammals and in man. They include the Kupffer cells of the liver sinusoids (*38*, *39*), alveolar macrophages (*36*, *40*), Hofbauer cells of the chorionic villi (*41*), and macrophages resident in the spleen (*35*). Several characteristics are common to all these macrophages and to those free in the peri-

toneal fluid and on the surface of the omentum. Among them are the qualities of the free surface, the vacuoles of widely varying sizes near the cell margin and within the cytoplasm, inclusion bodies such as those shown in figures 18 to 22, and random small vesicles in the cytoplasm which are similar to those associated with the Golgi apparatus. Ferritin is sometimes present, either situated in inclusions or scattered diffusely through the cytoplasm [fig. 19, (*35*, *36*, *40*)]. Its presence, particularly in the macrophages of the spleen, is not unusual in view of the role of the reticuloendothelial cells in the storage and processing of iron for return to the bone marrow (*42*). In this study, ferritin was often found in the macrophages of the C3H/An strain mice and observed only occasionally in the other mice.

Milky spots or analogous structures are present in human and all other mammalian omenta so far studied. The main constituent of these accumulations of connective-tissue cells is the macrophage, which occurs in both a resting and a mobilized state (*4*). In fact, the abundance of mobilized macrophages has caused the omentum to be likened to a tissue which is responding to inflammation (*43*). At present there is no other region of the peritoneum which is known to contain such a profusion of macrophages. That similar concentrations may occur in the other serous cavities is indicated in the reports of Kampmeier (*44*) and Mixter (*45*). In a study of the pleura of man and other mammals, they found discrete cell concentrations consisting chiefly of mobilized macrophages, which were most frequently localized in the retrocardiac mediastinal pleura. The pleural membrane was often netlike and the milky spots both vascular and avascular.

The absence of a basement membrane beneath the mesothelium of the omental network and the apposition of neighboring cells by merely adjoining or overlapping confirm earlier electron microscopic observations on the omenta of DBA/2 mice by Felix and Dalton (*27*). The present study shows the same to be true of the omental cells of two other mouse strains. It further shows that the mesothelial cells overlying the milky spots also lack a basement membrane and are contracted and discontinuous, thus forming actual openings as well as probable potential openings. In the earlier paper, Felix and Dalton (*27*) also presented observations on the visceral mesothelium from the liver, spleen, and intestine. Odor (*25*) studied the mesothelial covering of the ovary and Palade and Porter (*26*), in a paper on the endoplasmic reticulum, published an illustration of portions of two mesothelial cells from the surface of the intestine. The cells from all these visceral regions are less tenuous than those covering the omental network, possess a complete basement membrane, and meet by means of complicated interdigitation. Palade and Porter (*26*) show desmosomes or adhesion plates between the adjacent plasma membranes of the intestinal mesothelium and state that this is also true of the pleural and pericardial mesothelium which they examined. Two characteristics common to the mesothelial cells covering the viscera and the omentum are microvilli and small vesicles. The vesicles are

similar to those which were first described by Palade for endothelium (*46*).

The modified surface overlying the milky spots of the omentum is strikingly comparable to the sinusoidal linings of the blood vascular system. Capillary endothelial cells and mesothelial cells have a common origin, the mesoderm, and a similar function, the lining of channels and cavities to and from which fluids and substances pass. Beneath the endothelium of the majority of capillaries there is a complete basement membrane (*47*), and in many capillaries the adjacent cells seem to exhibit a mechanisn of intercellular binding, as shown by Bennett, Luft, and Hampton (*47*). The visceral mesothelial cells with their complete basement membrane and their complicated interdigitation may be compared to these capillaries. The only known capillaries where the lining cells are discontinuous and have no complete basement membrane are the sinusoids of the bone marrow (*48, 49*), the spleen (*50*), and the liver (*39, 51, 52*). Phagocytic cells with a morphology similar to that of the macrophages of the omental surface compose part of the lining of the liver sinusoids (*38, 48*). They are the most active of the sinusoidal macrophages of the blood vascular system, phagocytosing foreign material from the blood by contact.

In the peritoneal cavity the omentum is a free-hanging fold of tissue which can extend over a large area. It was once thought to be capable of movement (*53*). But this is not the case (*13, 54*). Florey and Carleton (*55*) showed it was incapable of intrinsic movement, but that posture and peristalsis and diaphragmatic movements could bring it into contact with infected or inflamed areas, to which it would adhere, or with foreign bodies, which it would encapsulate. The omentum has the ability to secrete a sticky, fibrinous fluid with great rapidity, a phenomenon which has been consistently observed by all those who have initiated experimental conditions with a view to studying its reactions (*3, 16, 34*). While the whole peritoneum apparently has this power (*56*), it is greater and more rapid in the omentum (*55*). Foreign particles can be washed free from all peritoneal surfaces except the omentum shortly after their inoculation. Fifteen minutes after injection Webb (*57*) found them sticking only to the milky spots.

These morphological and physiological characteristics of the omentum, coupled with the present finding that the cells covering the milky spots consist of discontinuous mesothelial cells interspersed with macrophages, would point to the existence of regions in the peritoneal cavity which are specialized, as the sinusoids of the blood vascular system are specialized, for the protection of the organism. The exudate might be a mechanism by means of which the omentum gathers material to be phagocytosed *in situ* or by means of which particles can gain entrance to the subadjacent tissue through intercellular openings, there either to be ingested by macrophages or to proceed to the lymphatics of the diaphragm (*16*). The intercellular openings, both actual and potential, might be a pathway for the mobilized macrophages of the milky spots to migrate to and from

the peritoneal fluid. It remains to be determined whether the macrophages on the surface function as sessile phagocytes, as do the Kupffer cells, or whether they have been caught in the act of migration.

The first question discussed in the introduction was the method of passage of fluids and substances over the mesothelium. These observations show that openings can exist between the mesothelial cells covering the omentum, a tissue which Higgins and Bain (*16*) demonstrated as a pathway for the passage of substances from the peritoneal cavity to the lymphatics of the diaphragm. Possibly there is a similar modification of the mesothelium directly over the endothelial lining of the lymphatic lacunae of the diaphragm.[3]

The second question considered in the introduction dealt with the views of some investigators that the large phagocytic cells of the peritoneal fluid are transformed mesothelial cells. In an area so rich in mobilized macrophages and their precursors and with a surface modification which makes them readily available, it hardly seems necessary to look further for macrophages to cope with the usual pathological conditions. Admittedly, omental mesothelial cells seem to shed more readily than those from other regions (*58*), and some particles (*11*) and pigment granules can appear in limited amounts in their cytoplasm (*58–60*). In addition, this study has shown small vacuoles in mesothelial cells which contain material similar to that in vacuoles in neighboring macrophages (figs. 16, 18, and 22). Nevertheless, the basic morphological differences between the two cells are marked. It remains to be determined with the electron microscope how mesothelial cells react to various kinds of stimulation in comparison with macrophages.

REFERENCES

(*1*) Ranvier, L.: Recherches sur la formation des mailles du grand epiploon. Arch. de Physiol., 2d series, 1: 421–428, 1874.

(*2*) ———: Du developpement et de l'accroissement des vaisseaux sanguins. Arch. de Physiol., 2d series, 1: 429–450, 1874.

(*3*) Buxton, F., and Torrey, J. C.: Absorption from the peritoneal cavity. IV and V. The function of the omentum. J. Med. Res. 15: 55–87, 1906.

(*4*) Maximow, A. A.: Bindegewebe und blutbildende Gewebe. *In* von Möllendorff's Handbuch der mikroskopischen Anatomie des Menschen. Berlin, J. Springer, Bd. II. 1. Teil, 1927, pp. 289–308.

[3] Since the completion of this manuscript the attention of the author was drawn to a paper concerned with the diaphragm:

French, J. E., Florey, M. W., and Morris, B.: The absorption of particles by the lymphatics of the diaphragm. Quart. J. Exper. Physiol. 45: 88–103, 1960.

This study describes a modification of the mesothelial cells overlying the lacunae. The lining cells are closer together and less flattened than elsewhere on the diaphragm and, when outlined with silver, the intercellular lines are wider. Use of the electon microscope demonstrates actual and potential openings between the mesothelial cells which permit the intercellular passage of erythrocytes and colloidal particles. Some particulate material is found within the cytoplasm of the mesothelial cells, contained in small vacuoles and vesicles. Nevertheless, in the authors' opinion the majority of particles make their way into the lymphatic lacunae by means of an intercellular route.

(5) VON RECKLINGHAUSEN, F. T.: Zur Fettresorption. Virchow's Arch. path. Anat. 26: 172–208, 1863.
(6) ———: The lymphatic system. *In* Stricker's Manual of Human and Comparative Histology. London, New Sydenham Soc., vol. I, chapt. 9, 1870.
(7) HERTZLER, A. E.: The morphogenesis of the stigmata and stomata occurring in peritoneal and vascular endothelium. Trans. Am. Micr. Soc. 22: 63–92, 1901.
(8) CUNNINGHAM, R. S.: The physiology of the serous membranes. Physiol. Rev. 6: 242–277, 1926.
(9) ALLEN, L.: The peritoneal stomata. Anat. Rec. 67: 89–99, 1936.
(10) SIMER, P. H.: The passage of particulate matter from the peritoneal cavity into the lymph vessels of the diaphragm. Anat. Rec. 101: 333–351, 1948.
(11) ODOR, D. L.: Uptake and transfer of particulate matter from the peritoneal cavity of the rat. J. Biophys. & Biochem. Cytol. 2, No. 4, Supp.: 105–108, 1956.
(12) COURTICE, F. C., and SIMMONDS, W. J.: Physiological significance of lymph drainage of the serous cavities and lungs. Physiol. Rev. 34: 419–448, 1954.
(13) WILKIE, D. P. D.: Some functions and surgical uses of the omentum. Brit. M. J. 2: 1103–1106, 1911.
(14) FELIX, M. D., and DALTON, A. J.: A phase-contrast microscope study of free cells native to the peritoneal fluid of DBA/2 mice. J. Nat. Cancer Inst. 16: 415–446, 1955.
(15) SHIPLEY, P. G., and CUNNINGHAM, R. S.: Studies on absorption from serous cavities. I. The omentum as a factor in absorption from the peritoneal cavity. Am. J. Physiol. 40: 75–81, 1916.
(16) HIGGINS, G. M., and BAIN, C. G.: The absorption and transference of particulate matter by the great omentum. Surg., Gynec. & Obst. 50: 851–860, 1930.
(17) DURHAM, H. E.: The mechanism of reaction to peritoneal infection. J. Path. & Bact. 4: 338–382, 1897.
(18) SCHOTT, E.: Morphologische und experimentelle Untersuchungen über Bedeutung und Herkunft der Zellen der serösen Höhlen und der sogenannten Makrophagen. Arch. f. mikro. Anat. 74: 143–216, 1909.
(19) WEIDENREICH, F.: Blutkörperchen und Wanderzellen. Jena, G. Fischer, 1911.
(20) TSCHASCHIN, W.: Ueber die "ruhenden Wanderzellen" und ihre Beziehungen zu den anderen Zellformen des Bindegewebes und zu den Lymphozyten. Folia Haemat. 17: 317–397, 1913.
(21) CUNNINGHAM, R. S.: On the origin of the free cells of the serous exudates. Am. J. Physiol. 59: 1–36, 1922.
(22) KIYONO, K.: Die vitale Karminspeicherung. Jena, G. Fischer, 1914.
(23) EVANS, H. M., and SCOTT, K. J.: On the differential reaction to vital dyes exhibited by the two great groups of connective tissue cells. Carnegie Contrib. Embryol. 10, No. 47: 1–56, 1921.
(24) SABIN, F. R., DOAN, C. A., and CUNNINGHAM, R. S.: Discrimination of two types of phagocytic cells in the connective tissues by supravital techniques. Carnegie Contrib. Embryol. 16, No. 82: 125–162, 1925.
(25) ODOR, D. L.: Observations of the rat mesothelium with the electron and phase microscopes. Am. J. Anat. 95: 433–467, 1954.
(26) PALADE, G. E., and PORTER, K. R.: Studies on the endoplasmic reticulum. I. Its identification in cells *in situ*. J. Exper. Med. 100: 641–656, 1954.
(27) FELIX, M. D., and DALTON, A. J.: A comparison of mesothelial cells and macrophages in mice after the intraperitoneal inoculation of melanin granules. J. Biophys. & Biochem. Cytol. 2, No. 4, Supp.: 109–114, 1956.
(28) DALTON, A. J.: A chrome-osmium fixative for electron microscopy. Anat. Rec. 121: 281, 1955.
(29) SHIPKEY, F. H., and DALTON, A. J.: Asodi-iso-butyronitrile (ADIB) as a catalyst for embedding tissue in methacrylate for electron microscopy. J. Appl. Physics 30: 2039, 1959.

(30) WARD, R. T.: Prevention of polymerization damage in methacrylate embedding media. J. Histochem. & Cytochem. 6: 398, 1958.

(31) MAXIMOW, A. A.: Ueber das Mesothel (Deckzellen der serösen Häute) und die Zellen der serösen Exsudate. Arch. exper. Zellforsch. 4: 1–42, 1927.

(32) FAWCETT, D. W., and PORTER, K. R.: A study of the fine structure of ciliated epithelia. J. Morphol. 94: 221–282, 1954.

(33) MUNGER, B. L.: A light and electron microscope study of cellular differentiation in the pancreatic islets of the mouse. Am. J. Anat. 103: 275–312, 1958.

(34) LATTA, J. S., and RUTLEDGE, D. I.: The reaction of omental tissue to trypan blue injected intraperitoneally, with special reference to interrelationships between cell types. Am. J. Anat. 56: 481–511, 1935.

(35) PALADE, G. E.: The endoplasmic reticulum. J. Biophys. & Biochem. Cytol. 2, No. 4, Supp.: 85–98, 1956.

(36) KARRER, H. E.: The ultrastructure of mouse lung: the alveolar macrophage. J. Biophys. & Biochem. Cytol. 4: 693–700, 1958.

(37) CHRISTENSEN, A. K.: Personal communication.

(38) PARKS, H. F., and CHIQUOINE, A. D.: Observations on early stages of phagocytosis of colloidal particles by hepatic phagocytes of the mouse. *In* Proc. Stockholm Conf. on Electron Microscopy, 1956. New York, Academic Press, Inc., 1957, pp. 154–156.

(39) HAMPTON, J.: An electron microscope study of the hepatic uptake and excretion of submicroscopic particles injected into the blood stream and into the bile duct. Acta Anat. 32: 262–291, 1958.

(40) POLICARD, A., COLLET, A., and PREGERMAIN, S.: Recherches au microscope électronique sur les cellules pariétales alvéolaires deupoumon des mammifères. Ztschr. Zellforsch. 50: 561–587, 1959.

(41) BARGMANN, W., and KNOOP, A.: Elektronmikroskopische Untersuchungen an Plazentarzotten des Menschen. Ztschr. Zellforsch. 50: 472–493, 1959.

(42) FINCH, C. A.: The role of iron in hemoglobin synthesis. Proc. of Conference on Hemoglobin. Nat. Acad. Sc.-Nat. Res. Council Publ. 557: 95–99, 1958.

(43) MAXIMOW, A. A.: Relation of blood cells to connective tissues and endothelium. Physiol. Rev. 4: 533–563, 1924.

(44) KAMPMEIER, O. F.: Concerning certain mesothelial thickenings and vascular plexuses of the mediastinal pleura, associated with histiocyte and fat-cell production in the human newborn. Anat. Rec. 39: 201–213, 1928.

(45) MIXTER, R. L.: On macrophagal foci ("milky spots") in the pleura of different mammals, including man. Am. J. Anat. 69: 159–186, 1941.

(46) PALADE, G. E.: Fine structure of blood capillaries. J. Appl. Physics 24: 1424, 1953.

(47) BENNETT, H. S., LUFT, J. H., and HAMPTON, J. C.: Morphological classification of vertebrate blood capillaries. Am. J. Physiol. 196: 381–390, 1959

(48) PEASE, D. C.: An electron microscope study of red bone marrow. Blood 11: 501–526, 1956.

(49) WEISS, L.: The organization of the connective tissues in the bone marrow. II. Reticular cells. Anat. Rec. 136: 300, 1960.

(50) ———: A study of the structure of splenic sinuses in man and in the albino rat with the light microscope and the electron microscope. J. Biophys. & Biochem. Cytol. 3: 599–610. 1957.

(51) FAWCETT, D. W.: Observations on the cytology and electron microscopy of hepatic cells. J. Nat. Cancer Inst. 15: 1475–1503, 1955.

(52) PARKS, H. F.: The hepatic sinusoidal endothelium and its histological relationships. *In* Proc. Stockholm Conf. on Electron Microscopy, 1956. New York, Academic Press, Inc., 1957, pp. 151–153.

(53) MORISON, R.: Remarks on some functions of the omentum. Brit. M. J. 1: 76–78, 1906.

(*54*) Rubin, I. C.: The function of the great omentum. Surg., Gynec. & Obst. 12: 117–131, 1911.

(*55*) Florey, H., and Carleton, H. M.: The nature of movements of the omentum. J. Path. & Bact. 29: 97–106, 1927.

(*56*) Hertzler, A. E.: The peritoneum. St. Louis, C. V. Mosby Co., vol. I., 1919.

(*57*) Webb, R. L.: Peritoneal reactions in the white rat, with especial reference to mast cells. Am. J. Anat. 49: 283–334, 1931.

(*58*) Cunningham, R. S.: The reaction of the cells lining the peritoneal cavity, including the germinal epithelium of the ovary, to vital dyes. Am. J. Anat. 30: 399–427, 1922.

(*59*) Cappell, D. F.: Intravital and supravital staining. IV. The cellular reactions following mild irritation of the peritoneum in normal and vitally stained animals with special reference to the origin and nature of the mononuclear cells. J. Path. & Bact. 33: 429–452, 1930.

(*60*) Baillif, R. N.: Reaction of rat peritoneum to acid colloidal pigments. Proc. Soc. Exper. Biol. & Med. 62: 264–269, 1946.

EXPLANATION OF PLATES

Abbreviations

BC, basal corpuscle.
D, mesothelial cell.
ER, ergastoplasm.
F, collagen fibers.
G, Golgi apparatus.
IB, inclusion.
L, lipide droplet.
M, mitochondrion.
MI, microvillus.
O, mesh.
PC, peritoneal cavity.
PH, macrophage.
S, discontinuity between surface cells.
V, vacuole.
VE, vesicle.
X, dense area in nucleus.

All figures except those in Plate 89 are electron micrographs. The line on each represents 1 μ. Original magnifications were between 5,000 and 5,600.

Omenta from two strains of mice, C3H/An and Swiss, were fixed in chrome-osmic, *p*H 7.2, and postfixed in 10 percent neutral formalin. Those parts which were embedded in methacrylate were pre-embedded in 2 percent agar.

Figures 5 through 8, 11, 16, and 19 through 21 show sections from the omentum of a C3H/An mouse. The final embedding was in methacrylate to which benzoyl peroxide was added as catalyst. Polymerization was completed at 65° C.

Figures 9, 10, 12 through 15, 17, 18, and 22 show sections from the omentum of a Swiss mouse. The final embedding was in methacrylate to which were added azodi-iso-butyronitrile (ADIB) as catalyst and uranyl nitrate. Polymerization was completed at 47° C.

PLATE 89

Phase-contrast photomicrographs of spreads of fixed omenta (figs. 1 and 4) and 1 μ cross sections of methacrylate-embedded omenta (figs. 1*a*, 1*b*, 2, 3, and 4*a*–4*c*) from a C3H/An and a Swiss mouse. They were mounted in glycerin on glass slides under coverslips. All magnifications were 650.

FIGURE 1.—Spread of a region from the netlike portion of the omentum of a C3H/An mouse. This illustrates texture of fabric formed by interwoven bundles of collagen. Variation in size and uneven distribution of the meshes (O) are shown. In some places only a narrow isthmus separates them (*arrows*).

FIGURE 1*a*.—Cross section of the network of omentum of a C3H/An mouse. Interruption of the fabric by the meshes (*arrows*) forms a characteristic series of segments. The extreme thinness that can be attained by the tissue of the network is illustrated. The long segment *below*, containing a mesothelial-cell nucleus on *right*, is an area which corresponds to that shown in the electron micrographs in figures 5 and 6.

FIGURE 1*b*.—Cross section of the network of omentum of a Swiss mouse. Tissue is thicker than that from the C3H/An mouse. Mesothelial cells tend to be less tenuous, and the nuclei are plumper. *Arrows* indicate the meshes.

FIGURE 2.—Cross section passing through a milky spot in the omentum of a C3H/An mouse. Surface cells are contracted compared with those on the netlike areas. Their longest diameter tends to be parallel to the tissue, giving it an undulated appearance. Vacuoles of a μ or more in diameter can be seen in the cytoplasm of some of the surface cells (*arrow*). At S there is a suggestion of a discontinuity between cells.

FIGURE 3.—Cross section through a milky spot in omentum of a Swiss mouse. Here the surface cells are also contracted, but their longest diameter tends to extend outward toward the peritoneal cavity, which gives the surface a jagged appearance. Several cells seem to be discontinuous, as at S.

FIGURE 4.—Spread of a region at the edge of a milky spot in omentum of a Swiss mouse. To *right* and in *center* are meshes of the network (O). To *left* is the edge of a milky spot, some cells of which project into the opening of the large, central mesh, much as others project from the surface toward the peritoneal cavity. The projecting cell at *arrow* appears attached to the tissue.

FIGURES 4*a*–4*c*.—Serial cross sections of a milky spot from omentum of a Swiss mouse. Cell indicated by *arrows* is similar to the one shown in figure 4. This illustrates that most cells on the surface of the milky spots of this mouse are anchored to the tissue. Due to thinness of sections, portions of the cells appear free of the tissue, which gives the impression of outside cells adherent to or caught against the omentum. An extended mesothelial cell sectioned through its nucleus appears on *left* in all three sections.

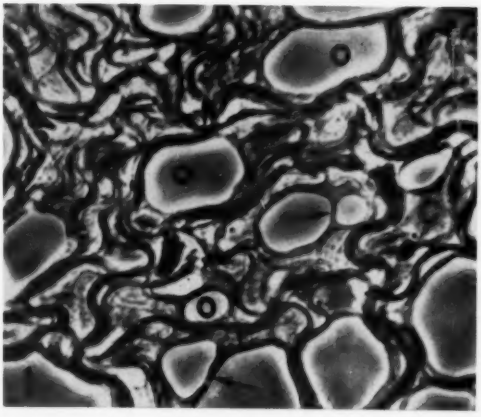

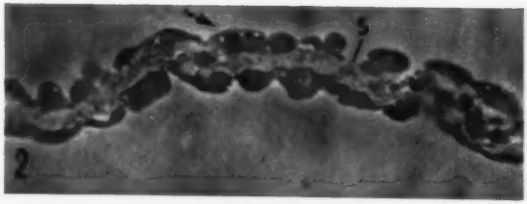

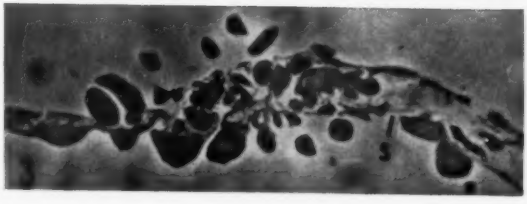

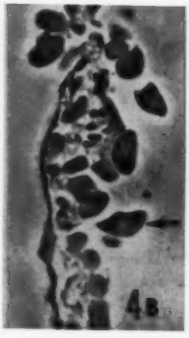

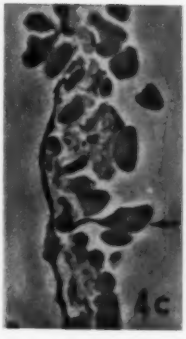

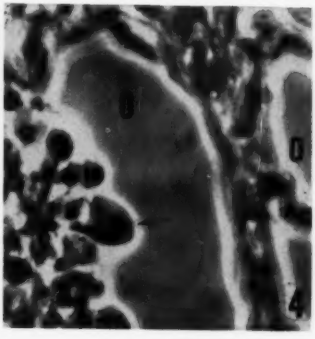

FELIX

731

603724—61——3

PLATE 90

FIGURE 5.—Electron micrograph of cross section of tissue from network of omentum of a C3H/An mouse. This would correspond to area referred to in figure 1*a*. Entire width of omentum is shown with peritoneal cavity (PC) on both sides. Between cytoplasm of mesothelial cells lie the collagen fibers (F). The fibrils are not clear cut in sections of the omentum from this mouse, due to poor fixation, polymerization damage, or to both. No microvilli appear on the free surface, and no basement membrane is apparent. This micrograph shows examples of the junctions of adjacent cells. On *left*, 2 cells meet by adjoining each other (*arrow*); on *right*, 4 cells meet by overlapping (1, 2, 3, 4). The thin edge of the inner cell (4) dips below some of the collagen fibers. Several small vesicles appear in cytoplasm (VE). An invagination of plasma membrane occurs next to the junction of the cells on *left*. × 26,500

FIGURE 6.—Electron micrograph of entire width of netlike area of omentum of a C3H/An mouse in a section of a cell containing a nucleus. The peritoneal cavity is at PC and the sparse collagen fibers at F. The extreme thinness which the tissue can assume is here apparent. At A, the narrowest part, it is less than 1 μ; at B, the widest part, it is less than 2 μ in spite of presence of the nucleus (N). This also illustrates the tenuousness which can be attained by the covering mesothelial-cell cytoplasm, which, at *arrow*, is only about 20 mμ. There is no basement membrane, although there are a few small areas where some material appears condensed against the basal plasma membrane. Free surfaces show no microvilli. The nucleus is flat and indented in places. This section shows no nucleolus, but there are two small circumscribed dense areas (X) which are surrounded by light areas. Near end of nucleus and near basal side of cell there is a vacuole (V) which has an electron-lucent interior and contains no granules. It seems to have no limiting membrane, but this might be the result of the obvious polymerization damage. × 26,500

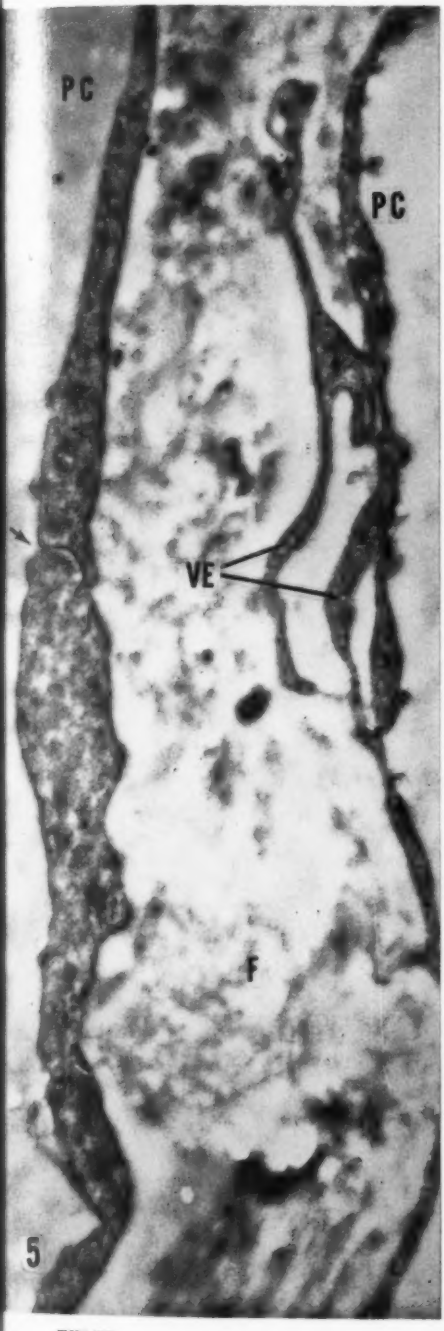
PC
PC
VE
F
5

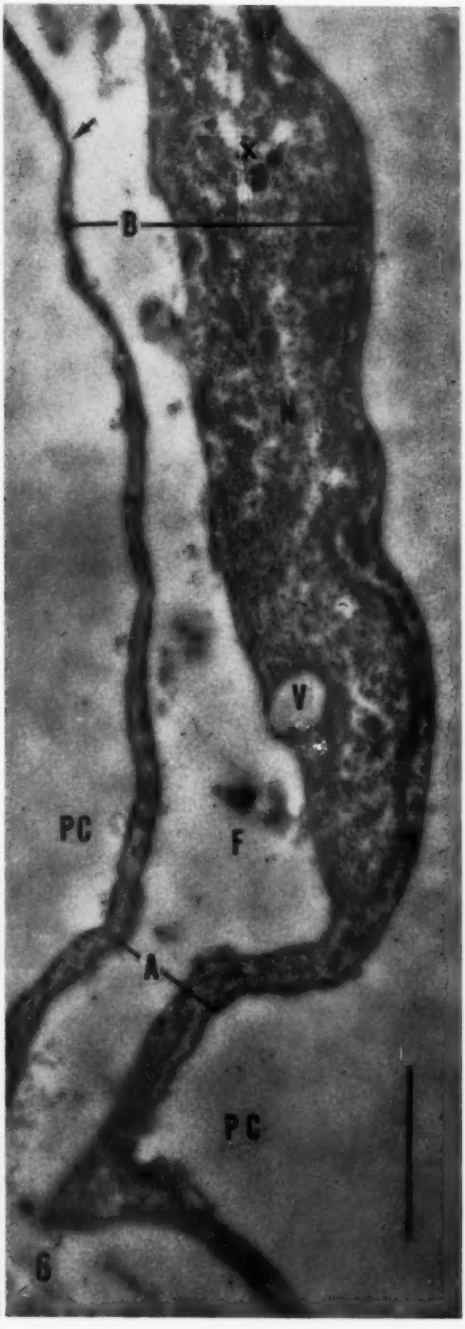
X
B
N
V
PC
F
A
PC
6

PLATE 91

FIGURE 7.—Electron micrograph of cross section of netlike region of omentum of a C3H/An mouse. Round segment at *lower center* of figure is a narrow isthmus between two meshes (O), as indicated in figure 1. Here again the tenuousness of the cytoplasm is evident. The isthmus is a bundle of collagen completely surrounded by mesothelial-cell cytoplasm. Only apparent place where there may be a junction of neighboring cells is at *arrow*. × 26,500

FIGURE 8.—Photomicrograph from a similar area to figure 7, showing a mesothelial-cell nucleus (N) beginning at edge of a mesh (O) and extending along one peritoneal surface (PC) of the omentum of a C3H/An mouse. Cytoplasm of the mesothelial cell continues around the edge of the mesh to the other surface of omentum and overlaps a cell on the other side (*arrow*). × 26,500

FIGURES 9 and 10.—Greater enlargements of micrographs showing the apposition of mesothelial cells on surface of network of omentum of a Swiss mouse. Figure 9 is the region outlined by the box in figure 12. It illustrates a contiguous junction. Figure 10 shows 2 cells (A and B) each adjoining a process of a third (C), with a process of a fourth (D) overlapping A and C. × 56,500

FIGURE 11.—An electron micrograph of cross section that passes through nuclear area of a mesothelial cell on surface of omentum of a C3H/An mouse. Part of a flagellum is shown in an approximately longitudinal section. Near the distal surface nucleus (N) exhibits a shallow depression. From one side of depression the basal corpuscle (BC) of flagellum extends to plasma membrane. Its center is less electron-dense than its periphery. Oval body (*arrow*) at *lower part* of the basal corpuscle might be either a centriole or a portion of the basal corpuscle, which appears partially separate because of the plane of the section. × 26,500

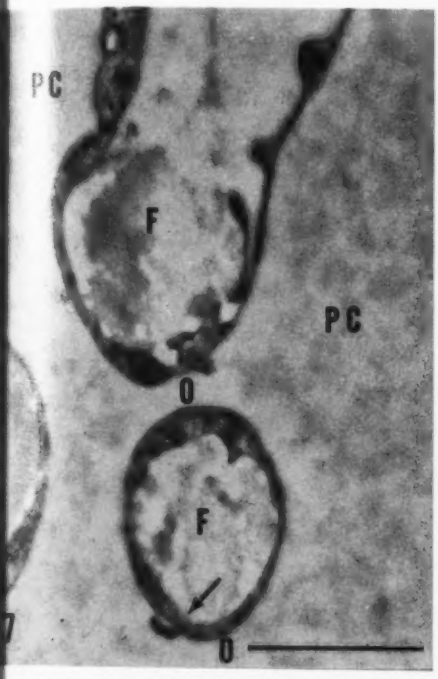

7

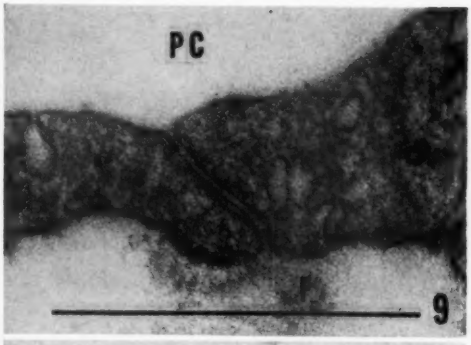

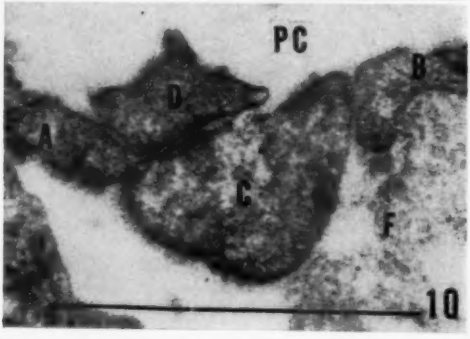

8

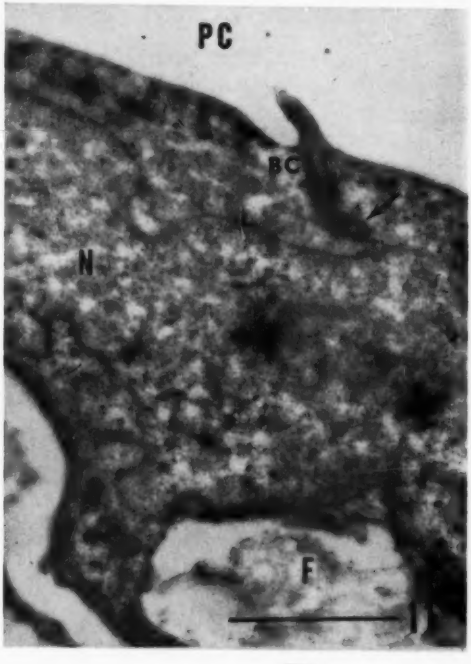

PLATE 92

FIGURE 12.—Electron micrograph of part of a mesothelial cell at the edge of a mesh (O) from netlike region of omentum of a Swiss mouse. The part of the cell not included in the micrograph extends along the peritoneal surface on *right*. Main body of the cell, which contains the nucleus (N), passes through the tissue and composes part of the surface of the opposite side. Collagen bundles (F) appear both *above* and *below*. A cell process on *right* continues around opening of the mesh and covers the bundle of collagen located there. It then abuts upon a short process of the same cell on the other side (*outlined area*). An enlargement of this junction is seen in figure 9. Vesicles (VE), appearing as invaginations of the plasma membrane and within the cytoplasm, are in evidence at both the distal and proximal membranes. Two vacuoles are at V. × 26,500

FIGURE 13.—Micrograph of a section through a narrow isthmus that separates the meshes of the omentum of a Swiss mouse. Both a bundle of collagen (F) and a cell within the tissue are surrounded by cytoplasm which seems to be from one mesothelial cell. Edges of the cytoplasm meet near *arrow;* due to knife damage it is difficult to discern the exact spot. Many small vesicles and a microvillus (MI) are in evidence. × 26,500

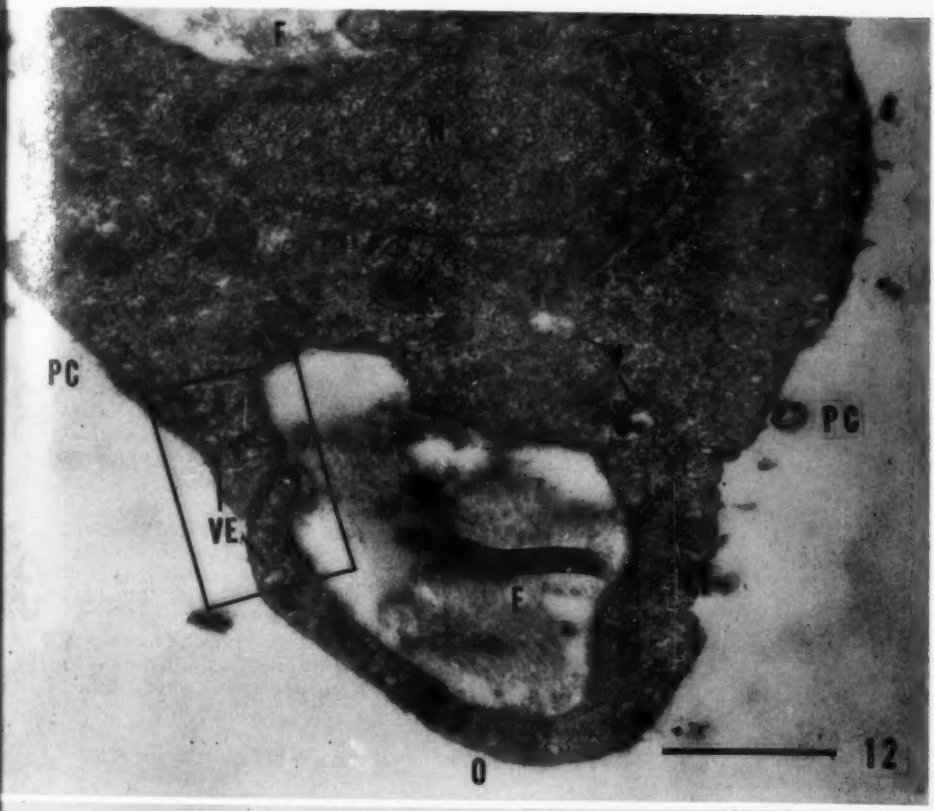
F
N
PC
PC
VE
F
O
12

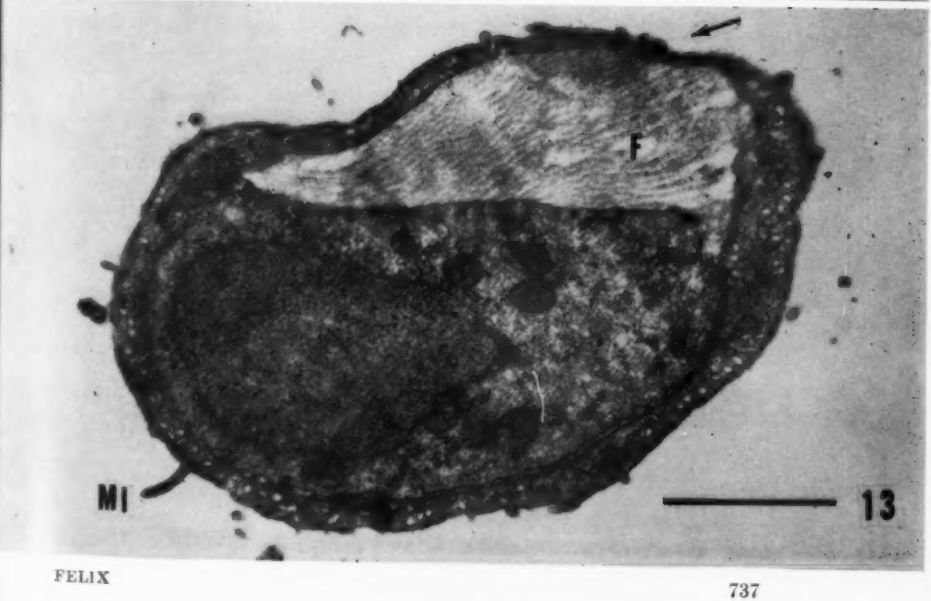
F
MI
13

PLATE 93

Electron micrograph of cross section of tissue from network of omentum of a Swiss mouse. Entire width of omentum is shown with peritoneal cavity (PC) on both sides. Since it was too wide for the plate, a central strip was eliminated, forming two figures which split the cell within the tissue.

FIGURE 14.—Expanse of the thin cytoplasm of a mesothelial cell that covers the surface of the network. Bundles of collagen fibers within the tissue are at F. Also within the tissue, above the collagen fibers, are parts of 2 cells. The better preservation obtained with the material from Swiss mouse is obvious. On free surface a few microvilli (MI) are shown. There is no basement membrane. Cytoplasmic processes can be seen extending into the fabric in two places (*arrows*), *upper one* appearing to be curved around some fibrils. This points to a mechanism for anchoring the surface cells. Prominent in the cytoplasm are small vesicles (VE), many of which are near the plasma membrane. Those near free surface are more numerous. Cross sections of several mitochondria (M) and scattered profiles of ergastoplasm (ER) are present. × 26,500

FIGURE 15.—Portions of 2 mesothelial cells on surface of network opposite that shown in figure 14. Collagen bundle appears at F, above which lies part of a cell. The cell showing part of its nucleus is typical, both in cytoplasmic and nuclear detail, of mesothelial cells on the net and on the cellular areas. The nucleus (N) is a flat oval with an infolding (small Y). It contains material of medium electron density, which shows even, though loose, distribution. At X there is a small region of more compact material surrounded by a paler area. No nucleolus is present in this section. In the cytoplasm are a few profiles of ergastoplasm (ER) in approximately parallel array. Two portions of the Golgi apparatus (G) lie near the free surface, one above a shallow nuclear indentation. Several membrane-bounded vacuoles (V) containing particulate material are apparent in both cells. Lipide droplets, which are characteristic cytoplasmic inclusions of the mesothelial cells of the Swiss mouse, are at L. There are scattered mitochondria, one cut tangentially or longitudinally (M), and small vesicles (VE) that lie chiefly near the free surface. Two microvilli (MI), one at the junction of the 2 cells (*arrow*) and one above it, are sectioned in a manner which shows their continuity with the cytoplasm. Other microvilli are shown in cross or tangential section. No basement membrane is present. × 26,500

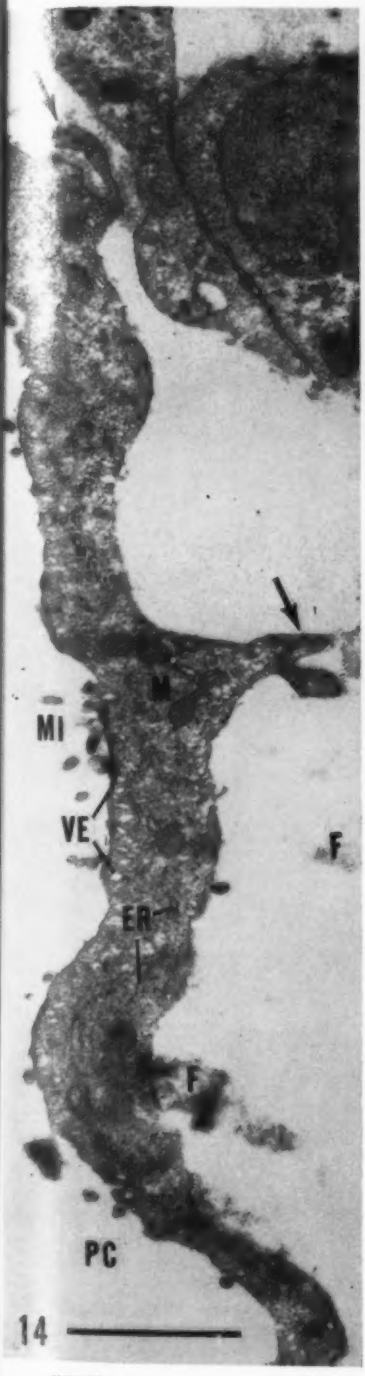

14

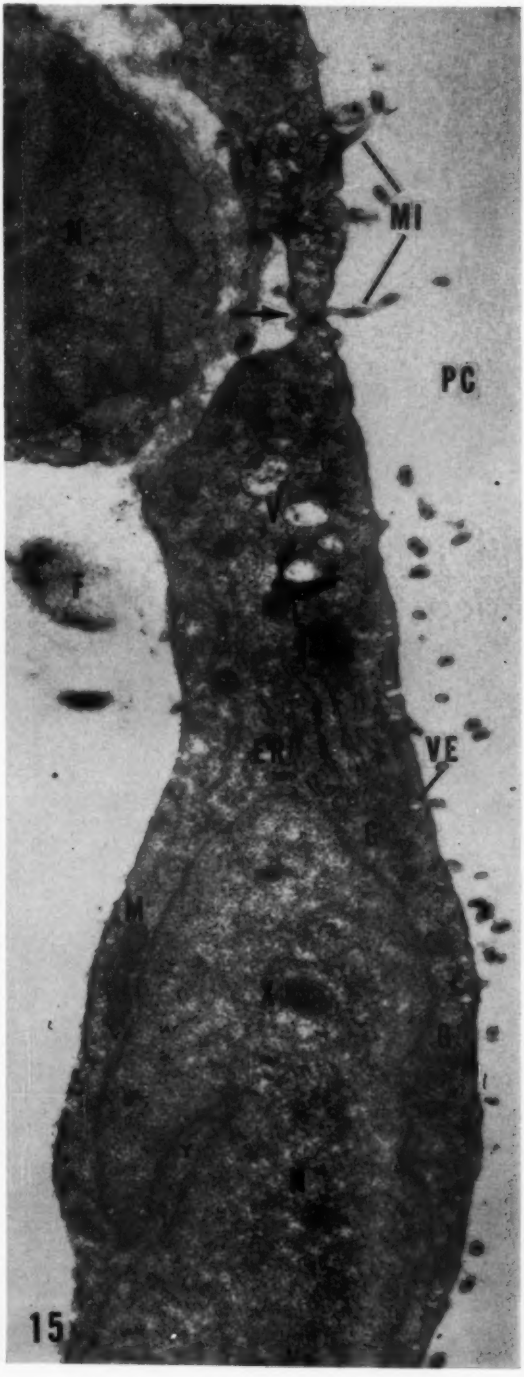

15

PLATE 94

FIGURE 16.—Electron micrograph of cross section passing through a milky spot in omentum of a C3H/An mouse. The entire width of the tissue is shown with peritoneal cavity (PC) on both sides. The tissue here is a dense array of fibers (F), which are indistinct in this material. An occasional process of a cell lies among them. The mesothelial cells are contracted as is obvious in comparison with those in figures 5 and 6. To *left* there is an interruption (S) of more than 1 μ between 2 mesothelial cells (D), exposing the underlying fibers to the surface. Nucleus of *upper* mesothelial cell is at N. To *right* is a highly vacuolated macrophage (PH) forming part of the surface continuity. Part of the body of cell lies directly on fibers of the tissue and part lies on tapering processes of adjacent mesothelial cells (D). One vacuole (V) in the macrophage is large enough to be visible in the phase-contrast microscope. $\times$ 26,500

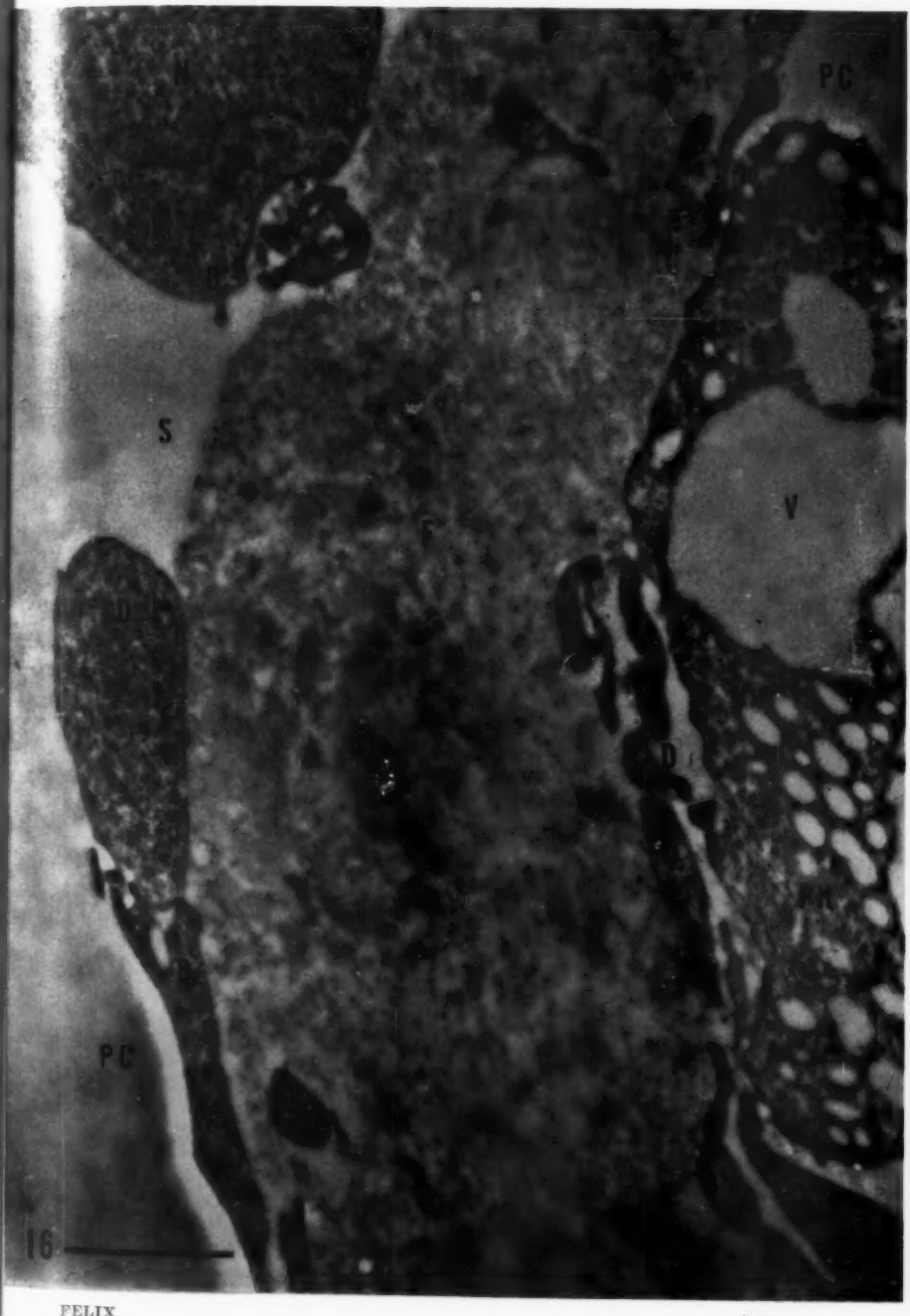
PC
S
V
PC
16

PLATE 95

Electron micrographs of portions of two cross sections through a milky spot in the omentum of a Swiss mouse.

FIGURE 17.—Discontinuities between surface cells. They occur between a macrophage (PH) and a process of a mesothelial cell (S_1) and between the same cell process and another mesothelial cell (S_2). The peritoneal cavity is at PC and collagen bundles at F. The cell process (*arrow*) is part of a cell lying within the tissue.

Note free surface of the mesothelial cell (D) for comparison with that of the macrophage in figure 18. Except for the microvilli (MI), which extend outward from surface with a more or less constant diameter from base to tip, the surface is smooth. Tiny, oval vesicles (VE), which occasionally appear as invaginations of the plasma membrane (*small arrow*), are usually near one of the surfaces and oriented with their longest diameter perpendicular to the membrane. Their size falls into a range of 20 to 60 mμ. × 23,000

FIGURE 18.—A macrophage sharing the surface of the omentum with a mesothelial cell (D). The difference in the free surface of the macrophage becomes apparent by comparing it with the mesothelial cell in figure 17. This macrophage shows the unevenness of surface and the blunt processes which are associated with its surface activity. In places a process seems to be folding over or meeting another to form a vacuole which sometimes contains a particle (*arrows*). At other places valleys between two processes are shown (small V). Vacuoles near surface of this macrophage are not oriented and range in size from approximately 30 to 150 mμ. Vacuole in cytoplasm at V contains material similar to that which appears in vacuoles of mesothelial cells in figure 15.

Nucleus (N) of the macrophage contains material of medium electron lucency which is evenly distributed but more compact than in mesothelial-cell nuclei. The cytoplasm is looser than that of mesothelial cells. In addition to mitochondria (M) membrane-bounded inclusions appear at IB. In this instance they contain a homogeneous substance of medium electron density. × 26,500

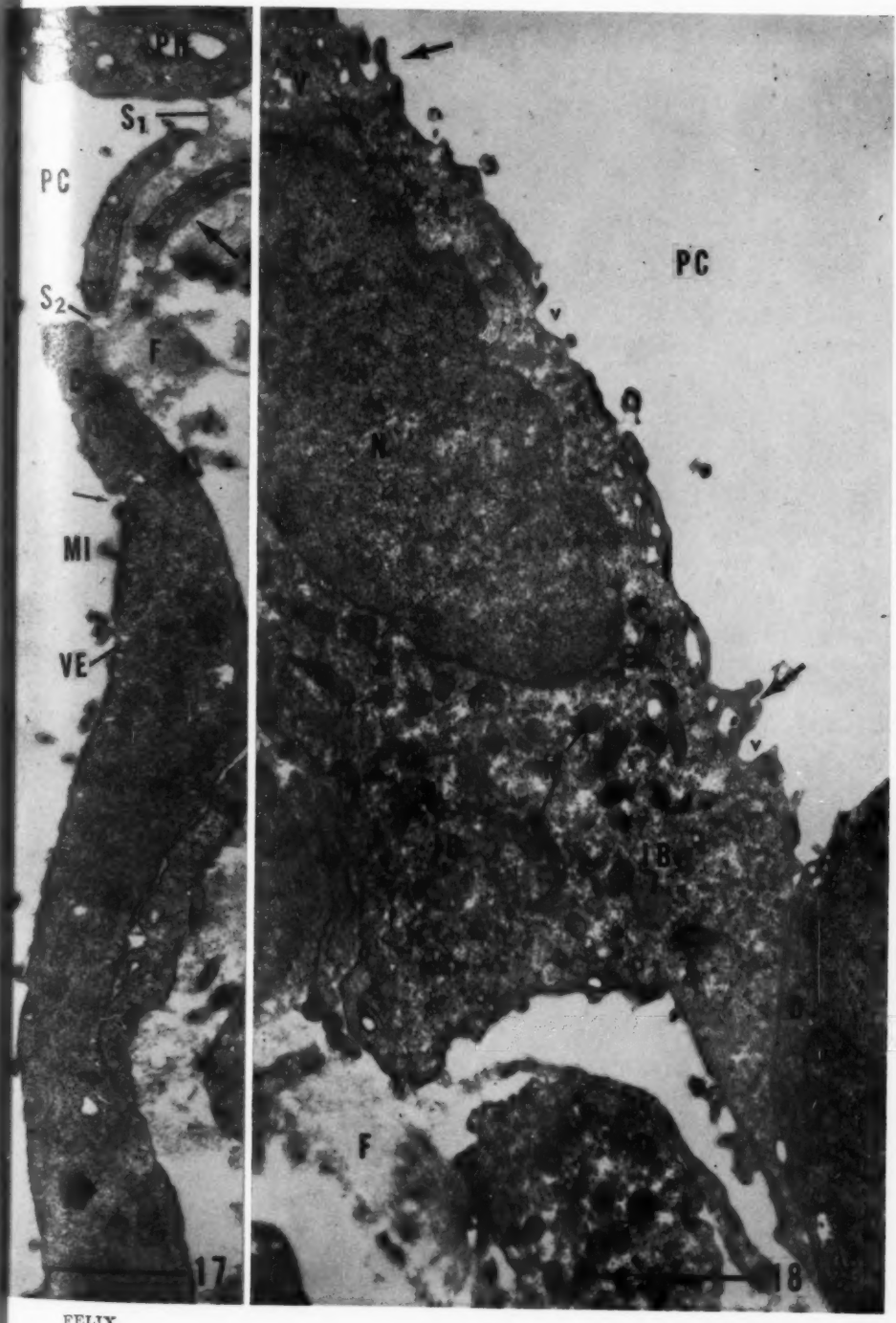
PC
S1
PC
S2
F
MI
VE
17
V
PC
N
IB
F
18

PLATE 96

Electron micrographs comparing portions of macrophages from the surfaces of the milky spots to macrophages free in the peritoneal fluid.

FIGURE 19.—A macrophage from surface of omentum of a C3H/An mouse. This detail is intended primarily to show the ferritin contained in macrophages found in this mouse strain. Two inclusions (IB) are indicated. In their homogeneous, gray matrices are a number of tiny black particles that are the iron component of the ferritin molecules. Ferritin molecules are also scattered diffusely through the cytoplasm. They do not appear within mitochondria (M). Vacuoles (V) are near the surface. Nucleus is at N. The use of benzoyl peroxide as catalyst caused clumping of the cytoplasm; this is more marked than in macrophage in figure 22 where ADIB and uranyl nitrate were used. × 45,000

FIGURE 20.—Portion of macrophage free in the peritoneal fluid of a normal DBA/2 mouse, which has characteristics in common with macrophages on surface of milky spots of omentum. Surface of the cell is undulant and shows several blunt processes. In one place a vacuole (*arrow*) seems in the process of being formed. Other vacuoles appear beneath the surface. The inclusions at IB are similar to those in the macrophage in figure 18. They are membrane-bounded and contain a homogeneous substance of medium electron density. The nucleus appears at N, several profiles of ergastoplasm at ER, and mitochondria at M. × 26,500

FIGURE 21.—Part of surface of macrophage free in peritoneal fluid of a DBA/2 mouse. Six days previously melanin granules had been inoculated into the peritoneal cavity. Surface is undulant and shows a short, blunt process. Beneath surface there are a number of vacuoles (V) which vary in size. In some, discrete particles of ingested melanin can be seen. Larger vacuole (ME) is completely filled with melanin particles. At VE there are two rows of vesicular profiles that might be associated with the fusion of the membranes of cytoplasmic processes. × 26,500

FIGURE 22.—Free surface of macrophage from a milky spot in omentum of a Swiss mouse. A number of blunt processes are apparent as well as several small vacuoles of irregular shape below the surface. Two larger vacuoles (V) within the cytoplasm are partially filled, one with particulate material and one with amorphous material. Three inclusions (IB) are indicated, the contents of which are not homogeneous. They contain membranes, vesicular-like structures, and electron-lucent areas. Mitochondria (M) and ergastoplasm (ER) are present. × 26,500

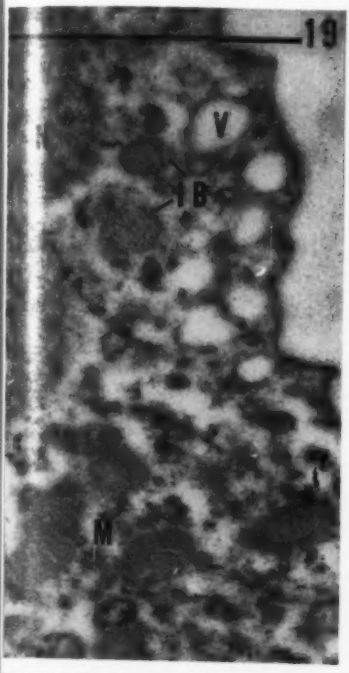
19
V
IB
M

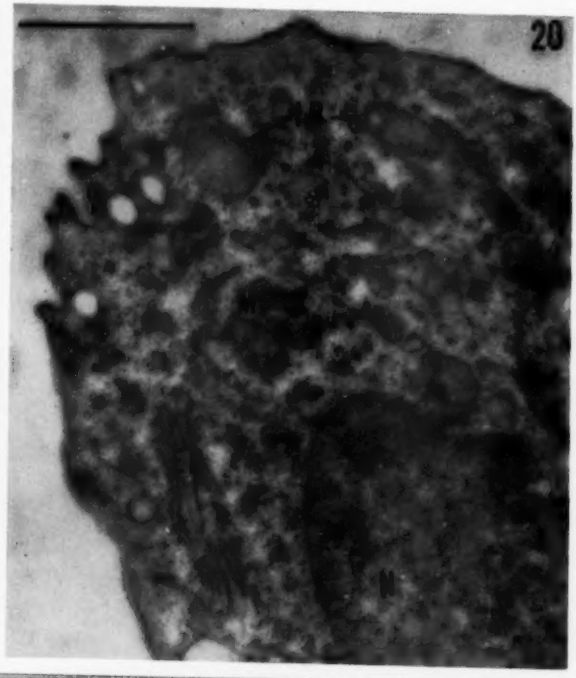
20
N

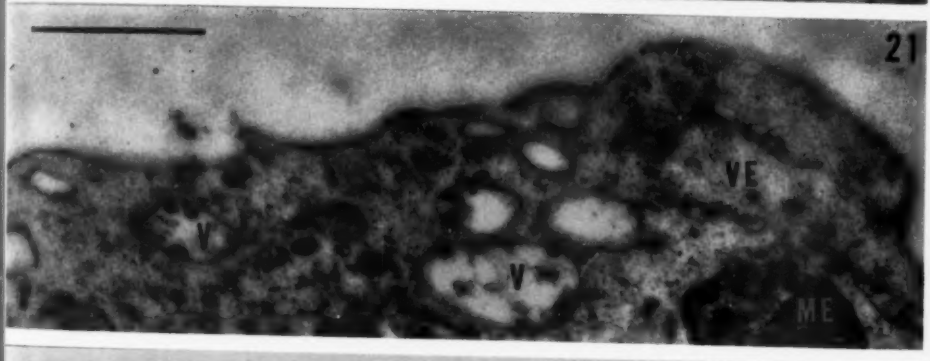
21
VE
V
V
ME

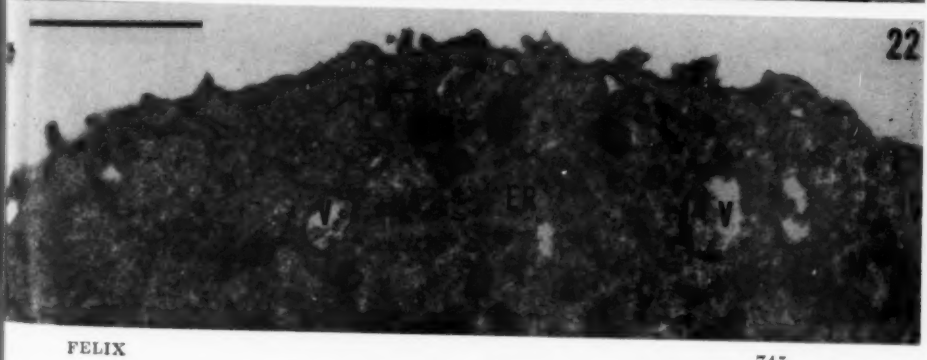
22
ER
V

An Electron Microscopic Study of a Series of Murine Lymphoid Neoplasms [1]

ALBERT J. DALTON, LLOYD W. LAW,[2] JOHN B. MOLONEY, *and* ROBERT A. MANAKER, *Laboratory of Viral Oncology and Laboratory of Biology, National Cancer Institute,[3] Bethesda, Maryland*

SUMMARY

Particles associated with a group of primary lymphoid neoplasms of the mouse were examined with the same electron microscope in tissues fixed, dehydrated, embedded, and stained in the same manner. The neoplasms studied were those induced with the Moloney, Gross, Manaker C-60 (Schwartz), and Friend agents, the strain C57BL/Ka radiation-induced lymphoid leukemia, and the spontaneous lymphoid leukemias of strain AKR and C3Hf/FgLw mice. No particles were associated with the radiation-induced leukemia of C57BL/Ka mice, but in all the other neoplasms, particles of characteristic size and fine structure were identified. Megakaryocytes of the spleen and bone marrow were the most satisfactory sources of particles, both from the point of view of frequency of occurrence and state of preservation. Particles were formed within megakaryocytes and retained in channels in the cytoplasm, apparently for relatively long intervals. Immature particles (with electron-lucent nucleoids) associated with 6 of the 7 leukemias studied had an average diameter of 100 mμ. Mature particles (with electron-dense nucleoids) associated with the Moloney and Manaker C-60 (Schwartz) leukemias also averaged 100 mμ in diameter, while mature particles associated with the Gross and Friend neoplasms and the spontaneous leukemias of strain AKR and C3Hf/FgLw mice were measurably smaller. Approximately 20 percent of the platelets of peripheral blood of Osborne-Mendel rats with lymphoid leukemia induced with the Moloney agent contained characteristic particles, and in the sections of platelet pellets numerous particles were identified lying free in the plasma between the platelets. The significance of these observations is discussed.—J. Nat. Cancer Inst. 27: 747-791, 1961.

IN RECENT years several mouse lymphoid leukemias (*1*, *2*) and a stem-cell leukemia (*3*) have been demonstrated to be of viral origin. In addition, chloroleukemias have been shown to be induced by cell-free extract (*4*). In a series of separate reports, the fine structure of particles associated with the Gross (*5*), Friend (*6*, *7*), Moloney (*8*, *9*), and Graffi (*10*) leukemias has been described, and examination of these contributions

[1] Received for publication June 21, 1961.

[2] Laboratory of Biology.

[3] National Institutes of Health, Public Health Service, U.S. Department of Health, Education, and Welfare.

603724—61——4

brings out the fact that, while the source of virus differed in some instances, the morphology of the particles is basically similar. Since minor differences have been noted in the size of these various particles, we decided to analyze, with the same electron microscope, a series of mouse neoplasms with which a leukemogenic virus was known to be or suspected of being associated and to use the same methods of fixation, embedding, sectioning, and staining. What follows is in good part a summary of the results of this analysis.

MATERIALS AND METHODS

Neoplasms induced with the Moloney, Gross (passage A), Manaker C-60 (Schwartz), and Friend agents, radiation-induced leukemia, and the spontaneous leukemias of strain AKR and substrain C3Hf/FgLw mice (*11*) were studied.

The Moloney agent, inoculated into 8 newborn BALB/c mice and 4 Osborne-Mendel rats, resulted in generalized lymphoid leukemia developing within 10 weeks.

The Gross passage-A material, inoculated into newborn C3Hf/BiLw mice, resulted in the appearance of generalized lymphoid leukemia or thymic lymphoma only in approximately 3 months.[4]

Tissue-culture fluids over explants of Schwartz Swiss mouse lymphoma were inoculated into newborn BALB/c mice, which later developed generalized lymphoid leukemia within 3 months.

Nine C57BL/Ka mice received a weekly exposure to 168 r for 4 weeks, beginning at 1 month of age. Leukemia, usually involving the thymus gland, developed in these mice at an average age of 5 months. Physical factors for radiation were: Two X-ray tubes placed opposite each other were operated at 200 kvp and 15 ma; filtration was by 0.25 mm Cu and 0.55 mm Al with a distance of 54 cm from each focal spot to the center of the mouse. Dose rate was 120 r per minute.

Approximately 90 percent of C57BL/KaLw mice irradiated at weekly intervals for 4 weeks, beginning at 1 month of age, became leukemic at an average age of 5 months.

Newborn NIH (Swiss) mice, inoculated with an extract of the Friend agent, exhibited signs of disease within 2 weeks. The material used was obtained from mice 8 days after inoculation.[5]

Six spontaneous leukemias of strain AKR mice, which developed at an average age of 8 months, and 7 leukemias of the C3Hf/FgLw mice, which developed at an average age of 10 months, were studied.

Samples of lymph node, thymus, and spleen of leukemic mice were removed as quickly as possible after cervical dislocation and diced with

[4] A virus preparation was obtained from Dr. L. Gross, which represented the 24th serial passage. Leukemic tissues from C3Hf/BiLw mice were homogenized, centrifuged, and filtered (Seitz 02). The filtrate inoculated into C3Hf/BiLw mice (1 to 22 days of age) induced lymphocytic neoplasms in all of 25 mice. The mean age at death from leukemia was 3¼ months.

[5] Mice inoculated with the Friend agent were obtained from Dr. W. P. Rowe, National Institute of Allergy and Infectious Diseases, National Institutes of Health.

razor blades in cold chrome-osmium fixative (*12*). We obtained bone marrow from these animals by cracking the shafts of the femur with hemostatic forceps. Platelet pellets were obtained by centrifugation of whole citrated blood at 700 rpm for 10 minutes in an International refrigerated centrifuge equipped with horizontal rotor #269. We then centrifuged the supernatant at 2500 rpm for 15 minutes to obtain the platelet pellet. After fixation for 1 hour (2 hours for bone marrow) the tissues were transferred to 10 percent neutral formalin for 1 hour, then through a graded series of ethyl alcohol (70, 80, 90, 95, and 100%). After absolute alcohol the tissues were immersed in a mixture of 1 part monomer (3 parts *n*-butyl, 1 part methyl methracrylate) and 1 part absolute alcohol, then transferred through two changes of the monomer mixture and finally into prepolymerized monomer mixture and held overnight. Polymerization was completed at 47° C if the accelerator was 0.25 percent azodiisobutyronitrile or at 80° C if the accelerator was 0.5 percent benzoyl peroxide. Sections were cut with a diamond knife on a Porter-Blum ultramicrotome or an LKB Ultrotome set to cut at 25 mμ, stained with monobasic lead acetate (*13*) and examined with a Siemens Elmiskop I electron microscope. Original magnifications of the electron micrographs varied from 5,000 to 40,000 diameters and the magnifications indicated were accurate within 2 percent as determined by comparison with a diffraction grating replica with spacing of $\frac{1}{28,800}$ inch.

RESULTS

The Moloney Leukemia

In sections of lymph node, thymus, and spleen, characteristic particles were regularly observed lying free in intercellular spaces. Occasionally small groups of particles may exhibit electron-lucent nucleoids (fig. 1), but when in a greater number the nucleoids are usually electron dense (fig. 2). The outer diameter of the latter particles varies considerably, and this variation is in part the result of differences in the space between the outer membrane and the central nucleoid. An average value for the diameter of this central nucleoid is 60 mμ and that for the whole particle, 100 mμ. In the majority of these extracellular particles, the nucleoid is electron dense [type-C particle of Bernhard (*14*)]. In particles in which the center of the nucleoid is electron lucent (figs. 1 and 3), the periphery of the nucleoid is consistently electron dense and reacts strongly with lead salts, the whole nucleoid giving the appearance of a ring in profile. The outer membrane of these particles is regularly circular or ovoid in outline, never exhibiting the wrinkling typical of extracellular particles with electron-dense nucleoids. Also in these particles a second membrane between the outer membrane and the central ring is regularly demonstrable. The average outer diameter of these particles is again 100 mμ, that of the intermediate membrane, 85 mμ, and that of the central ring or nucleoid,

60 mμ. These particles are regularly found in close approximation to the plasma membrane of the cells that are considered to be malignant lymphoblasts. These cells, characterized by their relatively high nucleocytoplasmic ratio, possess a relatively large ovoid, often indented nucleus which in turn contains a compact nucleolus. The cytoplasm contains but few elements of the endoplasmic reticulum and only rarely strands of ergastoplasm, *i.e.*, endoplasmic reticulum with associated ribosomes. Numerous closely packed ribosomes, however, fill most of the cytoplasmic area except for that occupied by a small Golgi complex and a few relatively large oval or short, rodlike mitochondria (fig. 4). These are not features which would make it possible to distinguish malignant lymphoblasts from normal ones; they are simply the fine structural characteristics of the cells which presumably have invaded and caused the enlargement of the lymph nodes, thymus, and spleen of animals in which leukemia has been induced by the introduction of the Moloney agent. No features have been identified by which a lymphoblast demonstrated to be involved in the formation of particles can be distinguished from those which are not, but it is from the plasma membranes of such cells that particles with the same fine structure as that in figure 3 may sometimes be caught in various stages of the process of budding (figs. 5 through 9). The first evidence of particle formation is a lifting and thickening of the plasma membrane. The raised portion of the plasma membrane is double and below it an electron-dense crescent is present (fig. 5). What is considered a later stage in particle formation is illustrated in figures 6 and 7. At this stage the plasma membrane is lifted still further and the electron-dense crescent has enlarged. Nearly completed particles are shown in figures 8 and 9. The bud is constricted at the base and the profile of the central nucleoid appears as an incomplete electron-dense ring. An intermediate membrane is interposed between the nucleoid and the surface membrane. Very rarely buds may form at the end of a long stalk (fig. 10).

While intercellular particles are regularly present in lymph nodes, thymus, and spleen, and particle formation by lymphoblasts may be noted after diligent search in any of these organs, the most satisfactory material for the study of particles is the megakaryocytes of the spleen and bone marrow.

In control animals the megakaryocytes of these two organs are similar in ultrastructure, possessing numerous specific granules, a moderate number of small mitochondria, occasional strands of ergastoplasm, separately grouped components of the Golgi complex usually located near the nucleus, and a system of intercommunicating channels lined by prominent membranes [platelet demarcating membranes of Yamada (*15*), figs. 11 through 14]. This system of channels varies in extent and complexity from one cell to the next (figs. 11, 12, and 13), usually extending through a wide band of cytoplasm up to within approximately 0.5 μ of the plasma and nuclear membranes (fig. 14).

Megakaryocytes of both spleen and bone marrow of animals made leukemic by introduction of the Moloney agent regularly contain numer-

ous particles identical in size to those seen in an extracellular position in lymph nodes, thymus, and spleen. As a rule the particles in any one megakaryocyte appear to be in the same stage of maturation (fig. 15). They frequently fill the system of channels, and their outer membranes may sometimes be seen in continuity with the membrane system lining the channels (fig. 16). Occasionally particles with electron-dense as well as those with electron-lucent nucleoids ("ring" forms) may appear in one cell (fig. 17). The significance of the presence of profiles of the cylindrical forms visible in figure 17 and seen in greater detail in figure 18 is not clear at present. Transitions between cylindrical and spherical forms have not been seen, though continuity of the outer membranes of spherical forms is a common occurrence (figs. 16 and 18). Whether the megakaryocytes are from bone marrow (figs. 15 through 18) or spleen (figs. 19 and 20), the fine structure and size of the spherical particles is the same (table 1).

It has been demonstrated that generalized lymphoid leukemia may be induced in rats with the Moloney agent (*9*). Again, the megakaryocytes of bone marrow and spleen of rats with leukemia so induced proved the most satisfactory source of particles (fig. 21). The particle size, fine structure, and distribution are the same as in leukemic mice (figs. 21 and 22).

The greater blood volume of the rat makes it readily feasible to collect and examine the platelets of peripheral blood. Examination of thin sections of platelet pellets from control rats reveals the presence of closely packed entities, the platelets, with their characteristic specific granules, occasional small mitochondria and vacuoles, and groups of ribosomes (fig. 23). The morphology of the platelets is clearly the same as the membrane-bound cytoplasmic areas present within mature megakaryocytes (figs. 13 and 14).

Approximately 20 percent of the platelets from leukemic rats examined contain particles with the characteristic fine structure of those seen in infected megakaryocytes (fig. 24). In addition to the particles, always within vacuoles, the infected platelets also contain the usual complement of small mitochondria, specific granules, and ribosomes. Occasionally platelets are observed which contain profiles of crystalloids (fig. 25). These structures have not been seen in platelets from control rats nor in megakaryocytes from control or leukemic animals. Of considerable added interest is the finding of fairly numerous 100 μ particles, the majority with electron-dense nucleoids, lying free in the plasma between the packed platelets (fig. 26).

The particles so far described, both those in an extracellular position and those within the channels of megakaryocytes and vacuoles of platelets, have consistently had the same ultrastructure (except for variations in electron density of the central nucleoid) and the same average size (100 mμ). However, on rare occasions in both leukemic rats and mice, another type of particle has been identified within the cytoplasms of cells considered malignant lymphoblasts. Usually these particles appear to

TABLE 1.—Particle measurement in megakaryocytes

		Outer diameter		Intermediate membrane		Nucleoid		Number measured
		Range	Average	Range	Average	Range	Average	
Moloney	Mature	85. 0–113. 2	97. 5			56. 6–79. 2	64. 7	30
	Immature	95. 0–110. 0	103. 5	75. 0–90. 0	81. 9	50. 0–65. 0	57. 7	30
Gross	Mature	74. 3–100. 0	88. 7			45. 7–64. 3	57. 4	30
	Immature	90. 6–113. 2	99. 8	75. 0–88. 7	81. 4	50. 9–75. 5	58. 0	30
Manaker C-60	Mature	91. 4–114. 3	101. 7			54. 3–71. 4	61. 4	30
(Schwartz)	Immature	90. 0–110. 0	98. 9	65. 0–80. 0	73. 5	45. 0–60. 0	53. 8	30
Friend	Mature	70. 4–101. 4	90. 7			45. 7–71. 4	53. 9	30
	Immature	92. 9–114. 3	100. 4	71. 4–92. 9	79. 6	47. 1–64. 3	53. 6	30
Spontaneous	Mature	83. 0–96. 2	90. 7			49. 1–73. 6	59. 2	15
C3Hf/FgLw	Immature	84. 3–114. 3	97. 0		*	48. 7–71. 3	58. 6	15
Spontaneous	Mature	66. 0–111. 3	95. 8			47. 2–75. 5	60. 3	15
AKR	Immature	88. 7–133. 3	103. 4		*	43. 4–94. 4	60. 4	15

*Diameter of intermediate membrane could not be measured accurately.

lie free in the cytoplasm, but on occasion are separated from the cytoplasm by a delicate, thin membrane (fig. 27). These particles are smaller, averaging 85 mμ and have never been seen to possess an electron-dense nucleoid. They differ also from the usual type particle in that they consist only of two concentric rings. They thus may be classified as type-A particles of Bernhard (*14*). No relationship between these particles and the larger common type-C particle in a topographical or developmental sense has been noted. The only relationship which can be considered of any possible significance is that they occur in the cytoplasm of the same cell type which is implicated in the production of the type-C particles by budding from the plasma membrane.

The Gross Leukemia

Since the megakaryocytes of spleen and bone marrow were the most satisfactory source of particles in animals carrying the Moloney agent, the greatest amount of time and effort has been expended on these cells in the study of the Gross and the other leukemias to be considered. As in the Moloney leukemia, numerous particles (type C) fill the channels of the megakaryocytes of mice carrying the Gross leukemia (fig. 28). When the nucleoids of these particles possess electron-lucent centers, the average outside diameter of the particle is 100 mμ and the diameter of the nucleoid 58 mμ (figs. 29 and 30). When the particles possess electron nucleoids, however, they are measurably smaller than the former, averaging 88+ mμ in diameter (fig. 29, table 1). Though smaller, their fine structure is similar to that of the Moloney particle. An intermediate membrane is sometimes identifiable in mature particles, but is much more readily resolved in particles with electron-lucent nucleoids than in those with electron-dense nucleoids. One way in which the Gross leukemia differs from the Moloney leukemia, as far as ultrastructure is concerned, is that particles are frequently found within the specific granules of megakaryocytes (figs. 28 and 30). This so far has not been noted in Moloney leukemia material. One other difference is that, while elongated particles have been seen occasionally (fig. 31), no true cylindrical forms have been observed.

The Manaker C-60 (Schwartz) Leukemia

Particles present in megakaryocytes of mice carrying this form of the Schwartz leukemia are almost identical in size and distribution to the 100 mμ particles of the Moloney leukemia. They occupy the channels of megakaryocytes (fig. 32), and they may possess a nucleoid with an electron-lucent center, in which case the intermediate membrane is readily resolved (fig. 33). The central nucleoid averages 58 mμ in diameter, the average diameter of the intermediate membrane 74 mμ, and the total diameter of the particle averages 100 mμ (fig. 34). In particles with electron-dense nucleoids, the outer diameter still averages 100 mμ. In only one instance has a particle been observed within a specific granule. On

the other hand, no cylindrical forms have been seen to date. As in the Moloney leukemia, extracellular particles possess distorted and wrinkled outer membranes (fig. 35), and occasionally particles may be observed in the process of budding from the plasma membrane of what are considered malignant lymphoblasts (figs. 35 and 36).

The Friend Neoplasm (Stem-Cell Leukemia)

Observations on the megakaryocytes of spleen and bone marrow of mice 8 days after inoculation of the Friend agent closely parallel those of de Harven and Friend (*6*, *7*). Numerous characteristic particles are present within the cytoplasmic channels, some showing continuity of their outer membranes, others apparently caught in the act of budding from the membranes lining the channels (fig. 37). At higher magnification, these particles can be seen to possess the same basic ultrastructure as the particles associated with the Moloney and Gross leukemias (fig. 38). Either an electron-dense or electron-lucent nucleoid is present and in the latter an intermediate membrane is readily visible between the nucleoid and the outer membrane. In confirmation of de Harven and Friend (*8*), measurement of the mature particles indicates that in size they more closely resemble the particles associated with the Gross leukemia than those of the Moloney leukemia. The nucleoids average 54 mμ in diameter, and the diameter of the whole particle averages 90 mμ. However, the measurements of particles with electron-lucent nucleoids more closely resemble those of the particles associated with the Moloney leukemia. Their outside diameter averages 100+ mμ, the diameter of the intermediate membrane 80 mμ, and that of the nucleoid 54 mμ (fig. 38 and table 1).

The C57BL/Ka Radiation-Induced Leukemia

In this material, cells which, with the light microscope, have the appearance of megakaryocytes, possess a very bizarre ultrastructure. While the cells possess multilobed nuclei, the cytoplasm is filled with closely packed, long strands of amorphous material of moderate electron density (fig. 39). In some of these cells there is evidence of past phagocytic activity (fig. 40), but none have particles with the ultrastructure of virus. No such particles are seen within or in association with any of the cells of the bone marrow, spleen, lymph nodes, or thymus.

Spontaneous Leukemia of Strain C3Hf/FgLw Mice

C3H mice of the Figge substrain have an incidence of spontaneous leukemia of approximately 80 percent at 10 months of age (*11*). The megakaryocytes of the bone marrow of mice that have developed gross signs of generalized leukemia do not contain the abundance of particles typical of megakaryocytes of mice with leukemia induced with cell-free extract. All megakaryocytes examined, however, contain particles. With but rare exceptions, only particles with electron-lucent nucleoids

are seen within specific granules (fig. 41), while particles with electron-lucent or dense nucleoids may occasionally be seen in the membrane-bound channels (fig. 42). Formation of the particles within specific granules occurs by inversion of the granule membrane back into the substance of the granule with the coincident development of an electron-dense crescent (figs. 42 and 43). This crescent later expands to form the electron-dense periphery of a central nucleoid. The largest immature particles measured had an outer diameter of 114 mμ and a central nucleoid of 71 mμ, while an average value obtained from measuring 100 clearly defined mature particles was 91 mμ for the outside diameter and 59 mμ for the diameter of the central nucleoid.

Spontaneous Leukemia of Strain AKR Mice

While there were few characteristic particles in the megakaryocytes of leukemic C3Hf/FgLw mice, they were nevertheless readily identified. This was not true in strain AKR mice. In this material, in some instances electron micrographs were taken of a moderate number of particles after they were observed within specific granules of megakaryocytes (fig. 44). In other instances no particles were seen and in still other instances there were so few particles that they were identified only in prints after electron micrographs of megakaryocytes were taken (figs. 45 and 46). Thus with the exception of radiation-induced leukemia where no particles were identified, evidence of characteristic particles in megakaryocytes was most difficult to obtain in leukemic AKR mice. In this material particles with electron-lucent nucleoids averaged over 100 mμ in diameter and the nucleoids 60 mμ (fig. 48). Particles with electron-dense nucleoids averaged 96 mμ in outside diameter and the nucleoids 60 mμ (fig. 47).

DISCUSSION

The primary purpose of this study, that of comparing the characteristic particles associated with this series of leukemias, with the use of the same electron microscope and the same preparative methods, has been accomplished. Of some interest is the fact that, in all but radiation-induced leukemia, particles of the same basic type (type C of Bernhard (*14*) [6] were identified in each. In the Moloney leukemia, in addition to the characteristic type-C particle, cylindrical particles as well as smaller intracytoplasmic particles (type A) were occasionally present. This is reminiscent of the Graffi leukemia in which type-A particles (*10*) as well as particles varying in diameter from 70 to 150 mμ have been identified (*16*). It is

[6] In this discussion a type-A particle is defined as consisting of 2 concentric spheres which in section appear as 2 concentric rings. The inner of the 2 rings is usually more electron dense and has a stronger affinity for lead salts than the outer and always surrounds an electron-lucent core. The type-C particle consists of a centrally located nucleoid which may possess an electron-lucent or electron-dense center, depending on the state of maturation. In immature particles of this type an intermediate membrane is regularly identifiable between the nucleoid and the outer membrane. These are basically the definitions of Bernhard (*14*), the classification of particles having been based on their structure at maturity, not on their appearance during development.

possible that examination of megakaryocytes in Graffi material would bring this leukemia into line with the present series.

This consistent presence of the type-C particle in animals made leukemic by inoculation of cell-free extract is considered significant, even though a positive correlation between number of particles and potency of extract has not as yet been demonstrated. In this connection the early appearance of clinical signs of disease after injection of the Moloney, Manaker C-60 (Schwartz), Gross, and Friend agents compared with the late appearance of spontaneous leukemias in AKR and C3Hf/FgLw mice may well be correlated with the large number of particles present in megakaryocytes of the former group and the small number in the latter. Also, neither typical megakaryocytes nor characteristic particles have been identified in the bone marrow of C57BL/Ka mice with radiation-induced leukemia, and cell-free extracts from such mice have failed to induce leukemia in several trials in this laboratory. Failure to find characteristic particles in other tissues from similar material has been reported previously (*17*). Since Gross (*18*) and Lieberman and Kaplan (*19*) were successful, it seems reasonable to assume that a virus in these animals "activated" by radiation was either not present or present in much lower concentration in ours.

In the details of particle size, location, and ultrastructure interesting informaticn has been obtained. Inspection of table 1 reveals that on the basis of particle size, the lymphomas may be separated into 2 groups, one in which the outside diameter is 100 mμ whether the central nucleoid is electron dense (mature) or contains an electron-lucent core (immature). This group includes the Moloney and Manaker C–60 (Schwartz) leukemias. The other group, in which particles with electron-dense nucleoids have an outside diameter of approximately 90 mμ, includes the Gross and Friend neoplasms and the AKR and C3Hf/FgLw spontaneous leukemias. It is pertinent at this point to discuss the measurement procedure. Choosing only those particles in which the membranes and nucleoids were clearly defined meant that for the most part the larger particles in any given electron micrograph were selected for measurements. It was felt that the use of this method would give results closer to the true dimensions of the particles than would have been true if all particles in an electron micrograph were measured. In sectioned material, part of the apparent variation in particle size is because only parts of many particles have been included in the section. Including the measurements of these smaller profiles in the determination of an average value of particle size would of necessity bring the figure down to well below the true value. The phenomenon of particle formation within specific granules of megakaryocytes appears characteristic of the leukemia induced with the Gross virus and of the spontaneous leukemias of AKR and C3Hf/Fg mice, but not of the other leukemias studied. It might be expected that the Gross and AKR leukemias would be similar in this respect, since Gross obtained his leukemia originally from AKR material (*1*). Size alone may not be a particularly dependable criterion for the classification

of particles under certain circumstances. For example, particles formed at the plasma membrane may be measurably larger than those formed on the endoplasmic reticulum (*20*). In the present case, however, the particles measured for comparison were all within cytoplasmic channels or within specific granules of megakaryocytes. In the Moloney and Manaker C-60 (Schwartz) leukemias, the outside diameter of the particles was very nearly identical and only by careful measurement of a large number of particles was it possible to determine that the intermediate membrane of the Moloney particles was larger than the corresponding entity of the Manaker particles (table 1). From the ultrastructural point of view, however, the presence of cylindrical forms in megakaryocytes of mice with the Moloney leukemia and their absence in the Manaker disease are a clearly distinguishing feature.

In the study of a series of megakaryocytes of control animals, part of the process of platelet formation was revealed. Platelets apparently do not form by the process of pinching off bits of peripheral cytoplasm of megakaryocytes, but rather by the development of an intricate system of intracytoplasmic channels which eventually divides the wide intermediate zone of cytoplasm into numerous small areas connected to each other by narrow bands of cytoplasm. These small areas, each with its share of specific granules, mitochondria, and ribosomes, are presumed to be immature platelets. While the final stage of this process has not been observed, it seems reasonable to believe that a shower of platelets is produced at one time by the disintegration of the peripheral zone of cytoplasm and release of the platelets, which leave behind only a narrow band of juxtanuclear cytoplasm. These results then, in general, confirm those of Yamada (*15*). Improvement in techniques and the development of heavy metal staining, however, have made possible a limited extension of Yamada's findings; *i.e.*, the greater electron density, the presence of but a single limiting membrane, and the absence of cristae are characteristic features that made the specific granules readily distinguishable from mitochondria.

The description by de Harven and Friend (*6*) of numerous characteristic particles present within the channels of megakaryocytes is obviously not an isolated phenomenon, since 5 other leukemias have been demonstrated to follow the same pattern. If these particles are accepted as being the morphological representations of oncogenic agents, then these are examples of a nonmalignant cell functioning as a site of replication of oncogenic virus. In the studies of Miller (*21*) cell-free extract demonstrated to be capable of inducing leukemia in intact mice (Gross, passage-A) was inoculated into thymectomized animals. These mice did not develop leukemia, but, after blind passages of cell-free extract through a series of thymectomized mice, extracts from the last of the series were introduced into intact mice and this was followed by the reappearance of leukemia. The possibility thus must be considered that megakaryocytes may have served as a site of virus replication in these studies. Only future analysis, however, will determine whether or not this is true.

There are two reasons why we believe megakaryocytes are the most satisfactory cells for the study of particles in these leukemias. 1) The particles are retained in an intracellular position and are thus protected to some degree from damage that could conceivably result from the technical procedures used in the fixation and embedding processes and from any circulating antibody. 2) Inspection of a mature megakaryocyte gives the observer the opportunity to view the results of a long series of past events. In other words, particles formed over a relatively long period are held within the cells until the final release of platelets. This gives the seeker a much better chance of finding particles than if he were studying malignant lymphoblasts in which particles are budded from the plasma membrane and released into the intercellular space.

The presence of particles in approximately 20 percent of the platelets of peripheral blood of rats with viral-induced leukemia is of some interest, but of greater interest is the presence of particles lying free in the plasma between the packed platelets. Since the centrifugation speed was only 2500 rpm in an International Centrifuge with the horizontal rotor #269, numerous particles presumably are in the blood plasma of rats carrying the Moloney leukemia. Thus peripheral blood of these rats should serve as a source of relatively pure virus. Studies at present under way to test this possibility have met with encouraging preliminary results, but will be dealt with in a separate report.

REFERENCES

(*1*) GROSS, L.: "Spontaneous" leukemia developing in C3H mice following inoculation, in infancy, with AK-leukemia extracts, or AK-embryos. Proc. Soc. Exper. Biol. & Med. 76: 27–32, 1951.

(*2*) MOLONEY, J. B.: Preliminary studies on a mouse lymphoid leukemia virus extracted from Sarcoma 37. Proc. Am. Assoc. Cancer Res. 3: 44, 1959.

(*3*) FRIEND, C.: Cell-free transmission in adult Swiss mice of a disease having the character of a leukemia. J. Exper. Med. 105: 307–318, 1957.

(*4*) GRAFFI, A.: Chloroleukemia of mice. Ann. New York Acad. Sc. 68: 540–558, 1957.

(*5*) BERNHARD, W., and GROSS, L.: Présence de particle d'aspect virusal dans les tissus tumoraux de souris atteintes de leucémies induites. Compt. rend. Acad. sc. 248: 160–163, 1959.

(*6*) DE HARVEN, E., and FRIEND, C.: Electron microscope study of a cell-free induced leukemia of the mouse: a preliminary report. J. Biophys. & Biochem. Cytol. 4: 151–156, 1958.

(*7*) ———: Further electron microscope studies of a mouse leukemia induced by cell-free filtrates. J. Biophys. & Biochem. Cytol. 7: 747–751, 1960.

(*8*) MOLONEY, J. B.: Biological studies on a lymphoid-leukemia virus extracted from Sarcoma 37. I. Origin and introductory investigations. J. Nat. Cancer Inst. 24: 933–951, 1960.

(*9*) ———: Properties of a leukemia virus. NCI Monogr. No. 4: 7–37, 1960.

(*10*) BERNHARD, W.: The detection and study of tumor viruses with the electron microscope. Cancer Res. 20: 712–727, 1960.

(*11*) LAW, L. W.: Present status of nonviral factors in the etiology of reticular neoplasms of the mouse. Ann. New York Acad. Sc. 68: 616–635, 1957.

(*12*) DALTON, A. J.: A chrome-osmium fixative for electron microscopy. Anat. Rec. 121: 281, 1955.

(*13*) DALTON, A. J., and ZEIGEL, R. F.: A simplified method of staining thin sections of biological material with lead hydroxide for electron microscopy. J. Biophys. & Biochem. Cytol. 7: 409–410, 1960.

(*14*) BERNHARD, W.: Electron microscopy of tumor viruses. A Review. Cancer Res. 18: 491–509, 1958.

(*15*) YAMADA, E.: The fine structure of the megakaryocyte in the mouse spleen. Acta anat. 29: 267–290, 1957.

(*16*) GRAFFI, A.: Personal communication, 1961.

(*17*) DMOCHOWSKI, L., GREY, C. E., and GROSS, L.: The role of viruses in x-ray-induced leukemia. *In* Radiation Biology and Cancer. Austin, Univ. Texas Publ., 1958, pp. 382–399.

(*18*) GROSS, L.: Serial cell-free passage of a radiation-activated mouse leukemia agent. Proc. Soc. Exper. Biol. & Med. 100: 102–105, 1959.

(*19*) LIEBERMAN, M., and KAPLAN, H. S.: Leukemogenic activity of filtrates from radiation induced lymphoid tumors of mice. Science 130: 387–388, 1959.

(*20*) DALTON, A. J., POTTER, M., and MERWIN, R.: Some ultrastructural characteristics of a series of primary and transplanted plasma cell tumors of the mouse. J. Nat. Cancer Inst. 26: 1221–1267, 1961.

(*21*) MILLER, J. F. A. P.: Recovery of leukemogenic agent from non-leukemic tissues of thymectomized mice. Nature, London 187: 703, 1960.

Figures 1 to 10, 15 to 22, and 24 to 27 are from mice with generalized leukemia induced with the Moloney agent. Figures 28 to 31 are from mice with generalized leukemia induced with the Gross passage-A agent. Figures 32 to 36 are from mice with generalized leukemia induced with the Manaker C-60 (Schwartz) agent. Figures 37 and 38 are from mice infected with the Friend agent. Figures 39 and 40 are from mice with radiation-induced leukemia. Figures 41 to 43 are from C3Hf/FgLw mice with spontaneous leukemia. Figures 44 to 48 are from AKR mice with spontaneous leukemia. All figures are taken from material fixed in chrome osmium and stained with monobasic lead acetate. *Line* on each figure or plate represents 1 μ unless otherwise indicated.

PLATES

PLATE 97

FIGURE 1.—Several extracellular particles lying free between 3 lymphoblasts in thymus of BALB/c mouse. Nucleoids of these particles are relatively electron lucent. One particle appears in process of budding (*arrow*). *Line* represents 0.1 μ. × 70,000

FIGURE 2.—Extracellular particles lying between lymphoblasts in thymus of BALB/c mouse. Nucleoids of these particles are relatively electron dense. *Line* represents 0.1 μ. × 70,000

FIGURE 3.—Three extracellular particles from thymus of a BALB/c mouse. Center one is cut near the midplane and exhibits electron-lucent nucleoid and intermediate membrane. *Line* represents 0.1 μ. × 140,000

FIGURE 4.—Parts of 3 cells considered to be malignant lymphoblasts from thymus of BALB/c mouse, showing profiles of typical mitochondria and the usual configuration of Golgi complex in these cells. A particle appears budding from plasma membrane of one cell (*arrow*). × 40,000

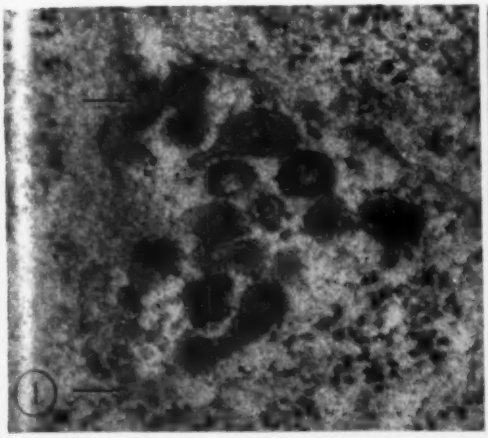

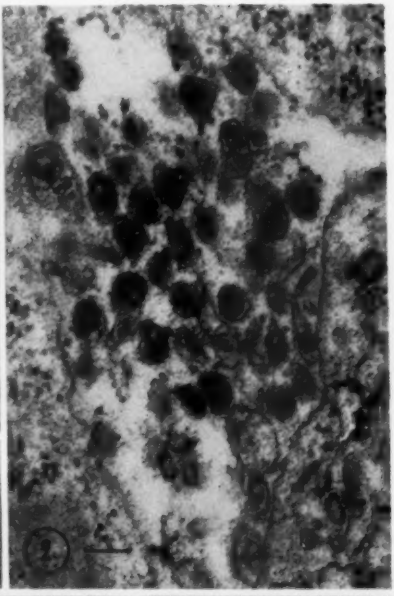

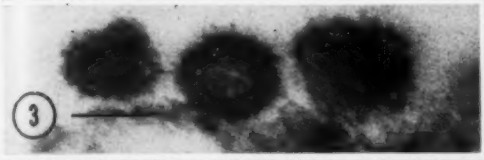

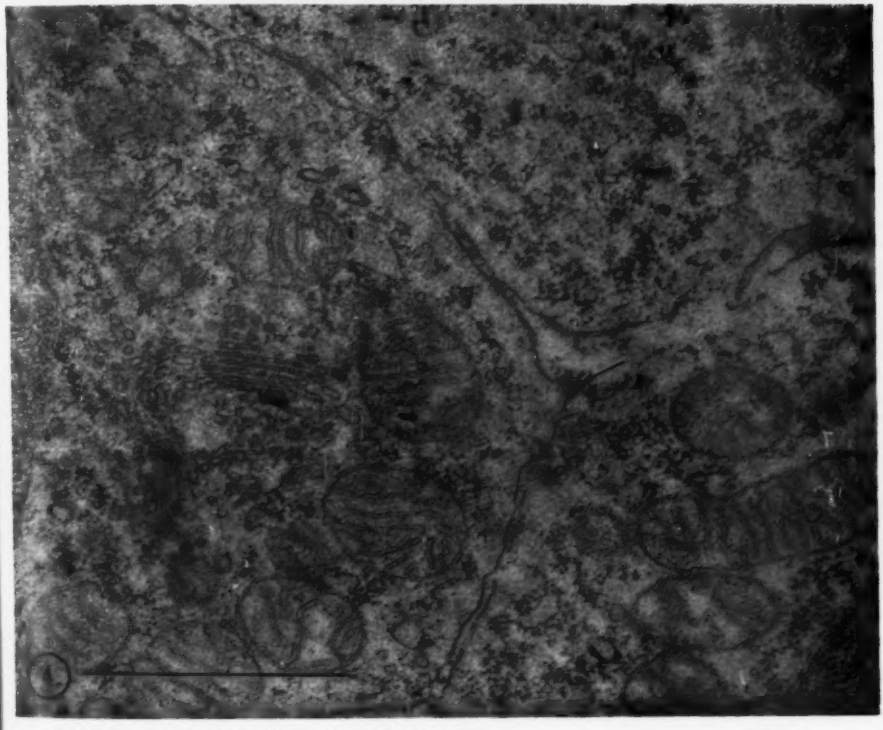

603724—61——5

PLATE 98

FIGURE 5.—Early stage in process of particle formation from plasma membrane of lymphoblast. Plasma membrane is lifted and double. The beginning of the nucleoid appears as slightly curved dense line below plasma membrane. *Line* on this figure is reference for plate and represents 0.1 μ. × 150,000

FIGURE 6.—Later stage in particle formation. Partly formed nucleoid is distinctly curved. × 150,000

FIGURE 7.—Two stages in particle formation, one to *left* slightly later than that in figure 6, one to *right* considerably farther advanced. × 150,000

FIGURE 8.—Late stage in particle formation in which nucleoid is nearly completed and bud shows constriction at base. × 150,000

FIGURE 9.—Slightly later stage in particle formation than that shown in figure 8. Electron-dense border of nucleoid is nearly complete and there is greater constriction at base of bud. × 150,000

FIGURE 10.—Two incomplete particles are visible in this figure, one appearing to be elongate or possibly double, the other forming at end of long stalk. This latter appearance is rare. × 150,000

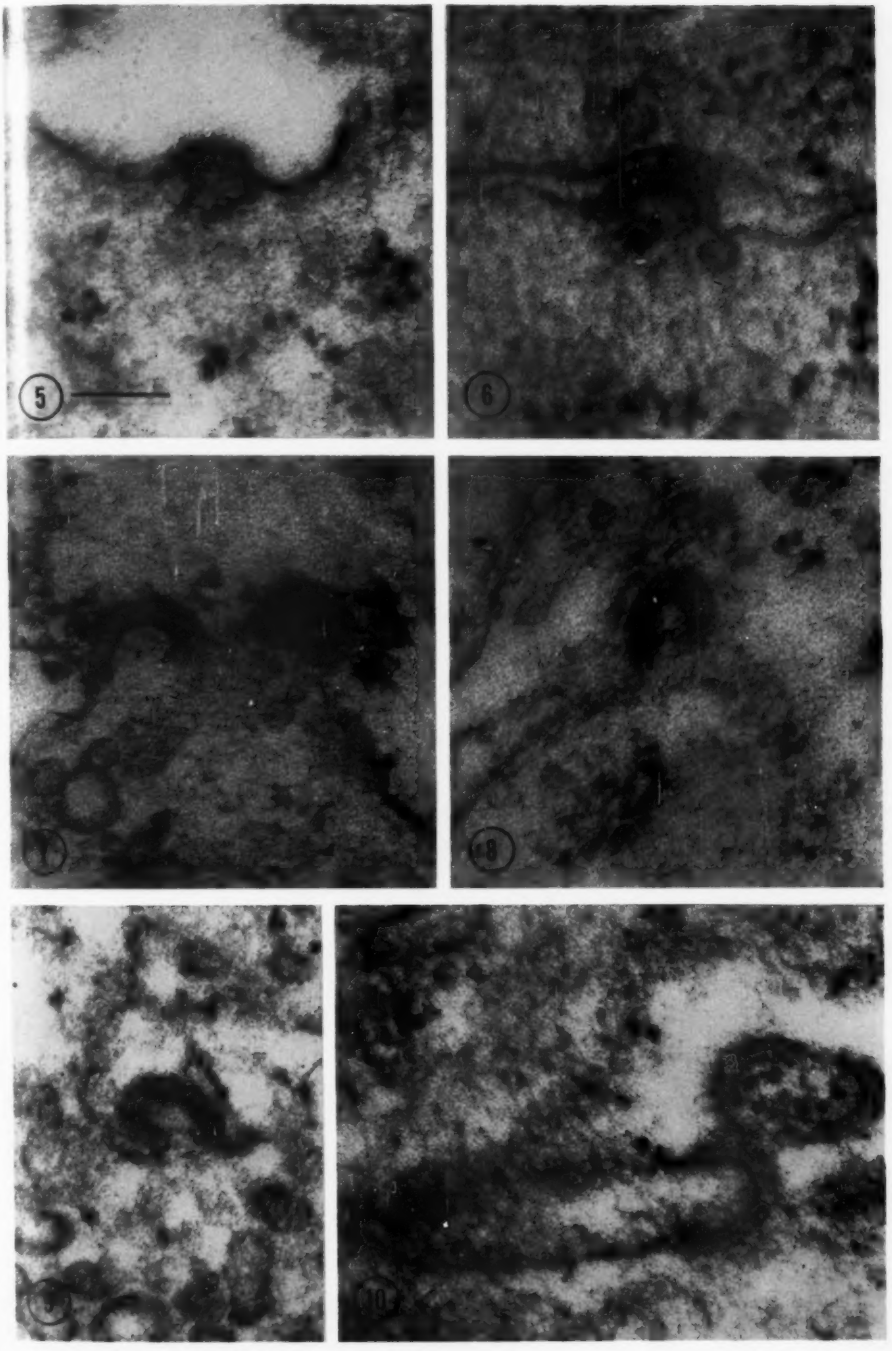
5
6
7
8
9
10

PLATE 99

FIGURE 11.—Part of megakaryocyte from bone marrow of control Osborne-Mendel rat. Specific granules (G) and small mitochondria (M) are numerous, but the "platelet demarcating membranes" of Yamada (*15*) are few in number. Part of Golgi complex is visible (*arrow*). × 35,000

FIGURE 12.—Part of megakaryocyte from bone marrow of control Osborne-Mendel rat. Platelet demarcating membranes (D) are more numerous than those in figure 11. Part of Golgi complex is present (*arrow*). × 35,000

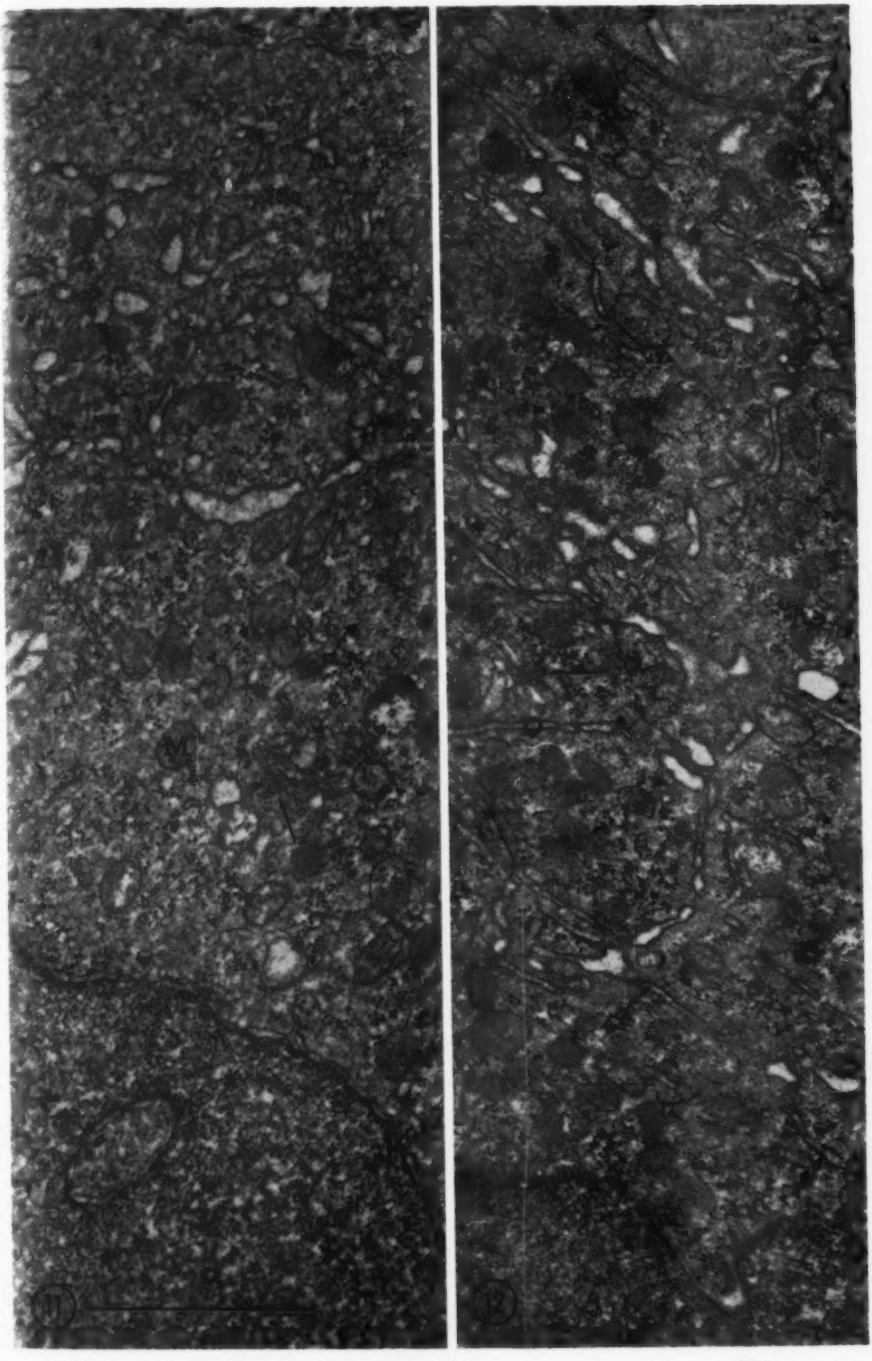

PLATE 100

FIGURE 13.—Part of megakaryocyte from bone marrow of control BALB/c mouse. Platelet demarcating membranes are numerous and distended, demarcating cytoplasmic areas destined to become individual platelets. × 35,000

FIGURE 14.—Part of megakaryocyte from bone marrow of control BALB/c mouse. Narrow cytoplasmic areas near nucleus and plasma membrane contain none of channels delimited by platelet demarcating membranes. × 35,000

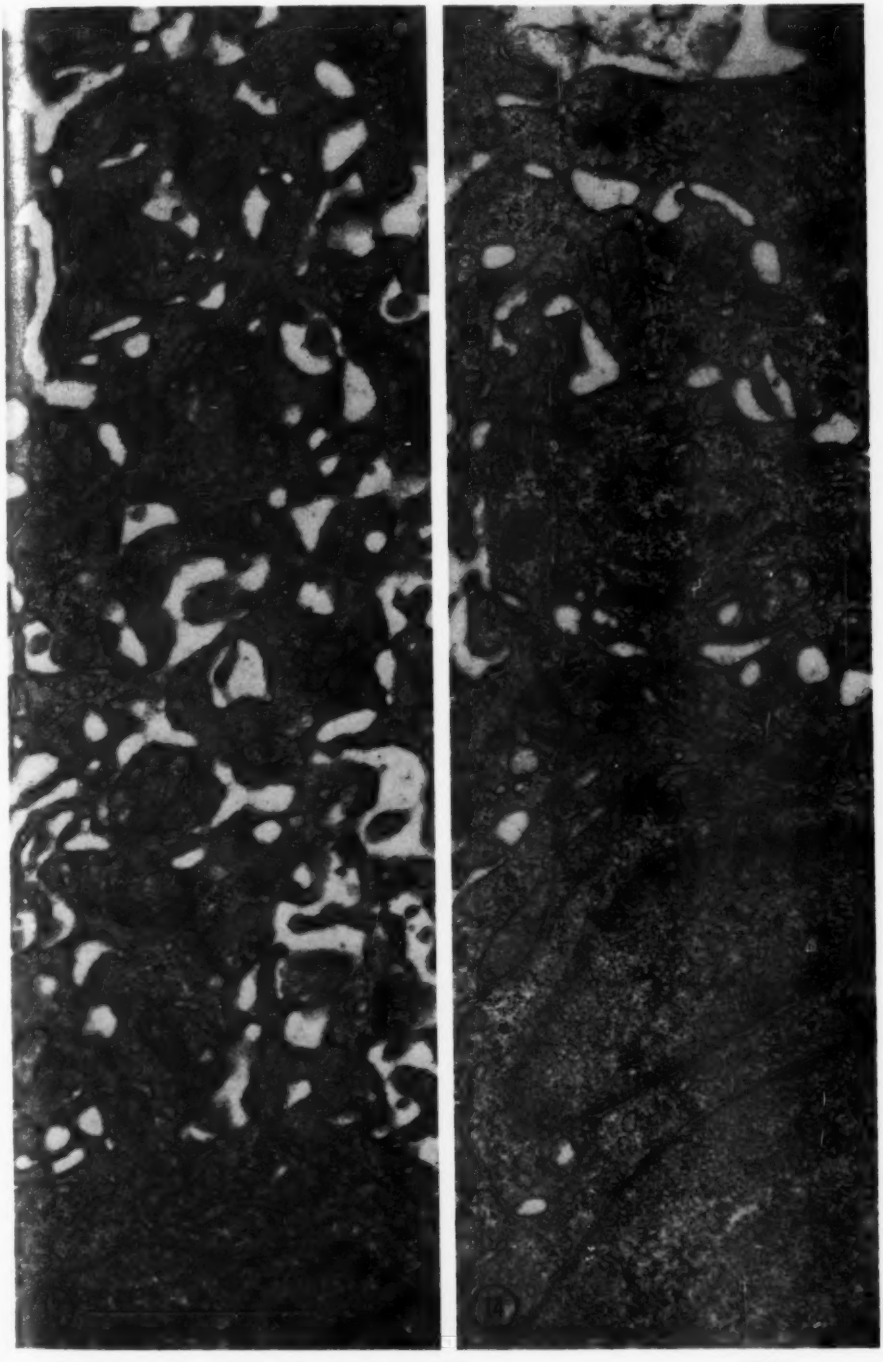

PLATE 101

FIGURE 15.—Low-power view of part of megakaryocyte from bone marrow of BALB/c mouse infected with the Moloney agent. Cytoplasmic channels are filled with numerous characteristic particles. × 35,000

FIGURE 16.—Part of cytoplasm of megakaryocyte from bone marrow of BALB/c mouse infected with the Moloney agent. Several particles are in process of formation (*long arrows*). Other groups of particles show continuity of their outer membranes (*short arrows*) and between their outer membranes and membranes lining the channels (X). × 53,000

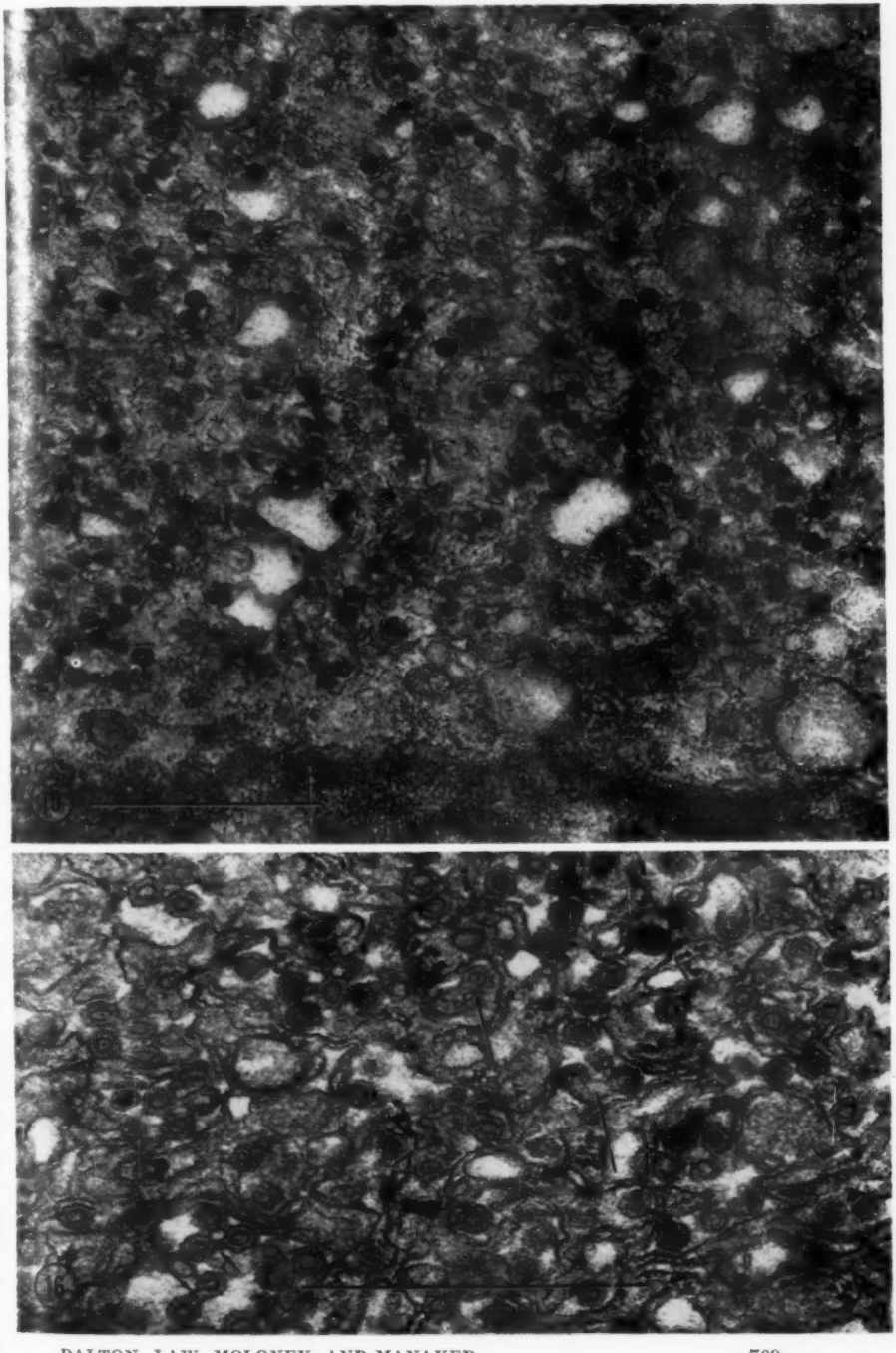

PLATE 102

FIGURE 17.—Part of cytoplasm of megakaryocyte from bone marrow of BALB/c mouse infected with the Moloney agent. Spherical particles with electron-lucent nucleoids are present to *left* and *upper left* (A). Particles with electron-dense nucleoids are in *upper right* (B). Cylindrical forms appear at *lower right* (C) and shorter cylinders in other areas. The significance of the extremely electron-dense bodies of variable size (X) is unknown. × 53,000

FIGURE 18.—Area of cytoplasm of megakaryocyte similar to that shown in figure 17 but at higher magnification, showing in greater detail one cylindrical form (A) and continuity of outer membranes of spherical particles (*arrow*). *Line* represents 0.1 μ. × 105,000

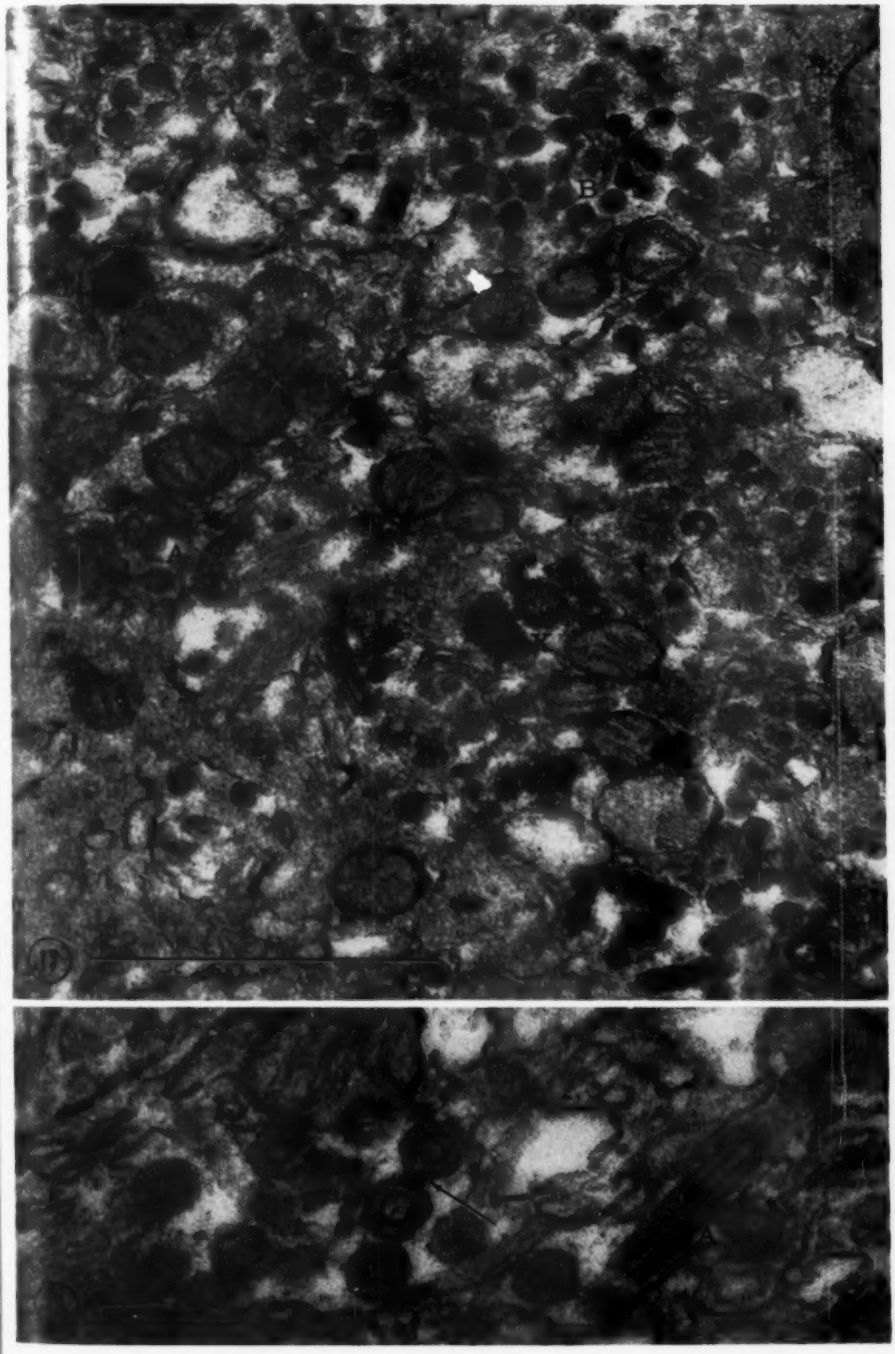
B
A

PLATE 103

FIGURE 19.—Low-power view of part of megakaryocyte from spleen of BALB/c mouse infected with the Moloney agent, showing that the distribution of particles is similar to that in megakaryocytes of bone marrow. × 53,000

FIGURE 20.—Higher magnification of part of cytoplasm of megakaryocyte similar to that in figure 19, showing details of particles. *Line* represents 0.1 μ. × 240,000

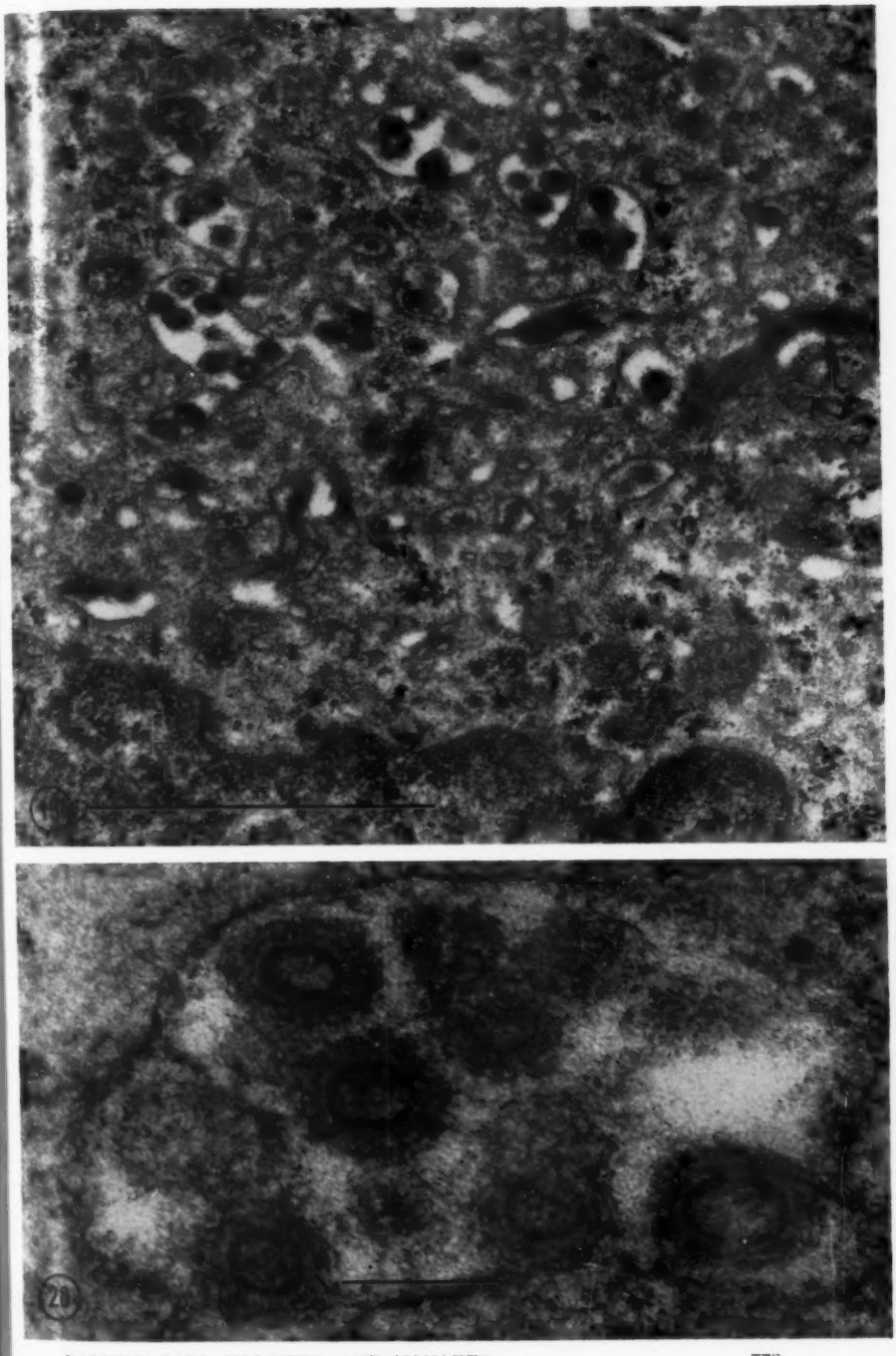

PLATE 104

FIGURE 21.—Part of cytoplasm of megakaryocyte from bone marrow of Osborne-Mendel rat infected with the Moloney agent, showing numerous characteristic particles and occasional specific granules and small mitochondria. Part of an engulfed granulocyte is visible at *lower right*. × 35,000

FIGURE 22.—Part of cytoplasm of megakaryocyte similar to that shown in figure 21, but at somewhat higher magnification. The majority of the characteristic particles possess electron-dense nucleoids, though 3 immature forms are visible (*arrows*). × 53,000

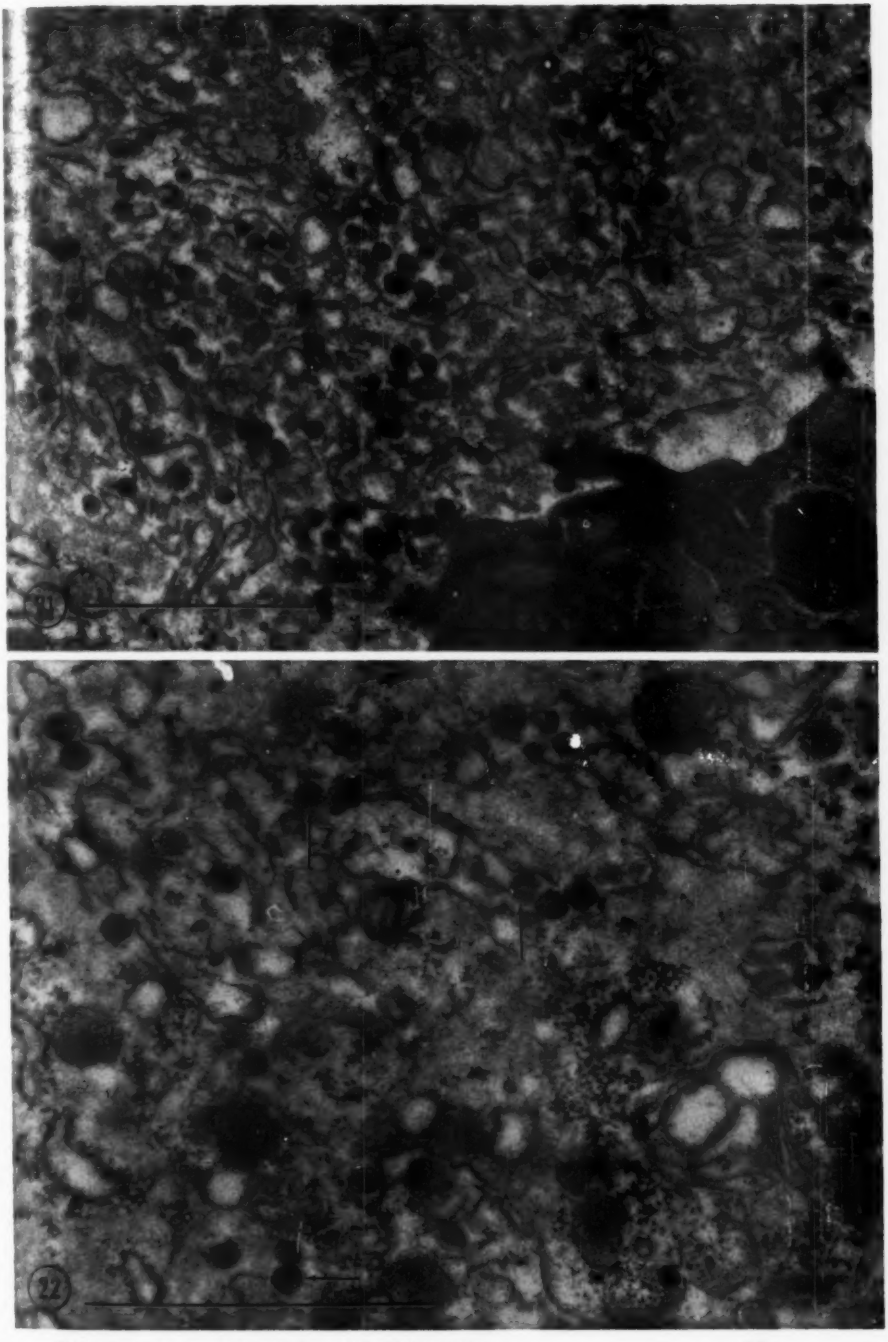
21
22

PLATE 105

FIGURE 23.—Platelets from peripheral blood of control Osborne-Mendel rat showing specific granules (G), mitochondria (M), and ribosomes (R). × 35,000

FIGURE 24.—Part of platelet from peripheral blood of Osborne-Mendel rat infected with the Moloney agent. As in figure 23, specific granules, mitochondria, and ribosomes are present, but in addition characteristic particles (P) of the Moloney leukemia are present in vacuoles. *Line* represents 0.1 μ. × 70,000

FIGURE 25.—Platelets from peripheral blood of Osborne-Mendel rat infected with the Moloney agent. Crystalloids of unknown significance, one showing periodicity (X) are present in both platelets. × 35,000

FIGURE 26.—Part of section of platelet pellet obtained from peripheral blood of Osborne-Mendel rat infected with the Moloney agent. Characteristic particles are visible lying free in spaces between platelets. × 53,000

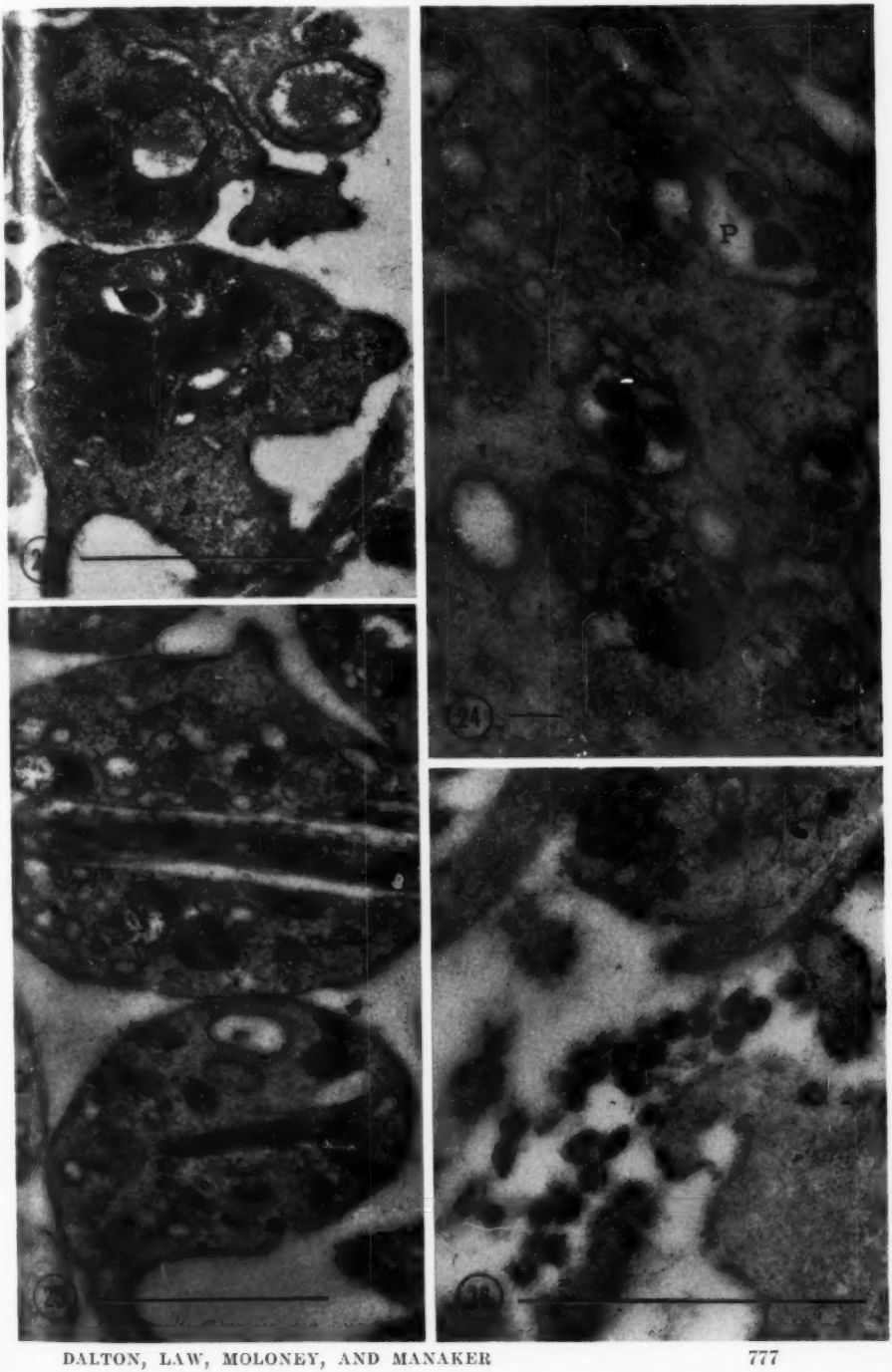

603724—61——6

PLATE 106

FIGURE 27.—Part of lymphoblast from thymus of BALB/c mouse infected with the Moloney agent. In cytoplasm are profiles of several particles which are made up of 2 concentric rings (type-A of Bernhard). These particles average 85 mμ in diameter. They do not appear to have been phagocytosed, since they are not within vacuoles, though a tenuous membrane appears to surround one particle (*arrow*). *Line* represents 0.1 μ. × 70,000

FIGURE 28.—Part of cytoplasm of megakaryocyte from bone marrow of a C3Hf/BiLw mouse with generalized leukemia, after injection of the Gross (passage-A) agent. Characteristic particles are present within cytoplasmic channels. Majority of these particles are mature. Occasionally particles are also present within specific granules (*arrows*). × 42,000

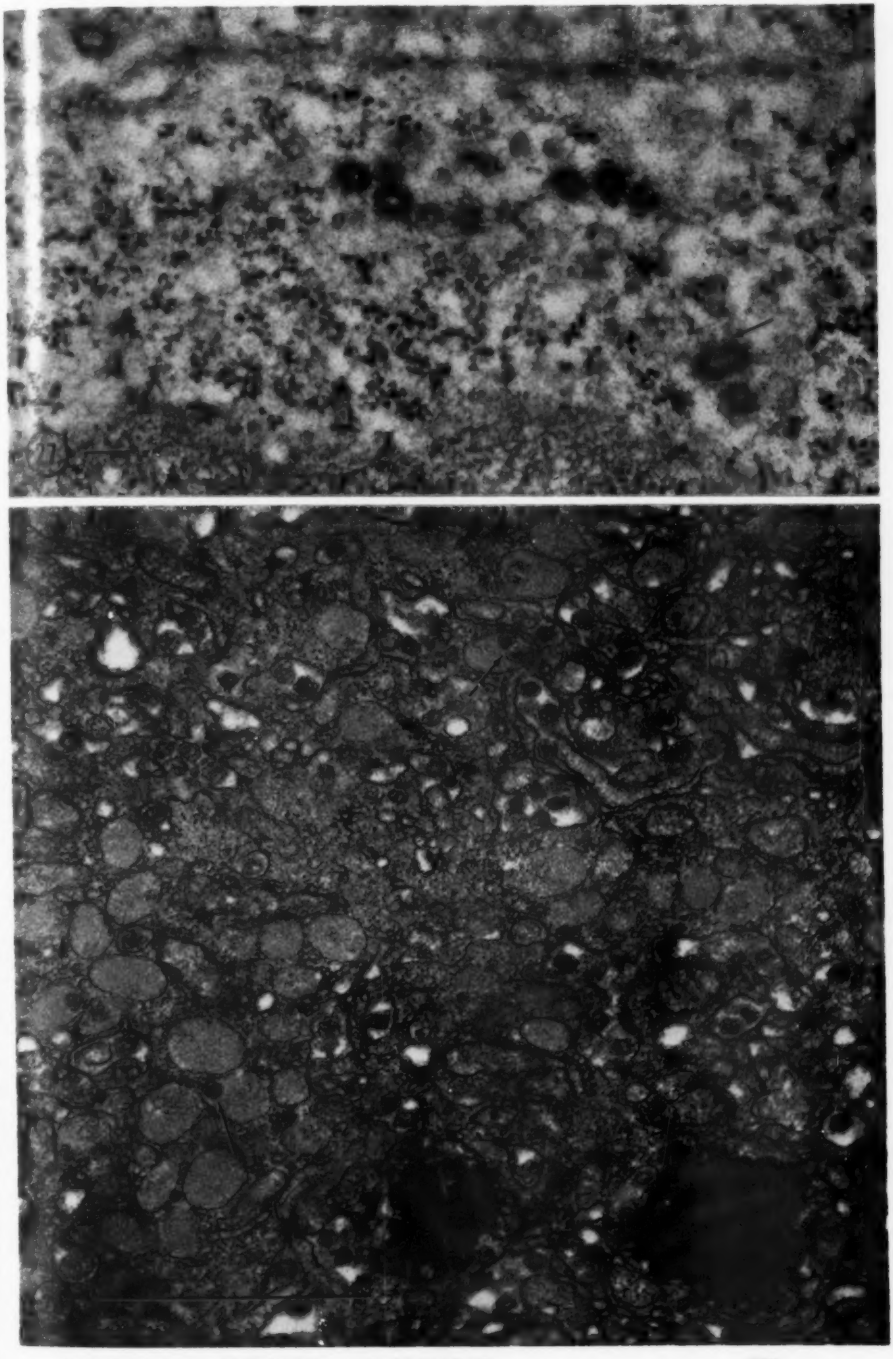

PLATE 107

FIGURE 29.—Part of cytoplasm of megakaryocyte similar to that shown in figure 28 but at higher magnification. Majority of particles in channels are mature but occasionally immature ones may be seen (*arrow*). *Line* represents 0.1 μ. × 70,000

FIGURE 30.—Part of cytoplasm of a megakaryocyte similar to that shown in figure 28. Immature particle is present within specific granule. *Line* represents 0.1 μ. × 70,000

FIGURE 31.—Part of cytoplasm of megakaryocyte similar to that shown in figure 28. All of these particles are immature and several are elongate (*arrows*). *Line* represents 0.1 μ. × 75,000

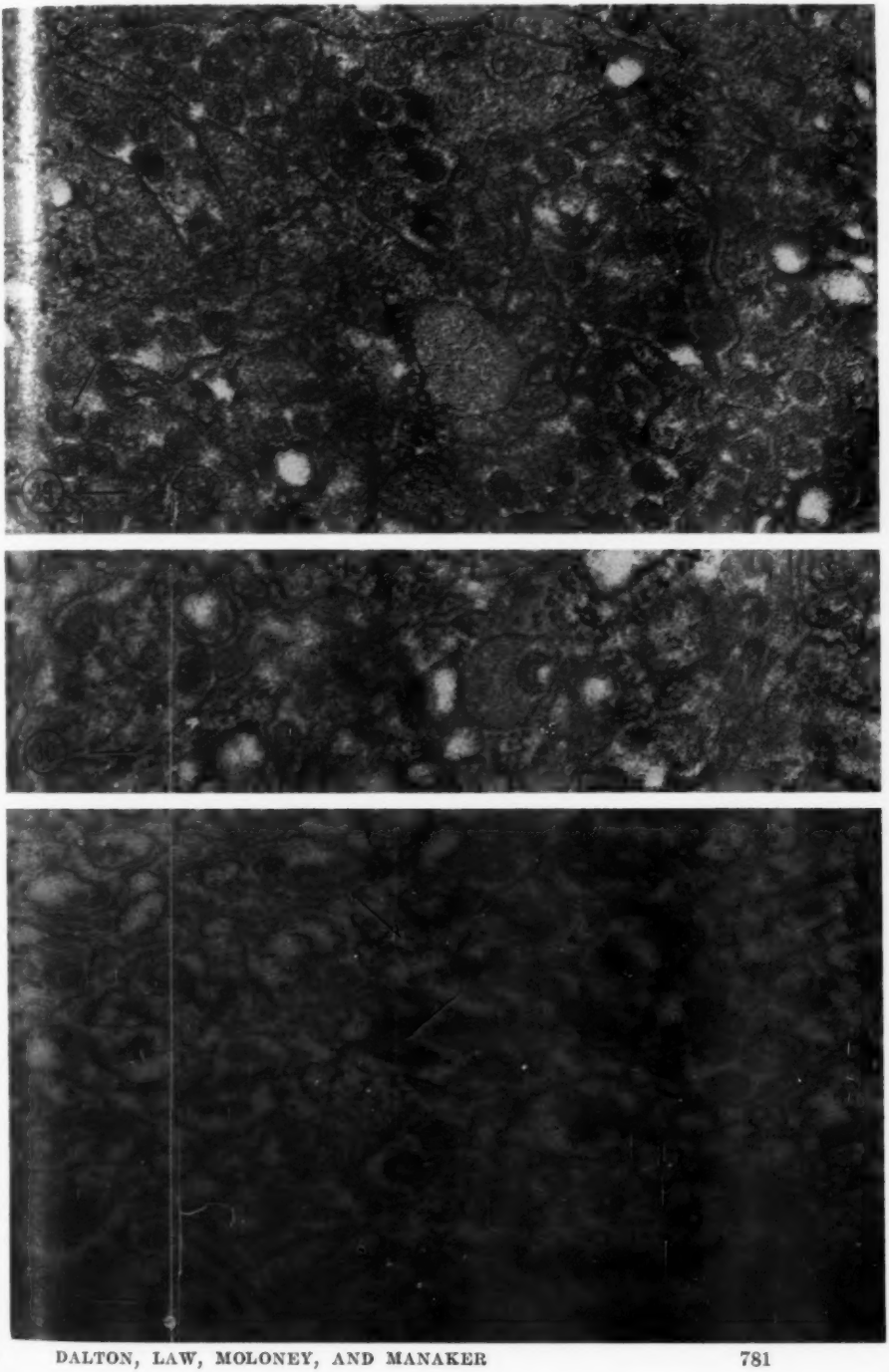

PLATE 108

FIGURE 32.—Part of cytoplasm of megakaryocyte from bone marrow of BALB/c mouse which developed generalized leukemia after introduction of the Manaker C–60 (Schwartz) agent. Characteristic particles are present in majority of cytoplasmic channels but not in specific granules. × 35,000

FIGURE 33.—Part of cytoplasm of megakaryocyte similar to that shown in figure 32. Majority of characteristic particles in cytoplasmic channels possess electron-lucent nucleoids (immature). Intermediate membrane is visible in some of particles between nucleoid and outer membrane (*arrows*). *Line* represents 0.1 μ. × 70,000

FIGURE 34.—Particles similar to those shown in figure 33 at higher magnification. *Line* represents 0.1 μ. × 200,000

FIGURE 35.—Characteristic extracellular particles in section of bone marrow from BALB/c mouse which developed leukemia after introduction of the Manaker C–60 (Schwartz) agent. Parts of cells near particles are considered to be lymphoblasts from the plasma membrane of one from which a particle is budding (*arrow*). *Line* represents 0.1 μ. ×88,000

FIGURE 36.—Characteristic particle forming at plasma membrane of lymphoblast similar to those shown in figure 35. *Line* represents 0.1μ. × 70,000

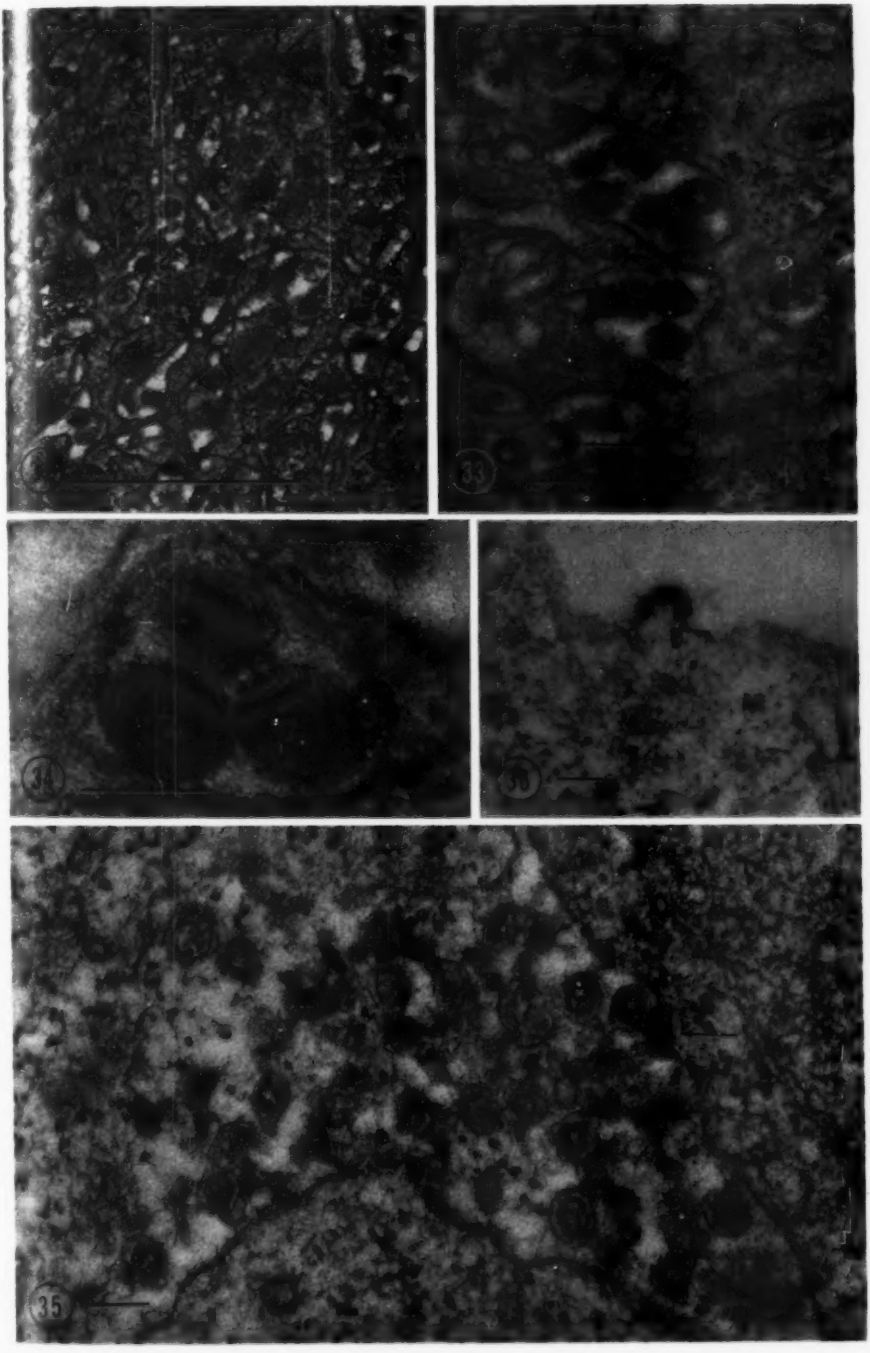
33
34
35

PLATE 109

FIGURE 37.—Part of cytoplasm of megakaryocyte from bone marrow of NIH (Swiss) mouse infected with the Friend agent. Numerous characteristic particles with electron-lucent nucleoids are present in channels. Outside diameter of these particles averages approximately 100 mμ. Rarely particles were found within specific granules (*arrow*). × 60,000

FIGURE 38.—Particles in megakaryocyte similar to the one illustrated in figure 37. Particles to *right* are immature, possessing electron-lucent nucleoids, those to *left* are mature, possessing electron-dense nucleoids. *Note* that the larger of the two particles to *left* has an outside diameter of 100 mμ while those to *right* are approximately 90 mμ in diameter. *Line* represents 0.1μ. × 150,000

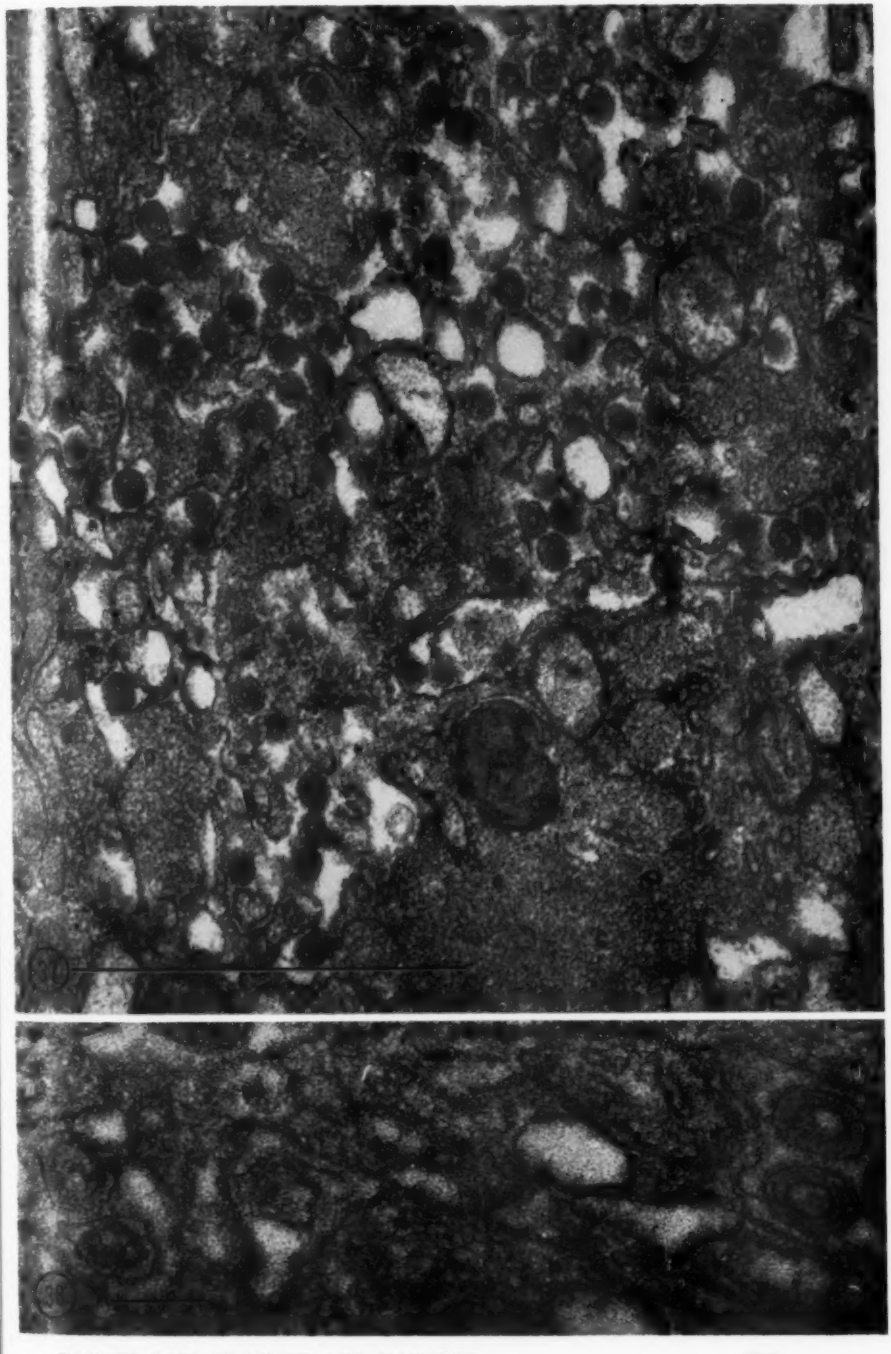

PLATE 110

FIGURE 39.—Part of cytoplasm of giant cell from bone marrow of a C57BL/KaLw mouse with radiation-induced leukemia. With the light microscope these cells have appearance of megakaryocytes. As this electron micrograph illustrates, these cells possess none of the fine structural features of megakaryocytes. Rather, they regularly contain numerous long strands of amorphous, moderately electron-dense material. × 26,000

FIGURE 40.—Part of cytoplasm of cell similar to that shown in figure 39. Bodies considered to be the result of phagocytosis, as well as amorphous strands, are present. × 53,000

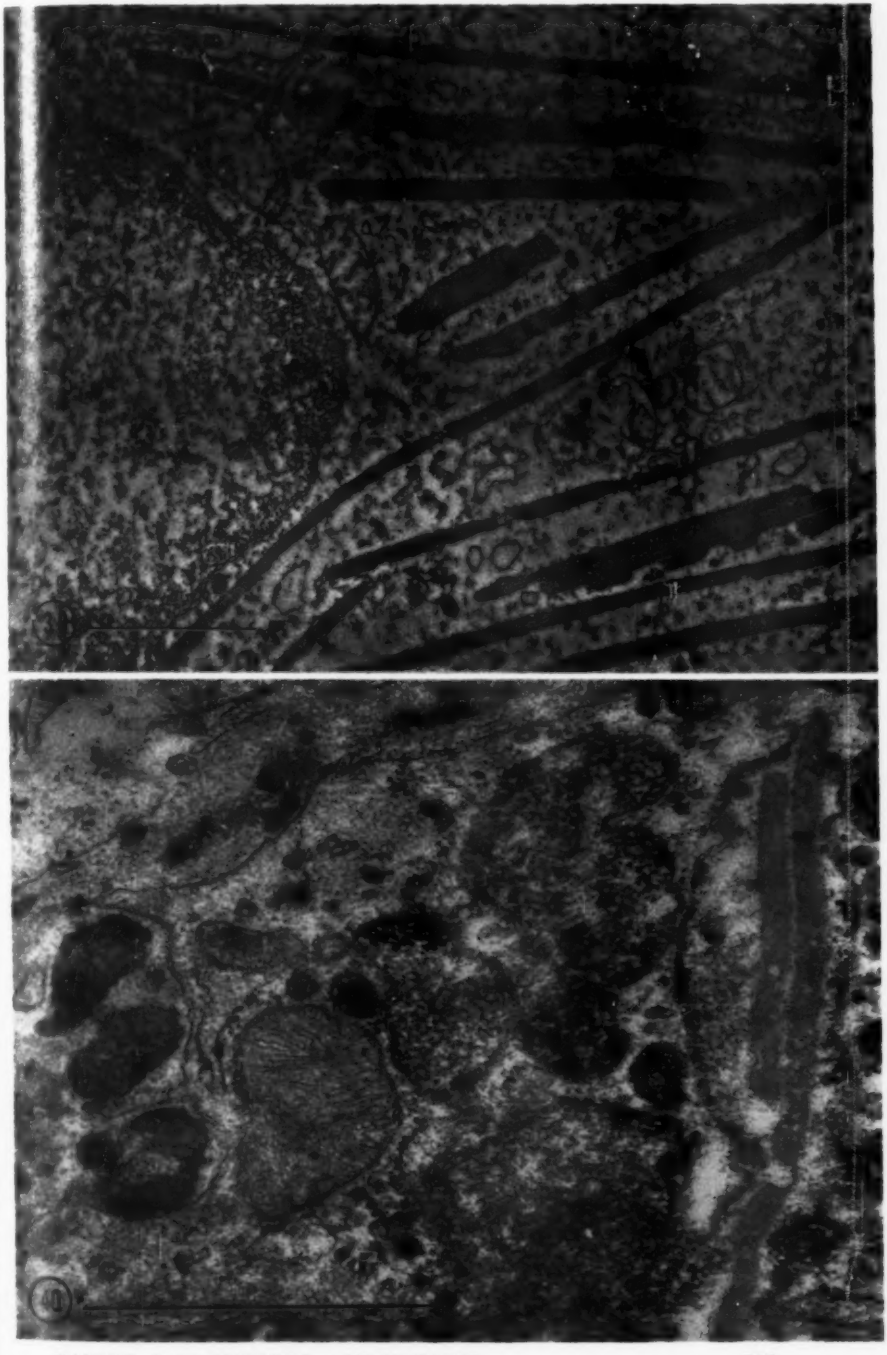

PLATE 111

FIGURE 41.—Part of cytoplasm of megakaryocyte from bone marrow of C3Hf/FgLw mouse with spontaneous generalized leukemia. Several characteristic particles are present within specific granules. × 53,000

FIGURE 42.—Part of cytoplasm of megakaryocyte similar to that shown in figure 41. Particles, some mature (A) and some immature (B), are present in cytoplasmic channels. One particle is in process of formation (*arrow*). × 53,000

FIGURE 43.—Part of cytoplasm of megakaryocyte similar to that shown in figure 41. One particle is in early stage of formation at border of specific granule. *Line* represents 0.1 μ. × 70,000

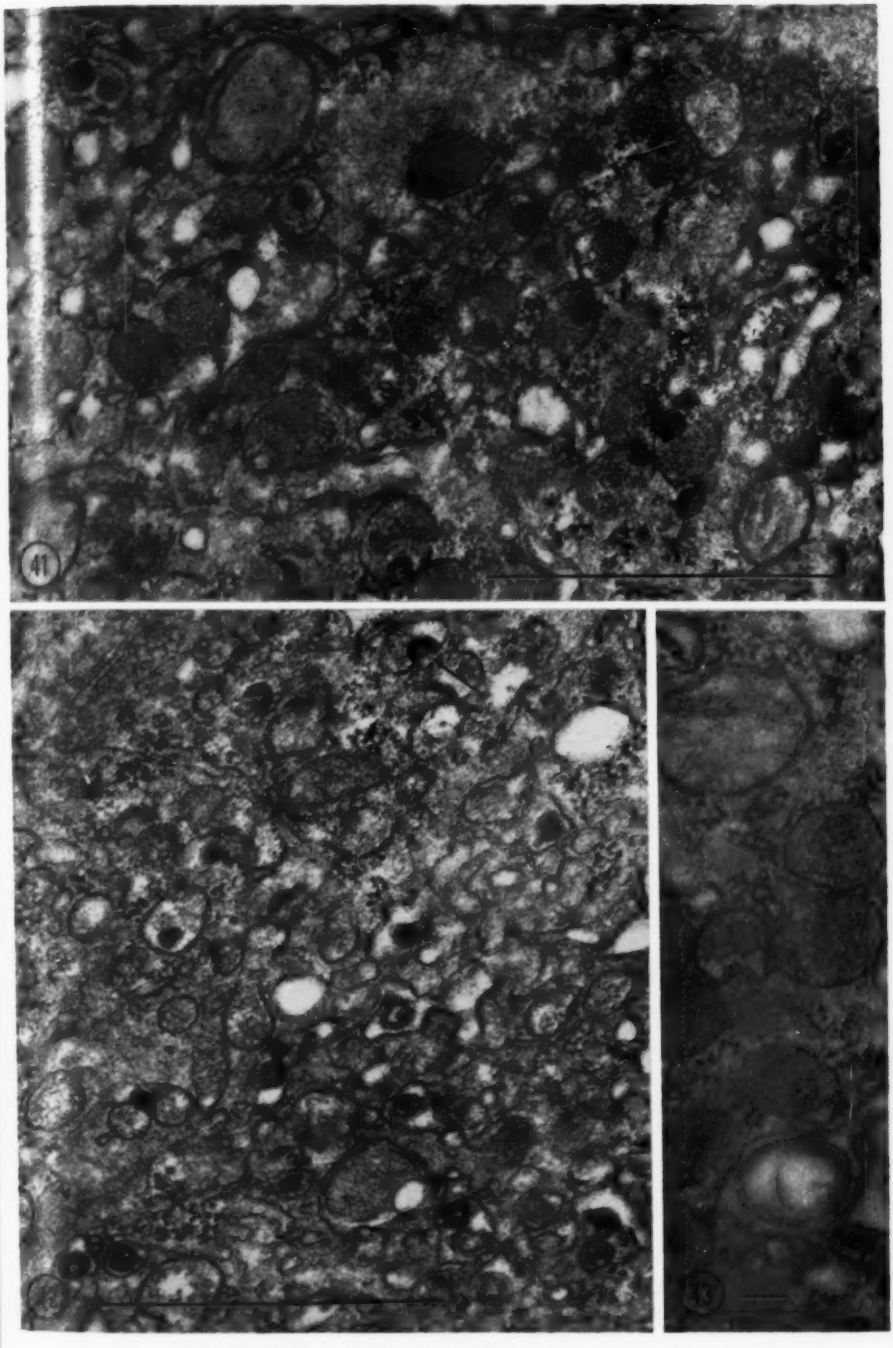

PLATE 112

FIGURE 44.—Part of cytoplasm of megakaryocyte from bone marrow of AKR mouse with spontaneous generalized lymphoid leukemia. Particles are present within specific granules, one in process of formation. *Line* represents 0.1 μ. × 75,000

FIGURE 45.—Part of cytoplasm of megakaryocyte similar to that shown in figure 44. Immature particles are present within cytoplasmic channels. × 53,000

FIGURE 46.—Part of cytoplasm of megakaryocyte similar to that shown in figure 44. Several immature particles including an elongated one (*arrow*) are present in cytoplasmic channels. × 53,000

FIGURE 47.—Three mature extracellular particles from bone marrow of AKR mouse with spontaneous lymphoid leukemia. Outside diameter of these particles averages approximately 90 mμ. *Line* represents 0.1 μ. × 90,000

FIGURE 48.—Three immature particles from bone marrow of AKR mouse with spontaneous lymphoid leukemia. Largest of these particles has outside diameter greater than 100 mμ. *Line* represents 0.1 μ. × 90,000

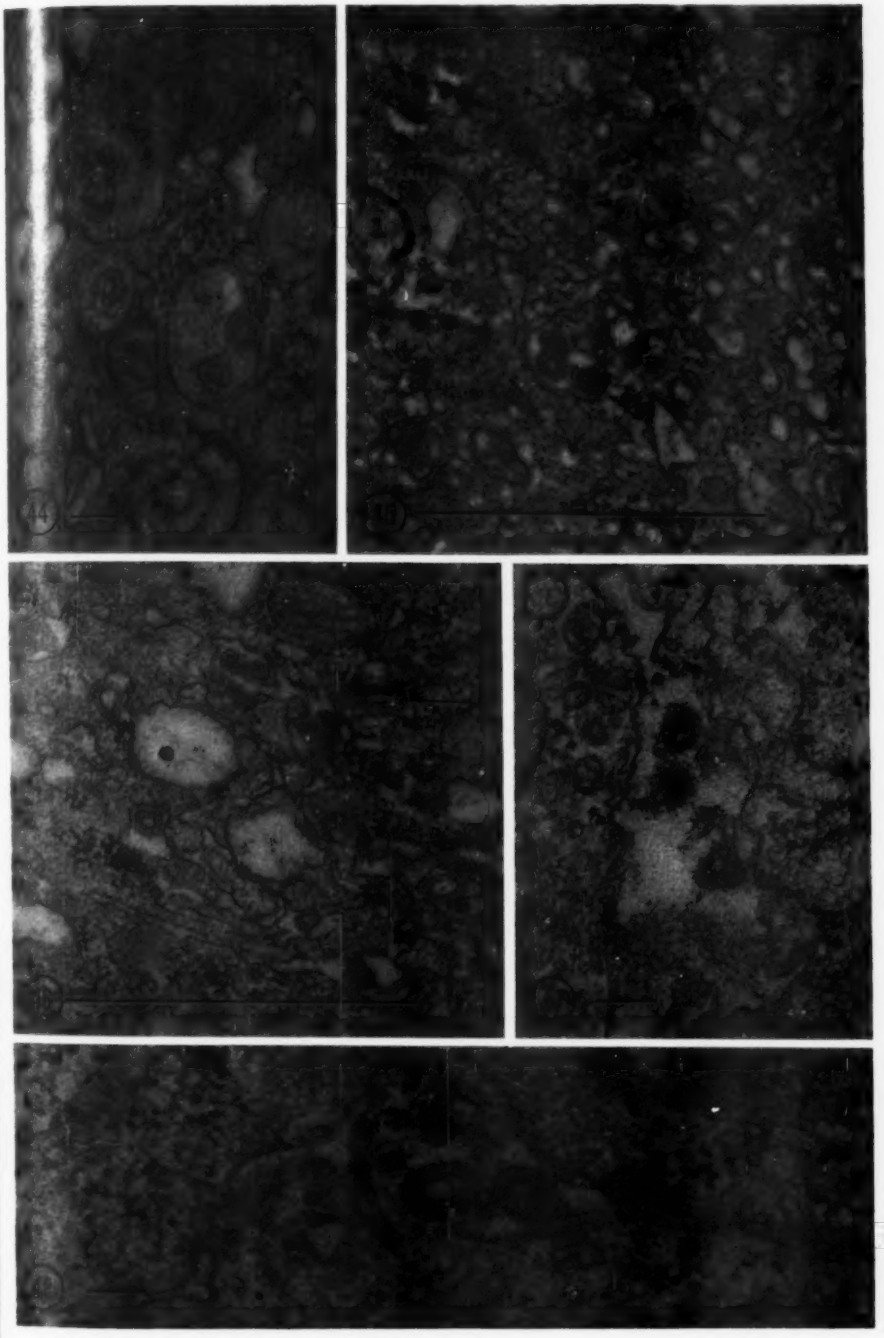

Persistent Theiler's Virus in Ependymoma Tissue Culture and the Problem of Virus-Like Bodies Seen by Electron Microscopy [1,2]

HAROLD E. PEARSON *and* RICHARD F. BAKER,
Departments of Public Health and Medical Microbiology, University of Southern California School of Medicine, and the Laboratory Division, Los Angeles County Hospital, Los Angeles, California

SUMMARY

Theiler's GDVII virus persistently infected mouse ependymoma cells in tissue culture; infectious virus might persist for longer than a year, or it might spontaneously disappear after several months. Electron-dense oval bodies approximately 85 mμ in diameter were found at the surface of cells infected only for 6 days and at a time when the viral titer was maximal. The nature of these bodies is unknown. Uninfected ependymoma cells of the strain studied contained electron-dense cytoplasmic bodies of another type. They were approximately 65 mμ in diameter, double-walled (type A Bernhard), and appeared to originate from the walls of cytoplasmic vacuoles. These were similar to bodies in various murine tumors described by other investigators.—J. Nat. Cancer Inst. 27: 793-805, 1961.

SEVERAL VIRAL and rickettsial agents are known to produce latent infections of tissue-culture cells. This relationship may occur only under special conditions such as the presence of immune serum, association with the interference phenomenon or cells resistant to virus for unknown reasons (*1*, *2*). The general recognition of this phenomenon, particularly as applicable to mammalian viruses, concomitant with the description of various electron-dense, polymorphic bodies in cells, has engendered numerous reports and much speculation as to whether such bodies are know or unknown viruses. This subject has been reviewed recently (*3–6*) and the bodies have been classified morphologically into several types (*3*, *4*). Although it usually has been assumed that these bodies are viruses, their viral nature mostly has not been established. The present study concerns persistent infection of murine ependymoma tissue cultures with mouse encephalomyelitis virus. The presence of 2 types of bodies found separately in these cells as seen by electron microscopy will be described. A preliminary report appeared elsewhere (*7*).

[1] Received for publication January 24, 1961; revised July 5, 1961.
[2] Aided by grants E-2721 and E-3468 from the National Institute of Allergy and Infectious Diseases, National Institutes of Health, Public Health Service.

603724—61——7

MATERIALS AND METHODS

A cell line, which possibly was a clone originally, was obtained from a chemically induced ependymoma in albino strain A mice. Prior to isolation of the tumor cell line the tumors were passed repeatedly by the subcutaneous route in albino A mice obtained from a commercial source; the genetic homogeneity of the mice is unknown. The cells had been maintained continuously for several years in tissue culture on glass at 37° C in Eagle's solution with 5 to 10 percent horse or calf serum (*8–10*). Fluid was changed twice weekly. The GDVII strain of Theiler's mouse encephalomyelitis virus has been carried by us for the past decade in tissue cultures of hybrid albino mouse brain. This virus killed mice in 2 to 14 days after intracerebral inoculation, with histologic changes of encephalitis; it produced cold hemagglutination of human red blood cells and was neutralized by rabbit serum prepared originally from animals immunized with the brains of infected mice. Virus titers were assayed by intracerebral injection of mice with serial tenfold dilutions of test material. Mouse brain tissue-culture virus usually had a titer of 10^{-5}. Before virus assay, infected tissue cultures were homogenized in the supernatant culture fluid for 10 minutes in a Raytheon 250W sonic oscillator. Cells were fixed in 1 percent osmic aicd, embedded in butyl methacrylate, cut on an ultramicrotome set to cut at 30 mμ thick, and examined with an EMU-1 electron microscope.

RESULTS

Ependymoma cells were infected with a 10^{-3} dilution (100 LD50) of virus, and the range of titers of virus attained after cultivation for various intervals was as follows: 2 days, 10^{-3}, $^{-4}$; 4 to 6 days, 10^{-4}, $^{-5}$; 7 days, 10^{-4}; 14 to 60 days, 10^{-1}, $^{-2}$. The maximal titer was found at 4 to 6 days, but virus persisted for prolonged periods of at least 7 to 16 months in several experiments; it disappeared spontaneously in different experiments after 2 to 4, 7 to 10, and 16 to 18 months. The virus was not noticeably cytolytic for these cells, but the presence of virus was associated after 1 to 2 days with the release of cells from the glass so that many cells were found in the supernatant tissue-culture fluid; vital staining of the floating cells with trypan blue showed that they were not viable. These cells were not examined with the electron microscope. Virus was constantly present in the supernatant fluid of persistently infected cultures. The percentage of cells infected at any given time was not determined. No differences were seen in the appearance of infected and noninfected cells grown for several days to months on coverslips and stained with hematoxylin-eosin. The presence of virus did not markedly affect the rate of cell proliferation as judged by mitotic indexes. The numbers of mitoses were counted for at least 600 cells from at least 3 cultures of infected and noninfected cells. Approximately 1 percent of cells was in mitosis.

Two types of electron-dense bodies were observed separately in the cells. The first type was present in large numbers in infected and noninfected cells. The bodies were seen only in the cytoplasm; they were approximately spherical and were double-walled with a less dense interior. They resembled the type A bodies of Bernhard and Guérin (*4*). During the present investigation, which extended over 2 years, it was noted originally that the bodies occurred in groups enclosed in vacuoles which resembled endoplasmic reticulum (fig. 1a). Recent photographs showed few vacuoles, and the enclosing membranes were less sharply demarcated than they were previously (fig. 1b). The bodies occurred with greatest frequency in the cell interior and seldom were seen near the cell boundaries. They were not related to the nucleus or any area of the cytoplasm such as the Golgi zone. The double membrane of the particle is clearly seen in figure 2 at medium magnification, while figures 3 and 4 show incomplete forms. A frequently observed form is in figure 4, in which elongations occur with a peripheral infolding of the double wall. In figure 4 the outer membrane is resolved as a doublet as is also the wall of the enclosing vacuole. A close relationship between the bodies and the enclosing vacuole is seen in figure 6, in which the wall of the vacuole is clearly continuous with the outer membrane of the type A body. This suggests that the body is pinched off from the vacuolar wall. Figure 5 shows a typical body in the cytoplasm with dimensions of approximately 650 A and with the components of the double membrane separated by an average distance of 75 A. The interior of the body is slightly more dense than the cytoplasmic matrix.

The second type of electron-dense body was seen only at the external surface of ependymoma cells infected with Theiler's virus and examined 6 days after infection, at which time the virus titer was maximal. These were also roughly spherical in section and were approximately 85 mμ in diameter (fig. 7). They were fairly uniform in density; some contained small areas of increased density. Such cells did not have cytoplasmic bodies of the type previously described, but this finding may not be valid if many more cells were examined. The infected cells did not differ in appearance from noninfected cells except for the presence of the electron-dense bodies just mentioned, and these were seen only in a few cells.

The presence of the first type of body described raised the question that possibly an unknown virus was carried by our stock ependymoma cells. As far as our cells are concerned, the bodies might be a developmental or a mature form of an unknown virus introduced by the calf- or horse-serum components of the culture medium, or they might be any murine virus that remained latent in the cells during 4 years that they had been maintained *in vitro*. The only viruses known to be present in the laboratory have been herpes simplex, polio, polyoma, and Theiler's. Herpes and polio virus probably can be excluded from consideration because bodies were not found similar to those described in cells known to be infected with these viruses (*11–13*). We have repeatedly subjected our stock culture cells to sonic disintegration in the presence of super-

natant culture fluid. This material was injected intracerebrally and intraperitoneally in suckling and 3-week-old Swiss mice; no disease developed. This finding tends to exclude the possibility that lymphocytic choriomeningitis (LCM), Theiler's, or mouse hepatitis viruses were present. Eight suckling and 8 adult DBA strain mice were similarly inoculated and killed 2 months later. There was no splenic enlargement suggestive of infection with Friend leukemia virus. Sonically disintegrated stock ependymoma culture cells were inoculated in tissue cultures of mouse fibroblasts known to be sensitive to lysis by polyoma virus. No lysis occurred during a period of 35 days. Electron microscopy of these fibroblasts after 5 and 10 days, respectively, did not reveal any abnormal component. Likewise no abnormal cellular particles were seen in fibroblasts continuously exposed in culture for 10 days to sonically fragmented ependymoma cells. The observations suggest that if mouse salivary-gland virus (SGV) (*14*, *15*) or other readily transmissible agents were present in our cells, these did not produce electron-dense bodies of the type under consideration.

DISCUSSION

Durable latent infection is now known to occur in relatively many cell-virus systems. This relationship demands that virus replication must be sufficiently slow to prevent destruction of all cells, but fast enough to maintain a continuing viral population. The relationship is a precarious one, since virus disappeared spontaneously from our cells, for reasons unknown, on 3 separate occasions. The nature of this cell resistance is unknown. It might result from chance combinations of factors that affect cell permeability, viral replication rates, and viral release.

Bernhard and Guérin (*4*) have classified virus-like cellular bodies (excluding crystal forms) into 3 morphologic types. The type A bodies, as in the present report, have been described mostly in the cytoplasm of mouse tumor cells, such as Ehrlich (*16–18*), mammary carcinoma (*3*, *19*, *20*), hyperplastic mammary nodules (*21*), leukemias (*4*, *22–25*), plasma-cell tumors (*26–28*), melanoma (*29*), and chemically induced carcinoma (*30*); they also were found in L cells (*31*). The nature of these particles is unknown. They may be a cell component peculiar to mouse tumor cells. They could represent a metabolic product used by the cell and associated with malignancy, or possibly they reflect a degenerative change occurring only in certain neoplastic cells; they are not found in all mouse tumors. Since those described so far are approximately the same size and uniform shape, it might be assumed that they have a common mechanism of production. However, multiple sites of origin (plasma membrane and mitochondria) have been described, and it has been suggested that the type A bodies may be variants of types B and C bodies (*3*, *28*). Our

present observations and those of others (*16, 18, 23, 28*) suggest that type A bodies can originate from the endoplasmic membranes or from cytoplasmic vacuoles, perhaps not connected with the endoplasmic reticulum. Those found in mouse mammary carcinoma cells may be closely associated with the Golgi zone (*3, 28*). Bernhard (*3*) points out that the endoplasmic reticulum frequently is altered in tumor cells and in response to various environmental changes. The high electron density of the particles might be expected, if they contain lipides, lipoproteins, or nucleoproteins. If the bodies are artifacts, it is difficult to understand why they should be peculiar to mouse tumors. The type A particles may represent known viruses, including tumor agents, or they may be unknown viruses associated with latent infections. This implies that they are capable of invasion of other cells in which they would find an environment suitable for their replication. Type A and type C virus-like particles found in 2 sublines of L cells were not transmissible to a third subline that did not contain them (*31*). Similar bodies found in mouse plasma cells could not be transmitted (*27, 28*). We were unable to pass our type A bodies to mouse fibroblasts in tissue culture. The bodies may be incomplete viruses not capable of extracellular survival. It has been suggested that the absence of a central, electron-dense nucleoid and the lack of extracellular occurrence support the concept that the bodies are not infectious virus (*27*); they sometimes are found outside the cell (*28*). The viral nature of these particles is difficult to establish and this has not been done.

The origin of the type B bodies seen at the surface of our infected cells is not clear. They might be a rarely occurring variant of the type A bodies; possibly they are Theiler's virus. If this were so, one would expect them to be much smaller than they appear to be. They might be another virus, possibly of murine origin that, in some unknown manner, had contaminated our Theiler's virus stock. If this were LCM virus, the particles should be smaller. Intracerebral passage in mice of our stock Theiler's virus has not resulted in infections that resemble LCM disease clinically or histologically. Our type B bodies resemble somewhat the spheres seen at the surface of chick chorio-allantoic entodermal cells infected with influenza virus (*32*). The latter presumably are infectious particles and contain an electron-dense, internal body 20 to 22 mμ in diameter.

The precise nature of the various bodies associated with viral infection of cells or found in cells thought to contain virus will not be determined by speculation or by description of the phenomenon. It will be necessary to utilize new techniques that permit qualitative identification of cell components. Of methods presently available, ferritin-conjugated antibody can be used to identify viral antigen within the cell and to localize its position by electron microscopy (*33*). New methods to stain cell components differentially are urgently needed. Possibly this can be done with heavy metals or other electron-dense substances that could be identified by electron microscopy.

REFERENCES

(1) Symposium on Latency and Masking in Viral and Rickettsial Infections. Minneapolis, Burgess Publishing Co., 1958.

(2) GINSBERG, H. S.: The significance of the viral carrier state in tissue culture systems. Med. Virol. 1: 36–58, 1958.

(3) BERNHARD, W.: Electron microscopy of tumor cells and tumor viruses. Cancer Res. 18: 491–509, 1958.

(4) BERNHARD, W., and GUÉRIN, M.: Présence de particules d'aspect virusal dans les tissus tumoraux de souris atteintes de leucémie spontanée. Compt. rend. Acad. sc. 247: 1802–1805, 1958.

(5) DMOCHOWSKI, L., and GREY, C. E.: Studies on submicroscopic structure of leukemias of known or suspected viral origin. Blood 13: 1017–1042, 1958.

(6) DMOCHOWSKI, L.: Viruses and tumors. Bact. Rev. 23: 18–40, 1959.

(7) PEARSON, H. E., and BAKER, R. F.: Latent infection of a mouse tumor with murine encephalomyelitis virus. Fed. Proc. 18: 591, 1959.

(8) PEARSON, H. E., and LAGERBORG, D. L.: Isolation of tumor cell colonies in tissue culture. Proc. Soc. Exper. Biol. & Med. 98: 247–249, 1958.

(9) ———: Propagation of Theiler's virus in murine ascitic tumors. Proc. Soc. Exper. Biol. & Med. 92: 551–553, 1956.

(10) ———: Growth of mouse encephalomyelitis virus in murine nervous tissue tumors. J. Immunol. 75: 134–136, 1955.

(11) MORGAN, C., *et al.*: Structure and development of viruses as observed in the electron microscope. I. Herpes simplex virus. J. Exper. Med. 100: 195–202, 1954.

(12) ———: Intranuclear crystals of herpes simplex virus observed with the electron microscope. Virology 5: 568–571, 1958.

(13) SJÖSTRAND, F. S., and POLSON, A.: Macrocrystalline patterns of closely packed poliovirus particles in ultra thin sections. J. Ultrastruct. Res. 1: 365–374, 1958.

(14) SMITH, M. G.: Propagation of salivary gland virus of the mouse in tissue cultures. Proc. Soc. Exper. Biol. & Med. 86: 435–440, 1954.

(15) BRODSKY, I., and ROWE, W. P.: Chronic subclinical infection with mouse salivary gland virus. Proc. Soc. Exper. Biol. & Med. 99: 654–655, 1958.

(16) FRIEDLANDER, M., and MOORE, D. H.: Occurrence of bodies within endoplasmic reticulum of Ehrlich ascites tumor cells. Proc. Soc. Exper. Biol. & Med. 92: 828–831, 1956.

(17) SELBY, C. C., *et al.*: Submicroscopic cytoplasmic particles occasionally found in the Ehrlich mouse ascites tumor. Cancer Res. 14: 790–794, 1954.

(18) ADAMS, W. R., and PRINCE, A. M.: An electron microscope study of the morphology and distribution of the intracytoplasmic "virus-like" particles of Ehrlich ascites tumor cells. J. Biophys. & Biochem. Cytol. 3: 161–170, 1957.

(19) BANG, F. B., *et al.*: Electron microscopic evidence concerning the mammary tumor inciter (virus); study of normal and malignant cells from mammary gland of mice. Bull. Johns Hopkins Hosp. 98: 255–285, 1956.

(20) GOLDFEDER, A., GELBER, D., and MOORE, D. H.: An electron microscope study of spontaneous mammary carcinomas in a subline of strain DBA mice. J. Nat. Cancer Inst. 25: 827–846, 1960.

(21) PITELKA, D. R., DEOME, K. B., and BERN, H. A.: Viruslike particles in precancerous hyperplastic mammary tissues of C3H and C3Hf mice. J. Nat. Cancer Inst. 25: 753–778, 1960.

(22) DE HARVEN, E., and FRIEND, C.: Electron microscope study of a cell-free induced leukemia of the mouse. A preliminary report. J. Biophys. & Biochem. Cytol. 4: 151–156, 1958.

(23) ———: Further electron microscope studies of a mouse leukemia induced by cell-free filtrates. J. Biophys. & Biochem. Cytol. 7: 747–752, 1960.

(*24*) HEINE, U., *et al.*: Virusartige Partikeln in zellfrei über-tragbaren Mäuseleukämien. Naturwissenschaften 44: 449–450, 1957.

(*25*) DMOCHOWSKI, L., and GREY, C. E.: Electron microscopy of tumors. Texas Rep. Biol. & Med. 15: 704–721, 1957.

(*26*) HOWATSON, A. F., and MCCULLOCH, E. A.: Virus-like bodies in a transplantable mouse cell tumor. Nature, London 181: 1213–1214, 1958.

(*27*) DALTON, A. J., POTTER, M., and MERWIN, R. M.: Some ultrastructural characteristics of a series of primary and transplanted plasma-cell tumors of the mouse. J. Nat. Cancer Inst. 26: 1221–1268, 1961.

(*28*) PARSONS, D. F., *et al.*: Electron microscopy of plasma cell tumors of the mouse. I. MPC-1 and X5563 tumors. II. Tissue cultures of X5563 tumor. J. Biophys. & Biochem. Cytol. 9: 353–368, 369–381, 1961.

(*29*) DALTON, A. J., and FELIX, M. D.: The electron microscopy of normal and malignant cells. Ann. New York Acad. Sc. 63: 1117–1140, 1956.

(*30*) THIERY, M., *et al.*: Virus-like particles in chemically induced carcinoma of the uterine cervix. Nature, London 183: 694–695, 1959.

(*31*) DALES, S., and HOWATSON, A. F.: Virus-like particles in association with L strain cells. Cancer Res. 21: 193–197, 1961.

(*32*) MORGAN, C., ROSE, H. M., and MOORE, D. H.: Structure and development of viruses observed in the electron microscope. III. Influenza virus. J. Exper. Med. 104: 171–182, 1956.

(*33*) MORGAN, C., *et al.*: Electron microscopic localization of intracellular viral antigen by the use of ferritin-conjugated antibody. Virology 14: 292–296 1961.

PLATES

603724—61——8

PLATE 113

FIGURE 1a.—Uninfected ependymoma cell. Electron-dense bodies in cytoplasmic vacuoles of noninfected ependymoma cell. This is typical of cells studied at beginning of a 2-year period.

FIGURE 1b.—Recent photograph of same cell line. There is less segregation of particles. Enclosing membrane is present but is less prominent. Portion of cell nucleus is at *upper right*; cell boundary is at *lower left*. × 29,500

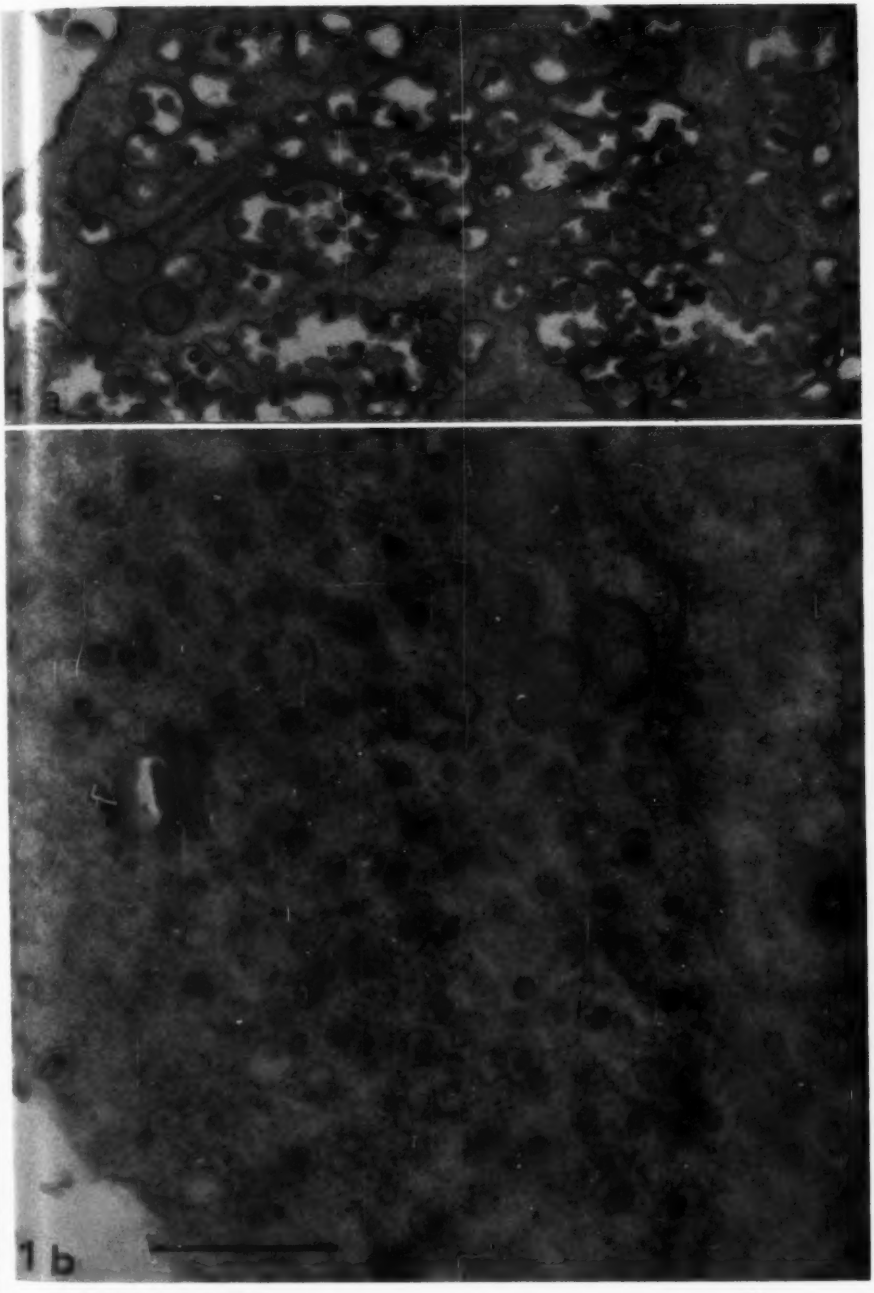
1 a
1 b

PLATE 114

FIGURE 2.—Uninfected ependymoma cell. Double-walled type A bodies in cytoplasm. The enclosing vacuole shown in figures 1a, 3, 4, and 6 is not seen in this view. × 100,000

FIGURES 3 and 4.—Uninfected ependymoma cell. Various forms of type A particles shown in relation to the bounding double-walled vacuoles. Figure 3 at *lower left* shows incomplete ring, while figure 4 illustrates indentations in wall of particles at midline. Outermost membranes of the particle are themselves doubled, as seen in figure 4. × 150,000

FIGURE 5.—Uninfected ependymoma cell. Only traces of enclosing vacuole are seen around this particle. Average dimensions of these type A bodies are 650 A, with double membrane separation averaging 75 A. Density of matrix in center of bodies is usually slightly higher than density of surrounding cytoplasm. × 230,000

FIGURE 6.—Uninfected ependymoma cell. Two type A bodies are connected to wall of the enclosing vacuole, suggesting a pinching off. Outer membrane appears to be continuous with wall of vacuole. × 71,500

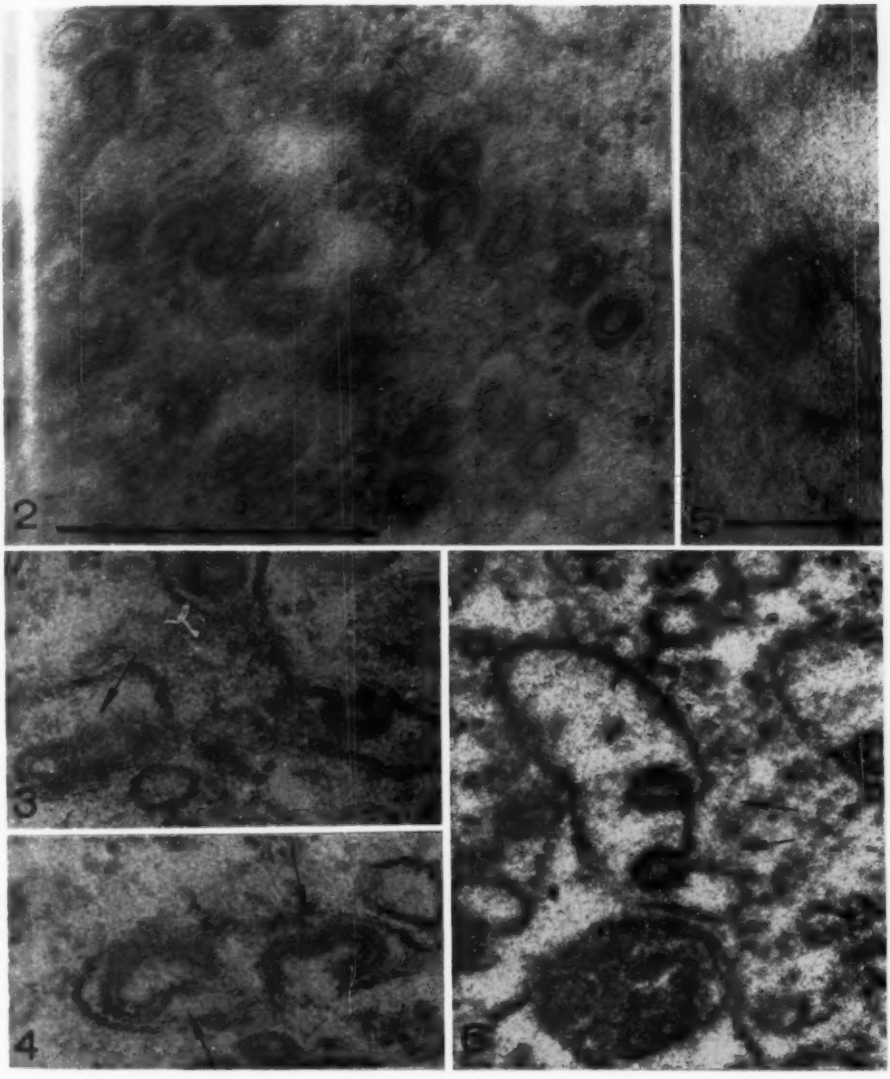
2
5
3
4
6

PLATE 115

FIGURE 7.—Ependymoma cell that had been infected with Theiler's virus for 6 days. Bodies are seen outside cell membrane. Type A particles were never seen in the same cell. × 94,000

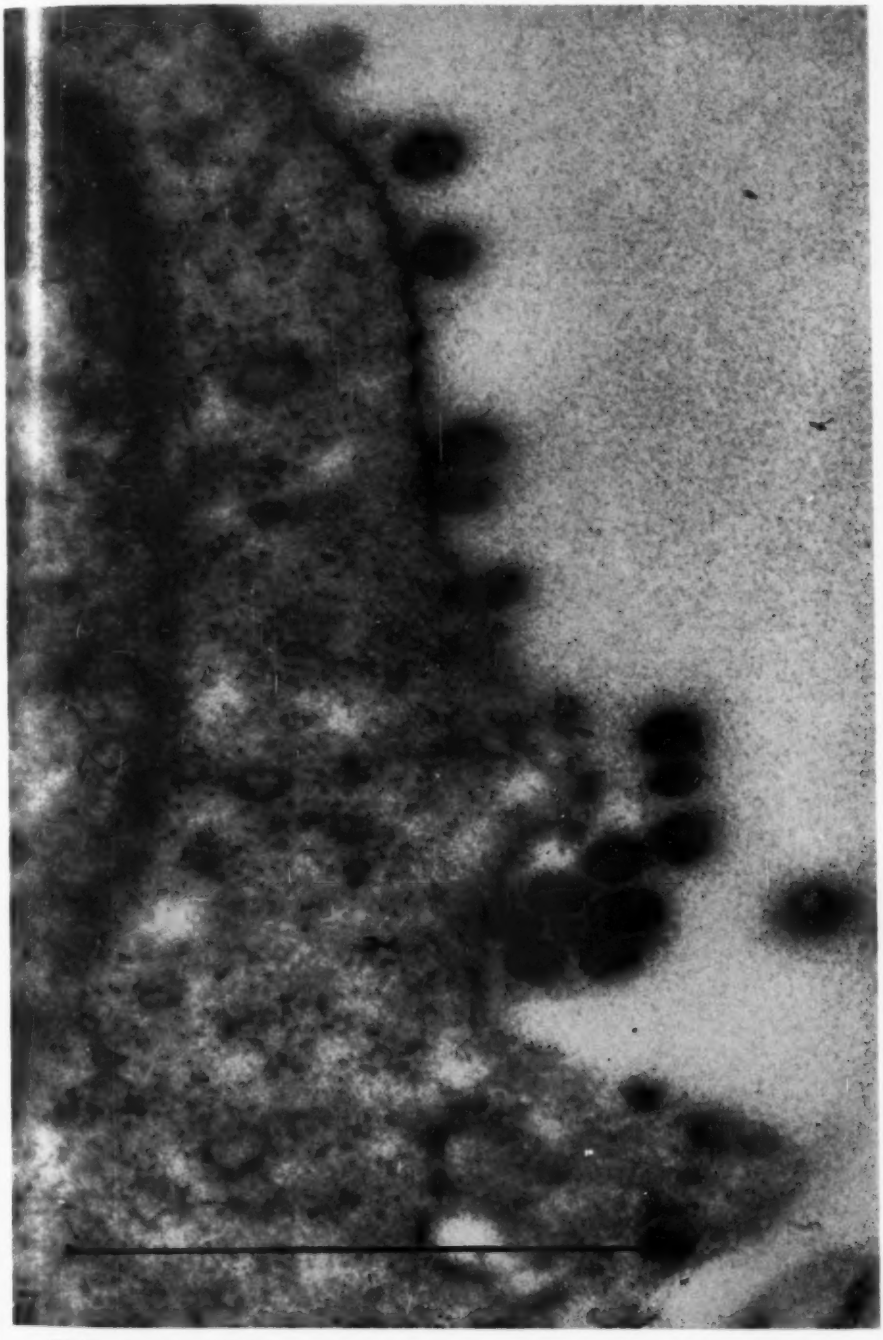

Evaluation of Inhibition of Human Tumor Tissue by Cancer Chemotherapeutic Drugs With an *In Vitro* Test [1,2]

JOSEPH A. DiPAOLO *and* JOHN E. DOWD,[3,4] *Roswell Park Memorial Institute, Buffalo, New York*

SUMMARY

An *in vitro* test system is presented that allows simultaneous testing of chemotherapeutic agents on human malignant tissue. Inhibition of dehydrogenase activity by the test compound is determined in an agar suspension of the homogenized tissue. Such a test system might be useful with biopsy material, since it allows selection of an agent, if any exists, that is effective on that particular material. Comparison of results with the use of normal and tumor tissue from the same patient demonstrated the topical toxicity of compounds. The fact that the most effective compounds were also the most toxic reaffirms the lack of specificity of these compounds for malignant tissue. From examination of over-all effectiveness at one concentration of drug, both compounds and tissue sites may be ranked: 5-Fluorodeoxyuridine was effective in the largest percentage, while *N*,*N*′,*N*″-triethylenethiophosphoramide was least effective. Amethopterin, Nitromin, and 5-fluorodeoxyuridine were consistently the most effective compounds. Bone and connective tissues were most sensitive, and hemopoietic and lymphatic tissues least sensitive. Thirty-four tissues (17%) were not affected by any drug, and many tissues responded to only one or two drugs, which indicated the general resistance of most tissues to known chemotherapeutic compounds.—J. Nat. Cancer Inst. 27: 807-815, 1961.

ALTHOUGH A FEW compounds of limited value are available for clinical cancer chemotherapy, there is little information as to the effectiveness of any drug against a specific tumor type. Agar-diffusion tests with ascites tumor cells have been used to evaluate potential cancer chemotherapeutic agents by the determination of dehydrogenase activity and possible general cytotoxicity (*1–4*). Studies of dehydrogenase inhibition of human tumor tissue with reference to *in vitro* effects of chemotherapeutic agents have also been reported (*5*, *6*).

[1] Received for publication March 9, 1961; revised July 13, 1961.

[2] Supported in part by research grant CY-3553 (C3) from the National Cancer Institute, National Institutes of Health, Public Health Service.

[3] The authors express their appreciation to the clinical staff of the Roswell Park Memorial Institute, in particular to Drs. G. E. Moore and A. Watne, for providing tissue specimens and for clinical evaluation of drug effectiveness, and to Mr. John Gallagher for able technical assistance.

[4] The di-(α-hydroxy-β-trichloroethyl)phosphine was supplied by Hooker Chemical Corporation, Niagara Falls, N.Y.

603724—61——9

The present report is an evaluation of the use of fresh surgical human malignant tissue in an *in vitro* test system based on the ascites agar method (7) for selecting from available compounds the best ones for clinical application. Tissue taken shortly after death is also being studied in a search for new agents for cancer chemotherapy.

MATERIALS AND METHODS

Technique.—Fresh, sterile, human malignant tissue and, when possible, "normal" tissue from the same patient were obtained directly from the operating room. Approximately 1 g of tissue, free of fat and other unwanted tissue, was transferred to a sterile petri dish. Protected within a hood, the tissue was finely minced with 2 scalpels fitted with #22 blades. In the event that cell separation proved difficult, 1 ml of ethylenediamine tetraacetate (3×10^{-4} M) containing 2×10^6 units of penicillin L was added. The mince was transferred to a glass homogenizer that was turned by hand two or three times after the addition of 10 ml of 0.25 M sucrose.

The suspension was centrifuged at 1000 rpm for 2 minutes after addition of more sucrose solution. The sucrose was discarded and the residue resuspended in 1 ml of normal saline. Tissue varied in hardness from sample to sample, at times requiring the addition of 0.25 percent trypsin and use of a magnetic stirrer subsequent to homogenizing, while other tissue was so soft that shaking in sucrose without homogenizing was sufficient to break it. Often the residue was examined under dark-contrast oil-immersion lens of a phase-contrast microscope to verify that the homogenate consisted mostly of tumor fragments and small clumps of cells.

The basic medium for the agar plates contained: peptone, 1 g; glucose, 0.5 g; sodium chloride, 0.25 g; hydrated sodium monohydrogen phosphate, 0.3 g; ionagar, 2 g; and distilled water, 100 ml. The *p*H of the medium was adjusted to 7.2. Cellular activity was determined with a 0.05 percent methylene blue solution as redox agent.

The drugs used in these experiments are presented in table 1. The concentration of drugs was determined as that which caused measurable and reproducible areas of inhibition under standardized conditions with Ehrlich ascites tumor in agar suspension. Excepting actinomycin D, solutions or suspensions were made to contain 1 mg of drug per ml; the amount placed on a 12.7 mm paper disc was 0.1 ml or 100 μg. Discs with actinomycin D contained 10 μg each of 100 μg per ml of solution. Discs were carefully dried under infrared lamp and stored in a deepfreeze until used.

For preparation of a pour plate, 8 ml of medium, 1.5 ml of rabbit plasma or pooled human serum after inactivation of complement, and the tissue homogenate in 1 ml of saline solution were mixed in a test tube and poured into a 90 mm petri dish. After the agar surface hardened, discs containing the drugs were added. Each plate had 10 discs. After

overnight refrigeration at 4° C, the plates were incubated for 5 to 7 hours at 37° C. Then the discs were removed, and plates washed with distilled water and covered with the redox agent. A circular glass plate was placed on the agar so that no air bubbles formed; the excess dye was poured off, and the petri dishes reincubated for a minimum of 3 hours or until the nondisc areas turned colorless. The area of unreduced dye indicating dehydrogenase inhibition or cell damage by the test drug was reported as + or − or as diameter measured in millimeters.

Reproducibility of method.—To examine the reproducibility of effect exhibited by a single compound applied to different discs on the same pour plate and by a single compound applied to different pour plates, a study was conducted using 10 agar pour plates containing mouse Ehrlich ascites

TABLE 1.—Results of *in vitro* and *in vivo* tests of inhibition of mouse Ehrlich ascites tumor, by the use of known cancer chemotherapeutic compounds

Code	Chemical*	Number of tests	Zone of inhibition *in vitro* (mm)		*In vivo*†
			Mean	Standard error	
HN2	2, 2′-Dichloro-*N*-methyldiethylamine hydrochloride	5	25. 8	±1. 3	+
TSPA	*N*, *N*′, *N*″-Triethylenethiophosphoramide	5	16. 0	±1. 0	+
AM	Amethopterin	5	17. 6	±1. 3	+
AD	Actinomycin D	5	18. 6	±1. 6	+
HN2O	Nitrogen mustard *N*-oxide	5	18. 0	±1. 8	+
6-MP	6-Mercaptopurine	5	12. 0	±0. 9	+
F	Fumagillin	5	16. 2	±0. 4	+
5-FUDR	5-Fluorodeoxyuridine	5	14. 6	±0. 4	+
AB-103	Benzyl *N*-bis-(ethylenimido)-phosphorocarbamate	5	14. 0	±0. 6	+
5-MU	5-Mercaptouracil	5	22. 6	±1. 8	−
5-MU + 5-FUDR	(5-Mercaptouracil + 5-fluorodeoxyuridine)	1	25. 0		+

*100 μg per assay, except 10 μg for AD.
† + indicates significant tumor inhibition as reported in the literature.

tumor and 6 drug-impregnated discs on each plate (table 1). The 10 tested compounds were distributed, 2 compounds to a plate, with 2 discs of each compound on each plate. The test was duplicated, making a total of 10 plates. Two blank discs were placed on each plate as a control. The pairs of compounds were placed on the plates at random, and individual discs were positioned on each plate at random.

Analysis of the variation in zone of inhibition for discs on the same plate containing the same drug shows an average standard deviation of 2.33 mm in diameter. For discs containing the same drug but on different plates, the average standard deviation of the zone of inhibition is 1.87 mm in diameter. Thus, results from the same drugs tested on different plates do not vary from results of the same drug on the same plates.

RESULTS AND INTERPRETATION

Comparison of *In Vitro* and *In Vivo* Results

Intermediate screening systems to bridge animal screening operations and clinical trials are needed in cancer chemotherapy. Compounds that are selected as effective in an *in vivo* screen, such as Ehrlich ascites tumors in mice, and that later show some clinical effectiveness should also be examined by the *in vitro* screen proposed here. A specific application might concern postoperative prophylactic treatment of cancer based on animal experimentation and the assumption that circulating cancer cells are more easily killed than attached cancer cells.

Table 1 lists the drugs used and compares the results found with the *in vivo* results obtained from various sources[5] (*8–10*). In both cases the compounds were tested against mouse Ehrlich ascites tumors. Inhibition was noted with the compounds used in the 2 tests with the exception of 5-mercaptouracil, effective *in vitro* but not *in vivo*.

Since most of the compounds tested were known to have some carcinostatic activity against Ehrlich ascites tumors, it is not surprising that both the *in vivo* and *in vitro* tests indicated the compounds as effective. Correlation was obtained with 17 of 25 compounds that had been tested with EF and ELD lines of Ehrlich ascites *in vivo* by Creech *et al.* (*11*).

Relationship of Ascites Results With Autopsy Material

Table 2, which lists the compounds tested, shows that whenever a compound was relatively effective on human malignant autopsy tissue it also produced a substantial zone of inhibition with the use of mouse Ehrlich

TABLE 2.—Correlation of *in vitro* tests with human autopsy tissue and Ehrlich ascites tumors

Compound	Human		Ehrlich
2-Amino-4-hydroxy-5-nitroso-6-hydroxy-pyrimidine	11/18*	15†	19‡
Di-(α-hydroxy-β-trichloroethyl)phospine	7/17	15	20
2-Thio-4,5,6-triaminopyrimidine	9/17	18	45
Iodoacetate	7/18	24	45
2,4,6-Triaminopyrimidine	5/17	15	30

*Number of specimens inhibited; total number tested.
†Average zone of inhibition for inhibited tumors.
‡Zones of inhibition in mm.

ascites tumors. Most compounds of unestablished chemotherapeutic value tested on various human autopsy material inhibited only 1 or 2 of the 17 specimens. Thus, on the basis of the experiments performed in this study, it cannot be concluded that complete correlation exists between the results of the 2 tests.

[5] Unpublished data of Dr. J. Ambrus.

Comparison of Normal and Malignant Surgical Specimens

Of the 203 human surgical specimens used in the agar-pour-plate tests, 59 were accompanied by specimens of "normal" nonmalignant tissue excised from a site adjacent to the malignant tissue. Drugs were tested on homogenates prepared from both the "normal" and tumor tissue. The results (table 3) indicate that drugs which inhibited dehydrogenase activity of the largest number of tumor cases were also most effective against the normal tissue. None of the compounds show selective toxicity to the tumor cells; a comparison of cases where the drug is inhibitory to tumor cells with cases where the drug is inhibitory to the "normal" cells shows only slight departure from a 1:1 ratio, which indicates no significant differences.

TABLE 3.—Comparison of *in vitro* test results on "normal" and tumor tissue from 59 patients

Drug	Normal and tumor	Effective on normal only	Tumor only	Neither
HN2	4	3	6	46
TSPA	1	1	2	53
AM	9	7	6	33
AD	9	7	13	30
HN2O	4	2	4	49
6-MP	2	3	6	48
F	0	3	4	52
5-FUDR	8	6	9	36
5-MU	7	8	6	38

Individual Drug Effects at Various Tissue Sites

Utilization of agents having laboratory evidence of antitumor activity would be facilitated by knowledge of site specificity.

Table 4 illustrates the effectiveness of the individual drugs at the concentration tested, as measured by the percentage of tissue specimens in which drug activity is exhibited. The over-all effectiveness of each drug is given in the final row of the table. 5-FUDR is effective in the largest percentage of cases, then AM, AD, HN2O, and HN2, all of which show little differentiation in over-all effect. It is possible that the differences in effectiveness between compounds do not fully reflect the therapeutic effectiveness of the compounds, since higher concentrations of a less effective compound might, without having adverse effects on normal tissue, produce the same effects as the compound showing greater effectiveness at the same concentration. Ideally, both tumor and normal tissue should be tested with several concentrations of each compound. The compound of choice in this test would be that which shows the greatest differential effectiveness at a minimal concentration. The tissue site referred to is the primary site of the tumor, though the specimen may be metastatic tissue from a different site. The percentages for the individual drugs at particular sites must be interpreted with some caution, since for some sites the number of specimens on which the percentages are based is quite small.

TABLE 4.—Drug effectiveness by site of tumor; percent of tissues on which drug was effective

Primary site of tumor	Number of tissues	HN2	TSPA	AM	AD	HN2O	6-MP	F	5-FUDR	Average percent for preceding drugs	AB-103	2,4,6-TAP	5-MU
											(46)*	(17)	(52)
Digestive organs and peritoneum	63	25	9	32	27	21	18	14	33	22	17	29	19
											(12)	(6)	(14)
Respiratory system	18	22	6	17	17	28	6	0	39	17	33	33	14
											(17)	(15)	(22)
Breast	32	25	9	47†	31	37	12	25	22	26	11	33	18
											(7)	(10)	(10)
Female genitals	17	29	18	12	18	24	24	18	24	21	28	20	0
											(5)	(4)	(8)
Malignant melanoma	9	11	0	22	22	11	0	0	44	14	20	0	13
											(16)	(14)	(21)
Bone and connective tissue	30	33	13	23	37	33	13	23	33	26	25	7	14
											(3)	(4)	(3)
Lymphatic and hemopoietic tissue	7	14	29	0	0	29	0	14	0	11	0	0	0
											(12)	(15)	(14)
Other sites	27	22	15	22	30	19	26	22	41	25	9	20	29
Total	(203)										(118)	(85)	(144)
Percentage		25	11	27	27	26	15	17	32	22	18	21	18

*In last 3 columns percentage is based upon number of tissues shown in parentheses.
†Effectiveness of drug at this site is significantly different from its over-all effectiveness.

Tissue and Site Sensitivity

A tissue specimen was regarded as sensitive to chemotherapy if it was inhibited by more than two drugs. Alternatively a tissue was regarded as resistant if it was affected by none or only one or two drugs. It is of interest to examine which agents were effective on those resistant tissues in which only one or two agents were effective, and which sites give rise to tissues either more sensitive or more resistant than other sites to chemotherapeutic agents.

Certain drugs show some departures from over-all performance. AM was effective by itself on almost three times as many tissues as expected by its over-all performance, while 5-FUDR and HN2O were effective alone twice as often as expected. On the other hand, TSPA and 2,4,6-TAP were almost never effective singly or with only one other compound. Deviations from expectation are significant at the 5 percent level for AM, TSPA, and 2,4,6-TAP but not for 5-FUDR and HN2O.

All sites taken together had more tissues resistant to all compounds than expected by the over-all performance (34 tissues observed vs. 19 tissues expected), but tissue resistance at specific sites could not be proved because of the small numbers of resistant tissues at any one site. Two sites did show some evidence of recalcitrance. Of the 17 female genital tissues tested, 5 were resistant to all drugs; of the 63 digestive and peritoneum tissues, 9 were resistant to all drugs. The effectiveness of some agents on recalcitrant tissues and the resistance of some sites observed are possibly artifactual. This could be due to the similar behavior of certain drugs so that related drugs would be effective on resistant tissues, and the isolated compound unrelated to the others is most likely to show up as singly effective.

Clinical and Experimental Correlation

An important criterion for the value of any test system for screening potential chemotherapeutic agents is the number of times an agent selected as effective by the system is also judged effective when used clinically against human tumors. It is equally important to know whether agents judged ineffective by the test system are also ineffective when used clinically.

On 76 patients referred to the Chemotherapy Service, biopsy material was obtained and included in the test system with the 10 previously mentioned agents. It was possible to obtain objective clinical impressions of the effectiveness of the compounds by noting either a decrease in primary tumor or metastases size or disappearance of ascites. Of the 76 patients, 42 received the selected drug and 10 showed objective improvement. No recommendations were made for 18 patients whose tissues were insensitive to all drugs. On the remaining 16, other drugs than those recommended were used. No improvement was noted in any of the 34.

Table 5 shows the relationship of objective clinical impressions to results of the *in vitro* test. A chi-square test of independence gives a

TABLE 5.—Relationship between effectiveness of drug as predicted by agar-pour-plate method and observed clinical impressions on 76 cases

Objective clinical impression	Agar-pour-plate test		
	Noneffective	Effective	Total
Noneffective	34	32	66
Effective	0	10	10
Total	34	42	76

value of 7.4 with 1 degree of freedom. This is significant at the 1 percent level. The evidence presented demonstrates that the agar-plate test is of some value in indicating compounds of potential clinical value. However, further studies involving dose-response relationships with the compounds and tissues used are required before definitive conclusions can be drawn.

DISCUSSION

A rational approach to selection of the drug to be used in therapy has many obvious advantages to the patient. Pharmacologically, it also permits evaluation of the best drug's effect without involvement of sequential effects of a variety of drugs.

Several potential agents may seem applicable according to preliminary animal screen. The essence of the screen reported herein is the use of a single human malignant tissue for the simultaneous evaluation of the group of compounds of potential chemotherapeutic value. The *in vitro* technique allows for simultaneous testing of drugs and provides for ranking of compound effectiveness on a particular tissue. It also readily provides preliminary information on the biological and biochemical properties of new classes of chemical agents.

Since many compounds currently in use as cancer chemotherapy agents have toxic effects on malignant and nonmalignant tissue, it is important to determine which agents have a high differential toxicity on tumor tissue and normal tissue. When specimens of both tumor material and normal tissue can be obtained from a patient, efficacy of a group of compounds can be tested. For each compound under test, the number of patients on which the compound affects tumor tissue but not normal tissue provides one measure of differential toxicity. This would be important in situations where the compound came into direct contact with both the tumor and surrounding normal tissue, as in topical application of the compound.

The concept of individual tumor growth, maintenance, and response to chemotherapy as primarily host-specific, and perhaps secondarily site-specific, has certain ramifications for cancer chemotherapy screening procedures. Extrapolation from animal and other screens to clinical studies in humans becomes more difficult to interpret when the extra dimension

of host specificity is added to that of species specificity of drug effect. Discrepancy between *in vitro* and *in vivo* results could be due to metabolic activation or inactivation of a drug that might occur in patients but not necessarily *in vitro*. This screening procedure attempts to overcome some difficulties of extrapolation of information of drug effects from one species of tumors to another, and allows for the comparison of various agents on a specific tissue.

REFERENCES

(*1*) Arai, T., and Suzuki, M.: A rapid agar dilution technique for the estimation of antitumor-cell activity. J. Antibiotics (Japan) 9: 169–171, 1956.

(*2*) DiPaolo, J. A., and Moore, G. E.: An evaluation of ascites tumor cell plating for screening chemotherapeutic agents. J. Antibiotics & Chemother. 7: 465–470, 1957.

(*3*) ———: The use of ascites tumors in solid agar for screening of cancer chemotherapeutic agents. Ann. New York Acad. Sc. 76: 870–880, 1958.

(*4*) Miyamura, S.: A determination method for anticancer action of antibiotics by the agar plate diffusion technique. J. Antibiotics & Chemother. 6: 280–282, 1956.

(*5*) Black, M. M., and Speer, F. D.: Further observations on the effects of cancer chemotherapeutic agents on the *in vitro* dehydrogenase activity of cancer tissue. J. Nat. Cancer Inst. 14: 1147–1158, 1954.

(*6*) Yamamoto, T., Nishioka, K., Oda, A., Sakurai, T., Yoshida, T., and Kikugawa, H.: A trial to the sensitivity test of human malignant tumor to antitumor agents. U.I.C.C. Symp. on the Chemotherapy of Cancer for the Pacific-Asian area and joint meeting with Cancer Chemotherapy Committee in Japan (Tokyo), 110–118, 1957.

(*7*) DiPaolo, J. A., and Moore, G. E.: An assay technique for testing cancer therapeutic agents for clinical use. Surg. Forum 9: 603–606, 1959.

(*8*) DiPaolo, J. A., Moore, G. E., and Niedbala, T. F.: Experimental studies with actinomycin D. Cancer Res. 17: 1127–1134, 1957.

(*9*) DiPaolo, J. A., Tarbell, D. S., and Moore, G. E.: Studies on the carcinolytic activity of fumagillin and some of its derivatives. *In* Antibiotics Annual. New York, Medical Encyclopedia, Inc., 1958–59, pp. 541–546.

(*10*) Sugiura, K.: Merits of ascites tumors for screening. Part I. Ann. New York Acad. Sc. 63: 962–973, 1956.

(*11*) Creech, H. J., Hauschka, T. S., Hankwitz, R. F., Jr., Littleton, B. J., and Andre, J.: Studies with four distinct lines of the Ehrlich ascites tumor for the evaluation of 27 potential inhibitors. Cancer Res. Supp. 3: 47–51, 1955.

Effects of Adrenocorticotropin and Insulin on Carcinogenesis in Hypophysectomized Rats [1, 2]

B. G. DODGE,[3] M. A. O'NEAL,[4] J. P. CHANG,[4] *and* A. C. GRIFFIN,[4] *Departments of Biochemistry, Baylor University College of Medicine, and The University of Texas M. D. Anderson Hospital and Tumor Institute, Houston, Texas*

SUMMARY

The administration of adrenocorticotropin and insulin to hypophysectomized rats fed 0.06 percent 3′-methyl-4-dimethylaminoazobenzene resulted in the highest incidence of liver tumors yet observed in the study of the effects on carcinogenesis of hormone replacement after hypophysectomy. The gross and histological precancerous changes observed in these animals appeared similar to those occurring in intact animals, which indicates that administration of the hormones had restored the same sequence that produces liver cancer in the intact rat. The liver concentrations of deoxyribonucleic acid, ribonucleic acid and riboflavine were also determined. In contrast to rather definite patterns observed in intact rats fed diets containing the carcinogen, there were no consistent or predictable changes observed in the livers of the hypophysectomized rats treated with adrenocorticotropin and insulin. The relative importance of the pituitary gland in cancer induction by fluorenamines and azo dyes is discussed.—J. Nat. Cancer Inst. 27: 817-825, 1961.

THE INDUCTION of tumors in the pituitary or its target glands, resulting from hormonal imbalances, has been firmly established. This important area of investigation has been adequately reviewed by Kirschbaum (*1*, *2*), Hertz (*3*), and Clifton (*4*). In contrast, the direct or indirect involvement of the pituitary gland on carcinogenic sequences not involving the endocrine glands has not been sufficiently elucidated.

Korteweg and Thomas (*5*) applied benzo[*a*]pyrene cutaneously to hypophysectomized mice and observed fewer skin epitheliomas and carcinomas than were present in the intact control mice. Findings from other laboratories substantiate this observation that cancer induction resulting from administration of benzo[*a*]pyrene may be delayed in the absence of the pituitary (*6*). Removal of the pituitary gland after the induction of tumors by dibenzanthracene produced no tumor regression, but did slow the growth rate of the tumors (*7*). Moon and Simpson (*8*) reported

[1] Received for publication March 27, 1961; revised July 17, 1961.

[2] Supported by grant CRTY-5021 from the National Cancer Institute, National Institutes of Health, Public Health Service, and by the Robert A. Welch Foundation.

[3] Cancer research trainee, Baylor University College of Medicine.

[4] The University of Texas M. D. Anderson Hospital and Tumor Institute.

that removal of the pituitary will delay considerably the onset of tumors in animals treated with methylcholanthrene. However, the hypophysis appears to exert little influence on carcinogenesis induced in rats by dimethylbenzanthracene (*9*).

During recent years we have found that hypophysectomy effectively inhibits liver-tumor formation in albino rats fed diets containing 3′-methyl-4-dimethylaminoazobenzene (3′MeDAB) (*10–12*) and fluorenamine derivatives (*13*). We attempted to determine the pituitary factors involved in the control of tumorigenesis resulting from the administration of these agents. Of the pituitary hormones, adrenocorticotropin (ACTH) and growth hormone were partially effective in restoring liver carcinogenesis in the hypophysectomized, azo-dye-fed rats (*11, 12*). Several other pituitary and steroid hormones were studied, but all were without appreciable effect. The present investigation was initiated to study in more detail other hormonal factors involved in liver carcinogenesis and to correlate, as far as possible, the hormonal influences with the biochemical and histochemical events that have been ascribed to liver-cancer induction.

MATERIAL AND METHODS

Male albino rats weighing 125 to 150 g were obtained from the Holtzman Rat Company, Madison, Wisconsin, and hypophysectomized by Endocrine Laboratories, Madison, Wisconsin. They were housed in wire cages in a well-ventilated animal room kept at 26 to 28° C. Food and water were administered *ad libitum*, and food intakes were recorded for each group. The composition of the basal synthetic diet has been previously described by Griffin *et al.* (*14*). 3′MeDAB was incorporated into this basal diet at a concentration of .06 percent. The animals were divided into experimental groups as follows:

Group number	Number of rats	Regimen
A	30	.06% 3′MeDAB + insulin
B	15	.06% 3′MeDAB + ACTH + insulin
1	58	Basal diet
2	100	.06% 3′MeDAB
3	105	.06% 3′MeDAB + ACTH + insulin

Group A received daily subcutaneous injections of 0.0075 units of protamine zinc insulin (Eli Lilly & Co., Indianapolis, Ind.). Groups B and 3 received daily subcutaneous injections of 0.5 units of ACTH (Cortrophin-Zinc, Organon, Inc., West Orange, N.J.) and 0.0075 units of the protamine zinc insulin.

Animals from groups A and B were killed after 20 weeks on the indicated regimens, and the livers were studied for the presence of tumors or other abnormalities. Animals from each of groups 1 to 3 were killed at 1, 2, 3, 4, 5, 9, 11, 13, 15, 17, and 20 weeks after the start of the specific regimens listed. Prior to 9 weeks, the animals were killed by decapitation.

Beginning with the 9th week, the rats were first anesthetized with an intraperitoneal injection of sodium pentobarbital (Nembutal) and exsanguinated at laparotomy by aortic puncture. The blood was centrifuged and the plasma stored at −10° C until analyses for corticosterone could be performed (*15*, *16*). According to procedures reported previously (*17*, *18*), the liver was removed and divided for the following histochemical observations: hematoxylin and eosin, mitochondria, glycogen, ribonucleic acid, and esterase. That portion of the liver allocated for chemical analysis was immediately frozen and stored at −10° C until the determinations of riboflavine (*19*, *20*), deoxyribonucleic acid (DNA) (*21*), and ribonucleic acid (RNA) (*22*) were carried out.

An additional 36 hypophysectomized rats weighing 125 to 150 g were obtained in the same manner and injected with 0.5 units of ACTH (Organon) at a specific hour (6:00 p.m.) each day for 14 days. Laboratory chow and water were administered *ad libitum*. After the fourteenth injection, 3 rats were killed at 2-hour intervals for 24 hours. Blood samples were collected, stored, and analyzed for corticosterone (*15*, *16*).

RESULTS

Fifty percent of the rats in group A (insulin + 3′MeDAB) survived the full 20 weeks. Of the survivors, 3 had definite liver tumors as established by both gross and histological examination. Approximately half of the animals had completely normal livers and the remainder exhibited varying degrees of cirrhosis and granularity. In group B (insulin + ACTH + 3′MeDAB), 8 of the 15 rats survived and all developed liver tumors after 15 to 20 weeks on this regimen. The livers also exhibited a considerable amount of enlargement, granularity, and cirrhosis. All the tumors in these and subsequent groups were confirmed by histological examination. The tumors observed were primarily cholangiocarcinomas as reported previously (*23*). From these results we concluded that both ACTH and insulin are involved in the restoration of azo-dye carcinogenesis in hypophysectomized rats, and the further detailed experiments that follow were carried out to study this effect.

Food intakes were similar in all groups in this series. The average food intake of group 1 was 7 g per day, and the intakes of the other groups averaged between 6 to 7 g per rat per day. The body weights of the group 1 animals remained constant throughout the study. Rats of all the other groups lost an average of 5 to 6 g during the 20 weeks maintained on the various regimens.

Histological changes in the dye-fed, hypophysectomized controls were negligible and no tumors were observed, in contrast to the near 100 percent liver-tumor incidence that occurs in intact rats after 12 to 14 weeks of carcinogen feeding. Gross observations revealed no nodular, cirrhotic, or tumorous livers in group 1 (basal diet) or group 2 (3′MeDAB) during the

entire 20 weeks of experimentation. Furthermore, livers of these 2 groups showed no evidence of precancerous changes, such as oval-cell or bile-duct proliferation, or glycogen depletion of hepatic cells surrounding the central vein.

The livers of animals from group 3 (3′MeDAB and ACTH + insulin) became grossly nodular at 11 weeks, showed microscopic oval-cell proliferation at 9 weeks and bile-duct adenomas at 15 and 17 weeks, with cholangiocarcinomas appearing at 20 weeks in 4 of the 5 animals killed. Depletion of the liver glycogen was apparent in the animals killed from group 3 at 5 to 9 weeks. New bile ducts appeared after 12 weeks and oval-cell proliferation became apparent from 9 to 20 weeks in the animals of this group. After the 15th week of combined carcinogen and hormone treatment, regenerative nodules, cholangiofibrosis, new bile ducts, and acinous arrangement of hepatic cells appeared in most of the animals killed. In brief, the morphological and histological picture is similar to that seen in intact dye-fed rats, though the onset of these changes was somewhat delayed in the hormone-treated rats of group 3.

This study was initiated to determine if there are differences in the DNA, RNA, and riboflavine levels in the livers of the hypophysectomized, dye-fed rats with or without administration of ACTH and insulin. While some trends were indicated, the results were inconclusive in the addition of any new information relative to chemical changes associated with liver-cancer induction. At 11, 15, and 20 weeks, the liver DNA concentration was highest in group 3 (3′MeDAB + ACTH + insulin). These results might correlate with the liver cirrhosis and proliferative activity seen in the animals of this group. A decrease in liver riboflavine was apparent in those animals receiving ACTH and insulin, the lowest values appearing after 20 weeks of treatment. In summary, the chemical determinations contributed little toward elucidation of the over-all mechanism of liver-cancer induction, and it is obvious that new approaches are essential to explain the ACTH-insulin effect on liver carcinogenesis.

The procedure used for plasma-corticosterone determination was not available until the 9th week of the experiment (table 1). The concentration of this hormone was slightly higher in those animals receiving ACTH (group 3), though the levels were not as high as would be expected in rats injected daily with ACTH. The high level of corticosterone apparent in group 3 after 20 weeks of dye feeding and hormone injections could not be accounted for on the basis of previous determinations, nor was there any evidence of pituitary remnants remaining in these animals. The only possible explanation was a variation of blood-corticosterone levels with time, after injection of ACTH. It was decided to study this phenomenon by the use of a time-response experiment. Our basic assumption had been that the long-acting ACTH, injected daily, would maintain the plasma corticosteroids at a high and relatively constant level. Table 2 shows that this was not the case. Within 2 hours after injection of ACTH, the plasma corticosterone had reached a maximum level and was declining. Within 6 hours, the concentration had dropped to less than one tenth of

TABLE 1.—Plasma corticosterone values in hypophysectomized rats (μg corticosterone per 100 ml plasma)

Weeks fed diet	Group 1	Group 2	Group 3*
	Basal diet	Basal diet + 3′MeDAB	Same as group 2 + ACTH and insulin
9	2.3 (1.8–2.8)	1.6 (1.0–2.0)	3.9 (3.6–4.6)
11	2.0 (1.1–2.4)	1.7 (1.0–2.6)	2.8 (2.4–4.4)
13	2.8 (2.2–3.4)	3.1 (2.5–4.2)	— —
15	2.1 (1.4–3.5)	1.7 (0.4–3.5)	4.9 (3.8–6.8)
17	2.3 (1.9–3.3)	2.7 (2.1–3.3)	3.5 (2.9–4.0)
20	3.0 (2.2–4.2)	1.2 (0.0–2.0)	15.6 (7.5–29.0)

*The time elapsed between the last ACTH injection and autopsy was 16 hours for the animals killed from 9 through 17 weeks, and 1.5 hours for the 20-week group.

TABLE 2.—Twenty-four-hour variation in the plasma corticosterone in hypophysectomized rats injected daily with 0.5 unit ACTH

Hours since injection of ACTH	Corticosterone (μg/100 ml plasma)	Hours since injection	Corticosterone (μg/100 ml plasma)
2.13	32.5	14.08	4.0
2.42	24.2	14.33	3.2
2.58	30.1	14.50	4.9
4.08	10.3	16.08	4.2
4.25	11.3	16.25	1.5
4.67	6.1	16.50	3.3
6.08	2.7	18.08	4.0
6.33	2.5	18.25	3.4
6.67	8.6	18.50	3.0
8.17	5.8	20.33	16.5*
8.33	4.0	20.58	2.0
8.67	6.2	20.83	3.0
10.17	3.7	22.00	10.0
10.42	5.2	22.17	3.0
10.58	4.0	22.42	4.0
12.17	11.4	24.08	4.6
12.33	5.2	24.33	4.1
12.58	5.2	24.58	3.0

*This animal had normal-appearing gonads and a pituitary tag.

the 2-hour value, and thereafter remained essentially constant at less than 6 μg percent for the remainder of the 24-hour period.

DISCUSSION

The complete absence of precancerous or tumor lesions in the hypophysectomized rats fed diets containing 3′MeDAB and the restoration of this cancer induction by the daily injection of ACTH and insulin emphasize again the important role of hormones in the initiation of certain carcinogenic sequences. Both gross and histological findings provided

further evidence that the livers of the hypophysectomized dye-fed rats were near normal, while administration of ACTH and insulin (groups B and 3) activated a sequence of changes observed by many investigators in dye-fed intact animals, which precedes the appearance of tumors. While it was hoped in the beginning that the interruption of carcinogenesis by removal of the pituitary gland and its restoration by administration of hormones would provide some new insight into the chemical changes associated with liver-cancer induction, the present findings indicate the complexity of the over-all process and suggest that changes in the concentration of DNA, RNA, etc., may be of secondary significance.

Administration of ACTH and insulin resulted in a higher incidence of liver tumors in dye-fed hypophysectomized rats (groups B and 3) than has been obtained by comparable treatment with ACTH, growth hormone, or insulin alone. We are unable to provide any direct explanation for this ACTH-insulin synergism, but may speculate as to their mode of action in restoring carcinogenesis. The obvious implication would be that adrenal integrity and one or more stages of carbohydrate metabolism are involved. There is some evidence that either adrenalectomy or suppression of adrenal activity by administration of large doses of deoxycorticosterone acetate or the trimethylacetate (*24*, *25*) is capable of inhibiting the initiation of carcinogenesis by the azo dyes. Our own attempts to determine whether adrenalectomy will influence 3′MeDAB carcinogenesis in the rat have not been conclusive (*11*, *12*), possibly because of the formation of accessory adrenals from rests or capsular remnants. Attempts to reinstate liver carcinogenesis in the hypophysectomized rats by restoration of adrenal corticoids have also been unsuccessful, though it may be virtually impossible to restore the hormonal equilibrium normally present in the intact rat. In the current study, the corticosterone analyses indicate that ACTH produced the expected effect on adrenal function, but that the plasma-corticosterone levels could not be maintained for more than 5 hours after the daily injection of ACTH. It would be of interest to ascertain whether or not the maintenance of a normal and constant corticosterone plasma level would accelerate the process of azo-dye liver tumorigenesis in the hypophysectomized rat to an even greater extent.

There are some indications that ACTH may possess extra adrenal functions or activities that might provide an alternative explanation for its effect on liver-cancer induction. For example, ACTH has been shown under certain conditions to inhibit the uptake of glucose by adipose tissue (*26*) or to stimulate lipide mobilization in fasting mice (*27*). ACTH in high doses has also been demonstrated to stimulate insulin secretion (*28*). Whether or not this extra adrenal function of ACTH will prove to have a direct involvement in liver carcinogenesis remains to be established. Engel has recently provided an excellent review of these extra adrenal functions of ACTH (*29*).

There are reports that liver-cancer induction may be associated with carbohydrate metabolism (*30*). However, in terms of the postulated mechanism of insulin action it is difficult to explain its stimulatory effect

on cancer induction in the hypophysectomized rats as was observed in this study. We may only conclude that glucose must be available in the liver cell for carcinogenesis to proceed. Since glycogen synthesis or storage becomes greatly reduced in the liver of intact dye-fed rats (*18*), it would appear that the insulin dependence of carcinogenesis might involve still another phase of carbohydrate metabolism.

The difficulties encountered in the assessment of data obtained from endocrinologically altered animals with respect to the carcinogenic mechanisms operating in animals with a normal endocrinological make-up are evident from the discussion. Nevertheless, it appears that whenever hormone replacement experiments reinstate liver carcinogenesis after hypophysectomy, the precancerous changes leading to malignancy are the same as those occurring in the intact rat. At this time, no single endocrine gland or hormone can be said to hold the key to induction of liver tumors by azo dyes or fluorenamine compounds since the pituitary, adrenal, and pancreas have all been implicated (*10–12, 24, 25, 31–33*). In addition, there is apparently a pituitary-thyroid gland relationship in fluorenamine carcinogenesis in the rat (*34*). Endocrinological control of liver-tumor induction by azo dyes is not the same as with the fluorenamines, however, since ACTH and insulin have no effect on liver-tumor incidence or precancerous changes in hypophysectomized rats fed *N*-2-fluorenyldiacetamide (*13*). A great many of the hormonal factors that regulate the action of these two classes of potent carcinogens have been well established, and it is expected that future investigation will be able to define the specific step(s) in the sequence of cancer formation regulated by each factor. Specific effects on carbohydrate metabolism appear to be among the earliest changes demonstrable in this process.

REFERENCES

(*1*) Kirschbaum, A.: The role of hormones in cancer: Laboratory aminals. Cancer Res. 17: 432–453, 1957.

(*2*) ———: The carcinogenic stimulus. *In* Fundamental Aspects of Normal and Malignant Growth (Nowinski, ed.). Amsterdam, Elsevier Press, Inc., 1960, chapt. 11, pp. 823–876.

(*3*) Hertz, R.: An appraisal of the concepts of endocrine influence on the etiology, pathogenesis, and control of abnormal and neoplastic growth. Cancer Res. 17: 423–431, 1957.

(*4*) Clifton, K. H.: Problems in experimental tumorigenesis of the pituitary glands, gonads, adrenal cortices, and mammary glands. *A review.* Cancer Res. 19: 2–22, 1959.

(*5*) Korteweg, R., and Thomas, F.: Tumor induction and tumor growth in hypophysectomized mice. Am. J. Cancer 37: 36–44, 1939.

(*6*) Agate, F. J., Jr., Antopol, W., Glaubach, S., Agate, F., and Graff, S.: The nonessentiality of the hypophysis for the induction of tumors with 3,4-benzpyrene. Cancer Res. 15: 6–8, 1955.

(*7*) Ball, H. A., and Samuels, L. T.: The relation of the hypophysis to the growth of malignant tumors. III. The effect of hypophysectomy on autogenous tumors. Am. J. Cancer 26: 547–551, 1936.

603724—61——10

(*8*) Moon, H. D., and Simpson, M. E.: Effect of hypophysectomy on carcinogenesis: Inhibition of methylcholanthrene carcinogenesis. Cancer Res. 15: 403–406, 1955.

(*9*) Simpson, M. E., and Evans, E. S.: Effect of pituitary hormones on carcinogenesis induced in rats by 7,12-dimethylbenzanthracene. Cancer Res. 19: 1096–1104, 1959.

(*10*) Griffin, A. C., Rinfret, A. P., and Corsigilia, V. F.: The inhibition of liver carcinogenesis with 3′-methyl-4-dimethylaminoazobenzene in hypophysectomized rats. Cancer Res. 13: 77–79, 1953.

(*11*) Griffin, A. C., O'Neal, M. A., Robertson, C. H., Hoffman, H. E., and Richardson, H. L.: Hormone factors involved in carcinogenesis. Acta Unio internat. contra cancrum 11: 671–674, 1955.

(*12*) Griffin, A. C., Richardson, H. L., Robertson, C. H., O'Neal, M. A., and Spain, J. D.: The role of hormones in liver carcinogenesis. J. Nat. Cancer Inst. Supp. 15: 1623–1632, 1955.

(*13*) O'Neal, M. A., Hoffman, H. E., Dodge, B. G., and Griffin, A. C.: Role of the pituitary in *N*-2-fluorenyldiacetamide carcinogenesis. J. Nat. Cancer Inst. 21: 1161–1168, 1958.

(*14*) Griffin, A. C., Nye, W. N., Noda, L., and Luck, J. M.: Tissue proteins and carcinogenesis. I. The effect of carcinogenic azo dyes on liver proteins. J. Biol. Chem. 176: 1225–1235, 1948.

(*15*) Silber, R. H., Busch, R. D., and Oslapas, R.: Practical procedure for estimation of corticosterone or hydrocortisone. Clin. Chem. 4: 278–285, 1958.

(*16*) Guillemin, R., Clayton, G. W., Smith, J. D., and Lipscomb, H. S.: Étude de la fonction corticosurrenalienne par la mesure simultanée de la corticosterone dans le sang périphérique et de l'acide ascorbique surrenalien. Compt. rend Acad. sc. 245: 1834, 1957.

(*17*) Chang, J. P., Spain, J. D., and Griffin, A. C.: Histochemical manifestations of early changes in rat liver during carcinogenesis induced by 3′-methyl-4-dimethylaminoazobenzene. Cancer Res. 18: 670–675, 1958.

(*18*) Spain, J. D., and Griffin, A. C.: A histochemical study of glycogen alterations in the livers of rats following azo dye administration. Cancer Res. 17: 200–204, 1957.

(*19*) Andrews, J. S.: A collaborative study of riboflavin assay methods. Cereal Chem. 20: 3, 1943.

(*20*) Conner, R. T., and Straub, G. J.: Combined determination of riboflavin and thiamine in food products. Indust. & Engng. Chem. (anal. ed.) 13: 385–388, 1941.

(*21*) Burton, K.: A study of the conditions and mechanism of the diphenylamine reaction for the colorimetric estimation of deoxyribonucleic acid. Biochem. J. 62: 315–323, 1956.

(*22*) Schneider, W. C.: Phosphorus compounds in animal tissues. I. Extraction and estimation of desoxypentose nucleic acid and of pentose nucleic acid. J. Biol. Chem. 161: 293–303, 1945.

(*23*) Richardson, H. L., O'Neal, M. A., Robertson, C. H., and Griffin, A. C.: The role of hormones in azo-dye induction of liver cancer and the adrenal-lipoid response in hypophysectomized rats. Cancer 7: 1044–1047, 1954.

(*24*) Eversole, W. J.: Inhibition of azo dye carcinogenesis by adrenalectomy and treatment with desoxycorticosterone trimethylacetate. Proc. Soc. Exper. Biol. & Med. 96: 643–646, 1957.

(*25*) DaVanzo, J. P., and Eversole, W. J.: The effects of adrenalectomy and deoxycorticosterones on liver enzymes and protein in rats fed 3′-methyl-4-dimethylaminoazobenzene. Cancer Res. 18: 796–801, 1958.

(*26*) Verner, J. V., Jr., and Engel, F. L.: The blocking effect of ACTH and the catechol amines on glucose uptake by adipose tissue. Am. J. Med. 27: 329, 1959.

(27) WHITE, J. E., and ENGEL, F. L.: Fat mobilization by purified corticotropin in the mouse. Proc. Soc. Exper. Biol. & Med. 102: 272–274, 1959.

(28) ENGEL, F. L., FREDERICKS, J., LOPEZ, E., and ALBERTSON, T.: Some extra adrenal actions of corticotropin on carbohydrate metabolism in the rat. Endocrinology 63: 768–777, 1958.

(29) ENGEL, F. L.: Extra-adrenal actions of ACTH. A review. *In* Vitamins and Hormones (Thimann, Harris, and Marrian, eds.). New York, Academic Press, Inc., 1960, vol. XVIII.

(30) GRIFFIN, A. C.: Biochemistry of cancer induction. *In* Cancer (Raven, R. W., ed.). London, Butterworth & Co., Ltd., 1957, vol. 1, chapt. 6, pp. 123–160.

(31) Skyorna, S. C.: Factors affecting liver carcinogenesis. Proc. Canad. Cancer Res. Conf. 1: 107, 1954.

(32) SALZBERG, D. A., and GRIFFIN, A. C.: Inhibition of azo dye carcinogenesis in the alloxan-diabetic rat. Cancer Res. 12: 294, 1952.

(33) BIELSCHOWSKY, F., and BIELSCHOWSKY, M.: Carcinogenesis in alloxan-diabetic rats. *In* Ciba Foundation Symp. on Carcinogenesis Mechanisms of Action, 1959, pp. 95–104.

(34) BIELSCHOWSKY, F.: Carcinogenesis in the thyroidectomized rat. The effect of injected growth hormone. Brit. J. Cancer 12: 231–233, 1958.

Cell Proliferation in Precancerous Liver: Relation to Presence and Dose of Carcinogen[1,2]

ANNA KANE LAIRD *and* A. D. BARTON, *Division of Biological and Medical Research, Argonne National Laboratory, Argonne, Illinois*

SUMMARY

The precancerous period in the livers of rats fed 2-acetylaminofluorene is divisible into two phases. During the first 4 to 8 weeks no significant change in the total number of liver cells occurs; thereafter the total number of liver cells increases at a constant rate. In the present study, when the rate of this constant cell proliferation was plotted against the relative dose of the carcinogen, the points approximated a function describing the properties of a first-order chemical reaction. When administration of the carcinogen was discontinued, the cell proliferation stopped after a short delay. These two findings considered together demonstrate a physiological relationship between the presence of the carcinogen and the preneoplastic cell proliferation in the target organ. It is suggested that the preneoplastic cell proliferation is a form of compensatory hyperplasia in response to the inactivation of some subcellular liver constituent, which is essential to life and is replaced only in association with cell division, and that this inactivation is accomplished by a first-order chemical reaction between the carcinogen and the essential cell constituent.—J. Nat. Cancer Inst. 27:827–839, 1961.

IN RECENTLY published studies (*1*, *2*) we have shown that the precancerous period in the livers of rats fed 2-acetylaminofluorene [3] (AAF) is divisible into two phases. During the first 4 to 8 weeks of administration of the carcinogen, no significant change in the total number of liver cells occurs; thereafter a relatively rapid increase in the total number of liver cells is observed, and this cell proliferation proceeds at a constant rate throughout the remainder of the precancerous period (tumors usually start to appear after 25 to 30 weeks of treatment with the carcinogen at the dose levels used).

In an effort to discover a relation between this cell proliferation and the presence of the carcinogen, we have determined the rate of cell proliferation when different doses of AAF were administered, and, in another experiment, the effect of withholding the carcinogen after the cell proliferation had become well established.

---

[1] Received for publication April 17, 1961; revised July 28, 1961.
[2] This work was performed under the auspices of the U.S. Atomic Energy Commission.
[3] *Chemical Abstracts'* nomenclature: *N*-2-fluorenylacetamide.

MATERIALS AND METHODS

In the first experiment, 250 male rats of the Holtzman strain were separated into three experimental groups of approximately 80 rats each, with average initial body weights of 201, 201, and 200 g, respectively, and a control group of 12 rats with an average initial body weight of 200 g. The experimental animals were all fed *ad libitum* a commercial grain diet with which AFF was mixed in concentrations of 0.015, 0.030, and initially 0.060 percent. The daily consumption of food and of AAF was recorded. Unusually high mortality of the animals in the third group, continuing into the 8th week of the experiment, necessitated reducing the concentration of the AAF in the diet from 0.060 to 0.045 percent. However, the animals of this group immediately increased their food intake, with the consequence that the consumption of AAF continued at the same constant rate as before, and the ratios of AAF actually consumed by the three experimental groups were maintained at 1.00:1.85:3.30 throughout the precancerous period. The control rats received the same diet without the carcinogen.

In the second experiment, 60 male rats with an average initial body weight of 282 g were fed AAF in an initial concentration of 0.060 percent, reduced after 19 days to 0.045 percent, because of unusual weight loss. At the 10th week, when cell proliferation was apparently well established, the rats were separated into two groups matched carefully with respect to the mean and range of body weight. For the remainder of the experiment, the AAF was withheld from one group and continued at the previous concentration in the diet of the other group.

For each experimental observation, 4 rats, matched to the entire experimental group with respect to the average and range of body weight, were selected at appropriate intervals and killed with ether. After samples were taken for histological study, the entire livers were pressed through a plastic tissue mincer that retains much of the connective tissue of the organ. Thus the liver pulp used in our studies is believed to consist of those cells of the liver lobules that are not closely embedded in the connective tissue of the portal areas; it would include the majority of the newly formed bile-duct cells (*3–5*) beyond the earliest days of their proliferation.

The liver pulp from the 4 rats was mixed together, and a weighed aliquot was homogenized in a glass apparatus of the Dounce type (*6*). Aliquots of the homogenate were analyzed for protein nitrogen (*7*), ribonucleic acid (RNA) (*8*), and deoxyribonucleic acid (DNA) (*8*), and similar aliquots were mixed in a 1:40 dilution with 3 percent acetic acid containing a nuclear stain, for enumeration of the nuclei. Under these conditions the nuclei are well dispersed and easily counted. The results are expressed as the total number of cells (nuclei) and as the total quantity of protein nitrogen or nucleic acid per average whole liver.

Our data were obtained in terms of "recovered nuclei." However, we feel that no great error is entailed, and communication of the over-all

biological significance of our results is favored, by reference throughout this paper to "liver cells" and "cell proliferation," for the following reasons:

1) Although binucleate cells occur in rat liver with considerable frequency (*9*), each binucleate cell is approximately two times the volume and mass of a mononucleate cell, and doubling of the total number of nuclei leads directly to a doubling of liver-cell mass.

2) Although it may be argued that all cells of the liver are by definition "liver cells," our method emphasizes the changes occurring during carcinogenesis in the total population of parenchymal liver cells, which we feel is the parameter of greatest importance in both normal and abnormal liver function.

3) Using this method, we have always found that the number of nuclei recovered per g of liver has been consistent with the histological appearance of the same livers: When the parenchymal cells are enlarged, as in the early stages of regeneration after partial hepatectomy (*10*), the number of nuclei recovered per g is reduced; when the liver cells are shrunken, as after a period of complete starvation (*11*), the number of nuclei recovered per g is greater than normal. And in all these cases, when the number of nuclei recovered per g is multiplied by the weight of the liver in g, the total number of nuclei (cells) per liver has always been consistent with the presence or absence of mitotic activity; *i.e.*, we do not find more cells per liver than normal unless there is sufficient mitotic activity to account for it.

RESULTS

Text-figure 1 shows the increase in the total number of liver cells and in the total protein nitrogen and RNA contents of the livers from the rats of the three experimental groups, in the first experiment. As in our previous studies (*1*, *2*), the precancerous period of about 25 weeks was divisible into two phases. An initial period lasted 4 to 8 weeks, in which the small increase in total cells in the experimental livers did not exceed that observed in the control livers (200 g male rats of this strain are still growing fairly rapidly, and for this reason some growth of the livers was observed during this early period in both control and experimental livers). This early period of normal liver growth was followed by one in which an excessive accumulation of new cells was maintained at a constant rate throughout the remainder of the preneoplastic period. The rate of net accumulation of cells varied from 211×10^6 to 322×10^6 new cells per week, as measured by the slopes of the lines of text-figure 1. Thus the rate of accumulation of new cells was greater when larger doses of AAF were used. The rate of increase of the protein and RNA was also greater with the larger doses of the carcinogen.

The slopes and intercepts of the lines drawn in text-figure 1, with their standard errors (SE), are given in table 1. For all the intercepts the SE is at least half the value of the intercept itself, and in a number of the

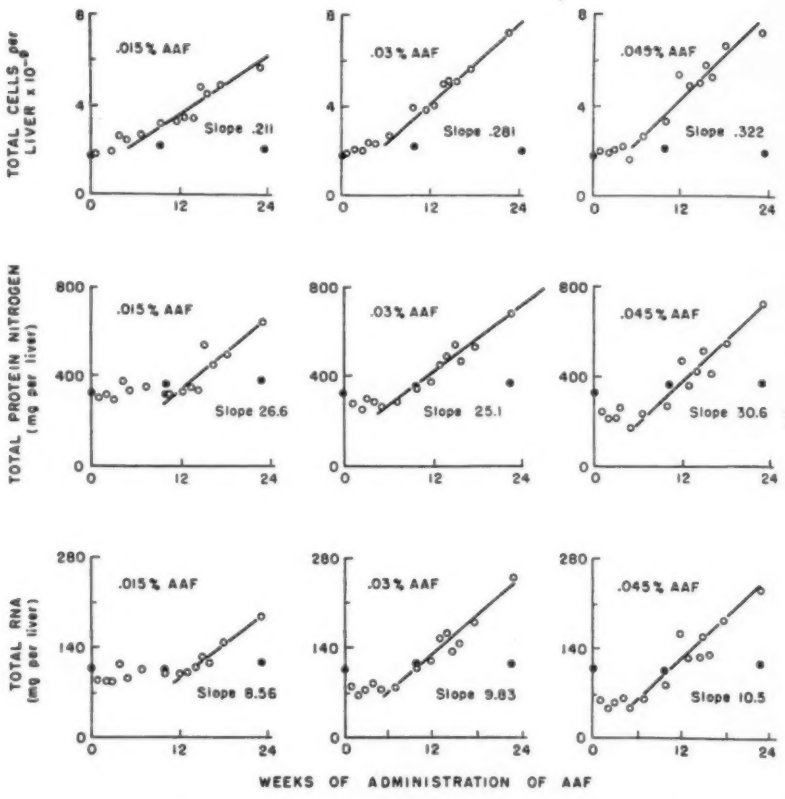

TEXT-FIGURE 1.—Changes in total number of liver cells (*top line*), total quantity of protein nitrogen (*middle line*), and in RNA (*bottom line*) in livers of rats fed AAF mixed in their diet in concentrations of 0.015 (*left column*), 0.030 (*middle column*), and 0.045 percent (*right column*). *Black circles* represent values obtained for control rats fed same diet without the carcinogen.

cases, the SE is greater than the value of the intercept. In the latter, the intercept is not significantly different from zero, and in the former it is very close to zero.

In text-figure 2, the rate of cell proliferation for each experimental group and for the control animals (*i.e.*, the slope of each line in the top row of text-fig. 1) is plotted against the relative dose of AAF consumed. The standard deviation for each experimental point is shown. It is evident that a number of different curves could be drawn through this series of points, each curve representing a mathematical function with a different theoretical interpretation. One such curve is shown in this text-figure; it represents the function $Y = \frac{4.2}{1 + 1/X}$. This function was derived by evaluation of the constants of the straight line obtained when

TABLE 1.—Statistical data accompanying text-figure 1

Concentration of AAF (percent)	Cells		Protein		RNA	
	Rate of increase (1×10^9 cells/week)	Y-intercept (1×10^9 cells)	Rate of increase (mg/week)	Y-intercept (mg)	Rate of increase (mg/week)	Y-intercept (mg)
0.015	0.211 ± 0.033	0.908 ± 0.549	26.6 ± 5.2	19 ± 81	8.56 ± 0.84	−10 ± 13.7
0.030	0.281 ± 0.022	0.747 ± 0.324	25.1 ± 3.4	106 ± 54	9.84 ± 1.2	8.2 ± 17.9
0.045	0.322 ± 0.035	0.471 ± 0.498	30.6 ± 3.4	0.82 ± 49	10.5 ± 1.4	−7.7 ± 19.9

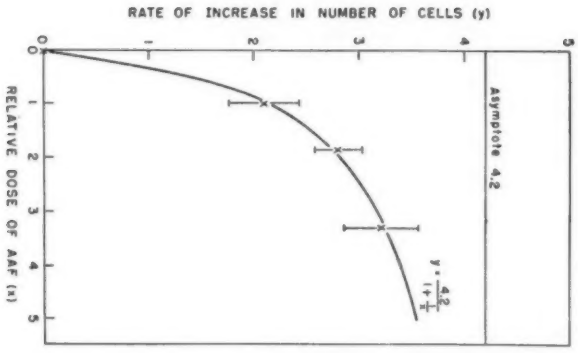

TEXT-FIGURE 2.—Rate of increase in total number of liver cells (shown by the slopes of the lines of text-fig.1) plotted against relative dose of AAF. The experimental points with their standard deviations are shown. The line is the theoretical curve representing the mathematical function $Y = \frac{4.2}{1 + 1/X}$, which was derived by evaluation of the constants of the straight line shown in text-figure 3.

the reciprocal of the rate of cell proliferation is plotted against the reciprocal of the relative dose of AAF consumed, as shown in text-figure 3. Such a plot was originally suggested by Lineweaver and Burk for the analysis of the dynamics of enzyme reactions (*12*); they showed that for first-order reactions a linear relation exists between the reciprocal of substrate concentration and the reciprocal of reaction rate. Since the reciprocals of dose and rate of cell increase plotted in text-figure 3 approximate a straight line, the function $Y = \frac{4.2}{1 + 1/X}$, representing the curve drawn through the points of text-figure 2, describes the properties of a first-order chemical reaction.

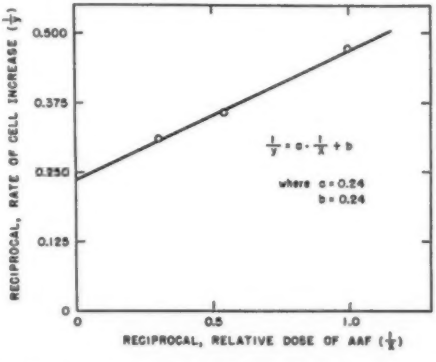

TEXT-FIGURE 3.—Reciprocal of rate of increase in total number of liver cells plotted against reciprocal of relative dose of AAF, as suggested by Lineweaver and Burk (*6*) for the analysis of first-order chemical reactions.

The growth of normal livers with age is shown in table 2; the data are taken from three experiments involving three different shipments of animals. As would be expected, the increase in body weight with age is accompanied by an increase in liver weight. However, the growth of the liver in adult animals can be accounted for mainly by an increase in the size of the average liver cell, rather than by an increase in the total number of liver cells. Thus the growth of normal adult liver contrasts sharply with that seen in preneoplastic liver, which is accompanied by a threefold increase in the number of cells present, and hence is a hyperplasia.

TABLE 2.—Growth of normal livers with age

Expt.	Age (weeks)	Body wt. (g)	Liver wt. (g)	Number of cells per g liver, (1×10^{-6})	Total No. cells/liver (1×10^{-6})	Wt. average liver cell (1×10^{-9}g)
A	5.5	153	9.2	180	1660	5.55
	7.5	205	11.6	159	1830	6.28
	10	300	15.3	148	2260	6.75
B	11	235	13.2	130	1720	7.70
	21	400	17.9	122	2180	8.20
	34	470	21.3	95	2020	10.5
C	9	288	17.1	168	2870	5.95
	19	440	20.6	124	2530	8.06
	29	451	21.0	156	3040	6.42

The content of DNA per average nucleus in this experiment is given in table 3. In general, the DNA per nucleus was lower in the experimental animals than in the controls, but there was no relation between the dose of AAF and the DNA content of the average nucleus. The DNA per nucleus was significantly reduced after the 7th week of AAF feeding, at all dose levels studied.

TABLE 3.—DNA per average nucleus during administration of AAF at 3 dose levels

Time (weeks)	Control	AAF 0.015 (percent)	AAF 0.030 (percent)	AAF 0.045 (percent)
0	19.5*	—	—	—
1	—	14.8	15.9	14.4
2	—	15.3	13.3	14.0
3	—	16.9	18.3	15.5
4	—	19.5	16.2	15.2
5	—	15.8	15.3	16.2
7	—	15.1	14.1	12.4
10	19.2	12.1	11.7	11.6
12	—	12.0	12.4	13.4
13	—	13.6	15.6	12.8
14	—	13.2	13.7	12.7
15	—	11.4	11.8	11.1
16	—	11.9	11.7	12.1
18	—	12.3	12.4	13.1
23	21.0	11.3	12.7	13.7
Mean, over-all.	—	14.0 ± 2.0	14.5 ± 1.8	13.5 ± 1.0
Mean, through 7th week.	—	14.8 ± 1.0	15.5 ± 1.2	16.2 ± 1.2
Mean, 10th through 23d week.	—	12.2 ± 0.6	12.8 ± 1.0	12.4 ± 0.8

*Units = 1×10^{-12} g per average nucleus.

Text-figure 4 shows the results of discontinuing the administration of AAF at the 10th week, after the cell proliferation had started. In this experiment the cell proliferation continued for 2 weeks and then stopped abruptly. It was not resumed in the course of the next 10 weeks, though during this time the further increase in the total number of liver cells in the rats remaining on the carcinogen-containing diet was as great as had already been observed before the 12th week.

The histological appearance of the livers in these experiments did not differ appreciably from that reported in an earlier study of hepatic carcinogenesis by AAF (*13*), or in similar histological studies by other authors (*3*, *4*). In general, during the first few weeks, when little or no net increase was noted in the total number of liver cells, the liver cells were uniformly smaller than normal. This reduction in cell size is probably related to the decreased food intake of the animals at this time [*compare* the effects of simple starvation (*11*)], and possibly also to the direct toxic

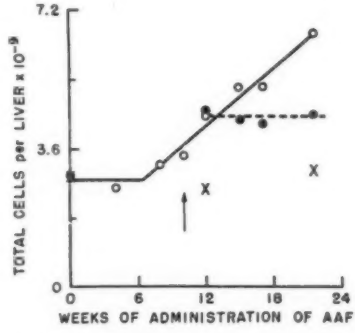

TEXT-FIGURE 4.—Effect of discontinuing the administration of AAF after cell proliferation has started in the liver. AAF was stopped at 10 weeks (↑); cell proliferation continued for another 2 weeks and then stopped. Points marked with an "X" represent values found for control animals not receiving AAF.

action of the drug. The reduction in cell size, which was also described in our earlier study (*13*), corresponds to an over-all reduction in liver weight and to the observed decrease in the total content of protein and RNA in these livers, as shown in text-figure 1. The normal lobular architecture was preserved, however, and there was no appreciable proliferation of ductular cells at this time. We observed very little cell death in these early livers; not more than about one cell per section showed condensation and crenation of the nucleus.

The early increase in the total number of liver cells was accompanied by a marked proliferation of ductular cells. As the increase in the total cell population continued, by the 10th week the normal lobular architecture of the liver had become completely disrupted, and parenchymal cells lay in dense sheets interspersed with disorganized clusters of bile ducts embedded in connective tissue. In the latest stages, small cysts were formed by the distension of these bile ducts; in our experiments, such cysts tended

to remain relatively small (up to a few mm in diameter) even after the appearance of tumors.

DISCUSSION

The data of text-figure 1, in agreement with our earlier observations (*1*, *2*), show that a net increase in the total number of liver cells occurs in preneoplastic livers, after a delay of several weeks during which the growth of the liver is no greater than that in control animals of the same age. This net increase appears to be linear, *i.e.*, it occurs at a constant rate, and it continues until tumors appear after 25 to 30 weeks. It must be emphasized that this is a net increase; a balanced turnover of the cell population may be occurring in addition to the measured increase in total cell number. We could measure such a turnover by labeling the DNA of the liver, but the present data give us no information bearing directly on this question. Other authors, on the basis of microscopic examination of preneoplastic livers, have described individual cell death and a slightly elevated mitotic activity in the first few weeks of administration of a carcinogen (*3–5*). It is clear that such turnover and proliferation in the early period are slight by comparison with the great proliferation of ductular and hepatic cells that occurs during the later phases; such proliferation of ductular cells can be very rapid in onset and may lead to invasion of half the liver lobule within a few days (*4*). We have observed (*14*) a 50 percent increase in the number of recovered liver cells at this time in the same livers studied by Price *et al.* (*4*).

The present data, however, measure the net accumulation of cells that occurs above and beyond any such turnover that may exist, and this accumulation results in an increase in the total liver-cell population to 3 times the normal value by the time tumors appear. Such a great increase in the total size of any cell population could theoretically occur only by immigration of cells from elsewhere in the body, or by proliferation of cells already present. We believe that the observed accumulation of cells in the present experiments is due to cell proliferation, and we have observed enough mitotic activity in such livers to account for the increase in cell number.

In the present experiments, the rate of such cell proliferation is greater with greater doses of AAF. We have suggested one mathematical function that would satisfactorily fit the relations observed, and a number of other such functions would fit equally well. But, whatever the exact mathematical relation may ultimately prove to be, the present data indicate a close physiological relation between the dose of AAF and the rate of cell proliferation in the target organ.

The total quantity of RNA and protein in such livers also increased at a steady rate when "net" cell proliferation was occurring. However, in the initial phase of the preneoplastic period, when the total cell number was essentially constant or even increasing slightly, the quantity of

RNA and protein decreased considerably, and for this reason the quantity of protein and RNA in the average liver cell at the start of the proliferative phase was much reduced from normal [*see* (*13*) and (*15*)]. Since the ensuing increase in cell number is accompanied by a parallel, linear increase in protein and RNA, we can conclude that the new cells being produced have, on the average, a constant composition with respect to protein and RNA. The quantities of protein and RNA in each cell fraction of the whole liver also increase in a linear fashion (*15*), and emphasize that on the average the new cells produced retain a constant gross chemical composition throughout the preneoplastic period.

The linear increase in all these quantities can be extrapolated back to the time of onset of administration of AAF, and in all our experiments to date, the intercept is very close to zero. This fact suggests that whatever physiological process is related to the action of AAF, the damage starts from the time AAF is first administered.

The evident reduction in the DNA content of the average nucleus during the preneoplastic period is almost certainly due to an increase in the proportion of diploid cells in these livers. The proliferating ductular cells are diploid (*16*), and the proportion of diploid to tetraploid cells in preneoplastic livers of rats receiving ethionine has been shown to shift from about 1:5 to 2.6:1 after 9 weeks of ethionine tretament (*16*).

While the evidence is thus far only circumstantial, we should like to suggest the following hypothesis: The carcinogen AAF combines, perhaps by a first-order chemical reaction, with some biologically essential chemical constituent of the liver, and as a consequence inhibits its biological activity. Such a constituent can be assumed to be essential for the survival of the animals, since many of them die at the time proliferation of liver cells starts in the survivors (*1*). If we further assume that such a substance is synthesized only in association with cell division, then the observed linear increase in the total number of liver cells during the second phase of the preneoplastic period could be explained in the following way: Since AAF is being consumed at a constant rate, its inactivation of a target substance would occur at a constant rate. Under these circumstances, if cell proliferation and its accompanying synthesis of this substance were exactly balancing its constant destruction, the cell proliferation would then proceed at a constant rate, which would give a linear increase in the total number of liver cells. The delay in onset of this compensatory cell proliferation would occur if the hypothetical target substance were normally present in excess; the triggering of active cell proliferation would occur as the quantity of this substance approached the minimum necessary for survival.

If we could identify and measure the target substance, we would expect to find that the curve describing the quantitative changes in this substance during the preneoplastic period would show a gradual reduction in quantity during the initial period of comparative cell constancy, and would reach a minimum value at the onset of hyperplasia. If, as we suggest, the hyperplasia only compensates the further loss of the target

substance, we would then expect that the quantity of this material per liver would remain at a constant low level throughout the period of hyperplasia.

That a close relation exists between the cell proliferation and the presence of the carcinogen is further demonstrated by the results of the experiment in which the carcinogen was withheld after the cell proliferation had become well established. After a delay of 2 weeks, the cell proliferation stopped completely and did not resume during the period of observation, which extended almost to the time tumors appeared in the animals still receiving AAF. Such a delay would be expected if a moderate excess of the target substance were to be restored.

It has been shown by others that when administration of a hepatic carcinogen is stopped early in the preneoplastic period, the cholangiofibrosis that accompanies the process remains indefinitely (*4*). In many animals exposed to hepatic carcinogens for brief periods longer than a minimum of 4 to 8 weeks, tumors appear eventually, but their appearance is much delayed (*17*, *18*). This was true in the present experiments; 5 of 6 rats in the group in which the administration of AAF had been discontinued outlived 7 survivors in the group still receiving AAF. All the animals that died in this period had neoplasms.

According to the view presented here, the new cells produced by the proliferation of the second phase of carcinogenesis would be considered to be incidental by-products of a process aimed at maintaining the total quantity of some substance in the liver at a level that permits the animal to survive. That is, this proliferation would constitute a compensatory type of hyperplasia, for which the stimulus is the loss of some subcellular biochemical constituent, rather than the loss of whole cells as is usually the case. According to this hypothesis, AAF would induce proliferation of liver cells through a disturbance of the mechanisms normally controlling growth of the liver, rather than by direct stimulation of mitosis.

It is known from the work of others (*17*, *18*) that administration of a hepatic carcinogen must be continued only through a critical period of 4 to 8 weeks to obtain the maximum incidence of tumor-bearing animals, and that if administration of the carcinogen is discontinued before this time, few if any of the animals will develop tumors. This critical period seems to correspond to that required to establish the proliferative activity described here. However, this cell proliferation is probably only indirectly related to the origin of the tumor cells whose presence will ultimately be demonstrated by the growth of grossly recognizable tumors. In our opinion, the drive toward cell multiplication is a physiological response to the damage produced by the carcinogen, and it produces at the same time both a linear increase in the number of liver cells and a malignant change in a few of them. If each tumor is composed of the progeny of a single cell that has undergone malignant transformation, then no more than about one in a million of the new cells produced during the precancerous period could be fully transformed and independently growing tumor cells (*1*). The nature and cause of the malignant trans-

formation that occurs in so few of the proliferating cells remains undefined. The tumors appear suddenly and only after a long precancerous period, because of their fundamentally exponential type of growth (*19*). At first so few potential tumor cells exist that their presence is not detectable against the background of linear growth of liver cells, but as the number of cells within each tumor focus increases exponentially, quite suddenly a mass of tumor cells becomes visible. Approximately 20 cell generations are required to produce a tumor mass 1 mm across (*1*), and therefore considerable growth takes place before a mass reaches a size great enough to permit its recognition on gross examination.

The evident separation of the preneoplastic period into two phases recalls the two-stage theory of carcinogenesis in skin (*20*). The analogy is strengthened by the fact that the second stage of skin carcinogenesis is characterized by active hyperplasia (*21*), whereas the stage of initiation does not require it (*22*). On the other hand, the results of the present study support the hypothesis that an essential step in liver carcinogenesis is the inactivation or "deletion" of some important cell constituent, probably a protein (*23*, *24*); this substance could be a self-marker protein of the sort suggested by Burnet (*25*). However, our hypothesis differs from the deletion hypothesis, as it is usually stated, in relating the action of the carcinogen to the hyperplasia in the preneoplastic tissue rather than to the initiation of the malignant change (*26*). In the present study, the nature of the malignant change remains undefined.

REFERENCES

(*1*) Laird, A. K., and Barton, A. D.: Cell growth and the development of tumours. Nature, London 183: 1655–1657, 1959.

(*2*) ———: Cell proliferation in precancerous liver: Linear growth curve. Nature, London 188: 417–418, 1960.

(*3*) Farber, E.: Similarities in the sequence of early histological changes induced in the liver of the rat by ethionine, 2-acetylaminofluorene, and 3′-methyl-4-dimethylaminoazobenzene. Cancer Res. 16: 142–148, 1956.

(*4*) Price, J. M., Harman, J. W., Miller, E. C., and Miller, J. A.: Progressive microscopic alterations in the livers of rats fed the hepatic carcinogens 3′-methyl-4-dimethylaminoazobenzene and 4′-fluoro-4-dimethylaminoazobenzene. Cancer Res. 12: 192–200, 1952.

(*5*) Popper, H., Kent, G., and Stein, R.: Ductular cell reaction in the liver in hepatic injury. J. Mt. Sinai Hosp. 24: 551–556, 1957.

(*6*) Dounce, A. L., Witter, R. F., Monty, E. J., Pate, S., and Cottone, M. A.: A method for isolating intact mitochondria and nuclei from the same homogenate, and the influence of mitochondrial destruction on the properties of cell nuclei. J. Biophys. & Biochem. Cytol. 1: 139–153, 1955.

(*7*) Umbreit, W. W., Burris, R. H., and Stauffer, J. F.: Manometric Techniques and Tissue Metabolism. Minneapolis, Burgess Pub. Co., 1949.

(*8*) Schneider, W. C.: Phosphorus compounds in animal tissues. I. Extraction and estimation of desoxypentose nucleic acid and of pentose nucleic acid. J. Biol. Chem. 161: 293–303, 1945.

(9) BEAMS, H. W., and KING, R. L.: The origin of binucleate and large mononucleate cells in the liver of the rat. Anat. Rec. 83: 281–297, 1942.

(10) PRICE, J. M., and LAIRD, A. K.: A comparison of the intracellular composition of regenerating liver and induced liver tumors. Cancer Res. 10: 650–658, 1950.

(11) LAIRD, A. K., BARTON, A. D., and NYGAARD, O.: Synthesis of protein and ribonucleic acid in rat liver during refeeding after starvation. Exper. Cell Res. 9: 523–540, 1955.

(12) LINEWEAVER, H., and BURK, D.: The determination of enzyme dissociation constants. J. Am. Chem. Soc. 56: 658–666, 1934.

(13) LAIRD, A. K., and MILLER, E. C.: Studies on the intracellular composition of livers from rats fed 2-acetylaminofluorene. Cancer Res. 13: 464–470, 1953.

(14) LAIRD, A. K.: Cell proliferation and changes in the large granule fraction during hepatic carcinogenesis. Proc. Soc. Exper. Biol. & Med. 77: 434–437, 1951.

(15) ———: Studies of cytoplasmic particulates. Ph.D. Thesis, Univ. Wisconsin, 1952, pp. 51–53.

(16) HOLZNER, J. H., BARKA, T., and POPPER, H.: Changes in the DNA content of rat liver cells during ethionine intoxication. J. Nat. Cancer Inst. 23: 1215–1225, 1959.

(17) WILSON, R. H., DEEDS, F., and COX, A. J.: The carcinogenic activity of 2-acetylaminofluorene. II. Effects of concentration and duration of exposure. Cancer Res. 7: 444–449, 1947.

(18) GLINOS, A. D., BUCHER, N. L. R., and AUB, J. C.: The effect of liver regeneration on tumor formation in rats fed 4-dimethylaminoazobenzene. J. Exper. Med. 93: 313–324, 1951.

(19) BASERGA, R., KISIELESKI, W. E., and HALVORSEN, K.: A study of the establishment and growth of tumor metastases with tritiated thymidine. Cancer Res. 20: 910–917, 1960.

(20) BERENBLUM, I., and SHUBIK, P.: A new quantitative approach to the study of the stages of chemical carcinogenesis in the mouse's skin. Brit. J. Cancer 1: 383–391, 1947.

(21) WALPOLE, A. L.: Initiation and promotion in carcinogenesis. *In* Ciba Foundation Symp. on Carcinogenesis. London, J. and A. Churchill, Ltd., 1959, pp. 41–54.

(22) BERENBLUM, I.: Some new implications of the two-stage mechanism in the study of skin carcinogenesis. *In* Ciba Foundation Symp. on Carcinogenesis. London, J. and A. Churchill, Ltd., 1959, pp. 55–69.

(23) MILLER, E. C., and MILLER, J. A.: Biochemical investigations on hepatic carcinogenesis. J. Nat. Cancer Inst. 15: 1571–1590, 1955.

(24) POTTER, V. R.: The biochemical approach to the cancer problem. Fed. Proc. 17: 691–697, 1958.

(25) BURNET, F. M.: The self marker hypothesis in relation to cellular proliferation and control. *In* Enzyme Antigen and Virus. Cambridge, Cambridge Univ. Press, 1956, chapt. 3, p. 81.

(26) LAWS, J. O.: Tissue regeneration and tumour development. Brit. J. Cancer 13: 669–674, 1959.

603724—61——11

Production of Viable Single Cell Suspensions From Solid Tumors[1]

ROBERT E. MADDEN[2] *and* DEAN BURK,[3] *Laboratory of Biochemistry, Cytochemistry Section, National Cancer Institute,*[4] *Bethesda, Maryland*

SUMMARY

A method is described for utilizing trypsin and DNAase to obtain suspensions of large numbers of single viable cells from a variety of solid tumor sources. Representative yields are reported. The viability index, which was obtained by vital staining, approached 100 percent. Metabolic studies disclosed little or no alteration in respiration and aerobic and anaerobic glycolysis of enzyme-processed cells, whether they were derived from solid tumors or from ascites cells and compared to unprocessed ascites cells. Processed cells derived from solid tumors showed consistently higher metabolic values than tissue slices of the tumor. Testosterone inhibited, and 2,4-dinitrophenol and endotoxin stimulated, certain metabolic parameters in tumor cells where such responses could be expected. The cells from one of two solid tumors tested compared favorably with equal numbers of the same strain ascites cells in ability to form tumors when injected back into mice of the host strain. Few, if any, morphologic differences were seen microscopically between stained cells derived from solid tumors and those from the ascites counterpart. Cells processed from a solid tumor were maintained in continuous tissue culture for 3 months. Time-lapse photography disclosed amoeboid motion. After 6 days in culture, biological virulence comparable to that in freshly derived cells was demonstrated by injection back into mice of the host strain.—J. Nat. Cancer Inst. 27 : 841–861, 1961.

A METHOD of producing suspensions of large numbers of viable, single cells from a variety of solid tumor sources appears desirable for quantitative work at the cellular level. The production of ascites from solid tumors has provided one successful method of obtaining such suspensions. It is common knowledge that purely mechanical disruption of solid tumors, without added enzymes, has usually yielded quantitatively unsuitable products because of clumping, debris, and low index of viability.

---

[1] Received for publication May 24, 1961.

[2] *Present address*: Department of Surgery, New York Medical College, Flower and Fifth Avenue Hospitals, New York, N.Y.

[3] The authors are grateful to Dr. Mark Woods and Mr. Jehu Hunter, National Cancer Institute, for valuable suggestions and help, and to Lt. Vernon Perry, National Naval Medical Center, Bethesda, Md., for collaboration in the tissue culture and time-lapse photography studies.

[4] National Institutes of Health, Public Health Service, U.S. Department of Health, Education, and Welfare.

Enzymatic preparation of cell suspensions from tissue-culture material was used as early as 1916 by Rous and Jones (*1*). It is an established technique in tissue culture today and has been used to produce cell suspensions from, *e.g.*, embryonic tissue (*2*), monkey kidney (*3*, *4*), and island ascites tumor (*5*).

In the present report a method is described in which two enzymes, trypsin and deoxyribonuclease, are used to obtain single cell suspensions from human and mouse solid tumors. The ability to obtain viable cell suspensions depends upon the breakdown of solid tissue and the separation of cells from stroma, with concomitant preservation of the cell. The viability of each cell is difficult to establish and probably depends ultimately on the definition of viability chosen. Staining, with trypan blue used in *all* cases, has been employed as a criterion of viability of individual cells; in some cases eosin and tetracycline were also used. In two of the mouse tumors, biological virulence was tested by quantitative mouse inoculation. Tissue-culture survival was demonstrated and extensive metabolic studies were carried out with the use of classical, and also more recent, Warburg manometric methods.

MATERIALS AND METHODS

Preparation of cell suspensions.—All preparations were carried out at room temperature. Freshly obtained tumor material was trimmed of gross necrosis, connective tissue, skin, and blood clots. It was rinsed in Earle's salt solution modified to contain the following in g per liter: NaCl, 6.8; KCl, 0.4; $NaH_2PO_4.H_2O$, 0.2; $NaHCO_3$, 2.2; dextrose 3.0; *p*H 7.4. The selected tumor material was blotted and weighed. The same solution with 0.25 percent crude trypsin [5] (T-solution) was added to the tumor, which was then cut with an iris scissors into particles about 1 mm^3. This suspension, containing not less than 10 cc T-solution per g of tissue, was transferred to a small Erlenmeyer flask or trypsinizing vessel. Six drops (0.3 cc) of a 0.04 percent deoxyribonuclease [6] (DNAase) solution per 10 cc tumor mixture were added and the mixture was allowed to stand, with occasional shaking, for one-half hour.

The supernatant (S-1) was decanted through two layers of cheesecloth and fresh T-solution and DNAase were added to the residue. This was agitated 1 hour on a magnetic stirrer and similarly filter-decanted, and yielded the first harvest (H-1). S-1 and H-1 were centrifuged separately at 200 $\times$ *g* for 10 minutes, and the pellets of cells resuspended by shaking in 1 or 2 cc of modified Earle's solution containing a drop of DNAase. S-1 was only occasionally used for further studies since it often contained considerable debris and red cells. The tumor cells were

[5] Crude trypsin, Difco Laboratories, Inc., Detroit, Mich., 1:250; hereinafter referred to as "trypsin." (Purified trypsin was not studied here.)

[6] Deoxyribonuclease crystallized once, Worthington Biochemical Corp., Freehold, N.J.

counted in a hemocytometer. A second harvest (H-2) was sometimes obtained by repeating the procedure with the residue from H-1. In most cases the yields were less than a quarter of H-1 and hence a second harvest was not used in the standard procedure.

Viability and biological virulence studies.—A drop of the suspension was stained with an equal volume of 0.25 percent trypan blue and the viability index was determined microscopically. In some instances the cells were also stained with 0.5 percent eosin, with results in excellent agreement with the trypan blue staining. The cells were observed once with ultraviolet light (350 mμ) after exposure to tetracycline (*6*) and a viability index approximately equal to that obtained with trypan blue was obtained. When there was difficulty in differentiating small tumor cells from inflammatory cells (lymphocytes and polymorphonuclear leukocytes), a sample of the suspension was taken up on a Millipore filter and examined after Papanicolaou staining.

Biological virulence was studied in mice by quantitative subcutaneous and intraperitoneal injection of prepared cell suspensions or ascites cells. Suitable dilutions were made in modified Earle's salt solution. Subcutaneous injections were made in the right thigh and the animals were examined daily. The 1st day a tumor was palpable at the inoculation site, and then persisted and grew, it was recorded. Survival time was recorded for animals receiving intraperitoneal tumor-cell injections. In one experiment the suspension material was obtained from tumor cells that had been maintained in roller tubes for 6 days in tissue culture in media described as follows.

Tissue-culture methods.—Cells were grown in roller tubes or Carrel D-3.5 flasks in NCTC 109, chemically defined media (*7*) supplemented with 10 volume-percent horse serum. Conventional and effective concentrations of SPAM (streptomycin, penicillin, aureomycin, and mycostatin) at, respectively, 200 μg, 200 units, 20 μg, and 20 units per cc of medium were added in most cases. In a replicate culture study, Earle's T-15 flasks were used. All cultures were gassed with 5 percent CO_2 and grown at 37.5° C. Appropriate fluid changes were made on the basis of *p*H change, usually every 3d or 4th day.

Replicate culture technique (*8*) was employed with one mouse tumor (MPC-3, a plasma-cell tumor) to test for viable cell survival and possible establishment in culture. Twenty-five T-15 flasks were inoculated from the stirring funnel, and triplicate to quintuplicate sacrifice was carried out periodically until the 10th day. The nuclear counts were interpreted as representing quantitatively the initial and subsequent total numbers of viable cells present (*8*). Time-lapse photography was undertaken on several Carrel flask cultures of this same tumor when they adhered to the glass.

Metabolic and manometric methods.—Respiratory oxygen consumption, and aerobic and anaerobic glycolysis, in the presence or absence of added 2,4-dinitrophenol (DNP), were measured in standard Warburg manometers with standard or newly designed vessels (*9*, *10*). Occasionally

Summerson manometry was employed, especially where direct measurements of respiratory carbon dioxide production and the respiratory quotient were also desired.

In the newly designed vessels used in aerobic experiments, the usual central well on the floor of the standard Warburg vessel is replaced by an elevated, wide-area trough further connected directly and confluently to a sidearm. To trough and sidearm are added, respectively, 0.4 and 0.6 cc of a mixture of 4 parts of 3 M $KHCO_3$ and 1 part 3 M K_2CO_3 containing up to 1 to 2 mg per cc commercial carbonic anhydrase, depending upon the relative purity of the latter. This buffer-enzyme mixture, with adequate shaking in the trough and sidearm, produces and maintains at 38° C a strictly constant and particular physiological pressure of CO_2 of about 5 percent-atm in the gas phase, so that any pressure decrease represents simply oxygen consumption, after correction against a thermobarometric control vessel containing the same potassium bicarbonate-carbonate-carbonic anhydrase mixture in the trough and sidearm but no living cells. When the latter mixture is omitted from a replicate experimental vessel, the difference in pressure changes between the two experimental vessels containing cells represents the sum of (*a*) the respiratory CO_2 production, plus (*b*) the CO_2 derived from aerobic glycolysis as a result of action of lactic or other acid on bicarbonate in the medium containing the living cells in the main vessel compartment. The aerobic glycolysis (*b*) may then be calculated by subtracting the respiratory CO_2 production (*a*), which may be estimated to be equal to the O_2 consumption (respiratory quotient = CO_2 produced/O_2 consumed, which is assumed to be 1, or possibly only 0.8), or obtained from direct measurements of CO_2 production made by Summerson manometry.

In anaerobic experiments, the gas phase was 5 percent CO_2 in nitrogen; or, at times, without distinguishable difference in result, 5 percent CO_2 in air with 0.01 M sodium azide (final concentration) in the cell-suspending medium (azide added from a stock 0.1 M azide solution in saline). DNP, when used, was added to provide 23 mg per liter (23 ppm) final concentraation, insulin at 0.4 units per cc, endotoxin P-45 (*Serratia marcescens*) at 1 ppm, and testosterone at 100 ppm. The cell-suspending medium [Krebs III, (*11*)] contained also 2 mg glucose per cc and 2 mg $NaHCO_3$ per cc initial concentration. Final *p*H values were checked at the end of most manometric runs.

Metabolic quotients are expressed as [7] $^*Q_{O_2}$ (oxygen consumption), $^*Q_A^{O_2}$ air (aerobic glycolysis, measured in 5% CO_2 in air), $^*Q_A^{N_2}$ (anaerobic glycolysis in 5% CO_2 in N_2 or in 5% CO_2 in air with 0.01 N NaN_3), and refer to mm^3 gas exchange per hour per *ca* 3 million tumor cells. Manometric measurements were usually made with 2 cc of cell suspension for a period of 2 hours.

[7] $^*Q$ values are based on cell count rather than mg dry wt as in the case of conventional Q values. However since *ca* 3 million of the tumor cells studied equal approximately 1 mg dry wt, $^*Q$ values approximate conventional Q values based on mg dry wt. Ordinary Q values reported for tissue slices are based on the conventional mg dry wt.

RESULTS

Yield of Viable Cells From Various Tumors

Table 1 shows the yield of viable single cells (determined by trypan blue staining) obtained from a variety of tumor sources. All yields are expressed as numbers of cells per g of starting material. The percentage of nonviable cells was subtracted from the total count. In no case, however, did this exceed 8 percent and it was usually 0 to 2 percent, and was regarded as negligible. A wide range of yields of viable cells was obtained from different tumors. Replicate determinations on different examples of the same transplantable tumors also showed considerable variation in yield. In two mouse tumors, melanoma S91 and MPC-3 (a mouse plasma-cell tumor obtained from the laboratory of Dr. Michael Potter, Laboratory of Biology, National Cancer Institute), the numbers of packed cells per mm^3 were determined to be 180,000 and 300,000, respectively. Thus the percentage yield of cells from the starting tumor could be calculated on a volume basis. The range was 9.1 to 14.4 percent with S91, and 5.0 to 19.8 percent with MPC-3, assuming a specific gravity of unity for tumor. The volume of packed processed cells was determined in a hematocrit centrifuged sufficiently to yield a minimum volume of cells. Thus, as a sample calculation for melanoma S91, a yield of 16.5 million cells obtained from 1 g wet weight starting material would represent a volume-percentage yield of $100 \times (16{,}500{,}000/180{,}000)mm^3$ per

TABLE 1.—Viable cell yields per gram wet weight of starting material

Tumors	Number of cells $\times 10^6$
Human	
Epidermoid carcinoma of cervix	1. 15
Epidermoid carcinoma, floor of mouth	1. 37
Inflammatory carcinoma of breast*	2. 23
Adenocarcinoma of cervix	2. 33
Epidermoid carcinoma of cervix	2. 68
Infiltrating duct carcinoma of breast	3. 20
Transitional-cell carcinoma of bladder	38. 9
Horse	
Melanoma, spontaneous	Nil
Mouse	
S91 melanoma	16. 5
	23. 3
	26. 8
MPC-3 (plasma-cell tumor), BALB/c	15. 1
	39. 6
	59. 5
MS-2 (sarcoma), BALB/c	19. 0
	24. 8
	70. 0
Mammary carcinoma, spontaneous, C3H	62. 1
Mammary carcinoma, spontaneous, C57BL	76. 0
Krebs-2	80. 0
Mammary carcinoma AMT-2, C3H	89. 6

*Treated with collagenase instead of trypsin.

1000 mm^3, or 9.1 percent. Such an expression of experimentally measured quantities represents, of course, less than the true percentage yield of viable tumor cells per original tumor cells, since the 1000 mm^3 wet weight of starting material contained much nontumorous material (stroma, blood, unavoidable necrotic material, etc.); moreover, not all tumor cells were released by the enzymatic and other processing, so that selection, significant or otherwise, was in some measure involved. No parameters of dry weight, nitrogen content, or deoxyribonucleic acid (DNA) or ribonucleici acid (RNA) content were measured, since they were beyond the immediate scope of interest of this study.

The variable yields obtained from different tumors and different samples of the same tumor line probably reflect differences in cellularity of the starting material, cell size, amount of necrosis, and amount of fibrous tissue stroma in the starting materials that not only represent some of the wet weight but also impede the release of cells. Trypsin acts slowly, if at all, on collagen and elastin under the conditions employed. In general, the spontaneous and transplantable mouse tumors yielded more cells than the spontaneous human tumors, which is not surprising since they were in general "softer," and thus gave better yields even in the absence of added enzymes.

Effects of Mechanical Processing Without Added Enzymes

In another series of experiments preparations obtained with mechanical agitation alone, *i.e.*, without enzymes, were compared with preparations with added enzymes. Three transplantable mouse tumors were each divided into two approximately equal parts. Each part was processed identically as described, but in one, the enzymes were omitted. The results are shown in table 2, and it is seen that several times as many viable cells were obtained with the enzymes as without. Furthermore, the products from two of the tumors showed a high percentage of dead cells when enzymes were not used. Column A of table 2 indicates that the viable cell yields with enzymes were virtually equal to the total cell yields, whereas column B shows that the viable cell yields were, respectively, 100, 75, and 50 percent of the total cell yields.

Metabolic Effects of Processing on Tumor Tissue

The possibility of damage to respiratory and glycolytic pathways in processing tumors cells was studied in four mouse tumor lines: MPC-3, Krebs-2, thymoma (Dalton–Schade), and S91 melanoma. The first three lines occur in both ascites and solid form. In table 3 the metabolic *Q values for cells processed from two solid tumors are compared with those of their untreated ascites counterpart. It is seen that in both there is a lower metabolic activity, per unit cellular material, in the cells processed from solid tumors.

TABLE 2.—Effects of mechanical agitation with and without enzymes

Tumor	A Viable cell yield with enzymes	B Viable cell yield without enzymes	Ratio $\frac{A}{B}$	Percentage of dead cells (B)
AMT-2	89.6×10^6	19.6×10^6	4.6	0
MPC-3	15.1×10^6	4.6×10^6	3.3	25
MS-2	25.4×10^6	3.7×10^6	6.9	50

TABLE 3.—Respiration and glycolysis in cells processed from solid tumor versus unprocessed ascites cells

	MPC-3		Krebs-2	
	Treated suspension	Untreated ascites	Treated suspension	Untreated ascites
$^*Q_{O_2}$	4.0	6.3		
$^*Q_A^{O_2}$	11.0	22.0		
$^*Q_A^N$	15.0	25.0		
$^*Q_{O_2}$ Control 8.4		11.2	4.8	5.7
DNP		13.2	7.0	16.8
$^*Q_A^{O_2}$ Control 8.2		10.0	22.0	25.0
DNP		21.2	39.0	64.0
$^*Q_A^N$ Control 10.8		24.0	22.0	38.0
DNP		17.2	19.0	41.0

*Q values refer to mm^3 gas per hour per 3.02×10^6 ascites cells or per 3.23×10^6 treated cells where each equals 6 mm^3 packed cells or 1 mg dry weight at 16.6 percent dry weight assumed.

It is doubtful, however, that these differences indicate significant metabolic alterations due to processing, since it has been a general observation in this laboratory and elsewhere that almost invariably ascites cells have much higher metabolic values than do slices of the corresponding solid tumor, and, further, that metabolic Q values between different solid tumors of the same tumor line or different ascites preparations of the same tumor can vary widely. This variability is likewise seen here between the two preparations of the MPC-3 tumor. It is most important to note that after enzymatic processing the cells still maintain that important property of virtually all cancer cells, namely, the ability to ferment glucose in the presence of oxygen. Furthermore, DNP is still able to evoke a marked uncoupling effect—increase in aerobic glycolysis and/or respiration—when used with the treated cells. The aerobic glycolysis with DNP may indeed often be greater than the anaerobic glycolysis. Badly damaged cells usually show little or no uncoupling by DNP, since both aerobic and anaerobic glycolysis may be so greatly inhibited as to be incapable of showing a true Pasteur effect.

A comparison between the treated and untreated aliquots of the same ascites preparation is seen in table 4. Here again the metabolic activity

TABLE 4.—Respiration and glycolysis in trypsin- and DNAase-treated MPC-3 ascites cells versus untreated ascites cells

		Treated ascites	Untreated ascites
$^{*}Q_{O_2}$		8.1	7.0
$^{*}Q_A^{N_2}$	Control	33.1	23.7
	DNP	47.3	39.6
$^{*}Q_A^{N_2}$		30.0	29.8

*Q values refer to mm³ gas per hour for 3.02×10^6 cells, where 3.02×10^6 cells = 6 mm³ packed cells = 1 mg dry weight at 16.6 percent dry weight assumed.

has not been greatly altered by treatment, and marked DNP uncoupling (increase in aerobic glycolysis) again is indicated.

The more subtle metabolic indexes of cancer metabolism were briefly and unextensively examined in S91 melanoma and the thymoma. Results are illustrated in table 5. In control, as well as test runs, the metabolism in the treated cell suspensions, whether measured by respiration or by fermentation, with or without oxygen, exceeds that of the tissue slices, just as ascites cells do. The data indicate that insulin had some stimulating effect on glycolysis in tissue slices of both tumors and in thymoma suspension. However, in the S91 melanoma suspension no insulin effect was observed (the control anaerobic glycolysis was already so high that insulin stimulation, as well as endotoxin stimulation, may have been precluded). Testosterone had its characteristic marked inhibitory effect which was well preserved in the treated cell suspensions. DNP

TABLE 5.—Response to insulin, endotoxin, and testosterone of cells processed from solid tumors versus tumor tissue slices

	S91 melanoma		Thymoma (Dalton–Schade)	
	Treated suspension	Tissue slice	Treated suspension	Tissue slice
$^{*}Q_{O_2}$ or Q_{O_2}	*Q	Q	*Q	Q
Control	7.0		4.3	3.0
Insulin†	7.0	3.0	4.3	3.2
Endotoxin	7.5	2.7		
Testosterone	3.8			
DNP	12.0		6.4	5.5
$^{*}Q_A^{N_2}$ or $Q_A^{N_2}$				
Control	6.3	2.9	11.2	
Insulin	5.0	4.6	12.2	
Endotoxin	14.0	3.9		
Testosterone	2.8			
DNP	5.0		26.0	
$^{*}Q_A^{N_2}$ or $Q_A^{N_2}$				
Control	20.0	4.4	25.0	13.5
Insulin	20.0	6.0	28.0	14.8
Endotoxin	20.0	5.3		
Testosterone	9.0	1.9		
DNP	19.0		32	19.0

† Insulin, 17 ppm (0.4 units/cc); endotoxin P-45, 1 ppm; testosterone, 100 ppm, and DNP, 23 ppm.

uncoupling occurred in most cases. The endotoxin effect of stimulating aerobic glycolysis, initially described by Woods, Landy, and Shear (*12*), was likewise seen in the suspension preparations of S91 melanoma. Various publications from this laboratory have shown that in general melanoma cells are more responsive as regards their insulin : anti-insulin system than are ascites cells, where such hormonal regulation is largely, though not completely, lost.

Preservation of Biological Potency

The ability of processed cells injected subcutaneously to cause tumors or ascites when compared with ascites cells of the same tumor was compared in both MPC-3 and Krebs-2 tumors. The former was used in its isologous strain of origin, BALB/c mice, and the latter in C3H mice. The results are given in tables 6 and 7; animals were examined daily for first appearance of the tumor. With the MPC-3–BALB/c system the processed cells are at least as virulent as the ascites cells. In the Krebs-2–C3H system, however, ascites cells proved more virulent. Table 8 shows the results of another such experiment with MPC-3 in BALB/c in which a presumed final endpoint of tumor formation was reached. The animals were observed for 60 days. The ascites cells displayed slight, if any, significant virulence over the treated cells. In these studies no growth comparisons were made between small numbers of ascites cells injected intraperitoneally as compared with subcutaneous injections.

Figure 1 is a photomicrograph of Papanicolaou-stained mouse sarcoma MS-2 cells processed from a solid tumor. A few leukocytes are present. This was true in most preparations, but a rough estimate would place the volume of such cells at less than one hundredth the volume of the tumor cells. Such contamination with leukocytes was less than that ordinarily found in ascites cell samples.

TABLE 6.—Biological virulence study—MPC-3–BALB/c system

Days after subcutaneous injection of cells for appearance of palpable tumors								
	Cell suspension				Ascites cells			
Number of mice	6	6	6	6	6	6	6	6
Number of cells injected	10,000	1,000	100	10	10,000	1,000	100	10
9 Days	0	0	0	0	0	0	0	0
11	0	0	0	0	1	0	0	0
12	3	0	0	0	4	0	0	0
13	3	0	0	0	5	1	0	0
15	5	1	0	0	6	2	0	0
16	5	2	0	0	6	3	0	0
19	5	2	1	0	6	3	0	0
20	6	2	2	0	6	3	0	0
21	6	2	2	0	6	4	0	0
35	6	2	2	0	6	4	0	0

TABLE 7.—Biological virulence study—Krebs-2–C3H system

Days after subcutaneous injection of cells for appearance of palpable tumors or ascites

	Cell suspension				Ascites cells			
Number of mice	6	6	6	6	6	6	6	6
Number of cells injected	100,000	10,000	1,000	100	100,000	10,000	1,000	100
8 Days	0	0	0	0	1	0	0	0
9	0	0	0	0	2	0	0	0
10	1	0	0	0	2	0	0	0
11	1	0	0	0	3	0	0	0
13	1	0	0	0	4	0	0	0
14	2	0	0	0	4	0	0	0
16	2	0	0	0	5	1	0	0
17	3	0	0	0	5	2	0	0
19	3	1	0	0	6	2	0	0
27	3	1	0	0	6	3	1	0
36	3	1	0	0	6	3	1	0

TABLE 8.—Biological virulence study—MPC-3–BALB/c system

Mice alive with tumor, or dead as a result of tumor, 60 days after subcutaneous inoculation

	Cell suspension		Ascites cells	
Number of cells inoculated	1, 000	100	1, 000	100
Tumor mice/total mice	17/20	9/10	20/20	18/19

Figure 2 shows a stained preparation of MPC-3 cells processed from a solid tumor, and figure 3 shows cells of the ascites counterpart of the same tumor. It can be seen that, after staining, the tumor cells from both sources are essentially identical, whereas the ascites preparation contains more leukocytes. Figure 4 shows a similarly stained preparation of cells from a solid S91 melanoma, for which no ascites form exists at present, in spite of numerous attempts to obtain one.

Tissue-Culture Studies

Text-figure 1 shows the graphed results of the replicate culture study of MPC-3. As would be expected in most primary cultures, the nuclear counts dropped initially. A later rise was noted with apparent leveling off at 10 days. These results represent only one experiment and cannot be considered representative or conclusive. All that can be said is that a logarithmic growth phase was not obtained by 10 days, neither was there extinction of growth.

Other cultures were kept in roller tubes at 12 revolutions per hour. After 6 days the cells were inoculated subcutaneously back into BALB/c mice. The results in table 9 prove that the cells survived in tissue culture for at least 6 days. These data, while semiquantitative with respect to tumor virulence, can perhaps be compared roughly to the data on fresh

cells of the same tumor given in tables 6 and 7. Processed cells from the MPC-3 tumor were maintained 3 months in culture before continuing growth ceased.

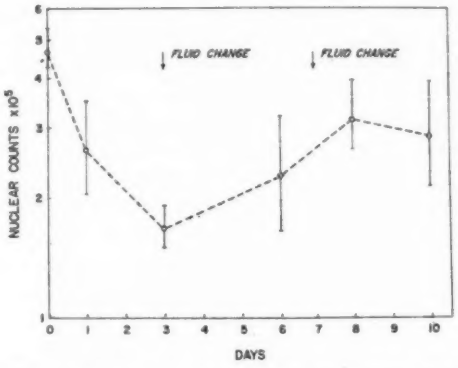

TEXT-FIGURE 1.—Nuclear counts of replicate culture study of MPC-3.

TABLE 9.—Biological virulence study—MPC-3*–BALB/c system

	Mice with tumors 42 days after inoculation	
Cells	100, 000	10, 000
Tumor mice/total mice	12/12	10/10

*Tumor cells used were obtained from a solid tumor and were maintained in culture in roller tubes for 6 days prior to subcutaneous inoculation.

Time-lapse photography was employed with some of the preparations in Carrel flasks. Minimal to moderate motion was observed. Figure 5 illustrates that the cells had adhered to the glass surface and exhibited cytoplasmic processes.

DISCUSSION

The ability to obtain single cell preparations from a wide variety of solid tumor sources has a number of applications. Our own immediate interest was an experimental study of circulating tumor cells in the mouse (*13*). There are certain advantages of suspensions from solid tumors over ascites tumors: The selection of tumors is not as limited. In fact, we have had at least a modicum of success in all but one tumor studied (table 1). The lone exception was a spontaneous horse melanoma in which most of the cells disintegrated during processing of the solid tumor. The experience of Klein (*14*), Belkin (*15*), and others has been that only a small percentage of solid tumors will readily convert to ascites. This is particularly true of adenocarcinomas. Our yields of massive amounts of cells from all portions of the solid tumor make it more likely that a population exhibits

average ploidy and genetic similarity to the parent tumor, but of course one cannot rule out some form of cell selection, significant or otherwise. Such a similarity may be lost in ascites strains due to cell selection (*14*). Cell type selection is possibly fundamental in ascites conversion. Boyse (*16*) recently published a report on trypsinized mouse mammary tumors and found no fundamental immunological changes due to trypsin. It is not inconceivable that single cells prepared along the lines indicated in this paper would yield higher percentages of conversion to the ascites form than other methods, in view of their initially dispersed state and preserved virulence.

It may be mentioned that we have examined two types of mechanical disruption of solid tumors. One method involved bumping a tube with tissue fragments in suspension. The Snell cytosieve method produced a similar type of result, *viz.*, a highly clumped product of very low viability index from which few viable single cells could be obtained by harvesting off a supernatant. A wet preparation of such material (mouse melanoma S91) stained with trypan blue is shown in figure 6. This may be compared in figure 7 with a corresponding preparation obtained by the processing described in this paper; only a single stained (and presumably nonviable) cell may be noted, located in the center of the field.

Kaltenbach (*17*) obtained fewer than one-third live (unstained) cells with his screening method. In our own method, mechanical agitation in the absence of enzymes yielded high percentages of dead cells in two cases (table 2). We have no certain explanation for this. It is probable that trypsin and DNAase secondarily digest some of the dead cells released during processing, which would account for viability indexes approaching 100 percent for the residual material. DNAase associated with liver mitochondria has been shown to be destructive of liver nuclei (*18*).

There is ample evidence that trypsin treatment of animal cells, bacteria, or fungi is not incompatible with their survival and subsequent propagation. This subject has been reviewed by Rinaldini (*19*). The application to tumors, however, is somewhat limited in the published literature. Rous and Jones' original report (*1*) mentions tumor tissue, but the subsequent course of growth was not followed. Other reports of the use of trypsin on tumor tissue involved the characterization of intercellular cement (*5*) or *in vitro* immunologic studies (*16*). The present report would indicate that no fundamental damage to biological virulence of the individual cells has accrued from the described treatment. It would also indicate a possible new source of tissue-culture lines since both short-term survival with preserved biological virulence and a long-term maintenance survival have been demonstrated.

Most uses of trypsin without DNAase on various tissues have resulted in a glairy, mucus-like residue, more or less resistant to a variety of enzymes, chelating agents, alkalinity, or hyaluronidase (*5*, *19*). We have found, along with, but independently of, Boyse (*16*), that this residue can be quickly and thoroughly dispersed with DNAase within a few seconds. The DNAase is apparently not attacked by the trypsin since its addition

at the start of the procedure gave equally good dispersion in our hands. There is no reason to doubt that the essential action of DNAase is enzymatic. That "The use of DNAase for the preparation of cells for *in vivo* or *in vitro* growth purposes raises the serious question of the effect of this enzyme on the genetic apparatus of the cells"—a suggestion seriously advanced to us—is a question beyond the scope of this investigation, as are the similar possibilities of genetic effects of other elements in our preparation.

There is undoubtedly considerable morphologic alteration of the cells during processing. This was not studied in detail in the present work. Edwards and Fogh (*20*) have reported profound intracellular alterations in human amniotic cells after 1 hour of trypsinization. Changes of similar magnitude may well have occurred in our own cells. From the cytologic appearance of stained cells under the microscope, no obvious changes took place (*cf.* figs. 1 and 2). Such possible morphologic changes notwithstanding, the cells were able to survive and multiply with the same virulence as their ascites counterparts. Viability tests, when positive, are the best evidence of lack of irreversible damage to cells.

The metabolic studies are of considerable interest. St. Amond and Tipton (*21*) separated grasshopper embryo neuroblasts with trypsin and hyaluronidase and reported active respiration. No comparison was made with untreated tissue. Kaltenbach (*17*) compared his screen-separated single cells to the same strain ascites cells and found the latter to have a somewhat higher anaerobic glycolysis but only slightly higher aerobic glycolysis. These findings agree closely with our own results comparing enzymatically separated cells with the ascites form (table 3). Similar results have frequently been reported as between solid tumor slices and their ascites forms. Perhaps the differences reflect a cell type selection in the conversion of solid to ascites form. In any case, the evidence suggests that trypsin is not responsible in the major part for a reduction in carbohydrate metabolism. This is further supported by the lack of significant alteration when ascites cells are treated directly (table 4).

Warburg (*22*) has attached great significance to the advent of ascites cancer "that consists of nearly 100 percent cancer cells." It is true that studies of respiration and fermentation on tissue slices always suffer because of the presence of unknown quantitites of stroma, red and white cells, and necrotic tumor cells. Some ascites preparations contain fairly large numbers of inflammatory reaction cells and it is usually best to examine all preparations microscopically. The resultant preparations obtained by the method described herein have all been examined microscopically and many have been collected on Millipore filters and stained. It is not claimed that any of them are fully "100 percent pure." They do, however, contain no stroma, virtually no red cells, a negligible amount of white cells on a volume basis, and a determined number of dead cells, usually below 2 percent.

The choice of medium deserves some discussive comment, since the presence of divalent cations promotes cohesive integrity of solid tissues,

and it was necessary to choose a medium without Ca^{++} or Mg^{++}. Earle's B solution was chosen from the available tissue-culture media as one such medium containing sufficient bicarbonate to buffer a heavy load of glycolyzing tumor cells over a 3- to 4-hour period.

REFERENCES

(1) ROUS, P. AND JONES, F. S.: A method for obtaining suspensions of living cells from the fixed tissues, and for the plating out of individual cells. J. Exper. Med. 23: 549–554, 1916.

(2) MEDAWAR, P. B.: Sheets of pure epidermal epithelium from human skin. Nature, London 148: 783, 1941.

(3) DULBECCO, R., and VOGT, M.: Plaque formation and isolation of pure lines with poliomyelitis viruses. J. Exper. Med. 99: 167–182, 1954.

(4) YOUNGNER, J. S.: Monolayer tissue cultures. I. Preparation and standardization of suspensions of trypsin-dispersed monkey kidney cells. Proc. Soc. Exper. Biol. & Med. 85: 202–205, 1954.

(5) ESSNER, E., SATO, H., and BELKIN, M.: Experiments on ascites hepatoma. I. Enzymatic digestion and alkaline degradation of the cementing substance and separation of cells in tumor islands. Exper. Cell Res. 7: 430–437, 1954.

(6) DU BUY, H. G., and SHOWACRE, J. L.: Selective localization of tetracycline in mitochondria of living cells. Science 133: 196–197, 1961.

(7) EVANS, V. J., BRYANT, J. C., FIORAMONTI, M. C., MCQUILKEN, W. T., SANFORD, K. K., and EARLE, W. R.: Studies of nutrient media for tissue cells *in vitro;* improved protein-free chemically defined medium for long-term cultivation of strain L-929 cells. Cancer Res. 16: 77–94, 1956.

(8) EVANS, V. J., EARLE, W. R., SANFORD, K. K., SHANNON, J. E., and WALTZ, H. K.: The preparation and handling of replicate tissue cultures for quantitative studies. J. Nat. Cancer Inst. 11: 907–927, 1951.

(9) WARBURG, O., and KRIPPAHL, G.: Further development of manometric methods. J. Nat. Cancer Inst. 24: 51–55, 1960.

(10) WARBURG, O.: Weiterentwicklung der zellphysiologischen Methoden und ihre Anwendung auf Krebs und Photosynthese. Stuttgart, Georg Thieme, and New York, Interscience. In press, 1961.

(11) KREBS, H. A.: Body size and tissue respiration. Biochim. et biophys. acta 4: 249–269, 1950.

(12) WOODS, M. W., LANDY, M., and SHEAR, M. J.: Effects of endotoxic polysaccharides on tumor glycolysis. Fed. Proc. 18: 355, 1959.

(13) MADDEN, R. E., and MALMGREN, R. A.: Quantitative studies on circulating cancer cells in the mouse. Cancer Res. In press.

(14) KLEIN, G., and KLEIN, E.: Conversion of solid neoplasms into ascites tumors. Ann. New York Acad. Sc. 63: 640–641, 1956.

(15) SATO, H., BELKIN, M., and ESSNER, E.: Experiments on an ascites hepatoma. III. The conversion of mouse hepatomas into the ascites form. J. Nat. Cancer Inst. 17: 1–21, 1956.

(16) BOYSE, E. A.: A method for the production of viable cell suspensions from solid tumors. Transpl. Bull. 7: 100–104, 1960.

(17) KALTENBACH, J. P., and KALTENBACH, M. H.: Comparative metabolic study of MC1M ascites and a suspension of whole cells obtained fom MC1M solid tumor. Ann. New York Acad. Sc. 63: 977–982, 1956.

(18) PHILPOT, J. ST. L., and STANIER, J. E.: Preservation of rat liver nuclei by potassium glycerophosphate. Nature, London 176: 1128–1129, 1955.

(19) Rinaldini, L. M. J.: The isolation of living cells from animal tumors. Internat. Rev. Cytol. 7: 587–647, 1958.

(20) Edwards, G. H., and Fogh, J.: Micromorphological changes in human amnion cells during trypsinization. Cancer Res. 19: 608–611, 1959.

(21) St. Amond, G. S., and Tipton, S. R.: The separation of neuroblasts and other cells from grasshopper embryos. Science 119: 93–94, 1954.

(22) Warburg, O.: On respiratory impairment in cancer cells. Science 124: 269–270, 1956.

603724—61——12

PLATE 116

FIGURE 1.—Mouse sarcoma MS-2 cell suspension. Papanicolaou stained. × 675

FIGURE 2.—Mouse plasma cell MPC-3 tumor suspension. × 645

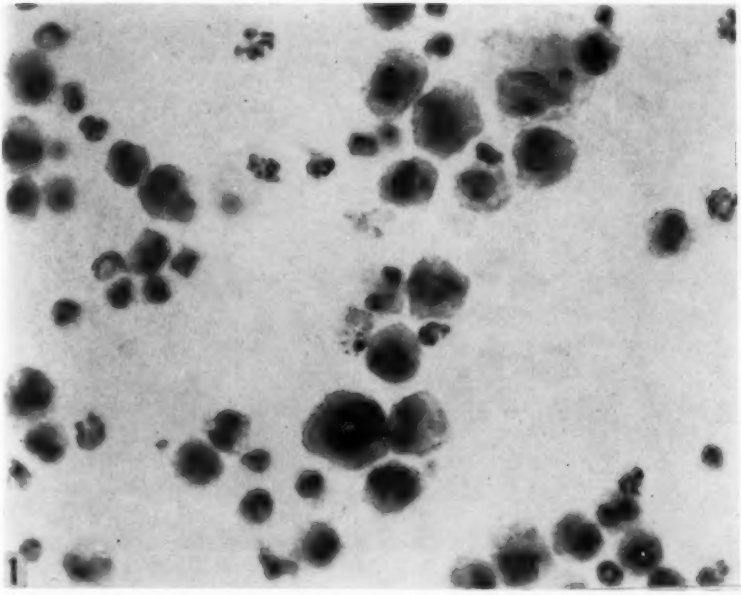

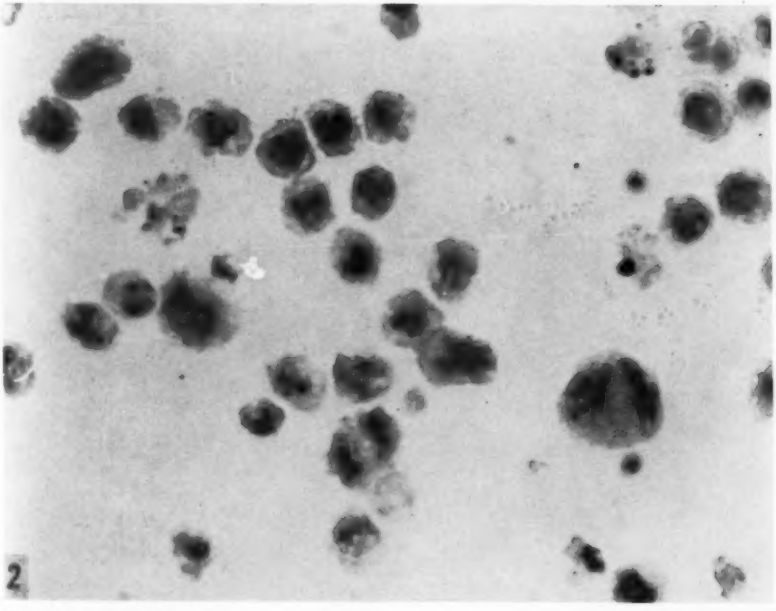

PLATE 117

FIGURE 3.—Mouse plasma cell MPC-3, ascites form. × 645

FIGURE 4.—Mouse melanoma S91 cell suspension. × 800

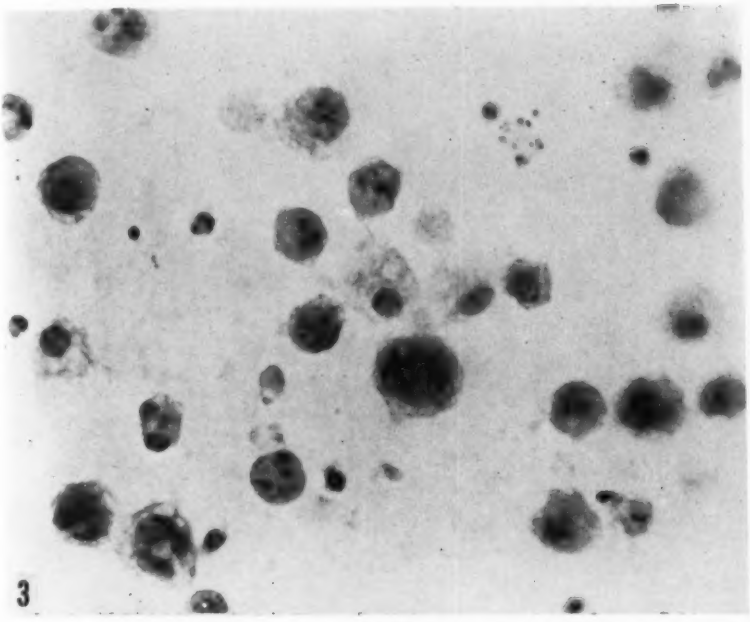
3

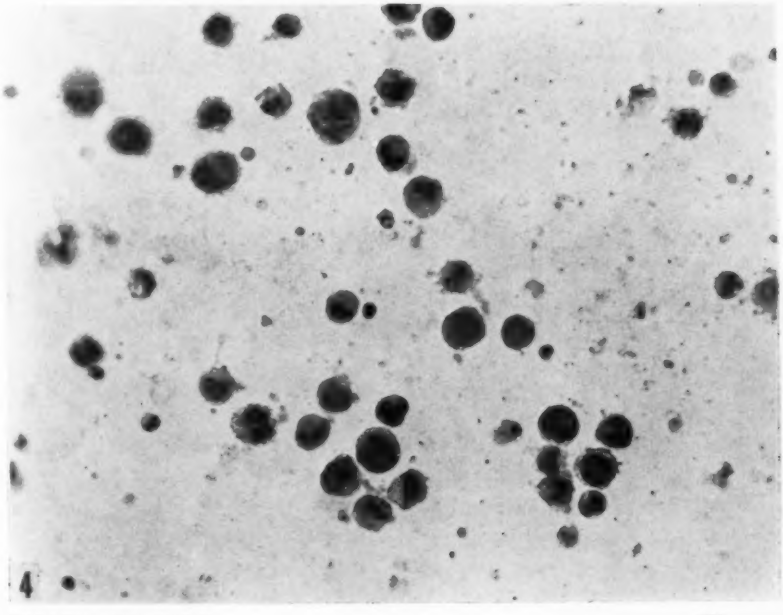
4

PLATE 118

FIGURE 5.—Mouse plasma cell MPC-3, adhering to glass surface of Carrel flask.

FIGURE 6.—Cytosieve preparation of mouse melanoma S91 cells. Stained with trypan blue. × 160

FIGURE 7.—Enzyme-processed cells of mouse melanoma S91. Stained with trypan blue. × 215

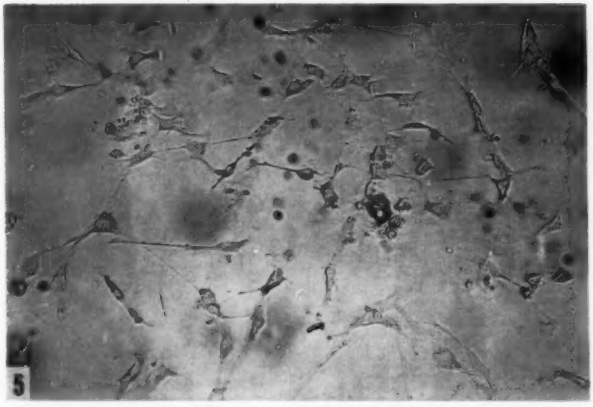
5

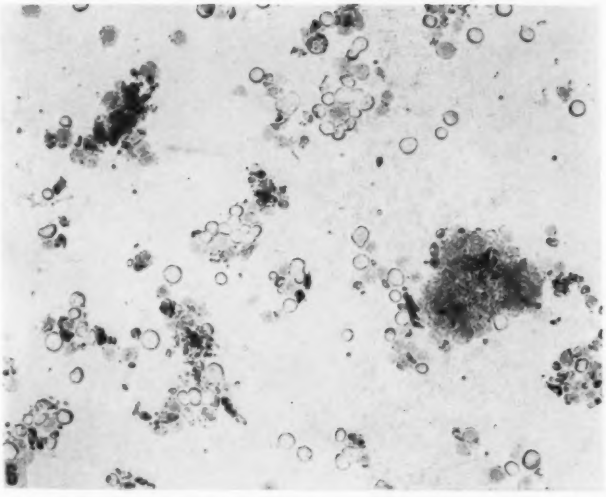

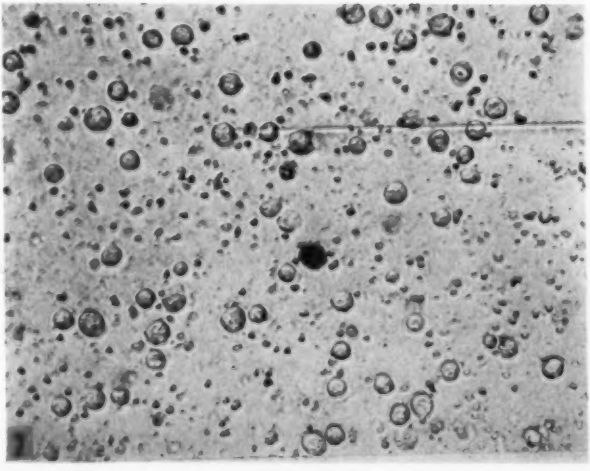

Glucose Metabolism of Tumors Induced by Rous Sarcoma Virus. II. Isotope Studies of Alternate Pathways [1,2]

JAMES ASHMORE, GEORGE WEBER, GOURI BANERJEE, *and* WILLIAM C. LOVE, *Departments of Pharmacology and Microbiology, Indiana University School of Medicine, Indianapolis, Indiana*

SUMMARY

Slices of Rous sarcoma virus-induced tumors were incubated with glucose-1-C^{14}, glucose-6-C^{14}, and pyruvate-2-C^{14} for the study of the intermediary metabolic pathways of this tumor. Glucose was readily metabolized and the rate of utilization was increased with rising concentration of the substrate. Preferential oxidation of carbon-1 of glucose was observed, which indicated operation of the direct oxidative pathway of glucose-6-phosphate in this tissue. The maximum contribution of this route did not exceed 4 percent of the glucose used. Incorporation into protein accounted for 1 to 2 percent of the glucose uptake. The Rous tumor utilized labeled pyruvate and approximately 15 percent was accounted for as $C^{14}O_2$. No significant incorporation of labeled carbon from pyruvate into tissue glycogen was observed.—J. Nat. Cancer Inst. 27: 863-867, 1961.

IN RECENT years isotope methods have been used for estimation of the relative contribution of alternate metabolic pathways in different isolated tissues. Bloom and Stetten (*1*) first suggested the use of glucose specifically labeled in carbon atoms 1 and 6 as a means of assaying extraglycolytic metabolism of glucose in liver, muscle, and kidney. Other workers (*2*, *3*) have employed various modifications of this method to study glucose metabolism in normal and neoplastic tissues. Estimates of the contribution of extraglycolytic pathways to the metabolism of glucose have been made in a number of mammalian tumors, *e.g.*, hepatomas (*4*, *5*), mammary adenocarcinoma (*4*), Ehrlich ascites (*6*), and Gardner lymphosarcoma (*6*).

Previous investigations in this laboratory (*7*) have indicated that in the Rous sarcoma, a tumor of viral etiology, lactic acid appears to be the major product of glucose metabolism as measured *in vitro*. In the present work, we incubated slices of Rous sarcoma virus-induced tumors with radioactive glucose, labeled either in carbon 1 (C-1) or carbon 6 (C-6), to estimate the extent of extraglycolytic metabolism. We also

[1] Received for publication June 1, 1961.

[2] This investigation was supported by grant C-4692 from the National Cancer Institute, National Institutes of Health, Public Health Service, and grants E-254 and E-212 from the American Cancer Society, Inc.

603724—61——13

carried out experiments with C^{14}-labeled pyruvate to characterize further the metabolic potential of this tumor.

MATERIALS AND METHODS

Tumors were produced by the injection of standardized preparations of Rous sarcoma virus (RSV) into the wing web and breast muscle of White Leghorn chicks. Material for study was harvested 6 to 9 days after inoculation and was carefully dissected away from non-neoplastic tissue.

Slices were prepared with a Stadie-Riggs hand microtome, and approximately 1 g of wet tissue was incubated in 12 ml of Ringer-bicarbonate buffer with labeled substrates. Glucose-1-C^{14}, glucose-6-C^{14}, and sodium pyruvate-2-C^{14} were obtained from Volk Radiochemical Company, Chicago, Illinois. Chemical and isotopic methods for glucose and CO_2 were identical with those previously described (*5*). Proteins were isolated and prepared for radioassay by the method of Manchester and Krahl (*8*). Pyruvate utilization was estimated colorimetrically (*9*), and the initial specific activity of this substrate was determined as the dinitrophenylhydrazone. All values were expressed in terms of μmoles of the original substrate incorporated into the various metabolic products by 1 g of wet tissue during the incubation period.

RESULTS AND DISCUSSION

Glucose utilization by Rous tumor slices was increased with increasing concentration of this substrate in the incubation medium (table 1). Such an effect has previously been noted with Rous tumors induced on the chorio-allantois of embryonated eggs. The amount of labeled carbon recovered as CO_2, protein, or lipide is similarly elevated at the higher substrate concentration.

With respect to glucose oxidation, the RSV tumor exhibits a preferential oxidation of C-1 of glucose. The C-1 : C-6 ratio observed in CO_2 averages about 4. This appears to be about the same ratio as that observed in several other tumors (*4*). Values greater than 1 are taken as evidence for an active glucose-6-phosphate direct oxidation pathway in the tissue. It should be noted that the ratio appears slightly higher with glucose 10 mM than at a concentration of 2.5 mM. This increase is due to the more pronounced effect of concentration change on C-1 oxidation than on C-6. Similarly increased C-1 oxidation with increased glucose utilization has been observed in adipose tissue (*10*). This effect is most probable because C-1 can be lost from the direct oxidation of glucose-6-phosphate, while C-6 oxidation results primarily via the citric acid cycle. If the intracellular glucose-6-phosphate concentration were less than that

TABLE 1.—Glucose metabolism by Rous virus-induced tumors—all values are expressed as μmoles per g wet tissue per 90 minutes

Substrate	Molarity	Observations	Uptake	CO_2	Protein	Lipide
Glucose-1-C^{14}	2. 5 mM	4	26 ± 0. 6*	0. 87 ± 0. 32	0. 37 ± 0. 16	0. 29 ± 0. 08
Glucose-1-C^{14}	10. 0 mM	3	56 ± 1. 7	1. 94 ± 0. 11	2. 0 ± 0. 35	0. 87 ± 0. 09
Glucose-6-C^{14}	2. 5 mM	4	26 ± 2. 6	0. 23 ± 0. 01	0. 43 ± 0. 18	0. 19 ± 0. 05
Glucose-6-C^{14}	10. 0 mM	3	57 ± 5. 0	0. 34 ± 0. 05	1. 7 ± 0. 50	1. 19 ± 0. 80

*Mean ± SD.

required for V_{max} of glucose-6-phosphate dehydrogenase, then any increase in glucose utilization resulting in an increase in glucose-6-phosphate within the cell might be expected to produce an increase in the direct oxidation.

If it is assumed that all the C-1 recovered as CO_2 was derived by the direct oxidation pathway, this metabolic route could account for no more than 4 percent of the labeled glucose metabolized.

The relative incorporation of C-1 and C-6 of glucose into fatty acids has been used as a basis for estimating the contribution of nonglycolytic pathways to the over-all metabolism of glucose in isolated tissues. Incorporation of glucose carbons into fat in RSV tumor apparently is primarily via the glycolytic route. Average values obtained with glucose present at 2.5 mM for the C-1 : C-6 ratio in fats are greater than 1 and indicate that probably all the glucose carbon recovered in this product had been derived via glycolysis. At the higher glucose concentration, a ratio of 0.75 was obtained, which indicates some contribution by the direct oxidation pathway to lipide synthesis.

The extent to which C^{14} was recovered in protein is rather surprising. Incorporation into protein accounts for 1 to 2 percent of the glucose used, and initial glucose concentration did not appear to affect markedly the percentage of the substrate used that was recovered.

In 4 experiments an average of 21 $\pm$ 0.7 μmoles per g per 90 minutes of labeled pyruvate was utilized by tissue slices *in vitro* and 10 to 15 percent of the substrate used was recovered as $C^{14}O_2$ (2.9 $\pm$ 0.4 μmoles). Although glycogen was present in the tissues (3.8 $\pm$ 0.2 μmoles per g), negligible amounts of labeled carbon from pyruvate were incorporated ($<$0.01 μmole).

From these studies the following conclusions may be drawn concerning the over-all metabolism of the RSV tumor:

1) Glucose is readily utilized and the rate of utilization is increased with increasing concentration of the substrate present.

2) Preferential oxidation of C-1 of glucose indicates the participation of the glucose-6-phosphate direct-oxidation pathway in this tissue, though the maximum contribution of this route does not exceed 4 percent of the glucose used.

3) Labeled pyruvate is utilized by Rous tumor and 10 to 15 percent of the substrate used can be accounted for as $C^{14}O_2$. No significant incorporation of labeled carbon from pyruvate into tissue glycogen was observed.

REFERENCES

(*1*) Bloom, B., and Stetten, De. W., Jr.: Pathways of glucose catabolism. J. Am. Chem. Soc. 75: 5446, 1953.

(*2*) Wood, H. G.: Significance of alternate pathways in the metabolism of glucose. Physiol. Rev. 35: 841–859, 1955.

(*3*) Katz, J., Abraham, S., Hill, R., and Chaikoff, I. L.: The occurrence and mechanism of the hexose monophosphate shunt in rat liver slices. J. Biol. Chem. 214: 853–868, 1955.

(4) WENNER, C. E., and WEINHOUSE, S.: Metabolism of neoplastic tissue. IX. An isotope tracer study of glucose catabolism pathways in normal and neoplastic tissues. J. Biol. Chem. 222: 399–414, 1956.

(5) ASHMORE, J., WEBER, G., and LANDAU, B. R.: Isotope studies on the pathways of glucose-6-phosphate metabolism in the Novikoff hepatoma. Cancer Res. 18: 974–979, 1958.

(6) KIT, S.: The role of the hexose monophosphate shunt in tumors and lymphatic tissue. Cancer Res. 16: 70–76, 1956.

(7) LEVINE, A. S., UHL, R., and ASHMORE, J.: Glucose metabolism of tumors induced by Rous sarcoma virus. I. Comparison of chorio-allantoic membrane with tumor of the chorio-allantois induced by Rous sarcoma virus. J. Nat. Cancer Inst. 27: 597–609, 1961.

(8) MANCHESTER, K. L., and KRAHL, M. E.: Effect of insulin on the incorporation of C^{14} from C^{14}-labeled carboxylic acids and bicarbonate into the protein of isolated rat diaphragm. J. Biol. Chem. 234: 2938–2942, 1959.

(9) FRIEDEMANN, T. E., and HAUGEN, G. E.: Pyruvic acid. II. The determination of keto acids in blood and urine. J. Biol. Chem. 147: 415–442, 1953.

(10) JEANRENAUD, B., and RENOLD, A. E.: Studies on rat adipose tissue *in vitro*. IV. Metabolic patterns produced in rat adipose tissue by varying insulin and glucose concentrations independently from each other. J. Biol. Chem. 234: 3082–3087, 1959.

Glucose Metabolism of Tumors Induced by Rous Sarcoma Virus. III. Carbohydrate Metabolic Enzymes in Rous Sarcoma [1, 2]

GEORGE WEBER, GOURI BANERJEE, ALVIN S. LEVINE, *and* JAMES ASHMORE, *Departments of Pharmacology and Microbiology, Indiana University School of Medicine, Indianapolis, Indiana*

SUMMARY

The carbohydrate metabolic enzymes of Rous sarcoma were investigated. Virus-induced tumors were obtained from the chorio-allantoic membrane of chick embryos and from wing webs of young chicks. In comparison with the normal chorio-allantoic membrane the Rous sarcoma exhibited an increased cellularity, but the nitrogen content was in the same range. The activities of glucose-6-phosphate dehydrogenase, 6-phosphogluconate dehydrogenase, and fructose-1,6-diphosphatase were similar in the normal and neoplastic tissues. Glucose-6-phosphatase activity was not demonstrable in either tissue. The enzymes, phosphoglucomutase, phosphohexoseisomerase, and lactic dehydrogenase, were markedly higher in Rous sarcoma than in chorio-allantoic membrane, which indicated a preferential synthesis of these specific proteins in this virus-induced tumor. The elevated activities of the glycolytic enzymes are in line with the markedly increased lactate production demonstrated in the Rous sarcoma.—J. Nat. Cancer Inst. 27: 869–873, 1961.

DURING THE past year in this Center, studies were carried out on the Rous sarcoma designed to elucidate the various biochemical mechanisms which play a strategic role in this virus-induced tumor (*1–5*). The present investigation describes the activities of enzymes involved in carbohydrate metabolism in the Rous sarcoma grown in the chorio-allantoic membrane of embryonated eggs or in the wing web of young chicks.

MATERIALS AND METHODS

Production of Rous sarcomas.—Rous sarcoma was induced by the standard Rous sarcoma virus (lot #842) obtained from Dr. W. Ray Bryan, of the National Institutes of Health. Chorio-allantoic membrane of 9-day chick embryos was infected with the virus and the sarcomas were harvested when the eggs were 16 days old. Chorio-allantoic membranes

[1] Received for publication June 19, 1961

[2] This investigation was supported by grants E-254 and E-212 from the American Cancer Society, Inc., and grant C-4692 from the National Cancer Institute, National Institutes of Health, Public Health Service.

of normal, uninfected, 10- to 16-day chick embryos were studied and compared with the tumors. Rous sarcomas were also produced in 10-day-old chicks by the inoculation of Rous virus ($10^{5.5}$ tumor-forming units) in the wing web or breast muscle. White Leghorn chickens and eggs obtained from a local dealer were used.

Preparation of homogenates and supernatant fluid.—The eggs were opened and chorio-allantoic membranes or tumors were rapidly excised and blotted on filter paper. The birds were killed by decapitation and exsanguinated. Tumors from the eggs or birds were carefully dissected free from necrotic, hemorrhagic, or apparent nontumor material. Tissues were chilled in a beaker on cracked ice for 5 minutes, then minced with scissors. Ten percent homogenates were prepared in isotonic KCl. Supernatant fluid was obtained by the centrifugation of the tissue homogenate at 100,000 $\times$ *g* for 30 minutes at 0° C. A refrigerated Spinco model L centrifuge was used.

Determination of cellularity.—The number of nuclei per g fresh tissue was counted by the technique described previously (*6*). Cellularity was expressed in millions of nuclei per g wet weight of tissue.

Biochemical procedures.—Nitrogen content was determined by the micro-Kjeldahl procedure. Lactic dehydrogenase and fructose-1,6-diphosphatase were measured according to Weber and Cantero (*7*). Glucose-6-phosphatase was assayed according to Cori and Cori (*8*), as modified by Weber and Cantero (*9*). Glucose-6-phosphate dehydrogenase and 6-phosphogluconate dehydrogenase were determined by the method of Glock and McLean (*10*). Phosphoglucomutase was assayed according to Najjar (*11*). Phosphohexoseisomerase was measured as described by Glock *et al.* (*12*). Glucose-6-phosphatase was assayed in the homogenate; the other enzymes were measured in the supernatant fluid. All enzymes were assayed under linear kinetic conditions.

Enzymatic activities were calculated as μmoles of substrate metabolized in 1 hour at 37° C. Enzymatic activities were expressed per unit of nitrogen and per average cell.

RESULTS AND DISCUSSION

The activities of the enzyme systems were found at the same level in Rous sarcoma grown in eggs and in the wing web of young chicks; therefore, all data are presented together, irrespective of the origin of the tumor. Since preliminary results demonstrated that the enzyme activities of 10- to 16-day chorio-allantoic membranes were in the same range, the means of these values are used as controls. Tables 1 and 2 compare the cellularity, nitrogen content, and activities of carbohydrate-metabolizing enzymes in Rous sarcoma and in normal chorio-allantoic membrane.

TABLE 1.—Comparison of nitrogen content and carbohydrate-metabolizing enzyme activities in normal chorio-allantoic membrane (CAM) and Rous sarcoma—values expressed per mg nitrogen*

	CAM	Rous	Percent†	P‡
Supernatant nitrogen §	3.8 ± 0.5	5.1 ± 0.2	134	
Phosphohexoseisomerase	472 ± 38.9	1474 ± 27.7	312	<0.01
Lactic dehydrogenase	161 ± 9.5	879 ± 34.1	546	<0.01
Phosphoglucomutase	10.7 ± 3.6	41.4 ± 8.3	387	<0.05
6-Phosphogluconate dehydrogenase	5.9 ± 1.4	9.7 ± 1.4	164	
Glucose-6-phosphate dehydrogenase	1.0 ± 0.4	0.5 ± 0.1	50	
Fructose-1,6-diphosphatase	1.6 ± 0.3	2.1 ± 0.3	131	
Glucose-6-phosphatase	Absent	Absent	—	

*Activities are expressed in μmoles of substrate metabolized per hour per mg *nitrogen* at 37° C. Means and standard errors represent 4 or more animals.

† Values of normal CAM are taken as 100 percent.

‡ Calculated *P*—value as compared with normal CAM. When no values are given the difference is >0.05 which is not accepted as significant.

§ Mg of nitrogen per g wet weight of tissue.

TABLE 2.—Comparison of cellularity, nitrogen content, and carbohydrate-metabolizing enzyme activities in normal chorio-allantoic membrane (CAM) and Rous sarcoma—values expressed per average cell*

	CAM	Rous	Percent†	P‡
Cellularity §	240 ± 20.7	357 ± 28.4	149	<0.05
Supernatant nitrogen ‖	2.0 ± 0.1	1.5 ± 0.2	75	
Phosphohexoseisomerase	863 ± 52.7	2222 ± 214	257	<0.01
Lactic dehydrogenase	332 ± 21.8	1374 ± 152	414	<0.01
Phosphoglucomutase	14.3 ± 2.8	69.2 ± 16.5	484	<0.05
6-Phosphogluconate dehydrogenase	10.5 ± 3.2	15.6 ± 3.0	149	
Glucose-6-phosphate dehydrogenase	0.9 ± 0.4	1.0 ± 0.2	111	
Fructose-1,6-diphosphatase	2.9 ± 0.7	3.0 ± 0.3	103	
Glucose-6-phosphatase	Absent	Absent	—	

*Activities are expressed in μmoles of substrate metabolized per hour per *average cell* × 10^{-6} at 37° C. Means and standard errors represent 4 or more animals.

† Values of normal CAM are taken as 100 percent.

‡ Calculated *P*—value as compared with normal CAM. When no values are given the difference is >0.05 which is not accepted as significant.

§ Millions of cells per g wet weight of tissue.

‖ Mg of nitrogen per cell × 10^{-6}.

Nitrogen Content and Cellularity

When the data were expressed per unit wet weight the nitrogen content showed an apparent, but statistically not significant, decrease in the Rous sarcoma. On the other hand, the cellularity of the Rous sarcoma was increased to 149 percent, which was significantly higher than that of the control tissue. Since the Rous sarcoma contains an increased number of cells, this increased cellularity must be considered in the interpretation of biochemical results obtained in this system.

Enzyme Results

Enzyme results are given as *specific activities* in table 1. It appears that when the enzyme data are expressed on a nitrogen basis there were no significant differences between the glucose-6-phosphate dehydrogenase, 6-phosphogluconate dehydrogenase, and fructose-1,6-diphosphatase activities of the Rous sarcoma and of the normal chorio-allantoic membrane. Glucose-6-phosphatase activity could not be demonstrated in either normal or neoplastic tissue. On the other hand, phosphohexoseisomerase was 312, lactic dehydrogenase, 546, and phosphoglucomutase, 387 percent of the values found in the normal chorio-allantoic membrane.

Enzyme activities are expressed on an *average cell* basis in table 2. This table demonstrates that when tumor cellularity is considered the marked increases in phosphohexoseisomerase, lactic dehydrogenase, and phosphoglucomutase activities are also statistically significant on the per cell basis. The enzymes, glucose-6-phosphate dehydrogenase, 6-phosphogluconate dehydrogenase, and fructose-1,6-diphosphatase exhibited apparent variations that, however, were not statistically significant.

Conclusions

The results show that certain carbohydrate enzyme systems exhibit the same activity in the Rous sarcoma and in the normal chorio-allantoic membrane. This is in line with the fact that the two tissues have about the same nitrogen content. On the other hand, certain glycolytic enzymes (phosphoglucomutase, phosphohexoseisomerase, and lactic dehydrogenase) are much higher in the Rous sarcoma than in the chorio-allantoic membrane, which indicates a preferential synthesis of these specific proteins in this virus-induced tumor. The marked activities of the glycolytic enzymes are in good agreement with the high glycolytic rate demonstrated in the Rous sarcoma by Burk (*13*) and others (*3–5*). The presence of glucose-6-phosphate dehydrogenase and 6-phosphogluconate dehydrogenase is in line with the report on the operation of the direct oxidative pathway in these tissues (*5*).

REFERENCES

(1) Ashmore, J., Uhl, R., and Levine, A. S.: Biochemical studies of viral induced neoplastic growth. Science 130: 1411, 1959.

(2) Levine, A. S., Stricker, F., Uhl, R., and Ashmore, J.: Effect of glucose concentration on respiration of Rous sarcoma and of chorio-allantoic membrane. Nature, London 188: 229–230, 1960.

(3) Weber, G., Banerjee, G., Levine, A. S., and Ashmore, J.: Metabolic studies on the Rous sarcoma. (Abstract.) Proc. Am. Assoc. Cancer Res. 3: 160, 1960.

(4) Levine, A. S., Uhl, R., and Ashmore, J.: Glucose metabolism of tumors induced by Rous sarcoma virus. I. Comparison of chorio-allantoic membrane with tumor of the chorio-allantois induced by Rous sarcoma virus. J. Nat. Cancer Inst. 27: 597–609, 1961.

(5) Ashmore, J., Weber, G., Banerjee, G., and Love, C. W.: Glucose metabolism of tumors induced by Rous sarcoma virus. II. Isotope studies of alternate pathways. J. Nat. Cancer Inst. 27: 863–867, 1961.

(6) Weber, G., and Cantero, A.: Studies on hormonal factors influencing hepatic glucose-6-phosphatase. Endocrinology 61: 701–712, 1957.

(7) ———: Fructose-1,6-diphosphatase and lactic dehydrogenase activity in hepatoma and in control human and animal tissues. Cancer Res. 19: 763–768, 1959.

(8) Cori, G. T., and Cori, C. F.: Glucose-6-phosphatase of the liver in glycogen storage disease. J. Biol. Chem. 199: 661–667, 1952.

(9) Weber, G., and Cantero, A.: Glucose-6-phosphatase activity in normal, precancerous, and neoplastic tissues. Cancer Res. 15: 105–108, 1955.

(10) Glock, G. E., and McLean, P.: Further studies on the properties and assay of glucose-6-phosphate dehydrogenase of rat liver. Biochem. J. 55: 400–408, 1953.

(11) Najjar, V. A.: The isolation and properties of phosphoglucomutase. J. Biol. Chem. 175: 281–290, 1948.

(12) Glock, G. E., McLean, P., and Whitehead, J. K.: Pathways of glucose catabolism in rat liver in alloxan diabetes and hyperthyroidism. Biochem. J. 63: 520–524, 1956.

(13) Burk, D., Sprince, H., Spangler, J. M., Kabat, E. A., Furth, J., and Claude, A.: The metabolism of chicken tumors. J. Nat. Cancer Inst. 2: 201–240, 1941.

Site Distribution of Cancer Deaths in Husband-Wife and Sibling Pairs [1]

WILLIAM Y. CHEN,[2] LYMAN B. CRITTENDEN,[3] NATHAN MANTEL,[4] *and* W. ROSS CAMERON,[5,6] *National Cancer Institute,*[7] *Bethesda, Maryland, and Washington County Department of Health, Hagerstown, Maryland*

SUMMARY

The problems of determining the importance of environmental and genetic factors contributing to observed familial aggregations of cancer are discussed. The distributions of 29 site classifications in 51 husband-wife pairs, 60 brother-sister pairs, 76 sister-sister pairs, and 44 brother-brother pairs dying of cancer are presented. The total number of pairs matched for detailed site on the death certificate for each type of pairing is compared to an expected number computed from the data in this study. Only the brother-sister pairing failed to show a significant excess of matched pairs. The fact that husband-wife pairings showed an excess suggests that common environment and common heredity should be considered in the explanation of observed familial aggregation of cancer. The Appendix indicates the derivation of the expectations of the sums of matched pairs and their variances for the case of the symmetrical and asymmetrical contingency table. Appropriate chi-square formulas are given for testing the deviations of the observed number of matched pairs from their expectations.—J. Nat. Cancer Inst. 27: 875–892, 1961.

THE OBSERVED familial aggregation of a chronic disease may be considered to be caused by multiple environmental and genetic factors that members of a family have in common (*1–3*). The degree of this association may be estimated in various ways, but interpretation on a purely environmental or genetic basis is unjustified except in the simplest cases where a single major cause may be isolated. This difficulty arises in human populations because genetically related individuals tend to share similar environments. These two classes of factors may be investigated independently only where unrelated people are observed in similar

[1] Received for publication June 12, 1961.

[2] Epidemiology Branch, National Cancer Institute. Requests for reprints should be addressed to: Dr. William Y. Chen, Environmental Cancer Field Research Laboratory, 1300 Pennsylvania Ave., Hagerstown, Md.

[3] Biometry Branch, National Cancer Institute. *Present address:* Regional Poultry Research Laboratory, 3606 E. Mt. Hope Rd., East Lansing, Mich.

[4] Biometry Branch, National Cancer Institute.

[5] Washington County Department of Health, Hagerstown, Md.

[6] The authors wish to express their appreciation for the constant encouragement of Dr. Michael B. Shimkin and Mr. Pope A. Lawrence and the able clerical assistance of Mr. Jack Gunderman, all of the National Cancer Institute.

[7] National Institutes of Health, Public Health Service, U.S. Department of Health, Education, and Welfare.

environments, related people are observed in random environments, or some correction is made for one effect or the other. Since these factors cannot be experimentally controlled, special types of family groupings must be located to shed light on the relative importance of environment and heredity in controlling the development of a chronic disease. [*See* Lush (*4*) for a discussion of a similar problem in cattle breeding.]

Twin studies are theoretically ideal, but the validity of assuming that all environmental factors have been removed by comparing monozygotic with dizygotic twin pairs has been questioned. This assumption, as well as the complete identity of genotypes of monozygotic twins, may bias these studies so that the role of heredity is overemphasized or oversimplified as pointed out by Osborne and De George (*5*). Systematic twin studies have contributed little to cancer research to date because of the large series of twins that must be located to study cancer of any particular site (*1*). Also biases may enter into the selection of twins for the study of a particular disease (*6*). Other potentially useful designs might use foster children (*7*, *8*), twins reared together and apart (*5*), and maternal and paternal half-siblings as compared with full-siblings. Studies involving special family situations become possible only when very large numbers of families are available for study and one does not have to depend entirely on interview methods.

Even though married couples are in general unrelated genetically and are intimately associated in the home environment during adult life, they have been used very little for the investigation of environmental association in relation to cancer. Ciocco (*9*) located 2,571 pairs of death certificates of married couples and classified them by 8 causes of death. For some of the causes he found more couples dying of the same cause than would be expected on the basis of the marginal totals of the 8×8 contingency table. He found that 29 pairs of death certificates gave cancer as a cause of death compared with an expected 19.9. Potter and Tully (*10*) were unable to confirm this in a study of a comparable number of death certificates.

Ciocco (*11*) investigated spouses and opposite-sex siblings of index cases dying of 8 causes of death. He again found a significant excess of cancer in spouses of cancer index cases and only a slight but insignificant excess in their siblings.

Woolf (*1*, *8*) and Macklin (*12*) investigated the mortality from cancer in the spouses of stomach-cancer patients as a check on the validity of the assumption of a genetic explanation for an observed familial aggregation. It should be recognized that husbands and wives share similar environments as adults, while siblings live together as children; thus the absence of association between husbands and wives does not rule out the possibility of an effect of a common environment on siblings. The 2 studies involved the spouses of 656 stomach-cancer patients. Matched controls and vital statistics rates were used for comparison. In contrast with Ciocco (*9*, *11*) neither author found excess deaths from cancer of all sites combined or from cancer of the stomach in spouses of individuals dying of stomach cancer.

Since most genetic studies in animals (*13*) and many in man show that genetic susceptibility to cancer is site-specific and controlled by multiple environmental and genetic factors (*1, 2, 12, 14–16*), one might expect that siblings and perhaps spouses would tend to die of cancer of the same site more often than would be anticipated. Woolf (*1, 7, 8*) and Macklin (*12*) found such a tendency for siblings, but not for spouses. Ciocco (*9, 11*) did not investigate cancer by site.

The present study is an analysis of paired death-certificate data to see if more spouses and/or siblings than expected tend to die of cancer of the same detailed site. Statistical methodology for this type of analysis will also be presented in the Appendix.

SOURCE AND COLLECTION OF DATA

More than 4,015 death certificates giving cancer as the cause of death were accumulated in Washington County, Maryland, between 1900 and 1960 as a part of a study of environmental influences on cancer described by Lawrence and Chen (*17*). Nine hundred and seventy-seven, or about one fourth of these, were assembled into "family" groups in which 2 or more members died of cancer. The following distribution of family groups with 2 through 7 cancer deaths was obtained:

Number of cancer deaths	Number of family groups
2	326
3	78
4	17
5	2
6	1
7	1
27	425

It was then decided to investigate specific family relationships. Seventy-nine husband-wife pairs were found. After a careful check, doubtful pairs that could not be verified by marriage certificate were removed, which reduced the number to 75. The following kinds of sibling groups also were found:

Number per group	Number of males	Number of females	Number of groups
2	2	—	53
	—	2	91
	1	1	111
3	3	—	3
	—	3	8
	2	1	7
	1	2	12
4	4	—	0
	—	4	1
	3	1	1
	2	2	2
	1	3	1

Of these, it was decided to analyze the 3 types of sibling pairs only because of the small number of 3- and 4-sibling groups and the difficulty of statistical analysis of groups larger than pairs. Removal of doubtful sibling pairs reduced the numbers used for analysis to 50 brother-brother, 87 sister-sister, and 100 brother-sister pairs.

To ensure valid comparison of organs of the same anatomical site, cases involving cancer of genital organs of both sexes and unclassified cancers were excluded. Of 75 husband-wife pairs, 24 pairs were excluded (7 pairs involved husbands with cancer of genital organs; 8 pairs involved wives with cancer of genital organs; 5 pairs involved husbands with unclassified cancer; 4 pairs involved wives with unclassified cancer). Of 100 brother-sister pairs, 40 pairs were excluded (15 pairs involved brothers with cancer of genital organs; 13 pairs involved sisters with cancer of genital organs; 6 pairs involved brothers with unclassified cancer; 6 pairs involved sisters with unclassified cancer). Of 50 brother-brother pairs, 6 pairs were excluded due to one or the other of the brothers having unclassified cancer. Of 87 sister-sister pairs, 11 pairs were excluded due to one or the other of the sisters having unclassified cancer.

Each death certificate was given one of 29 detailed site classifications as listed in table 5, as well as "unspecified" and "other" (*18*). Any pair in which an "unspecified" or "other" classification was observed for one member was eliminated. All pairs in which one member listed the genital organs were eliminated from the unlike sex pairings because matching would be impossible. When a primary cancer was listed, but not as the immediate cause of death, this was considered a cancer death for the present purposes.

RESULTS AND ANALYSIS

Tables 1, 2, 3, and 4 give the distribution of sites for the 4 types of pairings in contingency table form. Tables 1 and 2 show entries on both sides of the diagonal because pairings are restricted to those of unlike sex (comparable to a product-moment correlation table), but tables 3 and 4 show entries on only one side of the diagonal because pairings are unrestricted by any sex difference between individuals (comparable to the intraclass correlation). In each table the number of pairs that match for site are listed on the diagonal.

We now wish to determine if the method of pairing produces more pairs matching for site than would be expected, given the site distribution of all individuals entering into pairs, that is, given fixed marginal totals. Thus we are looking for excess site matching, disregarding any possible tendency for both members of a pair to die of cancer of any site. The problem then is to compare the sum of the matched pairs for each site ($\sum_i m_{ii}$) with the expected value of this sum [$E(\sum_i m_{ii})$]. A chi-square test of the general form

$$\text{chi square} = \frac{[|\sum_i m_{ii} - E(\sum_i m_{ii})| - 0.5]^2}{\textit{Variance} \sum_i m_{ii}}$$

TABLE 1.—Distribution of cancer sites for husbands and wives, both of which showed cancer as cause of death on the death certificate, Washington County, Maryland, 1900–60

Husbands: Group		International code (*18*)	Site	Wives: 1	2 A	2 B	2 C	2 D	2 E	2 F	2 G	2 H	3 A	3 B	3 C	3 D	4	7 A	7 B	8	9	10	11	12 A	12 B	Total pairs
1		140–148	Buccal cavity and pharynx			2																			2
2	A	150	Esophagus					2																	2
	B	151	Stomach			5		2	1	1	1											1		1	12
	C	152	Small intestine																						0
	D	153	Large intestine			2				1							1				1			1	6
	E	154	Rectum														1	1		1					3
	F	155	Liver and biliary passages					1		2										1					4
	G	157	Pancreas					1		1							3								5
	H	158	Peritoneum																						0
3	A	160	Nasal cavity																						0
	B	161	Larynx							1									1						2
	C	162–163	Lung, bronchus, and trachea					1														1			2
	D	164	Mediastinum																						0
4		170	Breast																						0
7	A	180	Kidney and ureter																						0
	B	181	Bladder and unspecified	1							1								1		1				4
8		190–191	Skin																						0
9		193	Central nervous system			1			1															1	3
10		194–195	Endocrine organs																						0
11		196	Bone																						0
12	A	204	Leukemia					1																	1
	B	200–203	Lymphoma					2																1	2	5
			Total	1	0	10	0	10	2	6	2	0	0	0	0	0	5	1	2	2	1	2	1	2	4	51

TABLE 2.—Distribution of cancer sites for brothers and sisters, both of which showed cancer as cause of death on the death certificate, Washington County, Maryland, 1900–60

Brothers: Group	International code (*18*)	Site	Sisters: 1	2 A	2 B	2 C	2 D	2 E	2 F	2 G	2 H	3 A	3 B	3 C	3 D	4	7 A	7 B	8	9	10	11	12 A	12 B	Total pairs
1	140–148	Buccal cavity and pharynx					2																		2
2 A	150	Esophagus						1																	1
B	151	Stomach			3		1		1	1						1						2		1	10
C	152	Small intestine																							0
D	153	Large intestine			1		1									3									5
E	154	Rectum				1								1		2					1				5
F	155	Liver and biliary passages	1		3				1										1			1	1		8
G	157	Pancreas							1	1						1									3
H	158	Peritoneum																							0
3 A	160	Nasal cavity																							0
B	161	Larynx							1																1
C	162–163	Lung, bronchus, and trachea	1				2									2		1						1	7
D	164	Mediastinum																							0
4	170	Breast																							0
7 A	180	Kidney and ureter																							0
B	181	Bladder and unspecified												1		2									3
8	190–191	Skin			2		1		1							2			1						7
9	193	Central nervous system							1																1
10	194–195	Endocrine organs						1																	1
11	196	Bone			1		1		1										1						4
12 A	204	Leukemia														1									1
B	200–203	Lymphoma																					1		1
		Total	2	0	10	1	8	2	7	2	0	0	0	2	0	14	0	1	3	0	1	3	2	2	60

TABLE 3.—Distribution of cancer sites for paired brothers, both of which showed cancer as cause of death on the death certificate, Washington County, Maryland, 1900–60

Brothers	Group		International code (*18*)	Site	Brothers																						Total cases: 88
					1	2								3				4	6			7		8	9	10	11	12	
						A	B	C	D	E	F	G	H	A	B	C	D		A	B	C	A	B					A	B	
Brothers	1		140–148	Buccal cavity and pharynx																				1					1
	2	A	150	Esophagus					1																				1
		B	151	Stomach			3		2	2						2			2				2	1					17
		C	152	Small intestines																									0
		D	153	Large intestines							1					1				1			2	1			1		10
		E	154	Rectum						1	1	1				1								1				1	8
		F	155	Liver and biliary passages							1										1						1		6
		G	157	Pancreas												1					1				1				4
		H	158	Peritoneum																									0
	3	A	160	Nasal cavity																									0
		B	161	Larynx																									0
		C	162–163	Lung, bronchus, and trachea												1													7
		D	164	Mediastinum																									0
	4		170	Breast																		1							1
	6	A	177	Prostate															1				4	1					9*
		B	178	Testis																									1
		C	179	Other male genital organs																									2
	7	A	180	Kidney and ureter																									1
		B	181	Bladder and unspecified																					1				9
	8		190–191	Skin																									4
	9		193	Central nervous system																									2
	10		194–195	Endocrine organs																									0
	11		196	Bone																									2
	12	A	204	Leukemia																							1		2
		B	200–203	Lymphoma																									1

*Note: Total cases for a given site can be obtained directly from the table. For example, the total number of pairs shown in row 6A is 6, while the total in column 6A is 3; 6 + 3 = 9 for a total of 9 brothers with cancer of the prostate. In effect, diagonal frequencies are properly counted twice. Counting these only once would give 8, the number of pairs involving prostate cancer.

TABLE 4.—Distribution of cancer sites for paired sisters, both showing cancer as a cause of death on the death certificate, Washington County, Maryland, 1900–60

	Group		International code (*18*)	Site	Sisters																								Total cases: 152
					1	2								3				4	5				7		8	9	10	11	12		
						A	B	C	D	E	F	G	H	A	B	C	D		A	B	C	D	A	B					A	B	
Sisters	1		140–148	Buccal cavity and pharynx																										0
	2	A	150	Esophagus							1																			1
		B	151	Stomach			2		1	1	3									3				3		1		1	1	18
		C	152	Small intestine																										0
		D	153	Large intestine					1									1		1										14
		E	154	Rectum							2							1		2										6
		F	155	Liver and biliary passages							1							1		2	1			1	2	1			1	17
		G	157	Pancreas																										0
		H	158	Peritoneum																										0
	3	A	160	Nasal cavity																										0
		B	161	Larynx																										0
		C	162–163	Lung, bronchus, and trachea															1	1									1	3
		D	164	Mediastinum																										0
	4		170	Breast														6		6	1	1	1	1	1				1	30
	5	A	171	Cervix															1	1	1							2		7
		B	172	Uterus (corpus)																3	1			1	1			1		26
		C	175	Ovary																	1					1				7
		D	176	Vagina and vulva																										1
	7	A	180	Kidney and ureter																										1
		B	181	Bladder and unspecified																										6
	8		190–191	Skin																										4
	9		193	Central nervous system																										3
	10		194–195	Endocrine organs																										0
	11		196	Bone																										4
	12	A	204	Leukemia																										3
		B	200–203	Lymphoma																										1

can be devised that tests the specific hypothesis in question with one degree of freedom. This is a more powerful test for the presence of correlation than the over-all test of the contingency table and also overcomes the problem of small expected values in many cells of the table. The covariances between the diagonal entries should be considered in calculating the variance of their sum (*19*). The appropriate formulas for the expectations and variances of the sums of the diagonals for both types are given in the Appendix.

Table 5 presents a summary of the observed and expected matches for each site and each type of pairing. Each type of pairing shows an excess of the sum of the matches for all sites over the expected, with only the brother-sister pairing failing to show significance at the 5 percent level. The total number of matches obtained from the 231 pairs was 43, twice the total of the expectations. Comparison of types of pairings or individual sites becomes more speculative because of the small numbers of pairs involved.

DISCUSSION

The limitations and biases entering into these data must be considered before extended discussion is warranted. The first point is the well-known inaccuracy of death certificates as to the specific primary site of cancer. As recently as 1947, it has been found that 18 percent of death certificates disagree with the case report as to major site classification and 24 percent for detailed site classification in 10 urban areas of the United States (*20*). There is no reason to believe that Washington County certificates are any more accurate, at least in the early years of this study. This in itself would probably only tend to dilute any true association between pairs. However, a potential source of bias arises when one considers this amount of error with the possibility that the same physicians may attend members of the same pair. This same source of bias should be found in Woolf's (*1*, *8*) and Macklin's (*12*) data on stomach cancer in spouses, but no excess was observed. Ciocco (*9*) investigated this source of bias and concluded that it was not important in his study of 8 causes of death.

Changing death rates from cancer of various sites over the 60 years observed could also produce more observed matches than the expected as calculated, because there is a correlation between the dates of death of the pairs. Calculations based on the examination of the change in the United States cancer-mortality rates at the various sites from 1930 to 1950 (*21*) showed that this source of bias could only account for a small proportion of the observed excess of matches.

A variety of other causes for correlation of cancer sites may be present. Cancer deaths occurring in the same age interval are more likely to be similar than deaths occurring in different age intervals. Deaths occurring in the same time interval may tend to be reported similarly, not only

TABLE 5.—Summary of the observed and expected number of paired couples and siblings, both of which showed the same cancer site as cause of death on the death certificate, Washington County, Maryland, 1900–60

Group	International code (*18*)	Site	Husband-wife		Brother-sister		Brother-brother		Sister-sister		All pairings	
			Observed matches	Expected matches	Observed matches	Expected matches	Observed matches	Expected matches	Observed matches	Expected matches	Observed matches	Expected matches
1	140–148	Buccal cavity and pharynx	0	0.04	0	0.07	0	0.00	0	0.00	0	0.11
2 A	150	Esophagus	0	.00	0	.00	0	.00	0	.00	0	.00
B	151	Stomach	5	2.35	3	1.67	3	1.56	2	1.01	13	6.59
C	152	Small intestine	0	.00	0	.00	0	.00	0	.00	0	.00
D	153	Large intestine	0	1.18	1	.67	0	.52	4	.60	5	2.97
E	154	Rectum	0	.12	0	.17	1	.32	0	.10	1	.71
F	155	Liver and biliary passages	2	.47	1	.93	1	.17	1	.90	5	2.47
G	157	Pancreas	0	.20	1	.10	0	.07	0	.00	1	.37
H	158	Peritoneum	0	.00	0	.00	0	.00	0	.00	0	.00
3 A	160	Nasal cavity	0	.00	0	.00	0	.00	0	.00	0	.00
B	161	Larynx	0	.00	0	.00	0	.00	0	.00	0	.00
C	162–163	Lung, bronchus, and trachea	0	.00	0	.23	1	.24	0	.02	1	.49
D	164	Mediastinum	0	.00	0	.00	0	.00	0	.00	0	.00
4	170	Breast	0	.00	0	.00	0	.00	6	2.88	6	2.88
5 A	171	Cervix	—	—	—	—	—	—	1	.14	1	.14
B	172	Uterus (corpus)	—	—	—	—	—	—	3	2.15	3	2.15
C	175	Ovary	—	—	—	—	—	—	1	.14	1	.14
D	176	Vagina and vulva	—	—	—	—	—	—	0	.00	0	.00
6 A	177	Prostate	—	—	—	—	1	.41	—	—	1	.41
B	178	Testis	—	—	—	—	0	.00	—	—	0	.00
C	179	Other male genital organs	—	—	—	—	0	.01	—	—	0	.01
7 A	180	Kidney and ureter	0	.00	0	.00	0	.00	0	.00	0	.00
B	181	Bladder and unspecified	1	.16	0	.05	0	.41	0	.10	1	.72
8	190–191	Skin	0	.00	1	.35	0	.07	0	.04	1	.46
9	193	Central nervous system	0	.06	0	.00	0	.01	0	.02	0	.09
10	194–195	Endocrine organs	0	.00	0	.02	0	.00	0	.00	0	.02
11	196	Bone	0	.00	0	.20	0	.01	0	.04	0	.25
12 A	204	Leukemia	0	.04	0	.03	1	.01	0	.02	1	.10
B	200–203	Lymphoma	2	.39	0	.03	0	.00	0	.00	2	.42
		Total	10	5.00	7	4.52	8	3.83	18	8.16	43	21.51
		Chi square	5.1		1.0		4.1		13.0		24.9	
		Probability*	<.012		>.10		<.025		<.001		<.00001	

*This probability is given as $\frac{\alpha}{2}$ because we are only interested in an excess over expected, thus the one-sided test was used.

because of the changing cancer rates for various sites but also because of changing diagnostic techniques and procedures. Related individuals under the care of the same physician or having other medical facilities in common are more likely to have similar diagnoses for their cancers than unrelated individuals.

These sources of bias are pointed out to indicate the preliminary nature of these data, which are being used to present a method and indicate suggestive results only.

One would like to compare husband-wife pairings with brother-sister pairings to evaluate the effect of a common environment in adult life compared with the effect of common heredity and environment shared in the first 15 to 20 years of life. These data (table 5) show a slight tendency for husbands and wives to show a greater association than sisters and brothers, but the difference between the 2 distributions is of doubtful statistical importance. Stomach cancer shows a consistent excess of about 2 times the expected number of matches for all pairings. The husband-wife excess conflicts with Woolf's (*1*, *8*) and Macklin's (*12*) results from a larger series with a somewhat different approach. Other trends may be noted in table 5. There is a consistent excess of matches for liver and biliary passages for all types of pairings. The excess of lymphoma for husbands and wives lends some weight to the suggestion of Razis *et al.* (*22*) that common environment may be important in the familial aggregation of Hodgkin's disease. The sister-sister pairings show a twofold excess of matches for breast cancer in contrast to Murphy and Abbey's (*23*) results but in agreement with most other family studies of breast cancer (*14*, *15*). Sister-sister pairings also show an excess for genital sites of cancer.

In general, the fact that husband-wife pairings showed an excess of total matches for site indicates that common environment may contribute to the familial aggregation of cancer of specific sites. We hope that these results stimulate further analysis of data where individuals from pairs can be classified in a large number of ways, and an association between pairs is looked for. This technique appears useful where large quantities of vital statistics and registry material are becoming available for matching in various ways for environmental and genetic study.

REFERENCES

(*1*) Woolf, C. M.: Investigations on genetic aspects of carcinoma of the stomach and breast. Univ. of Calif. Publ. in Pub. Health 2: 265–350, 1955.

(*2*) Wynder, E. L., and Day, E.: Some thoughts on the causation of chronic disease. J.A.M.A. 175: 997–999, 1961.

(*3*) Crittenden, L. B.: An interpretation of familial aggregation based on multiple genetic and environmental factors. Ann. New York Acad. Sc. In press, 1961.

(*4*) Lush, J. L.: Heritability of quantitative characters in farm animals. Proc. Eighth Internat. Cong. of Genetics. Hereditas (Supp.), 1949.

*This probability is given as $\frac{\alpha}{2}$ because we are only interested in an excess over expected, thus the one-sided test was used.

(*5*) Osborne, R. H., and De George, F. V.: Genetic Basis of Morphological Variation. Cambridge, Mass., Harvard Univ. Press, 1959.

(*6*) Graham, S., and Lilienfeld, A. M.: Genetic studies of gastric cancer in humans; an appraisal. Cancer 11: 945–958, 1958.

(*7*) Woolf, C. M.: A further study on the familial aspects of carcinoma of the stomach. Am. J. Human Genet. 8: 102–109, 1956.

(*8*) ———: The incidence of cancer in the spouses of stomach cancer patients. Cancer 14: 199–200, 1961.

(*9*) Ciocco, A.: On the mortality in husbands and wives. Human Biol. 12: 508–531, 1940.

(*10*) Potter, E. A., and Tully, M. R.: The statistical approach to the cancer problem in Massachusetts. Am. J. Pub. Health 35: 485–490, 1945.

(*11*) Ciocco, A.: On the mortality in brother-sister and husband-wife pairings. Human Biol. 13: 189–202, 1941.

(*12*) Macklin, M. T.: Inheritance of cancer of the stomach and large intestine in man. J. Nat. Cancer Inst. 24: 551–571, 1960.

(*13*) Heston, W. E.: Symposium: light from animal experimentation on human heredity; bearing of mouse genetics on our understanding of human cancer. Am. J. Human Genet. 4: 314–331, 1952.

(*14*) Anderson, V. E., Goodman, H. O., and Reed, S.: Variables Related to Human Breast Cancer. Minneapolis, Univ. Minnesota Press, 1958.

(*15*) Macklin, M. T.: Comparison of the number of breast-cancer deaths observed in relatives of breast-cancer patients, and the number expected on the basis of mortality rates. J. Nat. Cancer Inst. 22: 927–951, 1959.

(*16*) Crabtree, J. A.: Observations on the familial incidence of cancer. Am. J. Pub. Health 31: 49–56, 1941.

(*17*) Lawrence, P. A., and Chen, W. Y.: A project for studying the geographic distribution of cancer within a single county as related to environmental factors. Am. J. Pub. Health 49: 668–674, 1959.

(*18*) Manual of the International Classification of Diseases, Injuries, and Causes of Death, 6th rev. World Health Organization, 1948.

(*19*) Mantel, N., and Haenszel, W.: Statistical aspects of the analysis of data from retrospective studies of disease. J. Nat. Cancer Inst. 22: 719–748, 1959.

(*20*) Dorn, H. F., and Cutler, S. J.: Morbidity from Cancer in the United States. Pub. Health Monogr. No. 56. Washington, D.C., U.S. Gov't. Print. Office, 1959.

(*21*) Gordon, T., Crittenden, M., and Haenszel, W.: Cancer mortality trends in the United States, 1930–1955. NCI Monogr. No. 6: 133–350, 1961.

(*22*) Razis, D. V., Diamond, H. D., and Craven, L. F.: Familial Hodgkin's disease: its significance and implications. Ann. Int. Med. 51: 933–971, 1959.

(*23*) Murphy, D. P., and Abbey, H.: Cancer in Families, a Study of the Relatives of 200 Breast Cancer Probands. Cambridge, Mass., Harvard Univ. Press, 1959.

APPENDIX

Determination of Chi Square for Comparing the Number of Matched Pairs With Its Expectation

NATHAN MANTEL *and* LYMAN B. CRITTENDEN,
Biometry Branch, National Cancer Institute, Bethesda, Maryland

THE ASYMMETRICAL CASE (HUSBAND-WIFE, BROTHER-SISTER PAIRS)

Let the total number of cases in the i^{th} row category be r_i and in the j^{th} column category be c_j with

$$\sum_i r_i = \sum_j c_j = N,$$

where N is the total number of pairs of individuals in the study. The expectations, variances, and covariances of the cell frequencies (m_{ij}), that is, the number of pairs with one individual in row category i and the other in column category j are to be determined subject to the fixed r_i's and c_j's. In the absence of true association this can be visualized as a two-urn problem. Each urn contains N balls with r_i marked as representing category i in one urn and c_i so marked in the other. (For the data analyzed in this paper the row and column classifications are identical.) Balls are selected in pairs, one from each urn at random without replacement. Under this formulation, the expectations and variances of the m_{ij}'s are:

$$E(m_{ij}) = r_i c_j / N;$$

$$Var\ (m_{ij}) = r_i(N - r_i)c_j(N - c_j)/N^2(N - 1);$$

for $i =$ or $\neq j$.

The convariances of the m_{ij}'s are as follows:

$$CV(m_{ij},m_{ik}) = -r_i(N - r_i)c_j c_k/N^2(N - 1),\ j \neq k;$$

$$CV(m_{ij},m_{kl}) = -r_i r_k c_j(N - c_j)/N^2(N - 1),\ i \neq k;$$

$$CV(m_{ij},m_{kl}) = r_i r_k c_j c_l/N^2(N - 1),\ i \neq k,\ j \neq l.$$

In particular:

$$E(m_{ii}) = r_i c_i / N;$$

$$Var\ (m_{ii}) = r_i(N - r_i)c_i(N - c_i)/N^2(N-1);$$

$$CV(m_{ii},m_{ij}) = r_i r_j c_i c_j/N^2(N - 1),\ i \neq j;$$

$$E(\sum_i m_{ii}) = \sum_i E(m_{ii}) = \sum_i r_i c_i / N \quad \text{and}$$

603724—61——15

(*5*) OSBORNE, R. H., and DE GEORGE, F. V.: Genetic Basis of Morphological Variation. Cambridge, Mass., Harvard Univ. Press, 1959.

(*6*) GRAHAM, S., and LILIENFELD, A. M.: Genetic studies of gastric cancer in humans; an appraisal. Cancer 11: 945–958, 1958.

(*7*) WOOLF, C. M.: A further study on the familial aspects of carcinoma of the stomach. Am. J. Human Genet. 8: 102–109, 1956.

(*8*) ———: The incidence of cancer in the spouses of stomach cancer patients. Cancer 14: 199–200, 1961.

(*9*) CIOCCO, A.: On the mortality in husbands and wives. Human Biol. 12: 508–531, 1940.

(*10*) POTTER, E. A., and TULLY, M. R.: The statistical approach to the cancer problem in Massachusetts. Am. J. Pub. Health 35: 485–490, 1945.

(*11*) CIOCCO, A.: On the mortality in brother-sister and husband-wife pairings. Human Biol. 13: 189–202, 1941.

(*12*) MACKLIN, M. T.: Inheritance of cancer of the stomach and large intestine in man. J. Nat. Cancer Inst. 24: 551–571, 1960.

(*13*) HESTON, W. E.: Symposium: light from animal experimentation on human heredity; bearing of mouse genetics on our understanding of human cancer. Am. J. Human Genet. 4: 314–331, 1952.

(*14*) ANDERSON, V. E., GOODMAN, H. O., and REED, S.: Variables Related to Human Breast Cancer. Minneapolis, Univ. Minnesota Press, 1958.

(*15*) MACKLIN, M. T.: Comparison of the number of breast-cancer deaths observed in relatives of breast-cancer patients, and the number expected on the basis of mortality rates. J. Nat. Cancer Inst. 22: 927–951, 1959.

(*16*) CRABTREE, J. A.: Observations on the familial incidence of cancer. Am. J. Pub. Health 31: 49–56, 1941.

(*17*) LAWRENCE, P. A., and CHEN, W. Y.: A project for studying the geographic distribution of cancer within a single county as related to environmental factors. Am. J. Pub. Health 49: 668–674, 1959.

(*18*) Manual of the International Classification of Diseases, Injuries, and Causes of Death, 6th rev. World Health Organization, 1948.

(*19*) MANTEL, N., and HAENSZEL, W.: Statistical aspects of the analysis of data from retrospective studies of disease. J. Nat. Cancer Inst. 22: 719–748, 1959.

(*20*) DORN, H. F., and CUTLER, S. J.: Morbidity from Cancer in the United States. Pub. Health Monogr. No. 56. Washington, D.C., U.S. Gov't. Print. Office, 1959.

(*21*) GORDON, T., CRITTENDEN, M., and HAENSZEL, W.: Cancer mortality trends in the United States, 1930–1955. NCI Monogr. No. 6: 133–350, 1961.

(*22*) RAZIS, D. V., DIAMOND, H. D., and CRAVEN, L. F.: Familial Hodgkin's disease: its significance and implications. Ann. Int. Med. 51: 933–971, 1959.

(*23*) MURPHY, D. P., and ABBEY, H.: Cancer in Families, a Study of the Relatives of 200 Breast Cancer Probands. Cambridge, Mass., Harvard Univ. Press, 1959.

APPENDIX

Determination of Chi Square for Comparing the Number of Matched Pairs With Its Expectation

NATHAN MANTEL *and* LYMAN B. CRITTENDEN,
Biometry Branch, National Cancer Institute, Bethesda, Maryland

THE ASYMMETRICAL CASE (HUSBAND-WIFE, BROTHER-SISTER PAIRS)

Let the total number of cases in the i^{th} row category be r_i and in the j^{th} column category be c_j with

$$\sum_i r_i = \sum_j c_j = N,$$

where N is the total number of pairs of individuals in the study. The expectations, variances, and covariances of the cell frequencies (m_{ij}), that is, the number of pairs with one individual in row category i and the other in column category j are to be determined subject to the fixed r_i's and c_j's. In the absence of true association this can be visualized as a two-urn problem. Each urn contains N balls with r_i marked as representing category i in one urn and c_i so marked in the other. (For the data analyzed in this paper the row and column classifications are identical.) Balls are selected in pairs, one from each urn at random without replacement. Under this formulation, the expectations and variances of the m_{ij}'s are:

$$E(m_{ii}) = r_i c_i / N;$$

$$Var\ (m_{ii}) = r_i(N - r_i)c_i(N - c_i)/N^2(N - 1);$$

for $i =$ or $\neq j$.

The convariances of the m_{ij}'s are as follows:

$$CV(m_{ij},m_{ik}) = -r_i(N - r_i)c_j c_k/N^2(N - 1),\ j \neq k;$$

$$CV(m_{ij},m_{kj}) = -r_j r_k c_j(N - c_j)/N^2(N - 1),\ i \neq k;$$

$$CV(m_{ij},m_{kl}) = r_i r_k c_j c_l/N^2(N - 1),\ i \neq k,\ j \neq l.$$

In particular:

$$E(m_{ii}) = r_i c_i / N;$$

$$Var\ (m_{ii}) = r_i(N - r_i)c_i(N - c_i)/N^2(N-1);$$

$$CV(m_{ii},m_{jj}) = r_i r_j c_i c_j/N^2(N - 1),\ i \neq j;$$

$$E(\sum_i m_{ii}) = \sum_i E(m_{ii}) = \sum_i r_i c_i / N \quad \text{and}$$

603724—61——15

APPENDIX TABLE 1.—Illustrative computations for chi square for the asymmetrical case. Data obtained from text-table 1.

Group		r_i (1)	$N-r_i$ $\Sigma(1)-(1)$ (2)	c_i (3)	$N-c_i$ $\Sigma(3)-(3)$ (4)	r_ic_i (1) (3) (5)	$(N-r_i)$ $(N-c_i)$ (2) (4) (6)	m_{ii} (7)	$\frac{E(m_{ii})}{\Sigma(1)}$ (5) (8)
1		2	49	1	50	2	2450	0	0. 04
2	A	2	49	0	51	0	2499	0	0. 00
	B	12	39	10	41	120	1599	5	2. 35
	C	0	51	0	51	0	2601	0	0. 00
	D	6	45	10	41	60	1845	0	1. 18
	E	3	48	2	49	6	2352	0	0. 12
	F	4	47	6	45	24	2115	2	0. 47
	G	5	46	2	49	10	2254	0	0. 20
	H	0	51	0	51	0	2601	0	0. 00
3	A	0	51	0	51	0	2601	0	0. 00
	B	2	49	0	51	0	2499	0	0. 00
	C	2	49	0	51	0	2499	0	0. 00
	D	0	51	0	51	0	2601	0	0. 00
4		0	51	5	46	0	2346	0	0. 00
7	A	0	51	1	50	0	2550	0	0. 00
	B	4	47	2	49	8	2303	1	0. 16
8		0	51	2	49	0	2499	0	0. 00
9		3	48	1	50	3	2400	0	0. 06
10		0	51	2	49	0	2499	0	0. 00
11		0	51	1	50	0	2550	0	0. 00
12	A	1	50	2	49	2	2450	0	0. 04
	B	5	46	4	47	20	2162	2	0. 39
Total		51	1, 071	51	1, 071	255	52, 275	10	5. 00

$$\sum_i m_{ii} = \sum(7) = 10$$

$$E\left(\sum_i m_{ii}\right) = \sum_i r_i c_i / N = \sum(5)/\sum(1) = 255/51 = 5.00$$

$$Var\left(\sum_i m_{ii}\right) = \frac{1}{N^2(N-1)}\left[\sum_i r_i(N-r_i)c_i(N-c_i) + \left[\sum_i r_i c_i\right]^2 - \sum_i r_i^2 c_i^2\right]$$

$$= \frac{1}{[\sum(1)]^2[\sum(1)-1]}\left[\sum(5)(6) + [\sum(5)]^2 - \sum(5)^2\right]$$

$$= \frac{1}{51 \times 51 \times 50}[468{,}656 + 65{,}025 - 19{,}193] = 3.96$$

$$\left[\begin{array}{l} \sum(5)(6) = 2 \times 2{,}450 + 0 \times 2{,}499 + \cdots + 20 \times 2162 = 468{,}656 \\ [\sum(5)]^2 = 255 \times 255 = 65{,}025 \\ \sum(5)^2 = 2 \times 2 + 0 \times 0 + \cdots + 20 \times 20 = 19{,}193 \end{array}\right]$$

$$\text{chi square, corrected (1 df)} = [|\sum_i m_{ii} - E(\sum_i m_{ii})| - 0.5]^2 / Var\left(\sum_i m_{ii}\right)$$

$$= [|10 - 5.00| - 0.5]^2/3.96$$

$$= 20.25/3.96 = 5.11$$

$$Var(\sum_i m_{ii}) = \sum_i Var(m_{ii}) + \sum_{i \neq j} CV(m_{ii}, m_{jj})$$

$$= \frac{1}{N^2(N-1)} [\sum_i r_i(N - r_i)c_i(N - c_i) + \sum_{i \neq j} r_i r_j c_i c_j]$$

$$= \frac{1}{N^2(N-1)} [\sum_i r_i(N - r_i)c_i(N - c_i) + (\sum_i r_i c_i)^2 - \sum_i r_i^2 c_i^2].$$

A corrected chi square with one degree of freedom is given by

$$(|\sum_i m_{ii} - E(\sum_i m_{ii})| - 0.5)^2 / Var(\sum_i m_{ii}).$$

The computational procedure is illustrated in Appendix table 1 with the data from text-table 1.

It should be noted that the preceding result is not limited in application to studies of the kind covered here. The total expectation in any group of cells in a two-way contingency table and the corresponding variance can be determined with these formulas. In particular, one may select cells corresponding to anticipated positive (or negative) associations between the row and column classifications [*see* Mantel and Haenszel (*19*) for another instance in which frequencies have been combined to increase statistical power].

THE SYMMETRICAL CASE (LIKE SEXED TWIN AND SIBLING PAIRS)

Let the total number of cases in the i^{th} category be r_i so that $\sum_i r_i = 2N$, where N is the total number of pairs of individuals in the study. The expectations, variances, and covariances of the cell frequencies (m_{ij}), that is, the number of pairs with one individual in category i and the other in category j, are to be determined subject to the fixed r_i's. In the absence of true association, this is visualized as a single-urn problem. The urn contains $2N$ balls with r_i marked as representing category i. Balls are drawn at random from the urn without replacement. Under this formulation the expectations, variances, and covariances of the m_{ij}'s are:

$$E(m_{ii}) = r_i(r_i - 1)/2(2N - 1);$$

$$Var(m_{ii}) = r_i(r_i - 1)(2N - r_i)(2N - r_i - 1)/2(2N - 1)^2(2N - 3);$$

$$E(m_{ij}) = r_ir_j/(2N - 1),\ i \neq j;$$

$$Var(m_{ij}) = r_ir_j[(2N - 1)(2N - r_i - r_j - 2) + 2(r_ir_j)]/(2N - 1)^2(2N - 3),\ i \neq j;$$

$$CV(m_{ii}, m_{jk}) = r_ir_jr_k(r_i - 1)/(2N - 1)^2(2N - 3),$$

$i, j,$ and k, all different;

$$CV(m_{ii}, m_{ij}) = -r_ir_j(r_i - 1)(2N - r_i - 1)/(2N - 1)^2(2N - 3),\ i \neq j;$$

$$CV(m_{ii}, m_{jj}) = r_ir_j(r_i - 1)(r_j - 1)/2(2N - 1)^2(2N - 3),\ i \neq j;$$

$$CV(m_{ij}, m_{kl}) = 2r_ir_jr_kr_l/(2N - 1)^2(2N - 3),$$

$i, j, k,$ and l all different;

$$CV(m_{ij}, m_{ik}) = -r_ir_jr_k(2N - 2r_i - 1)/(2N - 1)^2(2N - 3),$$

$i, j,$ and k all different.

(In connection with these results, it is of interest to note that the regressions of any of the cell frequencies on the diagonal cell frequencies, the m_{ii}'s, are linear, while regressions on the off-diagonal frequencies are nonlinear. In the asymmetrical case all regressions are linear.)

Again for this case we are interested in the sum of the diagonal cell frequencies ($\sum_i m_{ii}$). Thus:

$$E(\sum_i m_{ii}) = \sum_i E(m_{ii}) = \sum_i r_i(r_i - 1)/2(2N - 1) \text{ and}$$

$$Var(\sum_i m_{ii}) = \sum_i Var(m_{ii}) + \sum_{i \neq j} CV(m_{ii}, m_{jj})$$

$$= \frac{1}{2(2N - 1)^2(2N - 3)} [\sum_i r_i(r_i - 1)(2N - r_i)(2N - r_i - 1) + \sum_{i \neq j} r_ir_j(r_i - 1)(r_j - 1)]$$

$$= \frac{1}{2(2N - 1)^2(2N - 3)} [\sum r_i(r_i - 1)(2N - r_i)(2N - r_i - 1) + (\sum r_i(r_i - 1))^2 - \sum_i r_i^2(r_i - 1)^2]$$

A corrected chi square may be calculated as before. The computational procedure is illustrated in Appendix table 2 with the data from text-table 3.

APPENDIX TABLE 2.—Illustrative computations for chi square for the symmetrical case. Data obtained from text-table 3.

Group		r_i (1)	$\frac{(2N-r_i)}{\sum(1)-(1)}$ (2)	$\frac{r_i(r_i-1)}{(1)[(1)-1]}$ (3)	$\frac{(2N-r_i)(2N-r_i-1)}{(2)[(2)-1]}$ (4)	m_{ii} (5)	$\frac{E(m_{ii})}{2[\sum(1)-1]}$ (6)
1		1	87	0	7482	0	0. 00
2	A	1	87	0	7482	0	0. 00
	B	17	71	272	4970	3	1. 56
	C	0	88	0	7656	0	0. 00
	D	10	78	90	6006	0	0. 52
	E	8	80	56	6320	1	0. 32
	F	6	82	30	6642	1	0. 17
	G	4	84	12	6972	0	0. 07
	H	0	88	0	7656	0	0. 00
3	A	0	88	0	7656	0	0. 00
	B	0	88	0	7656	0	0. 00
	C	7	81	42	6480	1	0. 24
	D	0	88	0	7656	0	0. 00
4		1	87	0	7482	0	0. 00
6	A	9	79	72	6162	1	0. 41
	B	1	87	0	7482	0	0. 00
	C	2	86	2	7310	0	0. 01
7	A	1	87	0	7482	0	0. 00
	B	9	79	72	6162	0	0. 41
8		4	84	12	6972	0	0. 07
9		2	86	2	7310	0	0. 01
10		0	88	0	7656	0	0. 00
11		2	86	2	7310	0	0. 01
12	A	2	86	2	7310	1	0. 01
	B	1	87	0	7482	0	0. 00
Total		88	2, 112	666	176, 754	8	3. 83

$$\sum_i m_{ii} = \sum(5) = 8$$

$$E\left(\sum_i m_{ii}\right) = \sum_i r_i(r_i - 1)/2(2N - 1) = \sum(3)/2[\sum(1) - 1] = 666/174 = 3.83$$

$$Var\left(\sum_i m_{ii}\right) = \frac{1}{2(2N-1)^2(2N-3)}\left[\sum_i r_i(r_i-1)(2N-r_i)(2N-r_i-1) + \left[\sum_i r_i(r_i-1)\right]^2 - \sum_i r_i^2(r_i-1)^2\right]$$

$$= \frac{1}{2[\sum(1)-1]^2[\sum(1)-3]}\left[\sum(3)(4) + [\sum(3)]^2 - \sum(3)^2\right]$$

$$= \frac{1}{2 \times 87 \times 87 \times 85}[3{,}830{,}856 + 443{,}556 - 98{,}556]$$

$$= 3.25$$

$$\left[\begin{array}{l} \sum(3)(4) = 0 \times 7{,}482 + 0 \times 7{,}482 + \cdots + 0 \times 7{,}482 = 3{,}830{,}856 \\ [\sum(3)]^2 = 666 \times 666 = 443{,}556 \\ \sum(3)^2 = 0 \times 0 + 0 \times 0 + \cdots + 0 \times 0 = 98{,}556 \end{array}\right]$$

$$\text{chi square, corrected (1 df)} = [|\sum_i m_{ii} - E(\sum_i m_{ii})| - 0.5]^2/Var\left(\sum_i m_{ii}\right)$$

$$= [|8 - 3.83| - 0.5]^2/3.25$$

$$= 13.47/3.25 = 4.14$$

In both the asymmetrial and the symmetrical cases chi square is calculated based on the comparison of $\sum_i m_{ii}$ with its expectation, the overall departure from expectation being related to the variance of the $\sum_i m_{ii}$. This procedure is statistically powerful in instances where the anticipated departure from independence is one in which matchings tend to be of like subjects.

Chromosome Constitution of Cells in Effusions of Cancer Patients [1,2]

TAKAAKI ISHIHARA, GEORGE E. MOORE, *and* AVERY A. SANDBERG,[3] *Roswell Park Memorial Institute, Buffalo, New York*

SUMMARY

The chromosome constitution was determined in 18 effusions from patients with cancer and in 13 benign effusions. In contrast to the sharp modes of 46 in nonmalignant effusions, there was a considerable spread in the chromosome numbers of the neoplastic fluids examined, only about 30 percent of the cells in the latter having the modal number. Eleven fluids had modes ranging from 44 to 56 chromosomes, 2 had a mode from 62 to 64, and the remaining effusions had unbalanced polyploid modes of 78 to 112. Karyotype analysis revealed a characteristic chromosomal profile for each effusion. On a morphologic basis, most of the chromosomes in malignant effusions could be grouped superficially into the normal categories of human chromosomes, but the total set was extremely unbalanced, even in pseudodiploid cells. "New" marker chromosomes were present in most effusions, including an unusual case with a pseudodiploid chromosome constitution characterized by the presence of 3 marker chromosomes. Therapy did not seem to affect the chromosomal constitution of the effusions studied.—J. Nat. Cancer Inst. 27: 893–933, 1961.

THE CHARACTERISTICS of the 46 human chromosomes in normal diploid somatic cells permit grouping into 7 fairly well-defined categories (*1–5*). These morphologic standards make it possible to compare the karyotypes of cancer cells with those of normal cells. Several studies of chromosomes in human cancer cells, obtained directly from effusions or tissues of patients with cancer and not grown *in vitro*, have been published previously (*6–10*). Analyses of the variations from the normal within the various chromosome groups, though attempted, were not definitive, primarily because of lack of knowledge at that time of the normal human karyotype. In addition, much of the pictorial material published in the past is scanty and of a technical quality which precludes exact chromosomal analysis (*6*, *8*, *9*). The data collected did indicate, however, that hyperdiploidy was a common occurrence in human cancer cells.

[1] Received for publication June 13, 1961.

[2] Supported in part by grants C-9749 and C-3435 from the National Cancer Institute, National Institutes of Health, Public Health Service

[3] The authors wish to thank Mrs. Lois H. Crosswhite for her invaluable technical assistance. We are also grateful to Dr. Theodore S. Hauschka of our Institute for his advice throughout the study and for his criticism in the preparation of the manuscript.

In this paper we report the detailed analysis of the chromosomes in cells obtained from effusions of patients with cancer. In addition to the number of chromosomes, the karyotypes of some of these cells will be presented in detail, including those of an unusual pseudodiploid tumor, according to the classification recently established for normal human chromosomes (*4*).

METHODS

Chromosomal analysis was performed on cells obtained from either pleural or peritoneal effusions. The freshly obtained effusion fluid was centrifuged for 5 minutes at 700 rpm in a table-top, clinical model centrifuge. Several drops of sedimented cells were then placed on a slide, an equal volume of tap water was added and mixed well with the cellular suspension. After 10 minutes, the freshly filtered acetic-orcein stain (2% orcein and 65% glacial acetic acid) was added and allowed to stand for 5 to 10 minutes. A coverslip was then put on the slide and squashing performed by even finger pressure on the coverslip. A minor modification of this procedure has been used with excellent results. The effusion fluid was spun in a centrifuge at 700 rpm for 5 minutes and the supernatant carefully decanted. To the volume of sedimented cells were added 3 to 5 volumes of water; the cells were suspended in the water and allowed to stand at room temperature for 10 to 15 minutes. The cells were again sedimented by centrifugation and the supernatant carefully decanted. The plug of cells was fixed in the test tube by the addition of freshly prepared 45 percent acetic acid and allowed to stand for 30 to 45 minutes. The fixative was decanted and the acetic-orcein stain added. The slides were prepared in the usual manner.

Only cells which appeared intact were examined, and exact counts of chromosomes were obtained on the cells which showed well-spread chromosomes without confusing overlap in intact metaphase plates. Broken metaphases suspected of being incomplete were not counted. Photographs were taken with an AO 97-X oil immersion objective (N.A. 1.25), achromatic condenser, standard photographic ocular, and a 35 mm camera supplied with an AO "Microstar." A Wratten 58 green filter increased the contrast, which facilitated the counting and photography. High Contrast Copy film (Microfile) was used and developed in D-76 at 20° C with continuous agitation for 9 minutes.

For the identification of homologous chromosomes, the Denver system of nomenclature was used (*4*), combined with the grouping system of Patau (*11*), as proposed by Hauschka (*12*).

It should be pointed out that the chromosomes were classified within the various groups (A–G) on the basis of their size and the position of the centromere. In no way does the labeling of a chromosome in a certain group imply that the chromosome is normal, but this purely morphologic arrangement of the chromosomes does facilitate analysis of the karyotypes in relation to the normal.

RESULTS AND DISCUSSION

In our laboratory, metaphases obtained by the "direct squash" method on cells from human control marrows contained 46 chromosomes in nearly 90 percent of the cells. About 7 percent of the cells contained 45 chromosomes and the remaining had either 44 or 47 chromosomes (*13*, *14*). Nearly 90 percent of the over 300 metaphases from 13 benign human effusions (pleural fluids in patients with heart failure, pneumonia, or tuberculosis, or ascitic fluids from subjects with cirrhosis of the liver) contained 46 chromosomes, and this finding is similar to those previously published (*15*). The deviations from the normal diploid number were not usually more than $\pm$ 1 chromosome. The karyotypes from these cells revealed a picture which did not differ, in essence, from the karyotypes obtained from the normal human marrow, skin, or blood cells.

A different picture was seen when the chromosomes were examined in the cells from freshly obtained malignant effusions (table 1). Many effusions contained cells with a modal range about the diploid number of chromosomes ($2n = 46$). In contrast to the sharp modes in nonmalignant effusions, there was a considerable spread in the chromosome numbers of the neoplastic fluids examined, only about 30 percent of the cells in the latter having the modal number. Eleven fluids had modes ranging from 44 to 56 chromosomes, 2 had a mode from 62 to 64, and the remaining had unbalanced polyploid modes from 78 to 112. Some effusions were bimodal or had a mode equally divided between 2 successive numbers. Of interest is the maintenance of the modal number of 56 in the effusion cells of patient G. T. (#10) over a period of 4 months, including a course of chemotherapy. Similar findings are shown for patient N. P. (#18). However, the effusion cells of patient M. S. (#4) changed from the mode of 46 to 54 to 55 in less than 3 weeks without any therapy. Therapy (radiation or chemotherapy) did not seem to affect the modal number of chromosomes or range of chromosome numbers in the effusions of the patients.

The high frequency of cells with a diploid or near-diploid modal number of chromosomes in the freshly obtained effusions contrasts with the hyperdiploid to near-tetraploid modes seen in cancer cells grown *in vitro* for long periods. These findings are reminiscent of those obtained in human subjects with leukemia. The determination of the number of chromosomes in the cells of the marrow by the "direct method" was more representative of the status *in vivo* than when the cells were grown *in vitro* (*14*).

Findings similar to those presented in table 1 have been published by Makino *et al.* (*10*) who examined the number and morphology of chromosomes in 13 effusions from subjects with various malignancies. In addition, these authors examined the chromosomes from 17 excised tumors. All chromosomes showed a pronounced variation in number within a wide range, with nearly half the effusions showing a mode near the diploid number. Makino *et al.* also found that in each case there was present a stemline of tumor cells occurring most frequently with a characteristic

TABLE 1.—Clinical data, date of sampling, chromosome number, and mode of effusions from patients with cancer

Case No.	Patient's initials, age, and sex	Diagnosis and source of effusion	Therapy	Chromosome sampling date	Modal number and distribution of chromosomes			Total cells counted
					Modal No.	<Modal No.	>Modal No.	
1	J. J. 64 ♂	Carcinoma of lung, pleural	Untreated	7/1/60	62 (20. 0) * 63 (20. 0)	46–61 (40. 0) *	64–121 (20. 0) *	10
2	S. R. 60 ♀	Carcinoma of breast, pleural	Radiation in 1959, androgens	7/8/60	47 (10. 0)	39–46 (40. 0)	48–98 (60. 0)	60
3	W. F. 44 ♀	Carcinoma of breast, pleural	Radiation to chest in 1959	7/15/60	78 (18. 7)	46–77 (37. 5)	79–106 (43. 7)	16
4	M. S. 59 ♀	Carcinoma of breast, pleural	Radiation? Androgens	7/19/60	83 (25. 0)	46–82 (50. 0)	87–254 (25. 0)	12
5	L. B. 66 ♀	Carcinoma of lung, pleural	Untreated	7/28/60	46 (50. 0)	— (0. 0)	47–90 (50. 0)	6
6	M. E. 47 ♀	Carcinoma of ovary, peritoneal	Two courses of radiotherapy to abdomen in 1960	8/11/60	46 (80. 0)	— (0. 0)	68 (20. 0)	5
7	A. G. 47 ♀	Carcinoma of stomach, peritoneal	Thio-tepa in 1960	9/2/60	64 (16. 0)	58–63 (28. 0)	65–123 (56. 0)	25
8	V. M. 63 ♀	Carcinoma of lung, pleural	Untreated	9/7/60	80 (33. 3)	78–79 (33. 3)	86–91 (33. 3)	6
				10/14/60	46 (42. 8)	— (0. 0)	49–52 (57. 1)	7
9	W. S. 56 ♀	Carcinoma of ovary, peritoneal	Untreated	1/11/61	46 (66. 6)	— (0. 0)	53 (33. 3)	3
				10/26/60	56 (17. 1)	50–55 (12. 2)	57–112 (70. 7)	41
			Untreated	11/3/60	56 (28. 5)	54–55 (14. 3)	57–67 (57. 2)	14
			Vincoleukoblastine	1/17/61	56 (29. 1)	54–55 (25. 0)	57–61 (45. 8)	25
10	G. T. 66 ♂	Carcinoma of stomach, peritoneal		1/31/61	56 (26. 9)	46–55 (19. 2)	57–62 (53. 8)	26

			Vincoleukoblastine	1/17/61	56 (29. 1)	54–55 (25. 0)	57–61 (45. 8)	25
10	G. T. 66 ♂	Carcinoma of stomach, peritoneal		1/31/61	56 (26. 9)	46–55 (19. 2)	57–62 (53. 8)	26
11	C. F. 60 ♀	Carcinoma of ovary, peritoneal	TSPA in 1960	9/26/60	46 (100. 0)	— (0. 0)	— (0. 0)	16
12	M. S. 72 ♀	Malignant melanoma, pleural	Untreated	11/21/60	46 (40. 0)	41–45 (20. 0)	47–49 (40. 0)	20
				12/7/60	54 (21. 0) 55 (26. 0)	44–53 (41. 0)	56–59 (12. 0)	100
13	E. K. 72 ♀	Carcinoma of ovary, peritoneal	Radiation in early 1960	1/17/61	112 (18. 2)	52–110 (59. 1)	113–180 (22. 7)	22
14	J. A. M. 49 ♂	Carcinoma of colon, peritoneal	Untreated	4/15/61	45 (24. 0) 46 (39. 0)	43–44 (7. 0)	47–114 (30. 0)	100
15	S. B. 59 ♀	Carcinoma of stomach, peritoneal	5-Fluorouracil, vincoleukoblastine in 1960	4/24/61	Diploid range 46 (80. 0); tetraploid range 102 (30. 0)	— (0. 0) 96–100 (60. 0)	47–48 (20. 0) 104 (10. 0)	10 10
16	G. R. 39 ♂	Malignant melanoma, peritoneal	Orthophenylenediamine, 6-MP-riboside	5/3/61	44 (37. 5)	43 (25. 0)	45–48 (37. 5)	32
17	M. B. 75 ♀	Carcinoma of stomach, peritoneal	Untreated	5/29/61	90 (15. 4)	63–89 (67. 6)	91–96 (16. 9)	65
			4 hours after 5-fluorouracil	5/29/61	90 (13. 0)	61–89 (69. 5)	92–94 (17. 3)	23
18	N. P. 51 ♀	Carcinoma of breast, pleural	Untreated	2/3/60	47 (20. 0)	41–46 (40. 0)	47–51 (40. 0)	64
			TSPA and radiation during Feb.–June, 1960	6/7/60	47 (19. 2)	40–46 (51. 0)	47–54 (29. 8)	43
				6/22/60	47 (24. 5)	40–46 (36. 5)	47–54 (39. 0)	59

* Numbers in parentheses indicate percent.

mode number. Hansen-Melander *et al.* (*9*) on 2 occasions studied the cells from the peritoneal effusions of a patient with cancer of the ovary. The mode was distributed about equally between 58 and 63 and showed only slight variations with time. Ising and Levan (*7*) found a hypertriploid number of chromosomes in the effusions of 2 patients with cancer.

From an analysis of the karyotypes studied, it appears that the preponderant number of chromosomes in cancer cells in effusions can be classified morphologically into the various groups defined for normal chromosomes. In most karyotypes a few abnormal "new" chromosomes were found that characterized the cells examined. A small percentage of cells was normal with respect both to their diploid chromosome number and structure (fig. 1). These cells may be malignant, but are more probably normal host elements. In those cases in which the modal number was 46, the karyotypes revealed a pseudodiploid picture with trisomy of some chromosomes, apparent monosomy in others, and entirely new elements. The karyotypes of some of the interesting cases will be discussed in some detail.

Patient J. A. M. (#14) with carcinoma of the colon, which had been resected about a half year before the fluid was examined, had not received radiation or chemotherapy. Most of the cells had 46 or fewer chromosomes, but detailed analysis revealed the presence, among the other anomalies (figs. 2 through 15), of at least 3 abnormal chromosomes. A very long, acrocentric chromosome, not previously described in a pseudodiploid cell, was present in 100 percent of the cells. A figure-eight-like ring chromosome was present in 70 percent of the cells counted and a minute chromosome in 63 percent. The distribution of these abnormal chromosomes in pseudodiploid and near-pseudodiploid cells is shown in table 2. Twenty-one cells that had a tetraploid or near-tetraploid number of chromosomes (not shown in table 2) contained 2 of the long, acrocentric chromosomes and some other abnormal chromosomes (figs. 14 and 15). In some cells a small metacentric chromosome was present also (figs. 4, 5, and 8 through 11). In some, a unit resembling the Y chromosome was seen (figs. 8, 9, 12, and 13). In addition, the short arms of chromosomes C9 or C10 were unusually small for these groups. In most cells 1 chromosome was missing in the B4 and B5 groups, 2 extra chromosomes were present in group A3, and several chromosomes were missing in groups E and F. In several metaphases 1 chromosome of group A1 was unusually long and the cells contained only 43 to 45 chromosomes (figs. 12 and 13). In many karyotypes 1 G22 chromosome was smaller than its homologue. Breaks were seen in some chromosomes, without any particular pattern of group involvement. In some cells an extra chromosome in group D was present and the satellited short arms of these acrocentrics were unusually prominent.

Even though the X chromosomes are labeled as such in the karyotypes of the cells of patient J. A. M., a question mark was put in, due to uncertainty in selection and identification of the X chromosomes and resemblance to some of the chromosomes in group C.

TABLE 2.—Frequency of marker chromosomes in cells of patient J. A. M. (#14)

Marker chromosomes*			Marker frequency in cells with the chromosome numbers of:						Total No. of cells
A	B	C	43	44	45	46	47	48	
1	1	1			2	31	4		37
1	1	0	1	2	15	3	1	1	23
1	0	1		2	4	3		1	10
1	0	0		2	3	1			6
1	1	2				1		1	2

*A = long acrocentric chromosome; B = ring chromosome; C = minute chromosome.

Several findings in this unusual pseudodiploid case are worth discussing. The occurrence in human cancer cells of at least 3 marker chromosomes is rare, especially in cells with 46 chromosomes. Makino *et al.* (*10*) have described a long, acrocentric chromosome, resembling the one in the cells of patient J. A. M., in the excised tissue of a mammary cancer with a hypotriploid number. Ring chromosomes have been described in human cancer cells by Ising and Levan (*7*), and the importance of such chromosomes in the propagation of cancer cells was discussed by Levan (*16*). The occurrence of other markers or abnormal chromosomes in the material of previously published studies is difficult to ascertain. Makino *et al.* did classify the chromosomes into 3 groups according to size and stated that a specific idiogram characterized each tumor which can differentiate it from other tumors and from normal tissue. These authors also believe there were indications that, concomitant with the numerical changes in the chromosomes, "structural and mutational changes of the stemline chromosome" had occurred.

Much cytochemical literature exists concerning the ploidy of nuclei of cancer cells. Although examinations of the amount of deoxyribonucleic acid (DNA) by spectrophotometric techniques have shown variable amounts, this method (even when used on individual metaphases and telophases) can discern only fairly gross quantitative changes in DNA. The structural changes or slight hyperdiploidy would escape detection. Pseudodiploidy can be identified only through rigorous karyotype analysis, as practiced in the present series.

The number of chromosomes cannot be used in arguments related to the role of chromosomal changes in cancer cells. As was demonstrated in J. A. M. (#14), cancer cells can have a mode of 46 chromosomes, yet be characterized by abnormal and new chromosomes. These findings indicate that careful analysis of the karyotypes of the cells is necessary before it can be stated that a cell probably has a normal chromosomal constitution. Even though, admittedly, the findings of the present study cannot shed light on the chromosomal aberrations as a cause of cancer, they do indicate that more detailed karyotypic analysis will have to be performed in cancer cells, diploid or pseudodiploid, to widen our knowledge about the relationship of karyotypic changes at the chromosomal level to the development and genesis of cancer (*17*).

Careful analysis of the karyotypes in effusion fluids would seem to be an additional criterion for the differentiation of malignant and non-malignant cells, even when the number of chromosomes is 46. A study related to this subject will be reported on separately.

Recently, the presence of a minute chromosome, which could belong either to pair G21 or G22 in the cultured blood cells of patients with chronic myelocytic leukemia, has been described (*18*). In our laboratory, the minute chromosome has been found consistently in the fresh, non-cultured marrow and blood cells of 10 subjects with chronic myelocytic leukemia, with use of the "direct squash" technique (unpublished data of Sandberg, A. A., Crosswhite, L. H., Ishihara, T., and Hauschka, T. S.). A similar finding was consistently observed in the cells of subject J. A. M. (#14), even though there may have been differences in the reduction in size of the various arms in the two conditions. The relation of this decrease in size of the G22 chromosome to cancer needs further investigation and observation.

The occurrence of new chromosomes (long, acrocentic, ring, minute) in the cells of patients, who had not been treated with radiation or chemotherapy, would indicate that translocation or the evolution of a new chromosome in cancer cells may be of considerable importance in the development and/or persistence of the cancer cells.

Another interesting patient was M. S. (#12). Most of the cells obtained from an ascitic effusion had 54 to 55 chromosomes (figs. 16 through 23). In the preponderant number of cells there was trisomy of groups A1, A2, A3, C9, C11, E16, F19, and 2 unusual chromosomes, a large metacentric one, and a small unit of uncertain homology. The large metacentric chromosome had a secondary constriction and was slightly smaller than the chromosomes in group A1. This large chromosome was present in 86 percent of the cells (table 3). In cells with 46 chromosomes (figs. 22 and 23) karyotype analysis revealed an abnormal picture in that some of the chromosomes were characterized by possible trisomy, while others were missing, including the abnormal chromosomes. In the cells obtained from the pleural fluid of a patient with cancer of the breast, the number of chromosomes ranged from 39 to 98, 70 percent of the cells having hyperdiploid numbers (fig. 24). Two ring chromosomes, one larger than the other, were present in 90 percent of the cells, and in 5 percent of the cells with a hypertetraploid number of chromosomes, 2 each of the ring chromosomes were present (table 4). This patient had been treated with radiation in the year previous to the analysis of the pleural fluid. The presence of 2 ring chromosomes in the cells is rather an unusual occurrence and, to our knowledge, has been described only once in human cells (*7*).

Cells obtained from the peritoneal fluid of patient G. T. (#10) with carcinoma of the stomach had a modal chromosome number of 56 (figs. 25 and 26). This number persisted for several months, including a period of chemotherapy. All the chromosomes could be grouped superficially

TABLE 3.—Frequency of marker chromosomes (with secondary constriction) in cells of patient M. S. (#12)

Marker chromosome	Marker frequency in cells with the chromosome numbers of:																					Total No. of cells
	44	45	46	47	48	49	50	51	52	53	54	55	56	57	58	59						
Present	1		5		2	2	2	4	11	10	21	26	5	4	2	1						86
Absent							3	1														14

TABLE 4.—Frequency of marker chromosomes (rings) in cells of patient S. R. (#2)

| Marker chromosomes* | | Marker frequency in cells with the chromosome numbers of: | | | | | | | | | | | | | | | | | | |

into the normal morphologic categories of human chromosomes, but the total set is extremely unbalanced.

In subject J. J. (#1), all the metaphases examined showed possible trisomy for 1 or more, or occasionally all, of the chromosomes in groups A, E, F, and G and from 5 to 10 extra chromosomes in group C. The Y chromosome was thought to be identifiable in all metaphases. An unusually large metacentric chromosome was present in group A2. Only 3 chromosomes were present in group D.

In patient W. F. (#3), analysis of the metaphases with the modal number 78 revealed the presence of an unusually long, acrocentric chromosome similar to, but somewhat smaller (group-B size) than, that described for J. A. M. In addition, there was possible trisomy of all the chromosomes in groups A, E, F, and G22, and possible trisomy (and occasionally tetrasomy) of the chromosomes in group C.

The subtetraploid metaphases in subject V. M. (#8) were characterized by possible trisomy of all the chromosomes in groups A, B, D, E, and F, and possible tetrasomy (and occasional pentasomy) of the C group of chromosomes. A large submetacentric chromosome of the A2 group was present in all the metaphases.

In 80 percent of the metaphases from the cells of patient M. B. (#17) a long, acrocentric chromosome (fig. 27), similar to that seen in J. A. M. (#14) was present. Four hours after the instillation of 5-fluorouracil into the peritoneal cavity, the number of mitoses decreased considerably, but the percentage of cells containing the marker chromosome remained unchanged.

In the effusion of N. P. (#18), the karyotype analysis revealed possible trisomy of groups A3, B5, and F19. Chromosomes were missing in groups C9, C10, and E18. A minute chromosome was present in 90 percent of the cells.

From an examination of our data it appears that the cells from each effusion were characterized by a karyotypic profile reflected in each cell, whether tetraploid, subtetraploid, or pseudodiploid. The maintenance and constancy of this karyotypic profile in the effusion cells over a period of time indicates considerable stability of the karyotypic changes. It will be interesting to study the karyotypes of various untreated human cancers to ascertain whether each kind of tumor is characterized by a specific karyotype, especially in the early phases of growth.

No attempt has been made to correlate, analyze, or speculate on the findings of this study in relation to carcinogenesis or the role of the chromosomes in cancer evolution or growth (*19*), since several complete and thorough reviews have been published (*20–24*). Instead, emphasis has been on thorough analysis of the pseudodiploid and other unusual karyotypes which should be of theoretical interest to workers in the field of chromosomes and cancer. It is hoped that a full presentation of such data will shed light on the individuality and the relative stability of chromosome constitutions in various human cancers.

REFERENCES

(1) TJIO, J. H., and LEVAN, A.: The chromosome number of man. Hereditas 42: 1–6, 1956.

(2) FORD, C. E., and HAMERTON, J. L.: The chromosomes of man. Nature, London 178: 1020–1023, 1956.

(3) CHU, E. H. Y., and GILES, N. H.: Human chromosome complements in normal somatic cells in culture. Am. J. Human Genet. 11: 63–79, 1959.

(4) HUMAN CHROMOSOME STUDY GROUP: A proposed standard system of nomenclature of human mitotic chromosomes. J. Heredity 51: 214–221, 1960.

(5) CHU, E. H. Y.: Chromosome complements of human somatic cells. Am. J. Human Genet. 12: 97–103, 1960.

(6) KOLLER, P. C.: Cytological variability in human carcinomatosis. Ann. New York Acad. Sc. 63: 793–817, 1956.

(7) ISING, U., and LEVAN, A.: The chromosomes of two highly malignant human tumors. Acta path. et microbiol. scandinav 40: 13–24, 1957.

(8) MANNA, G. K.: A study of the chromosome number of human neoplastic uterine cervix tissue. *In* Proceedings of the Zoological Society. Calcutta, Mookerjee Memorial Volume, 1957, pp. 95–112.

(9) HANSEN-MELANDER, E., KULLANDER, S., and MELANDER, Y.: Chromosome analysis of a human ovarian cystocarcinoma in the ascites form. J. Nat. Cancer Inst. 16: 1067–1081, 1956.

(10) MAKINO, S., ISHIHARA, T., and TONOMURA, A.: Cytological studies of tumors. XXVII. The chromosomes of thirty human tumors. Ztschr. Krebsforsch. 63: 184–208, 1959.

(11) PATAU, K.: The identification of individual chromosomes, especially in man. Am. J. Human Genet. 12: 250–276, 1960.

(12) HAUSCHKA, T. A.: Identification of individual human chromosomes with special reference to X and Y. *In* Methodology of Human Genetics. Salt Lake City, Univ. of Utah. In press.

(13) SANDBERG, A. A., KOEPF, G. F., CROSSWHITE, L. H., and HAUSCHKA, T. S.: The chromosome constitution of human marrow in various developmental and blood disorders. Am. J. Human Genet. 12: 231–249, 1960.

(14) SANDBERG, A. A., ISHIHARA, T., MIWA, T., and HAUSCHKA, T. S.: The in vivo chromosome constitution of marrow from 34 human leukemias and 60 nonleukemic controls. Cancer Res. 21: 678–689, 1961.

(15) ISHIHARA, T., and MAKINO, S.: Chromosomal conditions in some human subjects with nonmalignant diseases. Texas Rep. Biol. & Med. 18: 427–437, 1960.

(16) LEVAN, A.: Chromosomes in cancer tissue. Ann. New York Acad. Sc. 63: 774–789, 1956.

(17) BAYREUTHER, K.: Chromosomes in primary neoplastic growth. Nature, London 186: 6–9, 1960.

(18) NOWELL, P. C., and HUNGERFORD, D.: A minute chromosome in human granulocytic leukemia. Science 132: 1497, 1960.

(19) BOVERI, T.: Zur Frage der Entwicklung maligner Tumoren. Jena, 1912 (English translation by M. Boveri, "The Origin of Malignant Tumors"). Baltimore, Williams & Williams, 1929.

(20) HAUSCHKA, T. S.: Correlation of chromosomal and physiologic changes in tumors. J. Cell & Comp. Physiol. 52: 197–267, 1958.

(21) LEVAN, A., and BIESELE, J. J.: Role of chromosomes in cancerogenesis as studied in serial tissue culture of mammalian cells. Ann. New York Acad. Sc. 71: 1022–1053, 1958.

(22) LEVAN, A.: Relation of chromosome status to the origin and progression of tumors: The evidence of chromosome number. *In* Genetics and Cancer. Austin, Texas, University of Texas Press, 1959, pp. 151–182.

603724—61——16

(*23*) Hsu, T. C.: Chromosomal evolution in cell populations. In press.
(*24*) Hauschka, T. S.: The chromosomes in ontogeny and oncogeny. Cancer Res. In press.

Plate 119

Figure 1.—Normal karyotype, possibly a nonmalignant cell, from peritoneal fluid of patient (#6) with cancer of the ovary.

903724—61——17

PLATE 120

FIGURES 2 and 3.—Pseudodiploid metaphase (fig. 2) and karyotype of cell (fig. 3) from peritoneal fluid of patient (#14) with untreated cancer of the colon. *Note* extra chromosome in groups A3 and D14. Chromosomes are missing in groups B4, E16, E17, and E18. One G22 chromosome is smaller than its homologue. Of interest are the 3 marker chromosomes (question marks *below* them), a ring chromosome, a minute chromosome, and a very long, acrocentric chromosome, shown in the *lower* right-hand corner of figure 3.

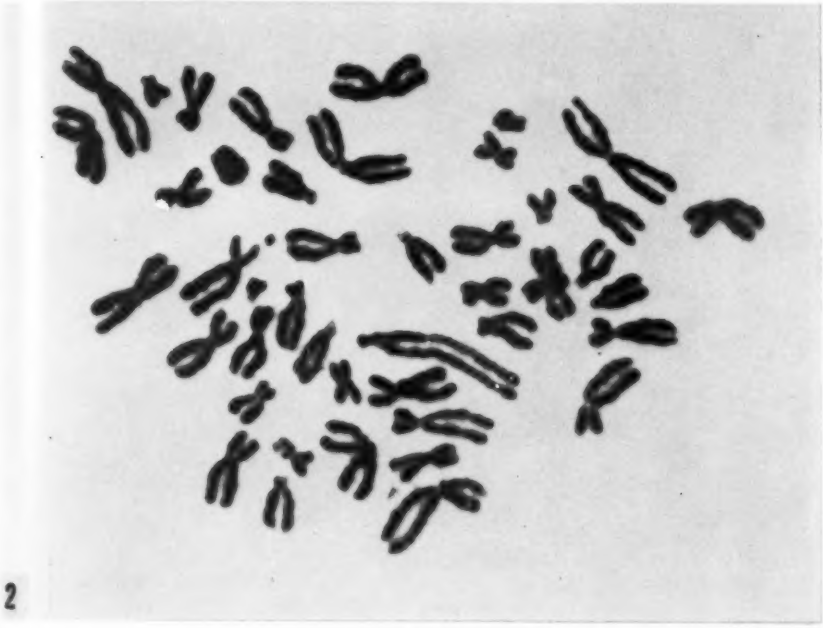

2

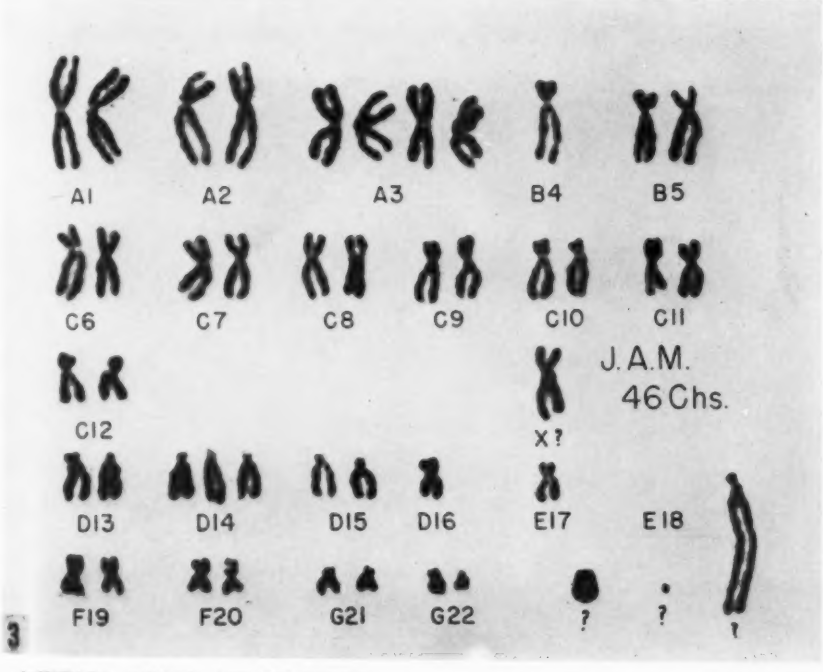
A1
A2
A3
B4
B5
C6
C7
C8
C9
C10
C11
C12
X?
J.A.M.
46 Chs.
D13
D14
D15
D16
E17
E18
F19
F20
G21
G22
?
?
?

3

PLATE 121

FIGURES 4 and 5.—Pseudodiploid metaphase (fig. 4) and karyotype of cell (fig. 5) from peritoneal fluid of patient (#14) with untreated cancer of the colon. *Note* 4 new chromosomes in *lower* right-hand corner of figure 5: a small metacentric chromosome, a minute chromosome, a figure-eight-like ring chromosome, and the very long, acrocentric chromosome present in every cell of this specimen. Two extra chromosomes are present in group A3. Chromosomes are missing in groups B4, D15, E16, E17, and E18. Chromosome shown in group E17 is somewhat larger than usually seen in this group, hence, the question mark. *Note* again, 1 G22 chromosome is smaller than its homologue.

4

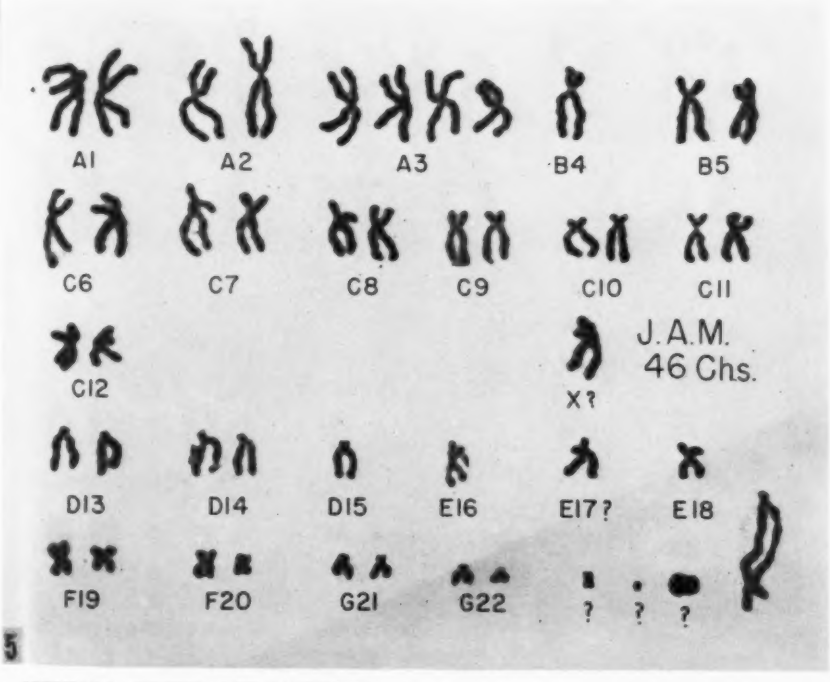
A1
A2
A3
B4
B5
C6
C7
C8
C9
C10
C11
C12
X?
J.A.M.
46 Chs.
D13
D14
D15
E16
E17?
E18
F19
F20
G21
G22
?
?
?

5

PLATE 122

FIGURES 6 and 7.—Pseudodiploid metaphase (fig.6) and karyotype of cell (fig. 7) from peritoneal fluid of patient (#14) with untreated cancer of the colon. *Note* 3 new chromosomes shown in *lower* right-hand corner of karyotype: a minute chromosome, a ring chromosome, and a very long, acrocentric chromosome. Again, 2 extra chromosomes are present in group A3. Chromosomes are missing in groups B5, E16, E17, and E18.

6

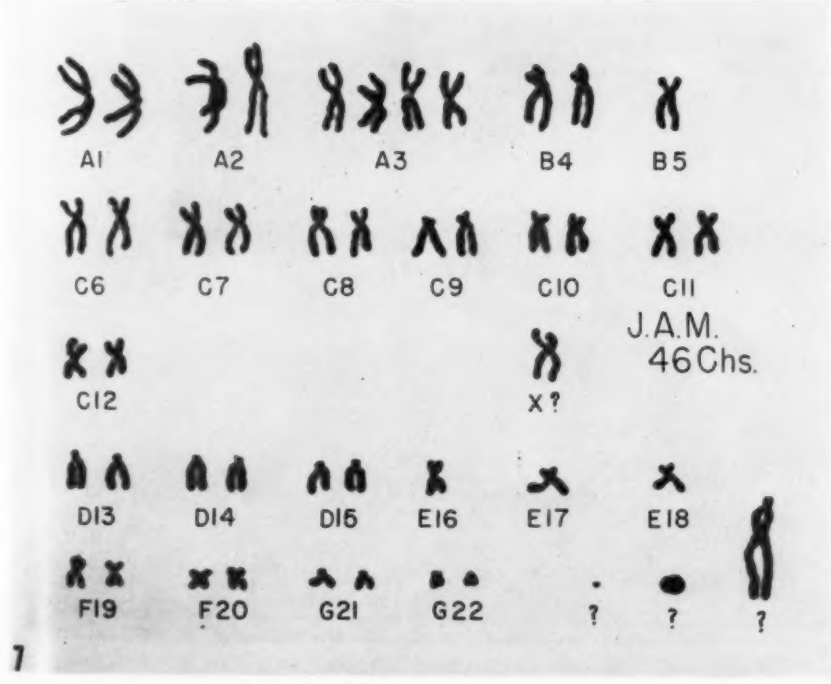
A1
A2
A3
B4
B5
C6
C7
C8
C9
C10
C11
J.A.M.
46 Chs.
C12
X?
D13
D14
D15
E16
E17
E18
F19
F20
G21
G22
?
?
?

7

PLATE 123

FIGURES 8 AND 9.—Metaphase with 45 chromosomes (fig. 8) in a cell from peritoneal fluid of patient (#14) with cancer of the colon. The karyotype (fig. 9) shows the 3 new chromosomes: a minute one, a figure-eight-like ring chromosome, and the very long, acrocentric chromosome. The Y chromosome was thought to be identifiable. Again, 1 G22 chromosome is smaller than its homologue. Two extra chromosomes are again present in group A3. Chromosomes are missing in groups B4, B5, D15, E16, E17, and E18.

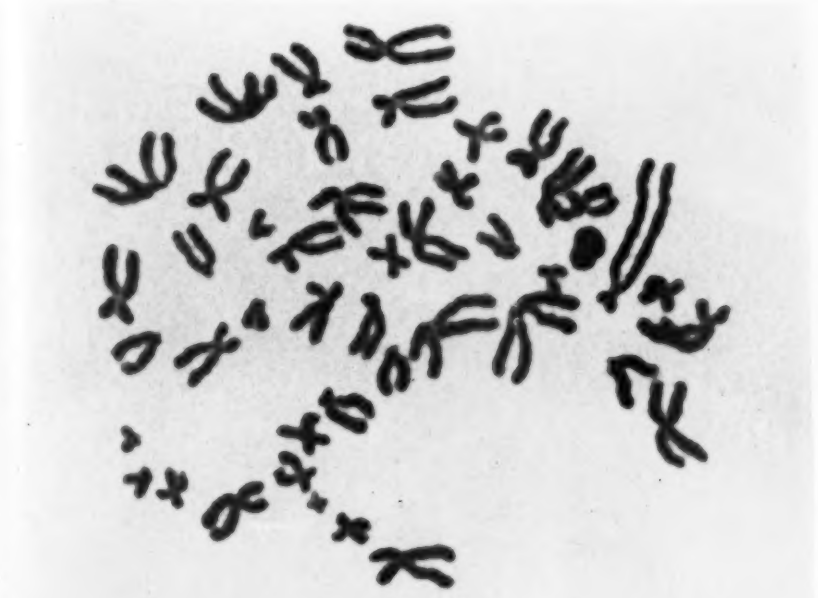

8

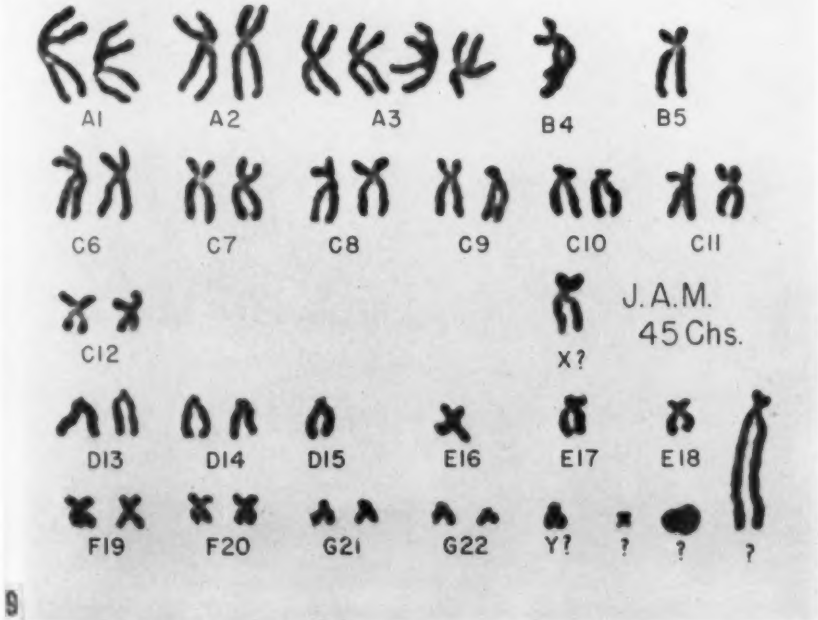
A1
A2
A3
B4
B5
C6
C7
C8
C9
C10
C11
C12
X?
J.A.M.
45 Chs.
D13
D14
D15
E16
E17
E18
F19
F20
G21
G22
Y?
?
?
?

9

PLATE 124

FIGURES 10 AND 11.—Metaphase with 46 chromosomes (fig. 10) and karyotype (fig. 11) of cell from peritoneal fluid of patient (#14) with cancer of the colon. Three new chromosomes are shown in *lower* right-hand corner of karyotype: a small metacentric, a minute, and a very long, acrocentric one. One G22 chromosome is smaller than its homologue. Only 1 extra chromosome is present in group A3. Chromosomes are missing in groups B5, E17, E18, and F19. Possible trisomy exists in group C12.

10

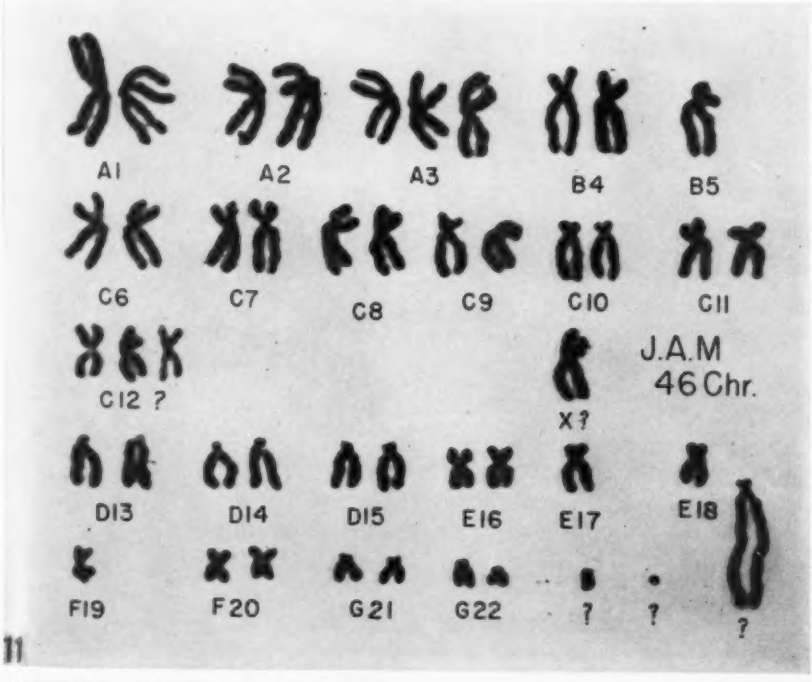
A1
A2
A3
B4
B5
C6
C7
C8
C9
C10
C11
C12 ?
X?
J.A.M
46 Chr.
D13
D14
D15
E16
E17
E18
F19
F20
G21
G22
?
?
?

11

PLATE 125

FIGURES 12 AND 13.—Metaphase with 44 chromosomes from cell of peritoneal fluid of case #14. Karyotype reveals a very large chromosome fitting into the general category, as far as the arm ratio is concerned, of group A1. Two other new chromosomes are present, a minute and the long, acrocentric one. The Y chromosome was thought to be identifiable. One G22 chromosome is smaller than its homologue. Two extra chromosomes were present in group A3. Chromosomes are missing in groups C10, C12, E16, E17, E18, and F19.

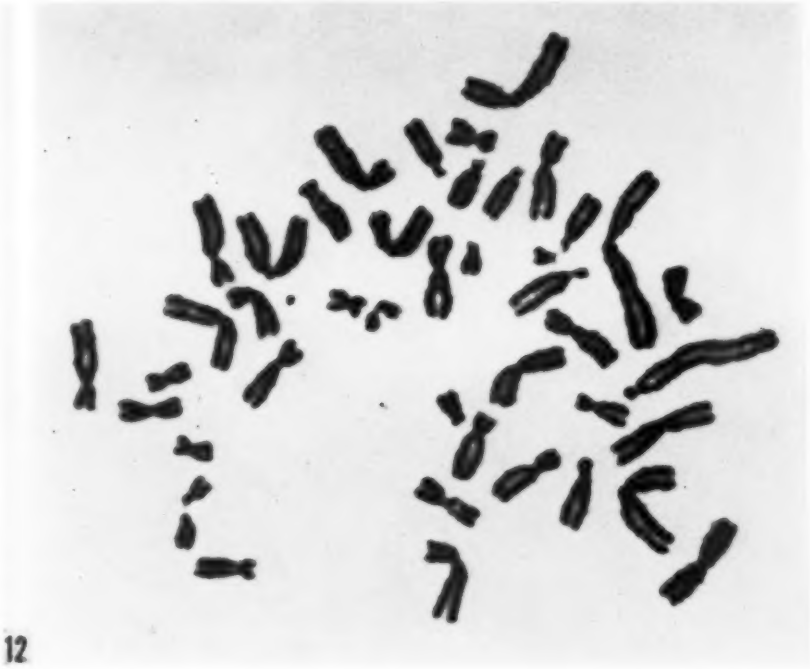

12

A1
A2
A3
B4
B5
C6
C7
C8
C9
C10
C11
C12
X?
J.A.M.
44Chr.
D13
D14
D15
E16
E17
E18
F19
F20
G21
G22
Y?
?
?

13

PLATE 126

FIGURES 14 AND 15.—Pseudotetraploid metaphase with 91 chromosomes from case #14. Karyotype reveals presence of 2 new very long, acrocentric chromosomes, 2 minutes, 1 small ring, and 2 medium-sized metacentric chromosomes, with secondary constrictions or twists. Two extra chromosomes are present in group A3. Chromosomes are missing from groups B5, C12, E16, E17, and E18.

14

A1
A2
A3
B4
B5
C6
C7
C8
C9
C10
J.A.M
91 Chs.
C11
C12
XX?
D13
D14
D15
E16
E17
E18
F19
F20
G21
G22

15

PLATE 127

FIGURES 16 and 17.—Two hyperdiploid karyotypes from peritoneal fluid of a patient (#12) with untreated malignant melanoma. Figure 16 contains 54 chromosomes, figure 17, 55. Possible trisomy of groups A1, A2, A3, C9, C11, and F19 is present in both karyotypes. In addition, in figure 17, trisomy of D14 and E16 was present, but only one G22 was found. A large chromosome with a secondary constriction and a "new" small chromosome were present in both karyotypes.

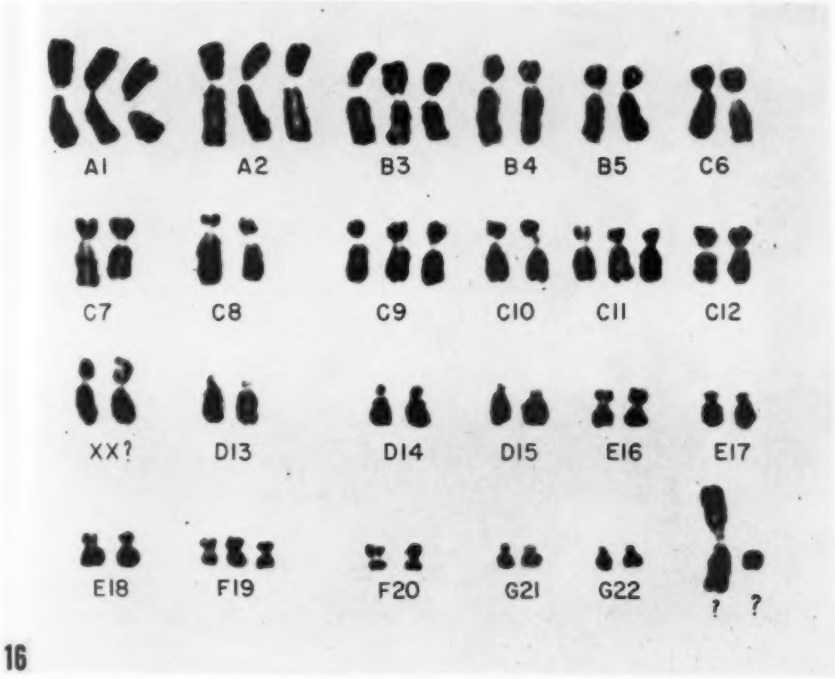

16

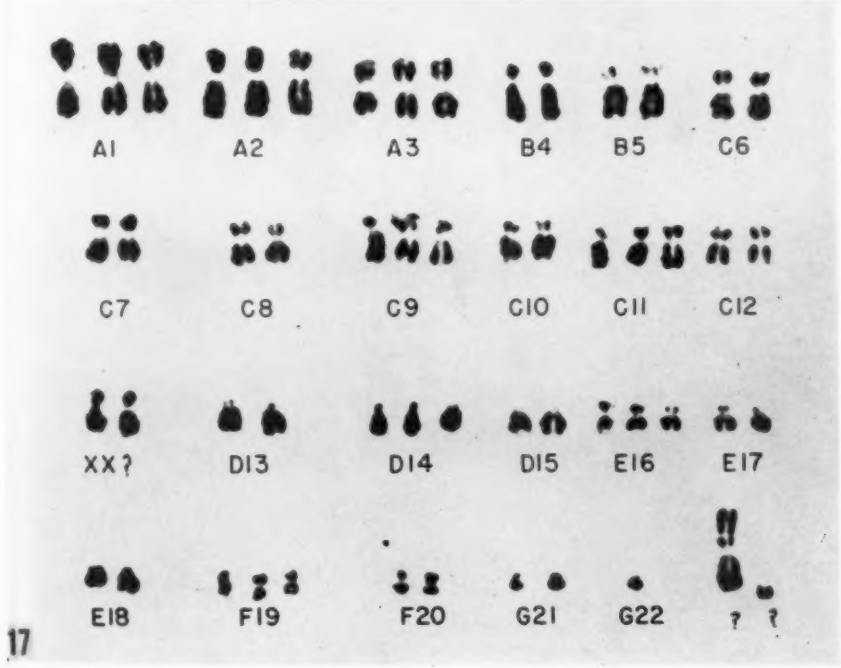

17

603724—61——18

PLATE 128

FIGURES 18 and 19.—Two hyperdiploid karyotypes (fig. 18 has 55 chromosomes, fig. 19, 53) from subject M. S. (#12). Possible trisomy for the following groups was present in both karyotypes: A1, A2, A3, C9, and E16. In figure 18, possible trisomy of groups C11 and D14 was also present. Only 1 G22 chromosome was present in figure 18. The 2 marker chromosomes were apparent in both karyotypes.

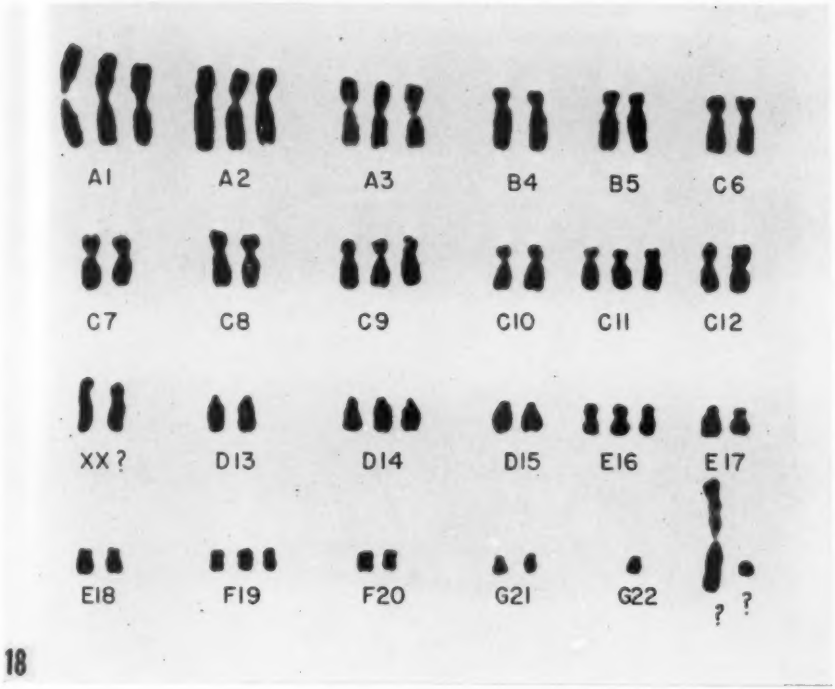
A1
A2
A3
B4
B5
C6
C7
C8
C9
C10
C11
C12
XX?
D13
D14
D15
E16
E17
E18
F19
F20
G21
G22
? ?

18

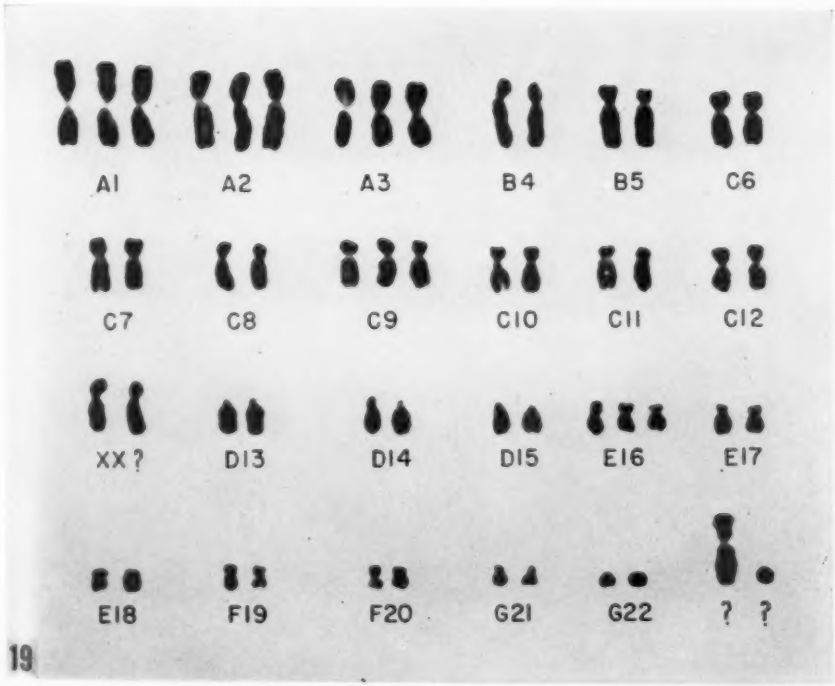
A1
A2
A3
B4
B5
C6
C7
C8
C9
C10
C11
C12
XX?
D13
D14
D15
E16
E17
E18
F19
F20
G21
G22
? ?

19

PLATE 129

FIGURES 20 and 21.—Two karyotypes with 54 chromosomes each from cells of peritoneal fluid of patient M. S. (#12). The distribution of possible trisomy is similar in both karyotypes, and each contains the 2 marker chromosomes.

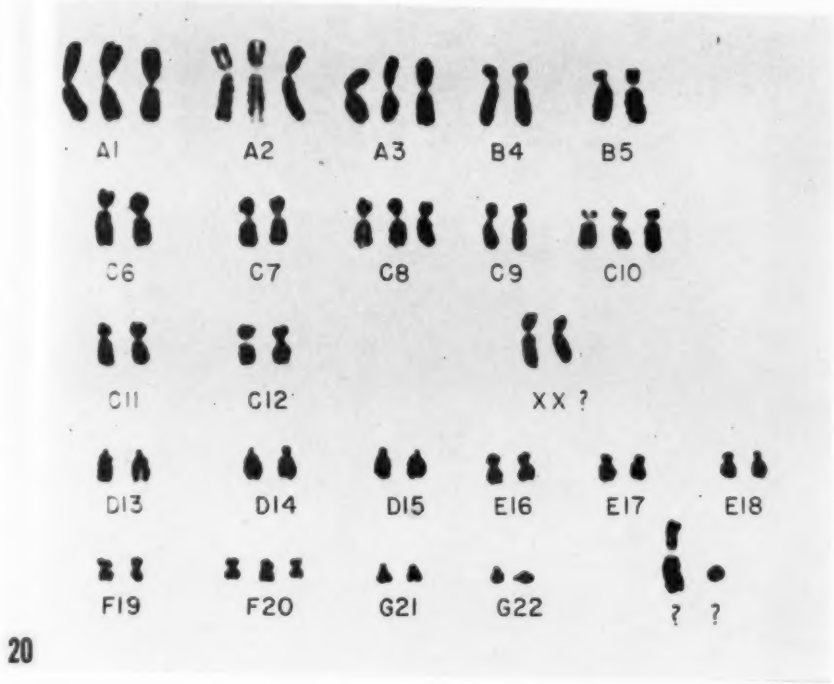
A1
A2
A3
B4
B5
C6
C7
C8
C9
C10
C11
C12
XX ?
D13
D14
D15
E16
E17
E18
F19
F20
G21
G22
? ?

20

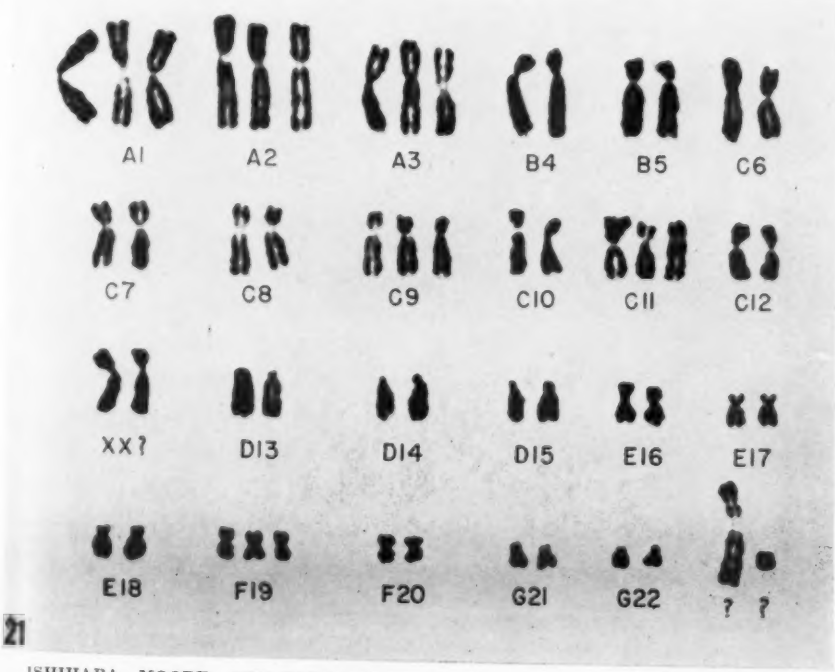
A1
A2
A3
B4
B5
C6
C7
C8
C9
C10
C11
C12
XX?
D13
D14
D15
E16
E17
E18
F19
F20
G21
G22
? ?

21

PLATE 130

FIGURES 22 and 23.—Two metaphase karyotypes, each with 46 chromosomes, from cells of peritoneal fluid of subject M. S. (#12). Even though these karyotypes contain 46 chromosomes, as do normal somatic human cells, the distribution among the various groups is abnormal. Figure 22 is characterized by possible trisomy of groups A1, A2 (*see* figs. 24 through 27) and missing chromosomes in groups C12, D15, E17, and G22. Two small, round chromosomes were present. In figure 23, possible trisomy of A1 and A3 was present. Chromosomes were missing from groups E18 and G22. One round, small chromosome was present.

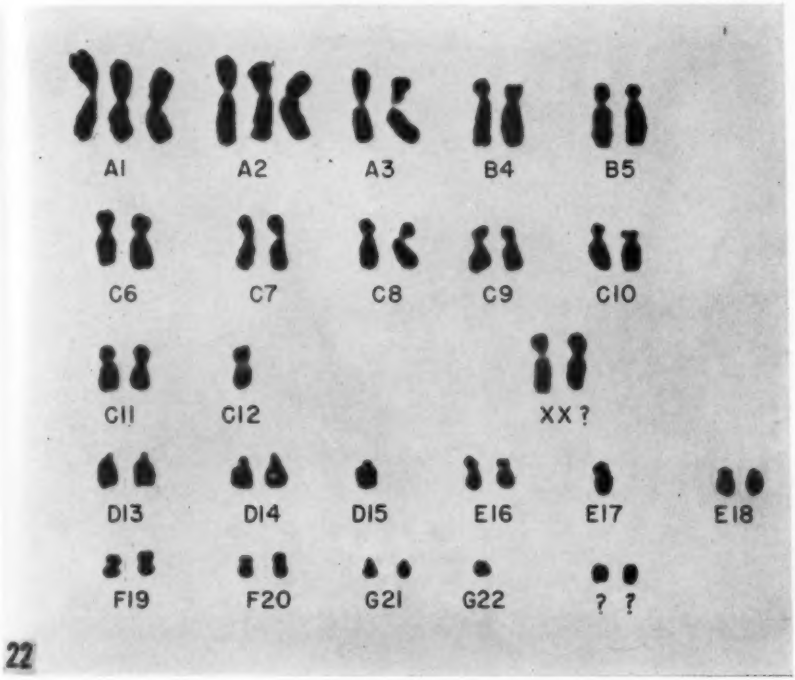
A1
A2
A3
B4
B5
C6
C7
C8
C9
C10
C11
C12
XX?
D13
D14
D15
E16
E17
E18
F19
F20
G21
G22
? ?
22

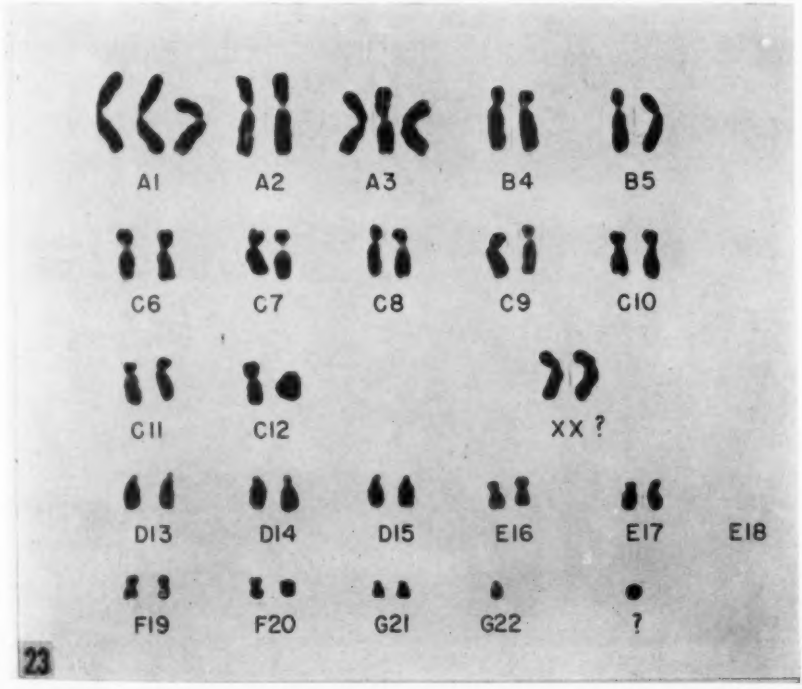
A1
A2
A3
B4
B5
C6
C7
C8
C9
C10
C11
C12
XX?
D13
D14
D15
E16
E17
E18
F19
F20
G21
G22
?
23

PLATE 131

FIGURE 24.—Subtetraploid (83 chromosomes) karyotype from S. R. (#2) obtained from cells of pleural fluid. (Patient had previously been treated with radiation for cancer of the breast.) *Note* 2 large ring and 5 new additional small chromosomes.

ISHIHARA, MOORE, AND SANDBERG

PLATE 132

FIGURES 25 and 26.—Two karyotypes from cells of subject G. T. (#10) obtained several months apart. Except for missing chromosome in group E16 in figure 25, the 2 karyotypes are identical.

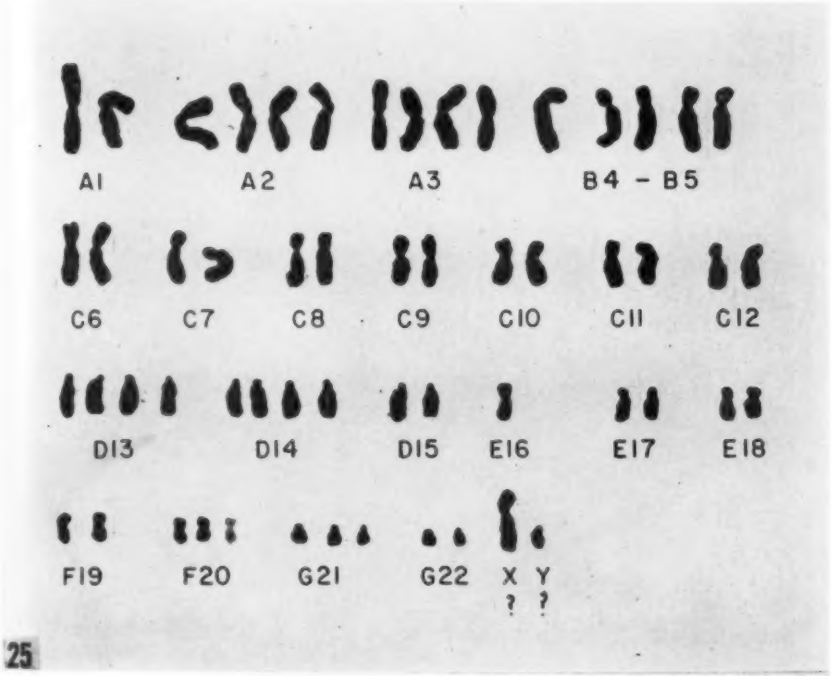
A1
A2
A3
B4 - B5
C6
C7
C8
C9
C10
C11
C12
D13
D14
D15
E16
E17
E18
F19
F20
G21
G22
X ?
Y ?

25

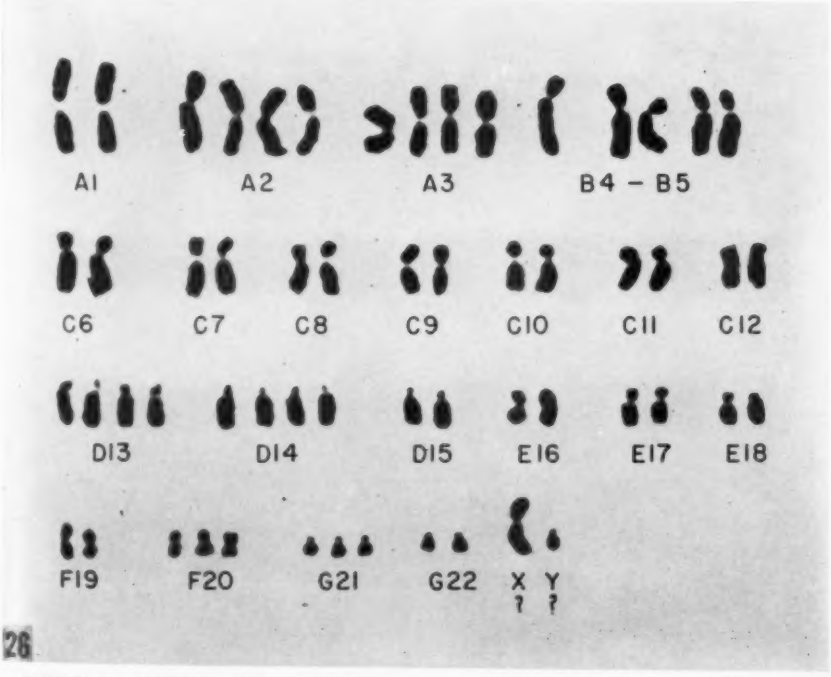
A1
A2
A3
B4 - B5
C6
C7
C8
C9
C10
C11
C12
D13
D14
D15
E16
E17
E18
F19
F20
G21
G22
X ?
Y ?

26

PLATE 133

FIGURE 27.—*Arrow* points to marker chromosome in metaphase from effusion cell of case #17.

27

Announcements

Symposium on Basic Problems in Neoplastic Disease

Columbia University College of Physicians and Surgeons will sponsor a 3-day symposium on "Basic Problems in Neoplastic Disease," March 12, 13, and 14, 1962. This symposium will commemorate the 50th anniversary of the Institute of Cancer Research at Columbia University and the 10th anniversary of its affiliated clinical facility, the Francis Delafield Hospital.

The sessions, in which outstanding scientists from the United States and abroad will participate, include: Nucleic Acid Structure and Synthesis; Viral and Genetic Studies; Protein Synthesis; Antibody Structure and Function. In addition there will be sessions on the clinical aspects of the biochemistry, pathological physiology, morphology, and therapy of cancer.

Further information may be obtained from the Institute for Cancer Research, Columbia University College of Physicians and Surgeons, 630 West 168th Street, New York 32, New York.

Manuscripts Approved for JNCI, August 15 to September 15, 1961

"Skin homograft tolerance in long-lived radiation chimeras and its abolition by injected lymphoid cells," by W. E. Davis, Jr. and L. J. Cole.

"Specific localization *in vivo* of antihepatoma antibodies in autochthonous rat hepatomas," by Eugene D. Day, Jakob A. Planinsek, and David Pressman.

"Inactivation by electron radiation of the capacity of goldenrod polysaccharide to induce vacuolization in ascites tumor cells," by John W. Preiss, Morris Belkin, and Walter G. Hardy.

"Plasma glycolytic, citric acid cycle, and transaminase enzyme levels in hamsters with a transplanted mammary adenocarcinoma," by M. West, M. Schwartz, and H. J. Zimmerman.

"Effect of enol-ether derivatives of dihydrotestosterone on 3-methylcholanthrene-induced rat mammary carcinoma," by Alberto Ercoli and Guiliano Briziarelli.

"Simple and radical mastectomy for breast cancer: A re-analysis of Smith and Meyer's report from Rockford, Illinois," by M. B. Shimkin, M. Koppel, R. R. Connelly, and S. J. Cutler.

"Intranuclear inclusions in *Rattus* (mastomys) *natalensis* infected with rat virus," by Alan S. Rabson, Lawrence Kilham, and Ruth L. Kirschstein.

"A virus isolated from a human eosinophilic granulosa," by Sarah Stewart, John C. Landon, and Mary A. Case.

"Studies on the exchange of fluids between host and tumor. II. The blood flow of hepatomas and other tumors in rats and mice," by Piero M. Gullino and Flora H. Grantham.

"Hormone-induced tumors. II. The flank-organ epithelioma of the Syrian hamster *in vitro*," by F. Thomas Algard.

"Effect of cortisone on skin maintained in organ culture," by Ronald W. Gillette, Angelica Findley, and Herbert Conway.

"Studies on the effects of surgery on transplanted animal tumors and their metastases," by Alfred S. Ketcham, Hilda Wexler, and Nathan Mantel.

"Biochemical and morphologic heterogeneity in a transplantable mast-cell neoplasm," by G. E. Mengel and J. S. Trier.

"Studies of the mammary-tumor agent of strain RIII mice," by H. B. Andervont and Thelma B. Dunn.

"Results of species-specific hemagglutination tests on 'transformed', nontransformed, and primary cell cultures," by K. G. Brand and J. T. Syverton.

"The failure of bone marrow to interfere with the augmentation of X-ray leukemogenesis by urethan," by I. Berenblum, F. E. Rewald, and N. Trainin.

"Intracellular localization of 'hematoporphyrin' in a transplanted tumor," by James Winkelman.

"Radiation response of mammalian cells grown in culture. II. The survival and recovery characteristics of several subcultures of HeLa S3 cells after X irradiation," by R. Z. Lockart, Jr., M. M. Elkind, and W. B. Moses.

"New metabolites of *N*-3-fluorenylacetamide," by Elizabeth Weisburger.

"The effect of azo-dye hepatocarcinogenesis upon the substrate induction of tryptophan pyrrolase activity," by Donald E. Kiser.

U.S. GOVERNMENT PRINTING OFFICE: 1961